UNIVERSITY OF SUSSEX

QUANTUM ELECTRODYNAMICS NEAR MATERIAL BOUNDARIES

by

Robert Zietal

A thesis submitted in partial fulfilment for the degree of Doctor of Philosophy

in the

Department of Physics & Astronomy

School of Mathematical & Physical Sciences

October 2010

Declaration of Authorship

I, Robert Zietal, declare that this thesis titled, 'Quantum electrodynamics near material boundaries' and the work presented in it are my own. I confirm that:

- This work was done wholly or mainly while in candidature for a research degree at this University.
- Where any part of this thesis has previously been submitted for a degree or any other qualification at this University or any other institution, this has been clearly stated.
- Where I have consulted the published work of others, this is always clearly attributed.
- Where I have quoted from the work of others, the source is always given. With the exception of such quotations, this thesis is entirely my own work.
- I have acknowledged all main sources of help.

Signed:

Date:

"I have had my results for a long time: but I do not yet know how I am to arrive at them."

Carl Friedrich Gauss

UNIVERSITY OF SUSSEX

Robert Jan Zietal, DPhil

Quantum electrodynamics near material boundaries

Quantum electrodynamics in free-space is a well-understood and a very successful theory. This is not the case when polarizable boundaries are present, which is a common scenario. The presence of reflective surfaces affects the photon field. Thereby the quantum-mechanical vacuum fluctuations of the electromagnetic field are constrained leading to changes in the interaction energies of charged particles which are directly measurable. One of the most famous examples of such an effect is the Lamb shift of an atom in front of a perfectly reflecting mirror, which depends on the distance of the atom from the mirror, thus giving rise to an attractive force - the so-called Casimir-Polder force. This thesis touches upon current challenges of quantum electrodynamics with externally applied boundary conditions, which is of increasing importance for nanotechnology and its applications in physics, chemistry and biology. When studying the abovementioned vacuum effects one can use models of various degrees of sophistication for the material properties that need to be taken into account. The simplest is to assume perfect reflectivity. This leads to simple boundary conditions on the electromagnetic field and thereby its quantum fluctuations. The difficulty of such calculations then lies only in the possibly complex geometry of the macroscopic body. The next possible level of sophistication is to allow imperfect reflectivity. The simplest way to achieve this is by considering a material with constant and frequency-independent refractive index. However, for all real material surfaces the reflectivity is frequency-dependent. Causality then requires that dispersion is accompanied by absorption. The aim of this project was twofold: (i) to construct, using well-understood tools of theoretical physics, the microscopic theory of quantum systems, like atoms, interacting with macroscopic polarizable media, which would facilitate relatively simple perturbative calculations of QED corrections due to the presence of boundaries, (ii) to apply the developed formalism to the calculation of the Casimir-Polder force between an atom and a realistic material.

Acknowledgements

It is a pleasure to thank Dr Claudia Eberlein for helping me to learn enough so that I could write this thesis. I am grateful not only for being my supervisor, but also for being a good friend in moments of crisis. Always patient, encouraging and supportive. This thesis would be nowhere near materializing if not for all the help, support and advice I received.

Contents

To my Parents.

Chapter 1

Thesis outline

Quantum electrodynamics in free-space is a well-understood and a very successful theory. This is not the case when polarizable boundaries are present, which is a common scenario. The presence of reflective and refracting surfaces affects the photon field. Thereby the quantum-mechanical vacuum fluctuations of the electromagnetic field are constrained leading to changes in the interaction energies of charged particles which are directly measurable. One of the most famous examples of such an effect is the Lamb shift of an atom in front of a perfectly reflecting mirror, which depends on the distance of the atom from the mirror, thus giving rise to an attractive force – the so-called Casimir-Polder force.

This thesis touches upon current challenges of quantum electrodynamics with externally applied boundary conditions, which is of increasing importance for nanotechnology and its applications in physics, chemistry and biology. The aim of this project was twofold: (i) to construct, using well-understood tools of theoretical physics, the microscopic theory of quantum systems, like atoms, interacting with macroscopic polarizable media, which would facilitate relatively simple perturbative calculations of QED corrections due to the presence of boundaries, (ii) to apply the developed formalism to the calculation of the Casimir-Polder force between an atom and a realistic dielectric material.

The problem is not new, and there exist a number of semi-phenomenological approaches e.g. a fluctuating-noise-current theory [1]. However, such elaborate theories are often opaque with respect to the underlying physical processes and are sometimes based on implicit assumptions thereby being prone to hidden pitfalls. Hence [2] *...the remarkable*

tendency to deal with such systems through simple models with explicit Hamiltonians, whose predictions are then evaluated by standard approximations of quantum mechanics or quantum field theory. From a fundamental field-theoretical point of view, the Casimir-Polder force is a result of changes to the atomic electron's self-energy, which in turn is due to the impact of the boundaries on the photon propagator. Therefore, the main task was to set up a microscopic and preferably gauge-independent model that would allow to work out corrections to the quantum photon propagator which arise due to the presence of realistic reflective boundaries.

There exist models of various degrees of sophistication to describe material's optical response to the electromagnetic field. The simplest is to assume perfect reflectivity. This leads to simple boundary conditions on the electromagnetic field and thereby its quantum fluctuations. The difficulty of such calculations then lies mostly in the possibly complex geometry of the macroscopic body. At an early stage of my PhD, on the request of the experimental cold-atom physics group at MIT, I used this simple model to derive previously unknown formulae designed to help experimental physicists to estimate magnitudes of the Casimir-Polder forces in their experiments, [3][4]. It is interesting to point out that the perfect-reflector model when applied to atoms seems to be grasping the essence of the realistic problem, whereas it completely fails when applied to the free electron. This is because electromagnetic field quantization in the presence of perfect reflectors suffers from a serious shortcoming - a lack of the evanescent modes. It turns out that these play a fundamental role in the interaction with quantum system that allows low-frequency excitations, so that the simple perfect-reflector model is fundamentally inadequate for describing such systems [5].

The next possible level of sophistication is to allow imperfect reflectivity. The simplest way to achieve this is by considering a material with constant and frequency-independent refractive index. The most important feature of this model is the inclusion of the evanescent field modes which arise from total internal reflection of a wave approaching the interface from inside the material. Such models are relatively uncomplicated, provided one refrains from studying configurations capable of wave-guiding. Then, the spectrum of the normal modes of the electromagnetic field becomes complicated as it gains a discrete part, in addition to the continuous one, related to the modes allowed within the wave-guide. This significantly complicates field operators, and any standard perturbative calculations that

require summations over all quantum numbers run into difficulties simply because it is non-trivial to combine a discrete sum with an integral. To explore the role of evanescent modes in the Casimir-Polder effect I addressed the problem of the interaction of an atom with a non-dispersive, single-layered dielectric. This exercise turned out to be an amazing experience of using beautiful mathematics. The results I obtained are relevant to current advancements in the atom-chip techniques and will be soon submitted to the journal Physical Review A.

For all real material surfaces the reflectivity is frequency-dependent (i.e. the material is dispersive). Causality then requires that dispersion is accompanied by absorption. From a quantum-mechanical point of view it means that the electromagnetic field needs to be coupled to additional quantum fields that would simulate the absorptive degrees of freedom. The Huttner-Barnett model of a dielectric interacting with the electromagnetic field does precisely this - it couples the electromagnetic field to the set of quantum fields. One of them, called the polarization field, is a field of harmonic oscillators that models polarization of the dielectric and the second, the so-called reservoir, is responsible for absorption. The model was shown to work very well in a homogeneous medium, however, its application to inhomogeneous media of even simple three-dimensional geometries is increasingly complicated and leads to unwieldy results. The best illustrating example is provided by the work of M. S. Yeung and T. K. Gustafson [6], where authors succeeded to calculate changes to spontaneous decay rates for an atom close to an absorptive half-space. However, the fundamental building block of their calculation – the photon propagator – turned out to be too complicated and necessitated the use of numerical methods thereby preventing a deep physical insight. For this reason, it seemed worthwhile to reconsider the problem and look for a remedy. The final stage of my PhD involved setting up and solving explicitly the inhomogeneous Huttner-Barnett model. I managed to show that starting from the multipolar rather than minimal coupling it is possible to solve the inhomogeneous Huttner-Barnett model in an entirely analytical and gauge-independent manner and obtain relatively simple expression for the photon propagator thereby opening the route to perturbative QED calculations using the Feynman's diagrammatic technique. I applied this formalism to calculate one-loop correction to the self-energy of the electron bound by a nucleus near a dielectric half-space. The set of final results forms a publishable content that is likely to be appreciated among experimental physicists worldwide.

Chapter 2

Introduction

2.1 Zero-point energy

The beginning of the twentieth century witnessed the development of one of the most remarkable and intellectually formidable of all physical theories - the quantum mechanics. The scope of quantum theory is to describe phenomena of the microscopic world that are entirely beyond human perception, where physical intuition, which is based on our experience of the macroscopic world has only limited, if any, applicability. Put it differently, quantum mechanics repeatedly happens to be counter-intuitive. For this reason, the only honest description of the microscopic world can be achieved in the language of abstract mathematics that is capable of reaching beyond limits of our perception.

In order to accommodate for one of the most profound surprises of quantum mechanics, the existence of the *zero-point energy*, Nature has to be described not by numbers but rather by objects that do not commute among themselves. Zero-point energy was as a matter of fact one of the first indications of the insufficiency of commutative algebras to spell out the laws of nature on the micro-scale. In the words of Dirac [7]:

...a new theory, which suggests that it is not the equations of classical mechanics that are in any way at fault, but that the mathematical operations by which physical results are deduced from them require modification.

The notion of the zero-point energy appeared in quantum theory as early as in 1911. It was then heuristically introduced by Planck in order to explain the spectrum of the radiation emitted by black body [8]. The zero-point energy is the lowest energy that a given quantum system can have and in contrast to classical physics this quantity is not zero. The most didactic example of this concept is a simple harmonic oscillator, first solved by Heisenberg using his matrix mechanics [9]. In one-dimensional case, the possible values of the energy that a simple harmonic oscillator can have are given by

$$E_n = \hbar\omega\left(n + \frac{1}{2}\right), \qquad n = 0, 1, 2\ldots \quad . \tag{2.1}$$

The lowest energy, energy of the ground state, is given by $E_0 = 1/2\hbar\omega$. The most elegant and fruitful way of modern derivation of the equation (2.1) is the well-known algebraical approach that stems from the work of Dirac [7]. It can be found in almost every elementary textbook on quantum mechanics, however, to allow for a relatively self-contained development brief summary will be given.

The Hamiltonian of a particle with mass m moving in the quadratic potential is given by

$$H = \frac{p^2}{2m} + \frac{1}{2}m\omega^2 x^2. \tag{2.2}$$

The transition to quantum mechanics requires us to impose an algebraical rule, known as commutation relation, on the canonically conjugate position x and momentum p,

$$[x, p] \equiv xp - px = i\hbar. \tag{2.3}$$

The algebraical method of solution is based on the introduction of non-Hermitean operators defined by

$$a = \frac{1}{\sqrt{2m\hbar\omega}}\left(p - im\omega x\right), \quad a^\dagger = \frac{1}{\sqrt{2m\hbar\omega}}\left(p + im\omega x\right), \quad [a, a^\dagger] = 1. \tag{2.4}$$

The normalization factors are not unique and, in fact, we only require that the Hamiltonian (2.2), when written out in terms of a and $a^\dagger$ takes the form

$$H = \frac{1}{2}\hbar\omega\left(a^\dagger a + aa^\dagger\right). \tag{2.5}$$

Using the fundamental commutators one observes that an operator $N \equiv a^\dagger a$, called number operator, commutes with the Hamiltonian (2.5). Therefore, it is possible to find simultaneous eigenstates of H and N. The defining eigenvalue problem is written as

$$N|n\rangle = n|n\rangle. \tag{2.6}$$

The expectation value of the number operator is given by $n = \langle n|a^\dagger a|n\rangle = (a|n\rangle)^\dagger a|n\rangle = |a|n\rangle|^2$. Therefore, n has to be a real and positive number or zero. It is not difficult to demonstrate using the commutators that if $|n\rangle$ is an eigenstate of N with eigenvalue n then $a|n\rangle$ or $a^\dagger|n\rangle$ are also eigenstates with eigenvalues $n-1$ or $n+1$, respectively. In fact we have

$$a|n\rangle = \sqrt{n}|n-1\rangle, \quad a^\dagger|n\rangle = \sqrt{n+1}|n+1\rangle \tag{2.7}$$

and, in particular, we note that the operator a generates the eigenstates of N with lower and lower eigenvalues that differ by unity. The process has to terminate at some point because we know that n is a positive or zero. From (2.7) it is seen to happen when $n = 0$. Therefore, we reach the conclusion that the spectrum of the number operator is given by the positive integers and zero. To show that equation (2.1) holds, we compute the expectation value of the Hamiltonian in the n^{th} state using the information we gained about the number operator:

$$E_n = \frac{1}{2}\hbar\omega\langle n|a^\dagger a + aa^\dagger|n\rangle = \frac{1}{2}\hbar\omega\langle n|a^\dagger a + a^\dagger a + 1|n\rangle = \hbar\omega\left(n + \frac{1}{2}\right). \tag{2.8}$$

We note that the appearance of the state-independent contribution, the zero-point energy, is intimately related to the non-commutativity of the canonically conjugate variables in (2.2).

Quantum mechanics of the simple harmonic oscillator is very well understood and in conjunction with Fourier analysis provides a very powerful and easily understandable method of quantizing complicated physical systems. Heuristically speaking, once the dynamics of the system is decomposed into harmonic components using Fourier analysis, one can put the Hamiltonian describing a single Fourier component into the form (2.2). Then, the route to quantization is open because the system can be viewed as a set of harmonic oscillators that we know how to treat quantum-mechanically. Obviously, in this way, the

physical system will inherit properties of a simple harmonic oscillator, most notably, the zero-point energy will appear in the Hamiltonian. It is in this way that the zero-point energy persists in modern physical theories. Here we will be mainly interested in electromagnetic zero-point energy. Therefore we would like to briefly demonstrate how the zero-point energy of a simple harmonic oscillator reappears in the theory of the quantized electromagnetic field.

The dynamics of the classical electromagnetic field in the absence of sources is described by the Hamiltonian

$$H = \frac{1}{2}\int \mathrm{d}^3\mathbf{r}\left[\epsilon_0 \mathbf{E}^2(\mathbf{r},t) + \frac{1}{\mu_0}\mathbf{B}^2(\mathbf{r},t)\right]. \tag{2.9}$$

The formalism of the classical field theory yields Maxwell's equations

$$\boldsymbol{\nabla}\cdot\mathbf{E}(\mathbf{r},t) = 0, \tag{2.10}$$

$$\boldsymbol{\nabla}\cdot\mathbf{B}(\mathbf{r},t) = 0, \tag{2.11}$$

$$\boldsymbol{\nabla}\times\mathbf{E}(\mathbf{r},t) = -\frac{\partial}{\partial t}\mathbf{B}(\mathbf{r},t), \tag{2.12}$$

$$\boldsymbol{\nabla}\times\mathbf{B}(\mathbf{r},t) = \frac{1}{c^2}\frac{\partial}{\partial t}\mathbf{E}(\mathbf{r},t). \tag{2.13}$$

Introducing the potentials $\mathbf{A}$ and ϕ such that

$$\mathbf{B}(\mathbf{r},t) = \boldsymbol{\nabla}\times\mathbf{A}(\mathbf{r},t), \quad \mathbf{E}(\mathbf{r},t) = -\frac{\partial}{\partial t}\mathbf{A}(\mathbf{r},t) - \boldsymbol{\nabla}\phi(\mathbf{r},t) \tag{2.14}$$

and choosing the Coulomb gauge $\boldsymbol{\nabla}\cdot\mathbf{A}(\mathbf{r},t) = 0$ allows to set $\phi(\mathbf{r},t) = 0$ (no sources) thereby reducing the Maxwell's equations to a single homogeneous wave equation for the vector potential [10]

$$\nabla^2\mathbf{A}(\mathbf{r},t) - \frac{1}{c^2}\frac{\partial^2}{\partial t^2}\mathbf{A}(\mathbf{r},t) = 0. \tag{2.15}$$

It is well known [11] that the monochromatic solutions of equation (2.15) reduce the Hamiltonian (2.9) to the simple harmonic form

$$H = \frac{1}{2}\left(P^2 + \omega^2 Q^2\right), \tag{2.16}$$

thereby demonstrating the equivalence of the monochromatic component of the electromagnetic field to the simple harmonic oscillator of the unit mass. This allows the quantization of the electromagnetic field by treating each mode of the field as a harmonic oscillator.

The technique of separation of variables allows us to write down the *real* monochromatic solution of equation (2.15) in the form

$$\mathbf{A}_{\mathbf{k}}(\mathbf{r},t) = N\left[a(0)\mathbf{f}_{\mathbf{k}}(\mathbf{r})e^{-i\omega t} + a^*(0)\mathbf{f}^*_{\mathbf{k}}(\mathbf{r})e^{+i\omega t}\right], \tag{2.17}$$

where the transverse vector mode function $\mathbf{f}_{\mathbf{k}}(\mathbf{r})$ is annihilated by the Helmholtz operator $\nabla^2+\omega^2/c^2$ and N is an arbitrary normalization constant. The transition from the classical Hamiltonian (2.16) to the quantum one is achieved by imposing the commutation relation on the canonically conjugate quantities Q and P. This procedure promotes the coefficient $a(0)$ in (2.17) to an operator that doesn't commute with its own Hermitian conjugate but rather satisfies the commutation relation $[\hat{a}(0), \hat{a}^\dagger(0)] = 1$. An analogous commutation relation was responsible for the quantum-mechanical properties of the simple harmonic oscillator. It is this relation through which the electromagnetic field acquires similar properties, including the zero-point energy. In the simplest case of the electromagnetic field in free-space, the full electric field operator in the Heisenberg picture is written as

$$\mathbf{E}(\mathbf{r},t) = -\frac{i}{(2\pi)^{3/2}}\sum_{\lambda}\int \mathrm{d}^3\mathbf{k}\sqrt{\frac{\hbar\omega}{2\epsilon_0}}\boldsymbol{\epsilon}_\lambda\left[a_{\mathbf{k}\lambda}(0)e^{i\mathbf{k}\cdot\mathbf{r}-i\omega t} - a^\dagger_{\mathbf{k}\lambda}(0)e^{-i\mathbf{k}\cdot\mathbf{r}+i\omega t}\right] \tag{2.18}$$

i.e. it is a 'sum' of monochromatic components. We observe how this construction satisfies the fundamental requirements of the theory. First, the mode functions $e^{i\mathbf{k}\cdot\mathbf{r}}$ take care of the spatial dependence of the operator so that together with time dependence $e^{-i\omega t}$ it satisfies the wave equation (or equivalently Maxwell equations). The transversality condition, as required by the Coulomb gauge (or first Maxwell equation), is satisfied by the introduction of the two polarization vectors $\boldsymbol{\epsilon}_\lambda$ such that $\mathbf{k}\cdot\boldsymbol{\epsilon}_\lambda = 0$, otherwise their choice is arbitrary. The quantum mechanical properties are embedded in (2.18) by one-to-one correspondence between each mode of the electromagnetic field, labelled by the composite of wave-vector and polarization index $(\mathbf{k},\lambda)$, and a unit-mass harmonic oscillator whose excitations, known as photons, are created and annihilated by the operators $a^\dagger_{\mathbf{k}\lambda}$ and $a_{\mathbf{k}\lambda}$, respectively. Thus, the state of the field is described by the state of infinitely many harmonic oscillators and can be written as $|...n_{\mathbf{k}\lambda}...\rangle$ meaning that the oscillator labelled by $(\mathbf{k}\lambda)$ is excited to the n^{th} level (n photons with momentum $\mathbf{k}$ and polarization λ). Finally, the normalization constant may vary and depends on the commutation relations that we choose to work with, their precise form is fixed by the expected form of the Hamiltonian

(2.9), which using equation (2.18) can be put in the form

$$H = \frac{1}{2}\int \mathrm{d}^3\mathbf{k}\hbar\omega \left(a^\dagger_{\mathbf{k}\lambda}a_{\mathbf{k}\lambda} + a_{\mathbf{k}\lambda}a^\dagger_{\mathbf{k}\lambda}\right). \tag{2.19}$$

Using the multi-mode generalization of the fundamental commutation relation between the creation and annihilation operators

$$\left[a_{\mathbf{k}\lambda}, a^\dagger_{\mathbf{p}\sigma}\right] = \delta^{(3)}(\mathbf{k}-\mathbf{p})\delta_{\lambda\sigma} \tag{2.20}$$

we obtain for the vacuum expectation value of the Hamiltonian

$$E_0 = \frac{1}{2}\delta^{(3)}(0)\int \mathrm{d}^3\mathbf{k}\hbar\omega. \tag{2.21}$$

The appearance of $\delta^{(3)}(0)$ in the above expression may seem strange at first. To shed some light on this we write

$$\delta^{(3)}(0) = \frac{1}{(2\pi)^3}\int \mathrm{d}^3\mathbf{r}e^0 = \frac{1}{(2\pi)^3}\int \mathrm{d}^3\mathbf{r} \tag{2.22}$$

and observe that the $\mathbf{r}$ integral is nothing but the infinite quantization volume. This problem disappears when the electromagnetic field is quantized in a finite box. What is really interesting is the divergence of the frequency integral in (2.21) that demonstrates that the zero-point energy of the electromagnetic field is in fact infinite, regardless of whether the quantization volume is infinite or finite.

The analogy between the simple harmonic oscillator and the monochromatic mode of the electromagnetic field immediately leads to the conclusion that

$$\langle \mathrm{vac}|\mathbf{E}(\mathbf{r})|\mathrm{vac}\rangle = 0, \qquad \langle \mathrm{vac}|\mathbf{E}^2(\mathbf{r})|\mathrm{vac}\rangle \neq 0, \tag{2.23}$$

i.e. on the average, the vacuum expectation value of the electric field operator vanishes but this by no means implies that there is no electromagnetic field present in the vacuum state. The non-vanishing expectation value of the square of the electric field operator informs us that, (especially) in the vacuum state, there are some fluctuations of the electromagnetic field around the mean value of zero. The (infinite) zero-point energy is the energy associated with these fluctuations. In the Heisenberg picture equations of motion

for operators are obtained by evaluating the commutators with the Hamiltonian. Since the zero-point energy is a c-number and not an operator it seems at first that it will not influence equations of motion[1]. However, as was first noted by Casimir and Polder [13], there are some observable consequences of the electromagnetic zero-point energy and we turn our attention to this fact now.

2.2 '...of some theoretical significance'

It is not possible to screen vacuum fluctuations. Therefore, every charged particle placed in vacuum will interact with the vacuum-state electromagnetic field. There are many manifestations of this interaction e.g. the deviation of the electron's g-factor from 2. In this work however, we will mainly concentrate on one in particular: the so-called Casimir-Polder effect.

An electron as a charged particle interacts with the vacuum electromagnetic field whether it is bound by a nucleus or not. For an electron within an atom, which is placed in an idealized unbounded space, this interaction is widely known as the Lamb shift and is position independent due to the translational invariance of empty unbounded space. What we are concerned with is the modification of this interaction due to the presence of a polarizable material. The spatial dependence of the vacuum fluctuations of the electromagnetic field is governed by Maxwell's equations. The introduction of polarizable boundaries imposes boundary conditions on the fields across interfaces. This breaks translation invariance thereby rendering the vacuum fluctuations position-dependent, which implies a position-dependence of the particles' interaction energies, and hence a force that is given by the gradient of this energy. This force, when acting on a neutral atom, is widely known as the Casimir-Polder force.

As is well-known, most problems in quantum mechanics don't have exact solutions and the present case is by no means an exception. However, one can study the Casimir-Polder effect using perturbative techniques. In such an approach the Hamiltonian of the system plays a central role, most notably its part that describes the interaction between the quantum system (electron or atom) and the electromagnetic field. There exist numerous

[1] It has been shown in [12] that the zero-point energy is in fact required to preserve the formal consistency of the quantum theory of the charged particles interacting with the electromagnetic field.

ways of formulating non-relativistic QED [14], and any particular choice is dictated merely by convenience. Throughout this dissertation we will restrict ourselves to a one-electron atom, for which the current and charge densities are given by

$$\mathbf{j}(\mathbf{r}) = -e\dot{\mathbf{q}}\delta^{(3)}(\mathbf{r}-\mathbf{q}), \quad \rho(\mathbf{r}) = -e\delta^{(3)}(\mathbf{r}-\mathbf{q}) + e\delta^{(3)}(\mathbf{r}), \tag{2.24}$$

i.e. the proton is immobile and placed at the origin whereas the electron has position $\mathbf{q}$. The Lagrangian of the system may be written as

$$L = \frac{1}{2}m\dot{\mathbf{q}}^2 + \int \mathrm{d}^3\mathbf{r}\Big\{\frac{\epsilon_0}{2}\left[\dot{\mathbf{A}}(\mathbf{r}) + \boldsymbol{\nabla}\phi(\mathbf{r})\right]^2 - \frac{1}{2\mu_0}\left[\boldsymbol{\nabla}\times\mathbf{A}(\mathbf{r})\right]^2 + \mathbf{j}(\mathbf{r})\cdot\mathbf{A}(\mathbf{r}) - \rho(\mathbf{r})\phi(\mathbf{r})\Big\}. \tag{2.25}$$

The Hamiltonian given in an arbitrary gauge may be obtained by a Legendre transformation

$$H = \frac{\left[\mathbf{p} + e\mathbf{A}(\mathbf{q})\right]^2}{2m} + \frac{1}{2}\int \mathrm{d}^3\mathbf{r}\left[\frac{1}{\epsilon_0}\boldsymbol{\Pi}^2(\mathbf{r}) + \frac{1}{\mu_0}\mathbf{B}^2(\mathbf{r})\right]. \tag{2.26}$$

The quantization is achieved as usual by imposing the commutation relations[2]

$$[q_i, p_j] = i\hbar\delta_{ij}, \quad [A_i(\mathbf{r}), \Pi_j(\mathbf{r}')] = i\hbar\delta_{ij}\delta^{(3)}(\mathbf{r}-\mathbf{r}'). \tag{2.27}$$

The interaction part of this Hamiltonian clearly reads

$$H_{\mathrm{INT}} = \frac{e}{2m}\left[\mathbf{p}\cdot\mathbf{A}(\mathbf{r}) + \mathbf{A}(\mathbf{r})\cdot\mathbf{p}\right] + \frac{e^2}{2m}\mathbf{A}^{\mathbf{2}}(\mathbf{r}). \tag{2.28}$$

Note that the electrostatic part of the interaction seems to be missing in (2.26). This however is not the case, it is encapsulated in the longitudinal part of the canonical electromagnetic momentum $\boldsymbol{\Pi}$, which is identified with the electric field $-\epsilon_0\mathbf{E}$, see [11]. It is well known that to study the Casimir-Polder force it is beneficial to transform the Hamiltonian (2.26) to the so called Power-Zienau-Wolley or multipolar form and then use the fact that the spatial dimensions of the atom are usually much smaller than the typical wavelength of the radiation involved. This last assumption is widely known as a *dipole approximation*.

[2]The reader should note that the commutation relation between $A_i(\mathbf{r})$ and $\Pi_j(\mathbf{r}')$ is gauge-dependent and the quantity appearing on the RHS should in general be considered as some "unit" tensor rather than standard delta-function. In particular, in the Coulomb gauge it becomes the well-known transverse delta-function.

The transformation can be achieved by several means. One can add a total time derivative to the Lagrangian (2.25) thereby leaving equation of motion unchanged [11] or perform a unitary transformation directly on the quantized Hamiltonian [15]. An alternative and very interesting method exploits the gauge transformations of the vector potential $\mathbf{A}$, as was discussed in a great detail in [16]. In multipolar formulation of the QED Hamiltonian the sources (2.24) are replaced by the polarization $\mathbf{P}(\mathbf{r})$ and magnetization $\mathbf{M}(\mathbf{r})$ associated with the atomic charges [14]

$$\mathbf{P}(\mathbf{r}) = -e\mathbf{q}\int_0^1 \mathrm{d}\lambda\delta^{(3)}(\mathbf{r}-\lambda\mathbf{q}), \quad \mathbf{M}(\mathbf{r}) = -e\mathbf{q}\times\dot{\mathbf{q}}\int_0^1 \mathrm{d}\lambda\lambda\delta^{(3)}(\mathbf{r}-\lambda\mathbf{q}), \tag{2.29}$$

where $\mathbf{q}$ is the electron's coordinate and the proton is placed at the origin. The Hamiltonian no longer depends on the vector potential $\mathbf{A}$ but takes the gauge-independent form [16]

$$H = \frac{\left[\mathbf{p} - e\int_0^1 \mathrm{d}\lambda\lambda\mathbf{q}\times\mathbf{B}(\lambda\mathbf{q})\right]^2}{2m} + \int \mathrm{d}^3\mathbf{r}\left\{\left[\frac{1}{2\epsilon_0}\mathbf{\Pi}^2(\mathbf{r}) + \frac{1}{2\mu_0}\mathbf{B}^2(\mathbf{r})\right] + \frac{1}{\epsilon_0}\mathbf{P}(\mathbf{r})\cdot\mathbf{\Pi}(\mathbf{r}) + \frac{1}{2\epsilon_0}\mathbf{P}^2(\mathbf{r})\right\}, \tag{2.30}$$

with the canonical electromagnetic momentum being now proportional to the displacement field $\mathbf{\Pi}(\mathbf{r}) = -\epsilon_0\mathbf{E}(\mathbf{r}) - \mathbf{P}(\mathbf{r})$. The appropriate commutation relations to accompany (2.30) are given by[3]

$$[q_i, p_j] = i\hbar\delta_{ij}, \quad [B_i(\mathbf{r}), \Pi_j(\mathbf{r}')] = \frac{\hbar}{(2\pi)^3}\epsilon^{ijm}\int \mathrm{d}^3\mathbf{k}k_m e^{i\mathbf{k}\cdot(\mathbf{r}-\mathbf{r}')}. \tag{2.31}$$

The assumption that the electromagnetic field varies slowly over the region in which the electron is permitted to move allows one to argue that magnetic interactions in (2.30) are negligible. This is because for a constant vector potential the magnetic field obtained from the vector potential by spatial differentiation vanishes. Assuming that the coordinate of the electron $\mathbf{q}$ is much smaller than any other length-scale in the problem lets us to write

$$\mathbf{P}(\mathbf{r}) = -e\mathbf{q}\int_0^1 \mathrm{d}\lambda\ \delta^{(3)}(\mathbf{r}-\lambda\mathbf{q}) \approx \boldsymbol{\mu}\delta^{(3)}(\mathbf{r}) + \ldots \tag{2.32}$$

[3] One should note that, in general, the issue of commutation relations for field operators in the presence of reflective boundaries forms a delicate question. Some care is needed when formulating the QED in the presence of dielectrics. We will address this problem in more detail in Chapter 4 of this thesis.

where $\boldsymbol{\mu} = -e\mathbf{q}$ is the electric dipole moment of the electron with respect to the origin. We note that in this picture the atom is envisaged to be a point-like electric dipole moment. The Hamiltonian in its final form is be written as [11]

$$H = \frac{\mathbf{p^2}}{2m} + V(\mathbf{r}) + \frac{1}{2}\int \mathrm{d}^3\mathbf{r}\left[\epsilon_0 \mathbf{E}_\perp^2(\mathbf{r}) + \frac{1}{\mu_0}\mathbf{B}^2(\mathbf{r})\right] - \boldsymbol{\mu}\cdot\mathbf{E}_\perp(0) = H_\mathrm{A} + H_\mathrm{F} + H_\mathrm{INT} \quad (2.33)$$

where $\mathbf{E}_\perp(\mathbf{r})$ is the transverse part of the electric field and $\boldsymbol{\mu}$ is the atomic electric dipole moment operator. In this formulation the interaction term

$$H_\mathrm{INT} = -\boldsymbol{\mu}\cdot\mathbf{E}_\perp(0) \quad (2.34)$$

emphasizes the physics of the problem: the interaction occurs, as in the classical case, via the coupling of the electric dipole moment of the atom to the transverse part of the electric field. $H_\mathrm{A} = \mathbf{p}^2/2m + V(\mathbf{r})$ is the part of the Hamiltonian that describes the isolated atom and H_F is the Hamiltonian of the free electromagnetic field. The transition from the Hamiltonian (2.26) to the Hamiltonian (2.33) is known in the literature as a Göppert-Mayer transformation. Here we have outlined the derivation which applies only in free-space. Its generalization to the case when polarizable boundaries are present has been developed in [17]. It turns out that the Hamiltonian of the atom plus the field corrected for the dielectric still retains the form (2.33) only that the electric field operator is no longer purely transverse but gains a longitudinal component due to the charge density arising on the surface of a dielectric. The major advantage gained here, as compared to the minimal coupling scheme, is the fact that the interaction term already encapsulates the electrostatic interaction energy between an atom and the surface thereby removing the need of separate treatment based on the Laplace equation, see e.g. [3].

The properties of a polarizable boundary present in the system are encoded in the specific form of the electric field operator, whose form, as we shall see, largely depends on the geometry of boundaries and on how complicated the dielectric's electromagnetic response is required. The method of obtaining the electric field operator is yet another problem that will form a great part of this dissertation. Throughout this work we will always employ $\boldsymbol{\mu}\cdot\mathbf{E}$ rather that $\mathbf{p}\cdot\mathbf{A}$ type of coupling to perform perturbative calculations. Having decided on the form of the interaction Hamiltonian we are in position to apply the

perturbation theory and demonstrate explicitly how the measurable effects of quantum vacuum arise in the simplest of possible scenarios:

A neutral atom placed in front of a perfectly reflecting mirror. Although the interaction between an atom and an electromagnetic wave is in principle time dependent it is sufficient to employ the time-independent perturbation theory in its standard formulation [18]. Given the interaction Hamiltonian (2.34) the shift of the i-th energy level is given by

$$\Delta W_i = \langle i;0|H_{\mathrm{INT}}|i;0\rangle + \sum_{\sigma,j\neq i}^{\prime} \frac{|\langle j;n_{\mathbf{k}\lambda}|H_{\mathrm{INT}}|i;0\rangle|^2}{E_i-(E_j+n_\sigma\hbar\omega)}. \tag{2.35}$$

In this formula the state of the combined system (atom + EM field) is described by the composite state $|i\rangle\otimes|n_\sigma\rangle \equiv |i;n_\sigma\rangle$ informing us that the atom is in the i-th state and the field contains n photons in the state σ. The index σ is a collective index that contains the photon quantum numbers. For example, in free-space $\sigma=\{\mathbf{k},\lambda\}$ i.e. it labels photons by their continuous momentum $\mathbf{k}$ and the two orthogonal polarization states $\lambda=1,2$. Note however that the character of the index σ may be quite different, its precise form largely depends on the geometry and the material properties of the polarizable media that are present in the system. We start by evaluating the first-order correction to the energy-level i which is simply an expectation value of the interaction Hamiltonian i.e.

$$\langle i;0|\boldsymbol{\mu}\cdot\mathbf{E}|i;0\rangle. \tag{2.36}$$

This contribution is easily seen to be vanishing. The form of the electric field operator, even in the presence of boundaries, will be the same as that of the free-space operator, cf. Eq. (2.18). When calculating the expectation value between the states in which there are no photons, the photon creation operator acting on vacuum will produce a 1-photon state $|1\rangle$ thereby contributing a vanishing inner product of the two orthogonal states, namely $\langle 0|1\rangle = 0$. On the other hand, the combination of the photon annihilation operator a acting on the vacuum state $|0\rangle$ vanishes by definition. Therefore, the first non-vanishing contribution to the energy shift will come from the second order of the perturbation theory. The combined integral and summation symbol that is present the last term of the formula (2.35) denotes the sum over all quantum numbers, as in the standard quantum-mechanical calculations. An unusual symbol used to denote it reminds us that it includes the sum over

the discrete atomic states j and the sum over the photon's quantum numbers σ, which can have both discrete and continuous spectra. The denominator in the second order part of (2.35) is obviously the energy difference between the intermediate states and the state for which we are calculating the shift. For reasons similar to those responsible for vanishing of the first term in (2.35) the summation in the second order correction will contribute only for one intermediate state, the state in which there is one photon and the atom in an arbitrary state j. Thus, effectively we have

$$\Delta W_i = \sum_{j\neq i} \sum\!\!\!\!\!\!\int_{\sigma} \frac{\left|\langle j; 1_{\mathbf{k}\lambda}\left|-\boldsymbol{\mu}\cdot\mathbf{E}(\mathbf{r}_0)\right|i;0\rangle\right|^2}{E_i-(E_j+\hbar\omega)}, \tag{2.37}$$

where we have explicitly indicated that the sum over the atomic states j is discrete in nature whereas the sum over the photon's degrees of freedom can be mixed. Note also that we work in the dipole approximation and the electric field operator is evaluated at the centre of the atom (which is no longer placed at the origin but we have shifted it away from the interface to position $\mathbf{r}_0$); therefore, it does not affect the atomic expectation value which consists of the integration over the electron's coordinates.

At this stage it is most convenient to work out the precise form of the electric field operator. For a perfectly reflecting plane mirror the standard method of electromagnetic field quantization by the normal-mode expansion can be applied [19]. The task of finding the electric field operator is split into two stages. First, one needs to solve the classical scattering problem (Maxwell's equations) i.e. find the normal-modes of the electromagnetic field that is excluded from the half-space, located at say $z<0$, as depicted in Fig. 2.1. Then, an arbitrary field is represented as a weighted sum of normal-modes. The quantum operator is obtained by promoting the expansion coefficients to the simple-harmonic creation and annihilation operators, as explained in the previous section.

It is convenient to work with the vector potential that satisfies the well-understood wave equation (2.15) rather than directly obtain the electric field from Maxwell's equations. For the normal modes of the vector potential $\mathbf{A}(\mathbf{r},t)=\mathbf{f}(\mathbf{r})e^{i\omega t}$ the wave equation yields an eigenvalue problem

$$-\nabla^2\mathbf{f}(\mathbf{r})=\omega^2\mathbf{f}(\mathbf{r}), \quad z>0 \tag{2.38}$$

i.e. the Helmholtz equation, which still needs to be supported by boundary conditions

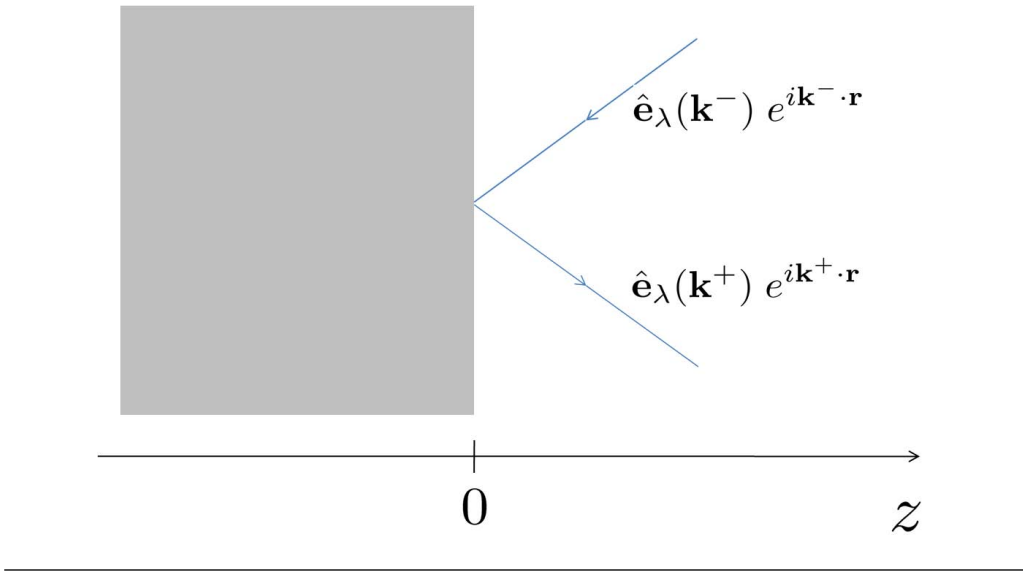

FIGURE 2.1: Electromagnetic wave scattering from the perfect reflector. The incident and reflected components form a single monochromatic mode of the electromagnetic field in this geometry.

appropriate for a perfectly reflecting surface. Maxwell's equations demand that the tangential component of the electric field $\mathbf{E}_\parallel$ is continuous across the surface. Since the electric field vanishes for $z < 0$ we have that $\mathbf{E}_\parallel(0^+) = 0$. This implies the same for the vector potential $\mathbf{A}_\parallel$, which is proportional to $\mathbf{E}_\parallel$. Next, $\mathbf{A}_\parallel(0^+) = 0$ implies that $B_\perp(0^+) \sim \partial_x A_y - \partial_y A_x = 0$. It is well known from the scattering theory [10] that these boundary conditions can be satisfied if one postulates that the solution of (2.38) consists of the incident and the reflected wave, cf. Fig. 2.1. Introducing wavevectors $\mathbf{k}^+ = (\mathbf{k}_\parallel, k_z)$ and $\mathbf{k}^- = (\mathbf{k}_\parallel, -k_z)$, which represent the wave propagating in the positive or negative z-direction, respectively, one may write down the scalar part of the solution as

$$\text{INCIDENT}: \quad e^{i\mathbf{k}^-\cdot\mathbf{r}} \qquad \text{REFLECTED}: \quad e^{i\mathbf{k}^+\cdot\mathbf{r}} \tag{2.39}$$

with $(\mathbf{k}^\pm)^2 = \omega^2$. This takes care of the spatial dependence of the mode function $\mathbf{f}(\mathbf{r})$. The transversality condition $\boldsymbol{\nabla}\cdot\mathbf{f}(\mathbf{r}) = 0$, which follows from the Coulomb gauge we are working in, imposes some restrictions on the vector character of the solutions. The divergence operator acting on the scalar solutions (2.39) drops down the wavevectors $\mathbf{k}^\pm$,

therefore the vector mode function might be written in the form[4]

$$\mathbf{f}(\mathbf{r}) = \theta(z)\left[\hat{\mathbf{e}}_\lambda(\mathbf{k}^-)e^{i\mathbf{k}^-\cdot\mathbf{r}} + R_\lambda\hat{\mathbf{e}}_\lambda(\mathbf{k}^+)e^{i\mathbf{k}^+\cdot\mathbf{r}}\right] \tag{2.40}$$

with the condition that the unit polarization vectors satisfy $\mathbf{k}^\pm\cdot\hat{\mathbf{e}}_\lambda(\mathbf{k}^\pm) = 0$. This removes one degree of freedom of the vector potential and in fact only two linearly independent vectors are needed to span the Coulomb-gauge vector potential $\mathbf{A}(\mathbf{r},t)$ in full. A very common choice in the literature is to work with the so-called transverse electric and transverse magnetic polarizations denoted TE and TM, respectively. In the TE mode the z-component of the electric field vanishes and in the TM mode the z-component of the magnetic field vanishes. The terminology originates from the theory of wave-guides [10]. In the geometry where the mirror coincides with the $z = 0$ plane the polarization vectors normalized to unity are given by

$$\hat{\mathbf{e}}_{\mathrm{TE}}\left(\mathbf{k}^\pm\right) = \frac{1}{|\mathbf{k}_\parallel|}(-k_y, k_x, 0), \quad \hat{\mathbf{e}}_{\mathrm{TM}}\left(\mathbf{k}^\pm\right) = \frac{1}{|\mathbf{k}_\parallel||\mathbf{k}|}\left(\pm k_x k_z, \pm k_y k_z, -\mathbf{k}_\parallel^2\right). \tag{2.41}$$

They satisfy the transversality condition $\mathbf{k}^\pm\cdot\mathbf{e}_\lambda(\mathbf{k}^\pm) = 0$ and are mutually orthogonal, in fact $\hat{\mathbf{e}}_{\mathrm{TM}}(\mathbf{k}^\pm) \propto \mathbf{k}^\pm \times \hat{\mathbf{e}}_{\mathrm{TE}}(\mathbf{k}^\pm)$ i.e. the set $\{\mathbf{k}^\pm, \hat{\mathbf{e}}_{\mathrm{TE}}(\mathbf{k}^\pm), \hat{\mathbf{e}}_{\mathrm{TM}}(\mathbf{k}^\pm)\}$ forms a *Dreibein* i.e. a set of three mutually orthogonal vectors. For a perfect reflector the reflection coefficient R_λ in (2.40) is of course equal to unity (up to a phase factor) but we wish to see how it follows from the boundary conditions. The continuity of the x-component of the electric field gives

$$\begin{aligned}
&\text{TE mode}: \quad \frac{k_y}{|\mathbf{k}_\parallel|}e^{i\mathbf{k}_\parallel\cdot\mathbf{r}_\parallel} + R_{\mathrm{TE}}\frac{k_y}{|\mathbf{k}_\parallel|}e^{i\mathbf{k}_\parallel\cdot\mathbf{r}_\parallel} = 0 \;\rightarrow\; R_{\mathrm{TE}} = -1,\\
&\text{TM mode}: \quad \frac{-k_x k_z}{|\mathbf{k}_\parallel||\mathbf{k}|}e^{i\mathbf{k}_\parallel\cdot\mathbf{r}_\parallel} + R_{\mathrm{TM}}\frac{k_x k_z}{|\mathbf{k}_\parallel||\mathbf{k}|}e^{i\mathbf{k}_\parallel\cdot\mathbf{r}_\parallel} = 0 \;\rightarrow\; R_{\mathrm{TM}} = 1,
\end{aligned} \tag{2.42}$$

and the continuity of the y-component of course yields the same. This in principle solves the problem but it is necessary to check that this is consistent with the condition that $B_\perp(0^+)$ vanishes. From Maxwell's equations it follows that $\mathbf{B} \propto \mathbf{k}\times\mathbf{E}$. Therefore, we see that for the TM mode the verification is trivial for the product $\mathbf{k}^\pm \times \hat{\mathbf{e}}_{\mathrm{TM}}(\mathbf{k}^\pm)$ is

[4]The modes in question, as a solution of the Hermitean operator's eigenvalue problem, form a complete set of modes. The discussion of the completeness relation as well as appropriate commutation relations for resulting operators is postponed to Chapter 5 where the question becomes non-trivial. In the case of perfect reflector the issue has been addressed for example in [20].

proportional to $\hat{\mathbf{e}}_{\mathrm{TE}}(\mathbf{k}^{\pm})$, for which the normal component vanishes identically. For the TE mode an explicit calculation gives

$$\left[\mathbf{k}^{-}\times\hat{\mathbf{e}}_{\mathrm{TE}}(\mathbf{k}^{-})+R_{\mathrm{TE}}\,\mathbf{k}^{+}\times\hat{\mathbf{e}}_{\mathrm{TE}}(\mathbf{k}^{+})\right]_{\perp}=\left[\left(\mathbf{k}^{-}-\mathbf{k}^{+}\right)\times\hat{\mathbf{e}}_{\mathrm{TE}}(\mathbf{k}^{-})\right]_{\perp}=0. \tag{2.43}$$

This confirms the consistency of equations (2.42). Once the mode functions are known the vector potential operator is given as the superposition of the monochromatic solutions, cf. Eq. (2.18),

$$\mathbf{A}(\mathbf{r},t)=\sum_{\text{all modes}}N\left[\hat{a}_{\mathbf{k}\lambda}(0)\mathbf{f}_{\mathbf{k}\lambda}(\mathbf{r})e^{-i\omega t}+\mathrm{H.C}\right], \tag{2.44}$$

where we have conveniently labelled the monochromatic modes by their momentum $\mathbf{k}$ and polarization λ. In this particular case of a perfect mirror the sum over all modes can be explicitly written out as

$$\sum_{\text{all modes}}\equiv\int_{-\infty}^{\infty}\mathrm{d}k_x\int_{-\infty}^{\infty}\mathrm{d}k_y\int_{0}^{\infty}\mathrm{d}k_z\sum_{\lambda}. \tag{2.45}$$

The restricted range of the k_z integration reflects the fact that fields are excluded from the $z<0$ half-space and therefore only the right-incident modes are allowed. The normalization constant in (2.44) is fixed by evaluating the field Hamiltonian (2.9) and comparing with the Hamiltonian of the harmonic oscillator fields (2.19)

$$N=\frac{1}{(2\pi)^{3/2}}\sqrt{\frac{\hbar}{2\epsilon_0\omega}}. \tag{2.46}$$

The electric field operator is obtained by the time derivative of the vector potential and for clarity we write it down in full

$$\begin{aligned}\mathbf{E}(\mathbf{r},t)=&-\frac{i}{(2\pi)^{3/2}}\int\mathrm{d}^2\mathbf{k}_{\parallel}\int_0^{\infty}\mathrm{d}k_z\sum_{\lambda}\sqrt{\frac{\hbar\omega}{2\epsilon_0}}\left[\hat{a}_{\mathbf{k}\lambda}(0)e^{-i\omega t}\mathbf{f}_{\mathbf{k}\lambda}(\mathbf{r})-\mathrm{H.C.}\right]\\&-\frac{i}{(2\pi)^{3/2}}\int\mathrm{d}^2\mathbf{k}_{\parallel}\int_0^{\infty}\mathrm{d}k_z\sum_{\lambda}\sqrt{\frac{\hbar\omega}{2\epsilon_0}}\left\{\hat{a}_{\mathbf{k}\lambda}(0)e^{-i\omega t}\left[\hat{\mathbf{e}}_{\lambda}(\mathbf{k}^{-})e^{i\mathbf{k}^{-}\cdot\mathbf{r}}+R_{\lambda}\hat{\mathbf{e}}_{\lambda}(\mathbf{k}^{+})e^{i\mathbf{k}^{+}\cdot\mathbf{r}}\right]-\mathrm{H.C.}\right\}.\end{aligned}$$

With the above electric field operator the second-order term of the *time-independent* perturbation series (2.37) takes the form

$$\Delta W_i=\sum_{j\neq i}\sum_{\lambda}\int\mathrm{d}^2\mathbf{k}_{\parallel}\int_0^{\infty}\mathrm{d}k_z\frac{\left|\langle j;1_{\mathbf{k}\lambda}\left|-\boldsymbol{\mu}\cdot\mathbf{E}(\mathbf{r}_0)\right|i;0\rangle\right|^2}{E_i-(E_j+\hbar\omega)}. \tag{2.47}$$

Because of the dipole approximation the electric field operator is evaluated at the position of the atom $\mathbf{r}_0$ and therefore the operation of integration hidden in the atomic expectation value is not affected by the mode functions $\mathbf{f}_{\mathbf{k}\lambda}(\mathbf{r}_0)$. We note that

$$\begin{aligned}\langle 1_{\mathbf{k}\lambda} \left|\mathbf{E}(\mathbf{r}_0)\right| 0\rangle &= \frac{i}{(2\pi)^{3/2}} \sum_\sigma \int \mathrm{d}^2\mathbf{p}_\parallel \int_0^\infty \mathrm{d}p_z \sqrt{\frac{\hbar\omega}{2\epsilon_0}} \mathbf{f}^*_{\mathbf{p}\sigma}(\mathbf{r}_0) \left\langle 1_{\mathbf{k}\lambda} \left| \hat{a}^\dagger_{\mathbf{p}\sigma} \right| 0 \right\rangle \\ &= \frac{i}{(2\pi)^{3/2}} \sqrt{\frac{\hbar\omega}{2\epsilon_0}} \mathbf{f}^*_{\mathbf{k}\lambda}(\mathbf{r}_0) \end{aligned} \tag{2.48}$$

and

$$\left|\langle j \left|\boldsymbol{\mu}\cdot\mathbf{f}^*(\mathbf{r}_0)\right| i\rangle\right|^2 = \langle j \left|\boldsymbol{\mu}\cdot\mathbf{f}^*(\mathbf{r}_0)\right| i\rangle \langle i \left|\boldsymbol{\mu}\cdot\mathbf{f}(\mathbf{r}_0)\right| i\rangle = f^*_n(\mathbf{r}_0) f_m(\mathbf{r}_0) \langle j \left|\mu_n\right| i\rangle \langle i \left|\mu_m\right| j\rangle , \tag{2.49}$$

so that Eq. (2.47) becomes

$$\Delta W_i = \frac{1}{(2\pi)^3} \sum_{j\neq i} \sum_\lambda \int \mathrm{d}^2\mathbf{k}_\parallel \int_0^\infty \mathrm{d}k_z \frac{\hbar\omega}{2\epsilon_0} f^*_n(\mathbf{r}_0) f_m(\mathbf{r}_0) \frac{\langle j \left|\mu_n\right| i\rangle \langle i \left|\mu_m\right| j\rangle}{E_{ji} + \hbar\omega}, \tag{2.50}$$

where the sums over the Cartesian indices n and m are implied. Also, to preserve clarity we have suppressed the subscripts indicating the obvious dependence of the components of the mode functions on the momentum $\mathbf{k}$ and polarization λ. The dipole matrix elements can be further simplified using the fact that we work with the atomic states of definite angular momentum $|l, m\rangle$ (in the following the spin of the electron is ignored). For the hydrogen-like atom the components of the electric dipole operator, when expressed in spherical polar coordinates, can be written in terms of the eigenfunctions of the angular momentum operator $\mathrm{Y}^m_l(\theta, \phi)$

$$\begin{aligned}\mu_x &= e|\mathbf{q}| \sqrt{\frac{2\pi}{3}} \left[\mathrm{Y}^1_1(\theta,\phi) - \mathrm{Y}^{-1}_1(\theta,\phi)\right] \\ \mu_y &= -ie|\mathbf{q}| \sqrt{\frac{2\pi}{3}} \left[\mathrm{Y}^1_1(\theta,\phi) + \mathrm{Y}^{-1}_1(\theta,\phi)\right] \\ \mu_z &= -e|\mathbf{q}| \sqrt{\frac{4\pi}{2}} \mathrm{Y}^0_1(\theta,\phi) \end{aligned}$$

Therefore, the problem is reduced to the evaluation of the quantities of the type

$$\langle l', m' | \mathrm{Y}^m_l(\theta,\phi) | l'', m''\rangle. \tag{2.51}$$

This can be done with the use of the commutator $[L_z, \mathrm{Y}_l^m(\theta,\phi)] = m\hbar \mathrm{Y}_l^m(\theta,\phi)$ where L_z is the z-component of the angular momentum operator. We write

$$\begin{aligned} 0 &= \langle l', m'|[L_z, \mathrm{Y}_l^m(\theta,\phi)] - m\hbar \mathrm{Y}_l^m(\theta,\phi)|l'', m''\rangle \\ &= \langle l', m'|L_z \mathrm{Y}_l^m(\theta,\phi) - \mathrm{Y}_l^m(\theta,\phi) L_z - m\hbar \mathrm{Y}_l^m(\theta,\phi)|l'', m''\rangle \\ &= \langle l', m'|m'\hbar \mathrm{Y}_l^m(\theta,\phi) - m''\hbar \mathrm{Y}_l^m(\theta,\phi) - m\hbar \mathrm{Y}_l^m(\theta,\phi)|l'', m''\rangle \\ &= \hbar(m' - m'' - m)\langle l', m'|\mathrm{Y}_l^m(\theta,\phi)|l'', m''\rangle, \end{aligned} \tag{2.52}$$

thereby arriving at the example of the m-selection rule [18]

$$\langle l', m'|\mathrm{Y}_l^m(\theta,\phi)|l'', m''\rangle \propto \delta_{m', m''+m}, \tag{2.53}$$

i.e. the matrix elements vanish unless $m' = m'' + m$. Now consider for example

$$\begin{aligned} \langle l', m'|\mu_x|l'', m''\rangle\langle l'', m''|\mu_z|l', m'\rangle &\propto \langle l', m'|\mathrm{Y}_1^1 - \mathrm{Y}_1^{-1}|l'', m''\rangle\langle l'', m''|\mathrm{Y}_1^0|l', m'\rangle \\ &\propto \left(\delta_{m', m''+1} - \delta_{m', m''-1}\right)\delta_{m', m''} = 0. \end{aligned}$$

Similarly we have

$$\begin{aligned} \langle l', m'|\mu_y|l'', m''\rangle\langle l'', m''|\mu_z|l', m'\rangle &\propto \langle l', m'|\mathrm{Y}_1^1 + \mathrm{Y}_1^{-1}|l'', m''\rangle\langle l'', m''|\mathrm{Y}_1^0|l', m'\rangle \\ &\propto \left(\delta_{m', m''+1} + \delta_{m', m''-1}\right)\delta_{m', m''} = 0. \end{aligned}$$

The remaining case is slightly less trivial. Computing the matrix elements gives

$$\langle l', m'|\mu_x|l'', m''\rangle\langle l'', m''|\mu_y|l', m'\rangle = |\langle l', m'|\mathrm{Y}_1^{-1}|l'', m' + 1\rangle|^2 - |\langle l', m'|\mathrm{Y}_1^1|l'', m' - 1\rangle|^2 \tag{2.54}$$

and we see that there are the contributions that do not vanish identically. However, the two terms can be shown to cancel out using the Wigner-Eckart theorem, see e.g. [18]. Alternatively, the vanishing of (2.54) can be argued on the rotational symmetry grounds i.e. one can always rotate the coordinate system from $\{x, y, z\}$ to $\{y, z, x\}$. Thus we have that

$$\langle l', m'|\mu_m|l'', m''\rangle\langle l'', m''|\mu_n|l', m'\rangle = \delta_{mn}|\langle l'', m''|\mu_n|l', m'\rangle|^2 \equiv |\mu_n|^2\delta_{mn} \tag{2.55}$$

and the formula (2.50) becomes

$$\Delta W_i = \frac{1}{(2\pi)^3}\sum_{j\neq i}\sum_{\lambda,n}\int \mathrm{d}^2\mathbf{k}_\parallel \int_0^\infty \mathrm{d}k_z \frac{\hbar\omega}{2\epsilon_0}\frac{|f_n^*(\mathbf{r}_0)|^2|\mu_n|^2}{E_{ji}+\hbar\omega}. \tag{2.56}$$

The reader is reminded that in fact $f_i^*(\mathbf{r}_0) = f_{i,\mathbf{k}\lambda}^*(\mathbf{r}_0)$. The situation is now ripe for the explicit form of the mode functions (2.40) to be plugged into (2.56). We have

$$|f_n^*(\mathbf{r}_0)|^2|\mu_n|^2 = |\mu_n|^2\Big[R_\lambda e_{n,\lambda}(\mathbf{k}^-)e_{n,\lambda}(\mathbf{k}^+)e^{-2ik_z z_0} + R_\lambda e_{n,\lambda}(\mathbf{k}^+)e_{n,\lambda}(\mathbf{k}^-)e^{2ik_z z_0} + e_{n,\lambda}^2(\mathbf{k}^-) + e_{n,\lambda}^2(\mathbf{k}^+)\Big] \tag{2.57}$$

where we have used the fact that $R_\lambda^2 = 1$ and the wave-vector $\mathbf{k}^\pm$ is always real i.e. there are no evanescent modes present in the radiation field. The terms that do not depend on the position of the atom z_0 are neglected as they are associated with the shift due to the free-space electromagnetic field. These are of course partially responsible for the Lamb shift. Since we are not interested in the Lamb shift itself but only in the corrections to that effect due to the presence of the boundary we neglect the z_0-independent terms. Formally, this 'renormalization' is achieved by calculating the energy shift using the free-space mode functions and subtracting the result from equation (2.56) i.e. $\Delta W_i^{\mathrm{ren}} = \Delta W_i - \Delta W_i^{\text{free space}}$. Therefore, the renormalized shift is written as

$$\Delta W_i^{\mathrm{ren}} = \frac{1}{2(2\pi)^3\epsilon_0}\sum_{j\neq i}\sum_{\lambda,n}|\mu_n|^2\int \mathrm{d}^2\mathbf{k}_\parallel \int_{-\infty}^{\infty}\mathrm{d}k_z \frac{|\mathbf{k}|}{E_{ji}/\hbar c + |\mathbf{k}|}R_\lambda e_{n,\lambda}(\mathbf{k}^+)e_{n,\lambda}(\mathbf{k}^-)e^{2ik_z z_0} \tag{2.58}$$

where $k = |\mathbf{k}| = \omega/c$. Note that the k_z integral range now spans from $-\infty$ to ∞. This is achieved by combining the two z_0-dependent terms in (2.57) by a simple change of variables $k_z \to -k_z$. Note also that the quantity $E_{ji} = E_j - E_i$, which is the energy difference between the atomic levels, could be in principle negative if one considers an excited state $|i\rangle$. In this case a prescription is needed on how to handle the pole at $E_{ji}/\hbar c + |\mathbf{k}| = 0$. This is done by adding a small imaginary part into the denominator and use of the distributional identity

$$\lim_{\eta\to 0}\frac{1}{x+i\eta} = \frac{\mathcal{P}}{x} - i\pi\delta(x) \tag{2.59}$$

where $\mathcal{P}$ stands for the Cauchy principal-value. Then, the principal part yields the energy

shift of the excited state $|i\rangle$ whereas the imaginary part of the energy shift $\Delta W_i^{\rm ren}$ is proportional to the change of the spontaneous decay rate[5]. In fact we have

$$\Delta\Gamma_i = -\frac{2}{\hbar}\mathrm{Im}\left(\Delta W_i^{\rm ren}\right). \tag{2.60}$$

The η-prescription would have arisen naturally if the time-dependent perturbation theory had been employed together with the adiabatic switching of the interaction.

The convergence of the expression (2.58) forms a delicate question and requires some attention. The most convenient way to deal with it is to use techniques of complex analysis and change the contour of the k_z-integration so that the resulting integrand contains the damping exponential $e^{-2k_z z_0}$. We reserve this way of extracting the finite result for the more interesting example of a dispersive dielectric worked out in Chapter 5. Here we will demonstrate yet another way of dealing with the apparently divergent expression (2.58). We start by writing out explicitly the sums over $\lambda = \{\mathrm{TE}, \mathrm{TM}\}$ and $n = \{x, y, z\}$

$$|\mu_n|^2\, R_\lambda e_\lambda^n(\mathbf{k}^+) e_\lambda^n(\mathbf{k}^-) = |\mu_x|^2\left(\frac{k_y^2}{|\mathbf{k}_\parallel|^2} + \frac{k_x^2 k_z^2}{|\mathbf{k}_\parallel|^2|\mathbf{k}|^2}\right) + |\mu_y|^2\left(\frac{k_x^2}{|\mathbf{k}_\parallel|^2} + \frac{k_y^2 k_z^2}{|\mathbf{k}_\parallel|^2|\mathbf{k}|^2}\right) - |\mu_z|^2\frac{|\mathbf{k}_\parallel|^2}{|\mathbf{k}|^2}$$

The coefficients of $|\mu_x|^2$ and $|\mu_y|^2$ are symmetric with respect to the interchange $k_x \leftrightarrow k_y$, therefore they are equal as we can always rename the integration variables. Slightly rewriting the above expression we arrive at

$$\Delta W_i^{\rm ren} = \frac{1}{2(2\pi)^3\epsilon_0}\sum_{j\neq i}\int \mathrm{d}^2\mathbf{k}_\parallel \int_{-\infty}^{\infty}\mathrm{d}k_z \frac{|\mathbf{k}|}{E_{ji}/\hbar c + |\mathbf{k}|} e^{2ik_z z_0} \times\left[\left(|\mu_x|^2 + |\mu_y|^2\right)\left(1 - \frac{k_y^2}{|\mathbf{k}|^2}\right) - |\mu_z|^2\frac{|\mathbf{k}_\parallel|^2}{|\mathbf{k}|^2}\right]. \tag{2.61}$$

The convergence of the integrals in (2.61) is still not obvious but, as we shall see, a physically meaningful result will emerge shortly. We carry out a series of changes of variables. First we note that in the k_z-integral only the even cosine contributes and, in fact, it is possible to restrict the integration range to the positive real axis. Next we go to polar coordinates by writing $k_x = |\mathbf{k}_\parallel|\sin\phi$ and $k_y = |\mathbf{k}_\parallel|\cos\phi$, then the ϕ-angle

[5] Spontaneous decay rates can of course be equivalently computed using Fermi's golden rule [18], which in fact seems to be a more intuitive way of approach.

integration is elementary and we arrive at

$$\Delta W_i^{\text{ren}} = \frac{1}{2(2\pi)^2\epsilon_0}\sum_{j\neq i}\int_0^\infty \mathrm{d}|\mathbf{k}_\parallel|\int_{-\infty}^\infty \mathrm{d}k_z \frac{|\mathbf{k}||\mathbf{k}_\parallel|}{E_{ji}/\hbar c + |\mathbf{k}|}\cos(2k_z z_0) \times\left[\left(|\mu_x|^2+|\mu_y|^2\right)\left(1+\frac{k_z^2}{|\mathbf{k}|^2}\right) - 2|\mu_z|^2\frac{|\mathbf{k}_\parallel|^2}{|\mathbf{k}|^2}\right]. \quad (2.62)$$

Introducing polar coordinates once more according to $k_z = k\cos\theta$ and $|\mathbf{k}_\parallel| = k\sin\theta$ we can quite easily perform the θ integral to get

$$\Delta W_i^{\text{ren}} = -\frac{1}{8\pi^2\epsilon_0}\sum_{j\neq i}\int_0^\infty \mathrm{d}k \frac{k^3}{E_{ji}/\hbar c + k}\left[2|\mu_z|^2\left(\frac{\sin(2kz_0)}{4k^3z_0^3} - \frac{\cos(2kz_0)}{2k^2z_0^2}\right) + \left(|\mu_x|^2+|\mu_y|^2\right)\left(\frac{\sin(2kz_0)}{4k^3z_0^3} - \frac{\cos(2kz_0)}{2k^2z_0^2} - \frac{\sin(2kz_0)}{kz}\right)\right]. \quad (2.63)$$

The convergence of the expression (2.63) is made apparent by an algebraical trick. Note that the following holds

$$\int_0^\infty \mathrm{d}k \frac{k^3}{E_{ji}/\hbar c + k}\left(\frac{\sin(2kz_0)}{2k^3z_0^3} - \frac{\cos(kz_0)}{2k^2z_0^2}\right) = -\frac{1}{2}\left(\frac{1}{z_0^3} + \frac{\partial}{\partial z_0}\frac{1}{z_0^2}\right)\int_0^\infty \mathrm{d}t \frac{\sin t}{2z_0E_{ji}/\hbar c + t} \quad (2.64)$$

where the last t-integral is a well-known special function [21, 5.2.12] commonly denoted $f(2z_0E_{ji}/\hbar c)$. We see that the trick is to represent the powers of k as derivatives with respect to the position of the atom. This procedure yields a nice and compact expression for the energy shift, which is susceptible for asymptotic analysis. Applying the outlined procedure to the expression (2.63) gives us the final result

$$\Delta W_i^{\text{ren}} = -\frac{1}{32\pi^2\epsilon_0}\sum_{j\neq i}\left[\left(|\mu_x|^2+|\mu_y|^2\right)\left(\frac{1}{z_0^3} + \frac{\partial}{\partial z_0}\frac{1}{z_0^2} + \frac{\partial^2}{\partial z_0^2}\frac{1}{z_0}\right) f\left(\frac{2z_0E_{ji}}{\hbar c}\right) - 2|\mu_z|^2\left(\frac{1}{z_0^3} + \frac{\partial}{\partial z_0}\frac{1}{z_0^2}\right) f\left(\frac{2z_0E_{ji}}{\hbar c}\right)\right]. \quad (2.65)$$

We now pause to discuss the meaning of the dimensionless quantity that has naturally appeared in the final result. To do so we rewrite it as

$$\zeta = \frac{2z_0E_{ji}}{\hbar c} = \frac{2z_0}{c}\omega_{ji} \propto \frac{\tau_\gamma}{\tau_a}. \quad (2.66)$$

Here $\tau_\gamma = 2z_0/c$ is the typical time needed by the virtual photon to make a round trip between the atom and the mirror, which are a distance z_0 apart. $\tau_a = \omega_{ji}^{-1}$ is proportional

to the typical time-scale at which the atomic state $|i\rangle$ evolves in, if the strongest dipole transition from state $|j\rangle$ goes to state $|i\rangle$. Therefore, the quantity ζ turns out to be a good indicator of whether the interaction between an atom and the mirror is retarded or not. In the case when $\zeta << 1$ the physical situation is as follows: the time needed by the photon to make a round trip between the mirror and the atom is much smaller than the typical time-scale over which the atomic state evolves. In other words, the atom has no chance to substantially evolve while the virtual photons with the mirror are exchanged. Then, the interaction is said to be non-retarded and in fact can be approximated by electrostatics where the speed of light is assumed to be infinite. In the opposite case, when $\zeta >> 1$, the interaction is said to be retarded as then the atom has changed significantly by the time the photon returns after it has been reflected by the mirror. Thus it seems natural to investigate the properties of (2.65) in these limiting cases. To do so one needs to work out the asymptotic behaviour of the special function $f(\zeta)$. This is straightforward when working with an alternative integral representation [21, 5.2.12]

$$f(\zeta) = \int_0^\infty \mathrm{d}t \frac{e^{-\zeta t}}{t^2+1} \approx \begin{cases} \displaystyle\int_0^\infty \frac{\mathrm{d}t}{t^2+1} = \frac{\pi}{2} & (\zeta << 1) \\ \\ \displaystyle\int_0^\infty \mathrm{d}t\; e^{-\zeta t} = \frac{1}{\zeta} & (\zeta >> 1) \end{cases} . \tag{2.67}$$

In the non-retarded limit, $\zeta << 1$, the exponential is approximated by unity whereas in the retarded limit we have used the fact that if $\zeta >> 1$, then the contribution to the integral comes essentially from the neighbourhood of $t = 0^+$. In this case the rational function in the integrand is well approximated by the first term of its Taylor series. The procedure outlined here is an example of a more general method of doing asymptotic analysis known as Watson's lemma [22]. With the result (2.67) it is a matter of simple differentiation to show that, in the limiting cases described above, the energy shift of the atomic *ground state* induced by the perfect mirror at a distance z_0 away is given by

$$\Delta W_g^{\mathrm{ren}} = -\frac{1}{64\pi\epsilon_0 z_0^3}\left(\langle\mu_x^2\rangle + \langle\mu_y^2\rangle + 2\langle\mu_z^2\rangle\right), \qquad (\zeta << 1), \tag{2.68}$$

$$\Delta W_g^{\mathrm{ren}} = -\frac{1}{16\pi^2\epsilon_0 z_0^4}\sum_{j\neq i}\frac{|\mu_x|^2 + |\mu_y|^2 + |\mu_z|^2}{E_{ji}}, \quad (\zeta >> 1), \tag{2.69}$$

with $\langle\mu_m^2\rangle \equiv \sum_{j\neq i}|\mu_m|^2 = \sum_{j\neq i}|\langle i|\mu_m|j\rangle|^2 = \langle i|\mu_m^2|i\rangle$. Equations (2.68) and (2.69) are

well-known results. The non-retarded limit of the energy shift (2.68) is seen to be an electrostatic interaction energy of a dipole with its own image, apart from the factor of 1/2 that arises due to the fact that in the process of bringing charges from infinity to form a dipole in the vicinity of a mirror one needs to do work only on the real dipole and not on its image. Quantum mechanics enters only via the expectation value of the atomic electric dipole moment operator $\boldsymbol{\mu}$. Equation (2.69) demonstrates the influence retardation has on the atom-mirror interaction and was first computed by Casimir and Polder in their remarkable paper [13] that ends with a following remark:

The very simple form of Eq. (2.69)[6] *(...) suggest that it might be possible to derive these expressions, perhaps apart from the numerical factors, by more elementary considerations. This would be desirable since it would also give a more physical background to our result, a result which in our opinion is rather remarkable. So far we have not been able to find such a simple argument.*

It is worth pointing out that Casimir & Polder arrived at equation (2.69) using the minimal ($\mathbf{p}\cdot\mathbf{A}$) rather than the multipolar ($\boldsymbol{\mu}\cdot\mathbf{E}$) coupling. This route seems to be more laborious and physically less transparent. The understanding of the physics of atoms interacting with the electromagnetic vacuum has progressed enormously since Casimir and Polder's milestone paper, for recent review see [23]. Their theoretical prediction awaited experimental confirmation for 45 years [24] but today there is a very little doubt about the physical interpretation of the Casimir-Polder effect. It can be seen one of the direct confirmations of the existence of the quantum vacuum of the electromagnetic field. The enormous progress in cooling and trapping of atoms (and more recently also of molecules) has meant that experimentalists now have unprecedented control over them, which includes the ability to trap or guide them in very close vicinity of material surfaces. Moreover, there is now a worldwide trend to miniaturize devices for trapping, guiding, and manipulating cold atoms and molecules by constructing so-called atom chips. In experiments using such microfabricated integrated devices atoms and molecules are now routinely very close to materials, so that e.g. the Casimir-Polder force is no longer a small and hard-to-measure effect but may be a dominant force. Precise knowledge of the Casimir-Polder force and related effects of the interaction of atoms, molecules, and other quantum systems with macroscopic objects

[6] Here we refer to the result, which is totally equivalent to that obtained by Casimir and Polder in their milestone paper.

in their vicinity is therefore essential for these developments. Knowing the significance of the Casimir-Polder and Casimir effect in the contemporary science it is interesting to note that it has been discovered as a by-product of the industrial research of colloidal systems. In 1983 H. B. G. Casimir himself seemed to not realize the impact his discovery will have and referred to it as '...of some theoretical significance' [25].

Considerations reported by Casimir and Polder are quite general and, in fact, the formula (2.65) contains some more physical information that can be extracted, namely the energy shift of the excited states and the change of the spontaneous decay rates. Bearing in mind the discussion after Eq. (2.58) we see that in order to compute the shift of the excited states and the change of the spontaneous decay rates we need to make sense of the function $f(2z_0E_{ji}/\hbar c)$ for $E_{ji} < 0$. As explained before this is done by adding a small imaginary part to the energy-difference denominator that arises in the second-order perturbation theory. In the language of formula (2.65) this translates to

$$\bar{f}\left(\frac{2z_0E_{ji}}{\hbar c}\right) = \int_0^\infty \mathrm{d}t \frac{\sin t}{2z_0E_{ji}/\hbar c + t + i\eta} = \int_0^\infty \mathrm{d}t \frac{\sin t}{t - 2z_0|E_{ji}|/\hbar c + i\eta}.$$

Using Eq. (2.59) we rewrite the above as

$$\int_0^\infty \mathrm{d}t \frac{\sin t}{t - 2z_0|E_{ji}|/\hbar c + i\eta} = \mathcal{P}\int_0^\infty \mathrm{d}t \frac{\sin t}{t - 2z_0|E_{ji}|/\hbar c} - i\pi \sin\left(\frac{2z_0|E_{ji}|}{\hbar c}\right). \tag{2.70}$$

By virtue of formula (2.60) and the fact that the Cauchy principal-value integral is necessarily real, we immediately obtain the expression for the change of the spontaneous decay rate

$$\Delta\Gamma_i = -\frac{1}{2\pi c^3\epsilon_0}\sum_{j<i}|\omega_{ji}|^3\left[|\mu_\parallel|^2\left(\frac{\sin|\zeta|}{|\zeta|^3} - \frac{\cos|\zeta|}{|\zeta|^2} - \frac{\sin|\zeta|}{|\zeta|}\right)\right.$$
$$\left. +2|\mu_z|^2\left(\frac{\sin|\zeta|}{|\zeta|^3} - \frac{\cos|\zeta|}{|\zeta|^2}\right)\right]. \tag{2.71}$$

where we have defined $|\mu_x|^2 + |\mu_y|^2 = |\mu_\parallel|^2$. Note that the sum over the atomic states is restricted to only those states for which $E_{ji} < 0$. This is an exact result, valid in any range of the parameter $|\zeta| = 2z_0|E_{ji}|/\hbar c$. It has been derived many times before, see e.g. [20], and describes the position-dependent corrections to the standard Einstein's A-coefficient due to the presence of a perfectly reflecting plane.

The calculation of the energy-level shifts for excited states is slightly more involved for one needs to evaluate

$$\mathcal{P}\int_0^\infty \mathrm{d}t \frac{\sin t}{t-|\zeta|} = \mathrm{Im}\left(\mathcal{P}\int_0^\infty \mathrm{d}t \frac{e^{it}}{t-|\zeta|}\right). \tag{2.72}$$

This can be done with the standard techniques of complex analysis. The Cauchy principal-value integral can be rewritten as follows

$$\mathcal{P}\int = \lim_{\epsilon\to 0}\left(\int_{C_1+C_\epsilon} - \int_{C_\epsilon}\right) \tag{2.73}$$

where the contour C_1 consists of the interval $t \in [0, |\zeta|-\epsilon] \cap [|\zeta|+\epsilon, \infty]$ and C_ϵ is a semi-circle of radius ϵ centred at $t = |\zeta|$ running in the negative (clockwise) direction. Since the integrand is analytic in the first quadrant of the complex plane we can rotate the contour of integration in the first integral in (2.73) to run along the imaginary axis. The second term, in the limit of small ϵ, is obtained by using the fractional residue theorem. After taking the imaginary part we get

$$\mathcal{P}\int_0^\infty \mathrm{d}t \frac{\sin t}{t-|\zeta|} = -|\zeta|\int_0^\infty \mathrm{d}s \frac{e^{-s}}{s^2+\zeta^2} + \pi\cos|\zeta| = -f(|\zeta|) + \pi\cos|\zeta| \tag{2.74}$$

where we have used the definition of the auxiliary function f, cf. Eq. (2.67). Therefore, the energy shift of the excited state $|i\rangle$ splits into two distinct contributions $\Delta W_i^{\mathrm{ren}} = \Delta W_i^1 + \Delta W_i^2$. The first contribution has exactly the same form as Eq. (2.65) with the exception that one needs to distinguish contributions from the states $|j\rangle$ that lie below the state $|i\rangle$ from those for which the state $|j\rangle$ lies above the state $|i\rangle$ as they differ in sign, cf. the first term of Eq. (2.74),

$$\Delta W_i^1 = -\frac{1}{32\pi^2\epsilon_0}\sum_{j\neq i}\mathrm{sgn}(E_{ji})\left[(|\mu_x|^2+|\mu_y|^2)\left(\frac{1}{z_0^3}+\frac{\partial}{\partial z_0}\frac{1}{z_0^2}+\frac{\partial^2}{\partial z_0^2}\frac{1}{z_0}\right) f\left(\frac{2z_0|E_{ji}|}{\hbar c}\right)\right.$$
$$\left. -2|\mu_z|^2\left(\frac{1}{z_0^3}+\frac{\partial}{\partial z_0}\frac{1}{z_0^2}\right) f\left(\frac{2z_0|E_{ji}|}{\hbar c}\right)\right]. \tag{2.75}$$

The second contribution to the energy shift of the excited state $|i\rangle$ arises due to the additional term (cosine) that emerged in Eq. (2.74). It has a nature similar to Eq. (2.71)

and can be explicitly evaluated by computing the derivatives

$$\Delta W_i^{\text{ren}} = -\frac{1}{4\pi c^3 \epsilon_0} \sum_{j<i} |\omega_{ji}|^3 \left[|\mu_{\parallel}|^2 \left(\frac{\cos|\zeta|}{|\zeta|^3} + \frac{\sin|\zeta|}{|\zeta|^2} - \frac{\cos|\zeta|}{|\zeta|} \right) + 2|\mu_z|^2 \left(\frac{\cos|\zeta|}{|\zeta|^3} + \frac{\sin|\zeta|}{|\zeta|^2} \right) \right]. \quad (2.76)$$

with $|\zeta| = 2z_0|Eji|/\hbar c$. These *exact* results are well-known in the literature, see e.g. [26][27][28]. It is worth noting that in the non-retarded limit $|\zeta| << 1$ the total shift $\Delta W_i^{\text{ren}} = \Delta W_i^1 + \Delta W_i^2$ still displays ground-state-like behaviour, Eq. (2.68). The situation is entirely different in the retarded limit when $|\zeta| >> 1$. The contribution ΔW_i^1 still yields Eq. (2.69) but it is dominated by contributions that come from equation (2.76). The energy shift no longer decays like z_0^{-4} but gains an oscillatory contribution for which the leading term behaves as z_0^{-1}.

We have demonstrated how one can use perturbation theory to study the quantum electrodynamics of atoms in the presence of boundaries. Even in the simplest possible example of an atom in the vicinity of a perfectly reflecting mirror the calculations turn out to be quite involved. Nevertheless they lead to unambiguous results that are physically meaningful. The effects described here tend to be tiny unless the atom-mirror distance is very small. What we calculated is a *boundary-dependent correction* to the Lamb shift, which in the case of a hydrogen atom is of the order of 1000 MHz. One needs to be careful and remember that the theory presented is valid only in the cases where there is no overlap between the atomic wavefunction and the wavefunction of the solid. In practice it means that the atom needs to be at least few Bohr radii away from the interface.

2.3 Casimir-Polder shift - how does one measure it?

As remarked earlier, although first derived in 1948, the Casimir-Polder force was unambiguously measured only in 1992-1993. On the other hand, the experimental verification of the oscillatory behaviour of the spontaneous decay rate predicted by Eq. (2.71) happened in 1970 in an experiment carried out by Drexhage [29], cf. Fig. 2.2. In general, there are two approaches to probe the Casimir-Polder potential. One can study directly the energy-level shifts by laser spectroscopy or one can base the experiment on kinematic

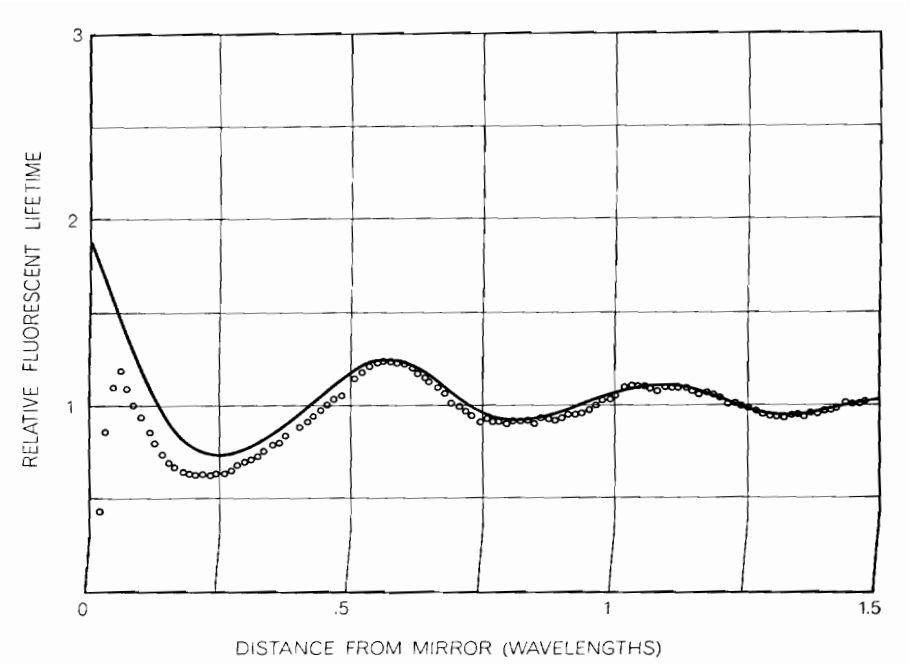

FIGURE 2.2: Picture taken from Sci. Am. **222**, 108(1970). The result reported by Drexhage was first considered suspicious for *'How can the emission of a photon be affected by an atom's environment when the atom can only "see" its environment by emitting a photon in the first place?' [11]*

effects thereby relying on Casimir-Polder forces that arise because of the position dependence of the energy-level shifts. In the early nineties a couple of experiments with sodium atoms [24][30] tested theoretical predictions of the Casimir-Polder effect with high precision. It was an experimental feat at the time and the first quantitative measurement of the interaction between an atom and a surface. In their first experiment [30] Sukenik et. al. effused sodium atoms through an oven slit and directed them through the micron-sized gold-plated cavity. Subsequently, the atoms were exited by a laser just before they left the cavity. Their excitation spectra were then obtained for various widths of the cavity. In this study the range of the atom-wall distances was such that the experiment probed essentially the nonretarded limit of the Casimir-Polder shifts, also known as the van der Waals shifts. An excellent agreement with the theory was observed, cf. Fig 2.3. The next experiment probed the Casimir-Polder potential for ground-state atoms in the retarded

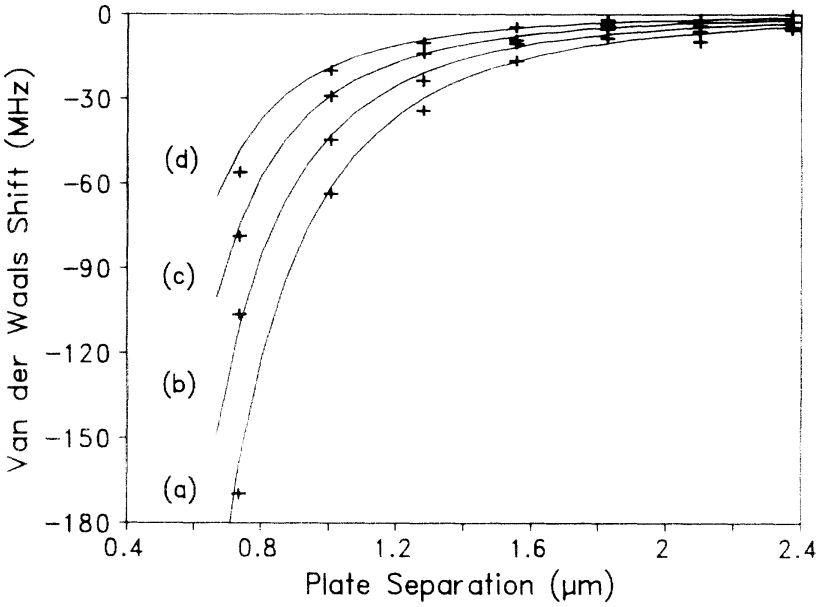

FIG. 4. van der Waals shifts vs plate separation for an atom at cavity center. Series *a*–*d* correspond to states $13S$–$10S$, respectively, with crosses indicating experimental data and lines corresponding to the calculated shifts.

FIGURE 2.3: Picture taken from Phys. Rev. Lett. **68**, 3432(1992).

regime [24]. The experimental set up was similar although the idea behind the measurement was completely different. This time the ground-state sodium atoms that emerged from the oven were passed through the cavity where some of them were deflected so much by the Casimir-Polder force that they were adsorbed by the walls of the cavity. The remaining atoms that managed to get through were ionised by a laser and directed to a channel electron multiplier where they could be detected. The idea behind the experiment was to measure the intensity of the emerging beam I as a function of the cavity width L. The results of this experiment were the first to unambiguously confirm the distance-dependence of the Casimir-Polder force in the retarded limit. In Fig. 2.4 we reproduce the results of this milestone paper where the plots of the quantity called opacity is presented. Opacity is defined as the inverse of the intensity of the emerging beam normalized to the intensity at the width of $6\mu m$.

The measurement of the Casimir-Polder force in the intermediate range of the atom-wall distances remained elusive until very recently. The breakthrough happened thanks

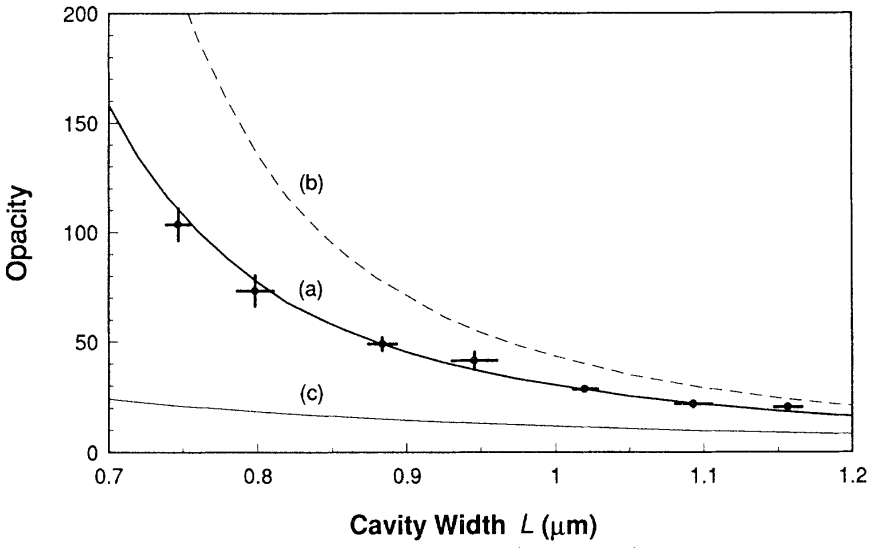

FIGURE 2.4: Picture taken from Phys. Rev. Lett. **70**, 560(1993). The different curves correspond to different theoretical results authors used to determine the opacity of the cavity: a) Casimir-Polder interaction, our Eq.(2.69), b) van der Waals interaction (non-retarded limit), our Eq. (2.68), c) no atom-wall interaction. The agreement of the theory and experiment is apparent.

to achievements in the field of cold-atom physics and development of evanescent-wave mirrors. Quantum reflection is a process in which a particle that is moving through a classically allowed region is reflected without reaching a classical turning point [31]. The idea that the atom could be reflected by the atom-wall interaction has been around since 1936 [32] however, in order to observe such an effect (hence probe the Casimir-Polder potential using the quantum reflection), the kinetic energy of atoms must be comparable with the atom-wall interaction energy. Therefore, ultra-cold atoms are required in order to succeed with this type of the experiment.

Recently a group of experimental physicists at the University of Tübingen, Germany, managed to carry out an experiment using the evanescent-wave mirror and quantum reflection that probed the Casimir-Polder potential in the transition region i.e. in between the retarded long-distance and nonretarded short-distance limits [33]. The idea behind the experiment was as follows. First, one creates a potential barrier close to the surface. This is achieved by superimposing the attractive Casimir-Polder potential of the solid with the repulsive potential generated by a laser beam which is incident from the inside the solid at such an angle that it is totally internally reflected. The maximum height H of the barrier

and its position Z can be adjusted by adjusting the laser's power. Remarkably, only H and Z need to be known in order to determine the Casimir-Polder potential at the point Z. But the properties of the barrier can be determined by studying the quantum reflection of cold atoms from it. This is done by trapping a cloud of ultra-cold Rubidium atoms close to the surface. Then, by suddenly shifting the minimum of the trapping potential the atoms can be moved towards the potential barrier with known velocity. The moving atoms undergo quantum reflection at the barrier, which allows the reflectivity of the barrier to be measured as a function of the atoms' incident velocity. This in turn allows the potential height H to be determined. By varying the laser power the position of the maximum height of the barrier Z with respect to the surface of the solid can be changed thereby allowing to probe the Casimir-Polder potential at these points. The result of the experiment is presented in Fig. 2.5

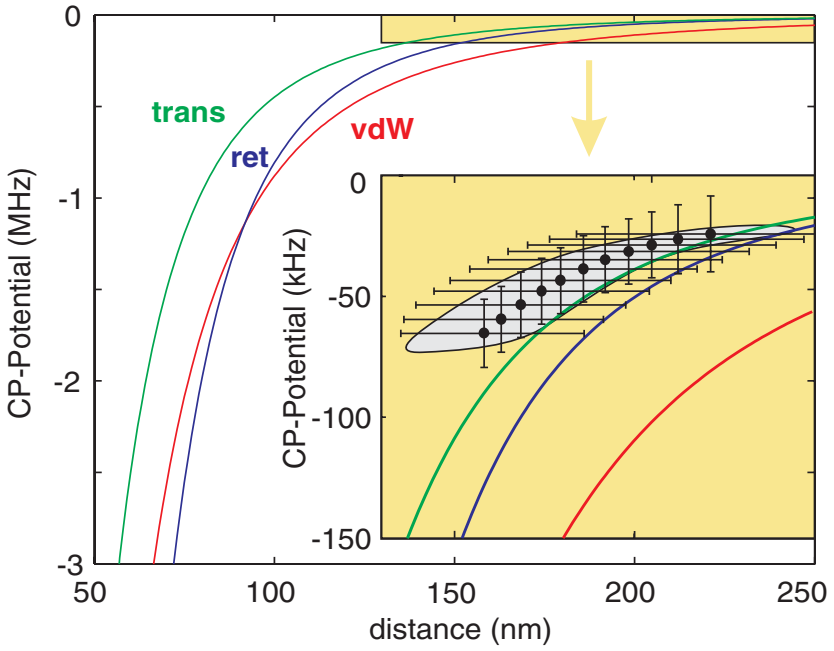

FIGURE 2.5: Picture taken from Phys. Rev. Lett. **104**, 083201 (2010). The different curves correspond to different theoretical results authors used to determine the atom-wall potential: (blue) Casimir-Polder limit, (red) van der Waals limit, (green) general formula. The agreement of the theory and experiment was observed but is disputable, especially for the high power output of the laser used in the evanescent-wave mirror. For details see [33].

Chapter 3

Retarded Casimir-Polder force on an atom near reflecting microstructures

3.1 Introduction

The explosive rate of developments in nanotechnology as well as in the manipulation of cold atoms has meant that interest in atom-surface interactions has increased strongly in recent years. What were once tiny, elusive effects are now dominant interactions, or, as the case may be, a major nuisance in some experimental set-ups. Motivated by a common type of microstructure, which consists of a protruding ledge fabricated by successive etching and possibly a thin electroplated top layer, we have recently studied the force on a neutral atom in close proximity of reflecting surfaces of either cylindrical geometry or that of a semi-infinite half-plane [3]. In the absence of free charges or thermal excitations, the interaction of the atom with the microstructure is dominated by Casimir-Polder forces [13], which are due to the interaction of the atomic dipole with polarization fluctuations excited by vacuum fluctuations of the electromagnetic field. If the atom is sufficiently close to the surface of the microstructure, then the interaction between the atomic dipole and the surface is purely electrostatic and retardation can be neglected, which was the case investigated in Ref. [3]. Then one does not need to quantize the electromagnetic field, but

can work with the classical Green's function of Poisson's equation. The only difficulty lies then in the geometry of the problem.

However, in experimental situations one more often finds that retardation is in fact important, as the distance of the atom from the surface of the microstructure is often commensurate or larger than the wavelength of a typical atomic transition. This is the case we investigate here, again for microstructures of two types of geometries: a cylindrical reflector of radius R and infinite length, and a reflecting half-plane.

Various versions of this problem have been studied before, both analytically and numerically. Probably the first to consider the interaction between an atom and a metallic wire, according to [34], was almost 75 years ago Zel'dovich [35]. This problem was then revisited and extended by Nabutovskii et al. [36], and subsequently by Marvin et al. [37]. In Nabutovskii's paper a dielectric cylinder is envisaged to be surrounded by a cylindrical shell of vacuum which in turn is surrounded by a rarefied gas of polarizable particles. The interaction energy of a single particle is then calculated through the work done by the force (obtained from the stress tensor) due to the fluctuating electromagnetic fields, in the limit of zero density of the surrounding gas. The asymptotic results obtained there (Eq. (23) and Eq. (24) of Ref. [36]) are, according to Ref. [34], valid only for dilute dielectric materials; they diverge in the perfect-reflector limit.

On the other hand, the work by Marvin et al.[37], motivated by [38, 39] and based on a normal-mode expansion and a linear-response formalism [40], gives the same general formula for the interaction between a point particle and a cylinder [their Eq. (4.10)] as the equivalent result in [36]. We have no reason to believe that the result in [37] is incorrect in the perfect-conductor limit, as it reduces to our previous result [3] in the electrostatic limit. Moreover, Ref. [37] manages to recover the original Casimir-Polder result [13] in the large-radius limit of the cylinder. This suggests that the general expression in [36] is probably correct, only that the perfect-conductor limit does not commute with the asymptotic limit of the zero radius (or large distance of the atom from the cylinder) studied there. In the small-radius limit, the result for the interaction between an atom and a metallic filament, in both retarded and non-retarded limits, is also given by [34].

Marvin et al.'s work [37] is certainly the most comprehensive, but due to its generality it is also quite cumbersome to apply, which is mainly done numerically for just a few examples

[41]. Further numerical studies of the interaction of atoms with macroscopic cylinders can be found in Refs. [42, 43, 44, 45].

By contrast, in this Chapter we are after a relatively simple theory that allows one to estimate the force between an atom and a cylindrical reflector at any distance and cylinder radius. To this end we are not interested in the precise dependence of the interaction on material constants of the reflector, and therefore we work with the model of a perfectly reflecting surface.

As discussed in Ref. [3], we also determine the force between an atom and a semi-infinite half-plane, in order to facilitate estimates for common types of microstructures that consist of a ledge protruding from a substrate. The Casimir-Polder interaction between an atom and such a half-plane has also been studied before, but only in the extreme retarded limit of very large distances of the atom from the surface [46]. To the best of our knowledge no formula for the interaction in the intermediate region, when the distance of the atom from the surface is comparable to the typical wavelength of an internal transition in the atom, has been derived yet. Recent work of Mendes et al. [47], dealing with wedges, does not include the general result in the half-plane geometry as a limiting case of a zero-angle wedge.

3.2 Field quantization and the energy shift

The complete system of an atom interacting with the quantized electromagnetic field is described by the Hamiltonian

$$H = H_{\rm Atom} + H_{\rm Field} + H_{\rm Int} \ . \tag{3.1}$$

We choose to work with $\boldsymbol{\mu} \cdot \mathbf{E}$ coupling, i.e. our interaction Hamiltonian is

$$H_{\rm Int} = -\boldsymbol{\mu} \cdot \mathbf{E} \ . \tag{3.2}$$

Quantization of the electromagnetic field is done by way of a normal-mode expansion of the vector potential in terms of photon annihilation and creation operators for each mode

λ and polarization σ,

$$\mathbf{A}(\mathbf{r},t) = \sum_{\lambda,\sigma} \frac{1}{\sqrt{2\varepsilon_0\omega_\lambda}} \left[a_\lambda^{(\sigma)} \mathbf{F}_\lambda^{(\sigma)}(\mathbf{r})\, e^{-\mathrm{i}\omega t} + \mathrm{h.c.} \right]. \tag{3.3}$$

To describe a mode we use the composite index λ instead of a wave vector, as we shall be working in cylindrical coordinates where the quantum number of the azimuthal part of the mode function is discrete, but the other two are continuous. We work in Coulomb gauge, $\boldsymbol{\nabla}\cdot\mathbf{A}(\mathbf{r}) = 0$, so that the normal modes $\mathbf{F}(\mathbf{r})$ satisfy the Helmholtz equation,

$$(\boldsymbol{\nabla}^2 + \omega^2)\,\mathbf{F}(\mathbf{r}) = 0\,. \tag{3.4}$$

The energy level shift due to the interaction (3.2) can be calculated perturbatively. For our system in state $|i;0\rangle$, i.e. the atom in state $|i\rangle$ and the electromagnetic field in its vacuum state $|0\rangle$, the lowest non-vanishing order of perturbation theory is the second, so that

$$\Delta W = \sum_{j\neq i} \frac{\left| \left\langle j; 1_\lambda^{(\sigma)} \right| -\boldsymbol{\mu}\cdot\mathbf{E} \left| i;0 \right\rangle \right|^2}{E_i - (E_j + \omega_\lambda)}\,. \tag{3.5}$$

As the relevant field modes can be expected to vary slowly over the size of the atom, we make the electric dipole approximation, which simplifies the expression for the energy shift to

$$\Delta W = -\sum_{\lambda,\sigma,j\neq i} \frac{\omega_\lambda}{2\varepsilon_0} \frac{\left| \langle j|\boldsymbol{\mu}|i\rangle \cdot \mathbf{F}_\lambda^{(\sigma)*}(\mathbf{r}) \right|^2}{E_{ji} + \omega_\lambda}\,, \tag{3.6}$$

where we have introduced the abbreviation $E_{ji} \equiv E_j - E_i$. The sum over intermediate states j in Eq. (3.6) is in practice limited to one or a few states to which there are strong dipole transitions from the initial state i. These strong dipole transitions dominate the internal dynamics of the atom, and the corresponding timescales are then given by $1/E_{ji}$, the inverse frequency of these dominant dipole transitions. Therefore, when we analyse the distance dependence of the energy shift, we shall use $1/E_{ji}$ for these transitions as the scale to which to compare the distance of the atom from the surface. We shall refer to E_{ji} as the frequency of a typical atomic transition.

Alternatively one can use the atomic polarizability, whose diagonal elements are

$$\alpha_{\nu\nu}(\omega) = \sum_j \frac{2E_{ji}\,|\langle j|\mu_\nu|i\rangle|^2}{E_{ji}^2 - \omega^2}\ , \tag{3.7}$$

and express the energy shift as an integral over the polarizability and the electric field susceptibility at imaginary frequencies [48]. In this formalism one can see most easily that the energy shift at large distances (in the so-called retarded limit) must always depend just on the static polarizability

$$\alpha_{\nu\nu}(0) = \sum_j \frac{2\,|\langle j|\mu_\nu|i\rangle|^2}{E_{ji}}\ . \tag{3.8}$$

For brevity and presentational clarity we shall henceforth abbreviate the matrix elements of the atomic dipole moment as

$$|\boldsymbol{\mu}| \equiv |\langle j\,|\boldsymbol{\mu}|\,i\rangle|\ . \tag{3.9}$$

3.3 Energy shift near a perfectly reflecting wire

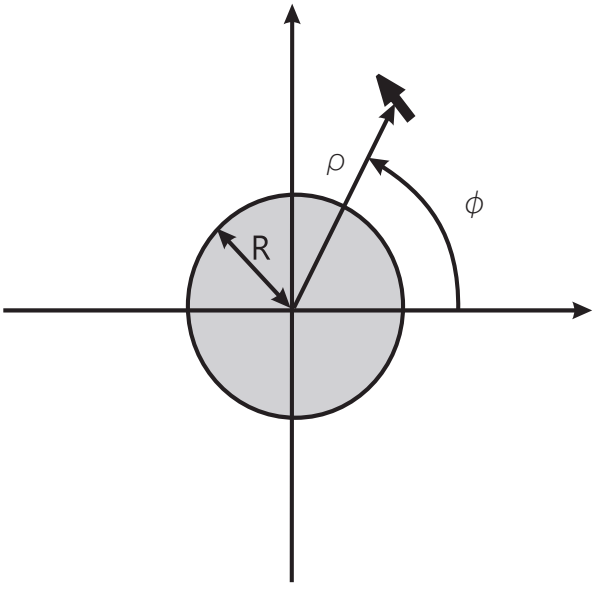

FIGURE 3.1: Atomic electric dipole moment in the vicinity of a perfectly reflecting cylinder of radius R. The normal modes $\mathbf{F}_\lambda^{(\sigma)}(\mathbf{x})$ in this geometry are given by Eqs. (3.15) and (3.16).

First we wish to calculate the energy shift of an atom near a perfectly reflecting and infinitely long cylindrical wire of radius R. It is advantageous to work in cylindrical coordinates, cf. Fig. 3.1.

In order to find two independent transverse vector field solutions of Eq. (3.4), we make use of the representation theorem for the vector Helmholtz equation [49, 10.411]. If $\Phi(\mathbf{x})$ is a solution of the scalar Helmholtz equation then the two independent solutions of the vector equation are given by

$$\mathbf{F}^{(1)}(\mathbf{r}) = (\nabla \times \hat{\mathbf{e}}_z)\,\Phi(\mathbf{r})\,, \tag{3.10}$$

$$\mathbf{F}^{(2)}(\mathbf{r}) = \frac{1}{\omega}\nabla \times (\nabla \times \hat{\mathbf{e}}_z)\,\Phi(\mathbf{r})\,. \tag{3.11}$$

The particular choice of the constant unit vector $\hat{\mathbf{e}}_z$ is motivated by the symmetry of our problem and lets us to identify the solutions $\mathbf{F}^{(1)}(\mathbf{r})$ and $\mathbf{F}^{(2)}(\mathbf{r})$ with the transverse electric (TE) and transverse magnetic (TM) modes, respectively. In cylindrical coordinates the scalar Helmholtz equation has solutions of the form

$$\Phi(\rho,\phi,z) = N\,[\,\cos\delta_m J_m(k\rho) + \sin\delta_m Y_m(k\rho)\,]\,e^{\mathrm{i}m\phi+\mathrm{i}\kappa z} \tag{3.12}$$

where $J_m(k\rho)$ and $Y_m(k\rho)$ are Bessel functions of the first and second kind [21, §9]. The separation constants satisfy $\omega^2 = k^2+\kappa^2$, and m is an integer. The phase shifts δ_m describe the superposition of regular and irregular solutions. In free space only regular solutions $J_m(k\rho)$ are admissible, and $\delta_m = 0$. In the presence of the perfectly reflecting wire, the phase shifts serve to make the electromagnetic fields satisfy the boundary conditions on the surface of the wire. The normalization constant N is chosen such that

$$\int \mathrm{d}^3\mathbf{r}\;\mathbf{F}^{(\sigma)*}_{\lambda'}(\mathbf{r})\cdot\mathbf{F}^{(\sigma)}_{\lambda}(\mathbf{r}) = \delta_{mm'}\delta(\kappa-\kappa')\frac{\delta(k-k')}{\sqrt{kk'}} \tag{3.13}$$

is met. Setting $\cos\delta_m = 1$, $\sin\delta_m = 0$, one can derive quite easily that $N = (2\pi k)^{-1}$.

On the surface of a perfect conductor, the tangential components of the electric field and the normal component of the magnetic field vanish. Therefore, at the surface $\rho = R$ of the cylindrical wire we must have $E_\phi = 0 = E_z$ and $B_\rho = 0$. These boundary conditions

determine the phase shifts as

$$\tan\delta_m^{\mathrm{TE}} = -\frac{J'_m(kR)}{Y'_m(kR)},\ \tan\delta_m^{\mathrm{TM}} = -\frac{J_m(kR)}{Y_m(kR)}\ . \tag{3.14}$$

According to Eqs. (3.10), (3.11), and (3.12), the normalized mode functions $\mathbf{F}_\lambda^{(\sigma)}(\mathbf{r})$, $\lambda = \{k, m, \kappa\}$, that satisfy the boundary conditions at $\rho = R$ are given by

$$\begin{aligned}\mathbf{F}_\lambda^{\mathrm{TE}}(\rho,\phi,z) = \frac{1}{2\pi}\Bigg[&\frac{\mathrm{i}m}{k\rho}\frac{J_m(k\rho)Y'_m(kR) - Y_m(k\rho)J'_m(kR)}{\sqrt{J'^2_m(kR)+Y'^2_m(kR)}}\,\hat{\mathbf{e}}_\rho \\ &- \frac{J'_m(k\rho)Y'_m(kR) - Y'_m(k\rho)J'_m(kR)}{\sqrt{J'^2_m(kR)+Y'^2_m(kR)}}\,\hat{\mathbf{e}}_\phi\Bigg]\, e^{\mathrm{i}m\phi+\mathrm{i}\kappa z},\end{aligned} \tag{3.15}$$

$$\begin{aligned}\mathbf{F}_\lambda^{\mathrm{TM}}(\rho,\phi,z) = \frac{1}{2\pi}\Bigg[&\frac{i\kappa}{\omega}\frac{J'_m(k\rho)Y_m(kR) - Y'_m(k\rho)J_m(kR)}{\sqrt{J^2_m(kR)+Y^2_m(kR)}}\,\hat{\mathbf{e}}_\rho \\ &- \frac{m\kappa}{\omega k\rho}\frac{J_m(k\rho)Y_m(kR) - Y_m(k\rho)J_m(kR)}{\sqrt{J^2_m(kR)+Y^2_m(kR)}}\,\hat{\mathbf{e}}_\phi \\ &+ \frac{k}{\omega}\frac{J_m(k\rho)Y_m(kR) - Y_m(k\rho)J_m(kR)}{\sqrt{J^2_m(kR)+Y^2_m(kR}}\,\hat{\mathbf{e}}_z\Bigg]\, e^{\mathrm{i}m\phi+\mathrm{i}\kappa z}.\end{aligned} \tag{3.16}$$

These mode functions can now be substituted into Eq. (3.6) for obtaining the energy shift of an atom positioned at $\mathbf{r} = (\rho, \phi, z)$. However, what we want to calculate here is only the correction to the energy shift caused by the presence of a perfectly conducting surface, rather than the whole energy shift due to the coupling of the atom to the fluctuating vacuum field, which would include the free-space Lamb shift. Therefore we need to subtract the energy shift caused by the vacuum fluctuations of the electromagnetic field in free space, which is obtained by either letting the phase shifts $\delta_m \to 0$ or equivalently taking the limit $R \to 0$. In the limit of vanishing radius R of the cylinder the behaviour of the mode functions (3.15), (3.16) is dominated by the singular behaviour of $Y_m(kR)$ and $Y'_m(kR)$ at the origin, which causes the phase shifts (3.14) to vanish. The renormalized energy shift $\Delta W^{\mathrm{ren}} = \Delta W - \lim_{R\to 0}\Delta W$ is found to be of the form

$$\Delta W^{\mathrm{ren}} = -\frac{1}{4\pi\varepsilon_0}\sum_{j\neq i}\left(\Xi_\rho|\mu_\rho|^2 + \Xi_\phi|\mu_\phi|^2 + \Xi_z|\mu_z|^2\right) \tag{3.17}$$

with

$$\Xi_\rho = \frac{2}{\pi}{\sum_{m=0}^{\infty}}' \int_0^\infty \mathrm{d}k\; k \int_0^\infty \mathrm{d}\kappa\; \frac{\omega}{E_{ji}+\omega} \times \left\{ \left(\frac{m}{k\rho}\right)^2 \left[\frac{\big(J_m(k\rho)Y'_m(kR) - Y_m(k\rho)J'_m(kR)\big)^2}{J'^2_m(kR)+Y'^2_m(kR)} - J^2_m(k\rho) \right] + \left(\frac{\kappa}{\omega}\right)^2 \left[\frac{\big(J'_m(k\rho)Y_m(kR) - Y'_m(k\rho)J_m(kR)\big)^2}{J^2_m(kR)+Y^2_m(kR)} - J'^2_m(k\rho) \right] \right\}, \tag{3.18}$$

$$\Xi_\phi = \frac{2}{\pi}{\sum_{m=0}^{\infty}}' \int_0^\infty \mathrm{d}k\; k \int_0^\infty \mathrm{d}\kappa\; \frac{\omega}{E_{ji}+\omega} \times \left\{ \left[\frac{\big(J'_m(k\rho)Y'_m(kR) - Y'_m(k\rho)J'_m(kR)\big)^2}{J'^2_m(kR)+Y'^2_m(kR)} - J'^2_m(k\rho) \right] + \left(\frac{m}{k\rho}\frac{\kappa}{\omega}\right)^2 \left[\frac{\big(J_m(k\rho)Y_m(kR) - Y_m(k\rho)J_m(kR)\big)^2}{J^2_m(kR)+Y^2_m(kR)} - J^2_m(k\rho) \right] \right\}, \tag{3.19}$$

$$\Xi_z = \frac{2}{\pi}{\sum_{m=0}^{\infty}}' \int_0^\infty \mathrm{d}k\; k \int_0^\infty \mathrm{d}\kappa\; \frac{\omega}{E_{ji}+\omega} \times \left\{ \left(\frac{k}{\omega}\right)^2 \left[\frac{\big(J_m(k\rho)Y_m(kR) - Y_m(k\rho)J_m(kR)\big)^2}{J^2_m(kR)+Y^2_m(kR)} - J^2_m(k\rho) \right] \right\} \tag{3.20}$$

where the primes on the sums indicate that the $m = 0$ term is weighted by an additional factor of $1/2$. It appears that the κ integrals fail to converge, but this is a common feature in such calculations caused by the dipole approximation, see e.g. [13]. As we shall see, convergence is in fact brought about by the Bessel functions, which come to bear if the k integral is replaced by an integral over $\omega = \sqrt{\kappa^2 + k^2}$.

As the Bessel functions $J_m(x)$ and $Y_m(x)$ are both oscillatory for large x, we wish to rotate the integration contour in the complex k plane, in order to get an integrand that is exponentially damped for large arguments. To this end we introduce the Hankel functions $H^{(1)}_m(x) = J_m(x) + iY_m(x)$ and $H^{(2)}_m(x) = [H^{(1)}_m(x)]^* = J_m(x) - iY_m(x)$, in terms of which we can rewrite the energy level shift in such a form that there are no poles in the first quadrant of the complex k plane, as is required for the rotation of the integration contour.

This step greatly simplifies further analysis.

$$\Xi_\rho = -\mathrm{Re}\,\frac{2}{\pi}\sum_{m=0}^{\infty}{}'\int_0^\infty \mathrm{d}k\,k\int_0^\infty \mathrm{d}\kappa\,\frac{\omega}{E_{ji}+\omega} \times\left\{\frac{\kappa^2}{\omega^2}[H_m'^{(1)}(k\rho)]^2\frac{J_m(kR)}{H_m^{(1)}(kR)}+\frac{m^2}{k^2\rho^2}[H_m^{(1)}(k\rho)]^2\frac{J_m'(kR)}{H_m'^{(1)}(kR)}\right\}, \quad (3.21)$$

$$\Xi_\phi = -\mathrm{Re}\,\frac{2}{\pi}\sum_{m=0}^{\infty}{}'\int_0^\infty \mathrm{d}k\,k\int_0^\infty \mathrm{d}\kappa\,\frac{\omega}{E_{ji}+\omega} \times\left\{[H_m'^{(1)}(k\rho)]^2\frac{J_m'(kR)}{H_m'^{(1)}(kR)}+\frac{m^2}{k^2\rho^2}\frac{\kappa^2}{\omega^2}[H_m^{(1)}(k\rho)]^2\frac{J_m(kR)}{H_m^{(1)}(kR)}\right\}, \quad (3.22)$$

$$\Xi_z = -\mathrm{Re}\,\frac{2}{\pi}\sum_{m=0}^{\infty}{}'\int_0^\infty \mathrm{d}k\,k\int_0^\infty \mathrm{d}\kappa\,\frac{\omega}{E_{ji}+\omega}\left\{\frac{k^2}{\omega^2}[H_m^{(1)}(k\rho)]^2\frac{J_m(kR)}{H_m^{(1)}(kR)}\right\}. \quad (3.23)$$

We now transform the k integration in Eqs. (3.21)–(3.23) into an integration over $\omega = \sqrt{\kappa^2+k^2}$, and note that on the interval $0 \le \omega \le \kappa$ the integrands become pure imaginary and therefore do not contribute if added to the real part of the integral. We can therefore shift the lower limit down to the origin

$$\int_\kappa^\infty \mathrm{d}\omega \longrightarrow \int_0^\infty \mathrm{d}\omega \quad (3.24)$$

without affecting the result. Further, we note that the functions $H_m^{(1)}(z)$ and $H_m'^{(1)}(z)$ have no zeros in the first quadrant of the complex plane [21, Fig. 9.6], so that the contour of the ω-integration can be rotated from the positive real to the positive imaginary axis, $\omega \to \mathrm{i}\omega$. Then the oscillatory Bessel functions turn into the modified Bessel functions according to [21, 9.6.3 & 5]

$$J_m(\mathrm{i}z) = e^{\mathrm{i}m\pi/2}I_m(z), \quad (3.25)$$

$$H_m^{(1)}(\mathrm{i}z) = -\frac{2\mathrm{i}}{\pi}e^{-\mathrm{i}m\pi/2}K_m(z)\,. \quad (3.26)$$

Taking the real part and going to polar coordinates, where the angle integrals are elementary, we find that

$$\Xi_\rho = \frac{2}{\pi}{\sum_{m=0}^{\infty}}' \int_0^\infty \mathrm{d}k\; k \left\{ \left(\sqrt{E_{ji}^2 + k^2} - E_{ji} \right) \frac{I_m(kR)}{K_m(kR)} [K_m'(k\rho)]^2 \right. \\ \left. + \frac{m^2}{k^2\rho^2} \left(\frac{E_{ji}^2}{\sqrt{E_{ji}^2 + k^2}} - E_{ji} \right) \frac{I_m'(kR)}{K_m'(kR)} [K_m(k\rho)]^2 \right\}, \tag{3.27}$$

$$\Xi_\phi = \frac{2}{\pi}{\sum_{m=0}^{\infty}}' \int_0^\infty \mathrm{d}k\; k \left\{ \left(\frac{E_{ji}^2}{\sqrt{E_{ji}^2 + k^2}} - E_{ji} \right) \frac{I_m'(kR)}{K_m'(kR)} [K_m'(k\rho)]^2 \right. \\ \left. + \frac{m^2}{k^2\rho^2} \left(\sqrt{E_{ji}^2 + k^2} - E_{ji} \right) \frac{I_m(kR)}{K_m(kR)} [K_m(k\rho)]^2 \right\}, \tag{3.28}$$

$$\Xi_z = \frac{2}{\pi}{\sum_{m=0}^{\infty}}' \int_0^\infty \mathrm{d}k\; k \left\{ \frac{k^2}{\sqrt{E_{ji}^2 + k^2}} \frac{I_m(kR)}{K_m(kR)} [K_m(k\rho)]^2 \right\}. \tag{3.29}$$

Note that the effect of our manipulations has been that the integration variable k in Eqs. (3.27)–(3.29) has been rotated by $\pi/2$ in the complex plane compared to Eqs. (3.21)–(3.23).

The final result for the energy shift, Eq. (3.17) with Eqs. (3.27)–(3.29), is a sum over a series of rapidly converging integrals, which, unlike Eqs. (3.18)–(3.20), is reasonably easily evaluated numerically. However, as the functions $\Xi_{\rho,\phi,z}(E_{ji}, d, R)$ are quite cumbersome and it is not possible to find exact closed form expressions for them, we now look at their asymptotics in various limiting cases, which is very useful for analytical estimates.

3.3.1 Asymptotic regimes

There are three length scales in the problem: the distance of the atom from the surface of the cylinder $d = \rho - R$, the radius of the cylindrical wire R, and the wavelength of a typical transition in the atom $\lambda_{ji} \propto 1/E_{ji}$. Accordingly we get six different asymptotic regimes, three non-retarded and three retarded. The criterion as to whether retardation matters is the relative size of the distance d of the atom from the surface and the wavelength λ_{ji} of a typical transition: if the atom is very close to the surface then its interaction with the

surface is entirely electrostatic [3], whereas retardation begins to play a role once $d \sim \lambda_{ji}$ or larger, because then the internal state of the atom is then subject to non-negligible evolution during the time a virtual photon mediating the interaction would take to travel from the atom to the surface and back. First we shall deal with the three non-retarded cases, and then with the three retarded ones.

3.3.1.1 $d \ll R \ll \lambda_{ji}$

If λ_{ji} is larger than any other lengthscale, we can take the limit $E_{ji} \to 0$ in Eqs. (3.27)–(3.29). This gives the same result as a purely electrostatic calculation [3]. If the distance d of the atom from the surface is small, then the atom does not feel the curvature of the surface, and one expects to get the same energy shift as one would close to a plane surface. This is indeed the result we get when we take the limit $d \to 0$ by using uniform asymptotic expansions for the Bessel functions [3]; we obtain

$$\Xi_\rho \approx \frac{1}{8d^3} \ , \quad \Xi_\phi \approx \frac{1}{16d^3} \ , \quad \Xi_z \approx \frac{1}{16d^3} \ . \tag{3.30}$$

3.3.1.2 $d \ll \lambda_{ji} \ll R$

In this regime the energy shift behaves in exactly the same way as in the previous case, because the radius of the wire has no influence on retardation, so that the relative size of R and λ_{ji} does not matter. All that matters is that the distance d of the atom from the cylinder is still much less than the wavelength λ_{ji} of the relevant transition in the atom. In mathematical terms, the electrostatic limit ($E_{ji} \to 0$) and the large-radius limit ($R \to \infty$) of the energy shift commute.

The limit of large radius was studied in great detail in [37]. Application of the summation formula derived in Appendix A of [37] to Eqs. (3.27)-(3.29) leads to the original Casimir-Polder result [13] for the interaction between an atom and a plane, perfectly reflecting mirror:

$$\Xi_\rho = \frac{1}{2\pi d^3} \int_0^\infty \mathrm{d}\eta \frac{e^{-2dE_{ji}\eta}}{(1+\eta^2)^2} \ , \tag{3.31}$$

$$\Xi_\phi = \Xi_z = \frac{1}{2\pi d^3} \int_0^\infty \mathrm{d}\eta \frac{e^{-2dE_{ji}\eta}}{(1+\eta^2)^2} \frac{1-\eta^2}{1+\eta^2} \ . \tag{3.32}$$

If we now take λ_{ji} to be much greater than d, we reproduce the result (3.30) of the previous section.

3.3.1.3 $R \ll d \ll \lambda_{ji}$

In this case we again start by taking the limit $E_{ji} \to 0$ in Eqs. (3.27)–(3.29) and obtain the electrostatic expression derived in [3]. In the limit of the radius of the wire being much smaller than the distance d, the energy shift is dominated by summand with lowest m in Eqs. (3.27)–(3.29) [3]. Asymptotically one gets

$$\Xi_\rho \propto \frac{1}{d^3 \ln d}, \quad \Xi_\phi \propto \frac{R^2}{d^5}, \quad \Xi_z \propto \frac{1}{d^3 \ln d} ,$$

which is not very helpful numerically though, as logarithmic series converge only very slowly.

3.3.1.4 $\lambda_{ji} \ll d \ll R$

When λ_{ji} is smaller than the distance d of the atom to the surface of the wire, then the interaction is manifestly retarded. As λ_{ji} is the smallest of the three lengthscales, we first take the limit $\lambda_{ji} \to 0$, i.e. $E_{ji} \to \infty$, in Eqs. (3.27)–(3.29) and find that the leading terms in all three integrals go as $1/E_{ji}$. Thus the energy shift (3.17) indeed depends only on the static polarizability (3.8) of the atom, as mentioned at the end of Section 3.2. The remaining integration over k is then quite similar to those found in the non-relativistic calculation in [3] and can be tackled by the same means. Scaling k to $x = k\rho/m$ and realizing that the dominant contributions to the integrals and sums come from large x and large m, one can approximate the Bessel Functions by their uniform asymptotic expansions and then gets a geometric series, which is easy to sum. In this way one finds the following

approximations

$$\Xi_\rho \approx \frac{1}{2\pi E_{ji}\rho^4}\left\{\rho^4\int_0^\infty \mathrm{d}k\, k^3 \frac{I_0(kR)}{K_0(kR)}[K_1(k\rho)]^2 + \int_0^\infty \mathrm{d}x\, x\left(\sqrt{1+x^2}+\frac{1}{\sqrt{1+x^2}}\right)\frac{A(A^2+4A+1)}{(A-1)^4}\right\}, \tag{3.33}$$

$$\Xi_\phi \approx \frac{1}{2\pi E_{ji}\rho^4}\left\{\rho^4\int_0^\infty \mathrm{d}k\, k^3 \frac{I_1(kR)}{K_1(kR)}[K_1(k\rho)]^2 + \int_0^\infty \mathrm{d}x\, x\left(\sqrt{1+x^2}+\frac{1}{\sqrt{1+x^2}}\right)\frac{A(A^2+4A+1)}{(A-1)^4}\right\}, \tag{3.34}$$

$$\Xi_z \approx \frac{1}{\pi E_{ji}\rho^4}\left\{\rho^4\int_0^\infty \mathrm{d}k\, k^3 \frac{I_0(kR)}{K_0(kR)}[K_0(k\rho)]^2 + \int_0^\infty \mathrm{d}x\, \frac{x^3}{\sqrt{1+x^2}}\frac{A(A^2+4A+1)}{(A-1)^4}\right\}, \tag{3.35}$$

with $A(x)$ given by

$$A(x) = \left(\frac{R}{\rho}\right)^2\left(\frac{1+\sqrt{1+x^2}}{1+\sqrt{1+x^2\frac{R^2}{\rho^2}}}\right)^2 \exp\left[2\left(\sqrt{1+x^2\frac{R^2}{\rho^2}}-\sqrt{1+x^2}\right)\right]. \tag{3.36}$$

These are easy to evaluate numerically and provide a reasonable approximation to the energy shift in the retarded limit, as shown in Fig. 3.2.

In the limit of the distance $d = \rho - R$ being much smaller than the radius R of the wire, the above approximations yield

$$\Xi_\rho \approx \Xi_\phi \approx \Xi_z \approx \frac{1}{4\pi d^4}\frac{1}{E_{ji}}, \tag{3.37}$$

which agrees with the retarded energy shift of an atom in front of a perfectly reflecting plane mirror, as calculated by Casimir and Polder [13]. This is what one would expect because an atom that is very close to the surface is not susceptible to the curvature of the surface.

3.3.1.5 $\lambda_{ji} \ll R \ll d$

In this case we again start by taking the limit $E_{ji} \to \infty$ in Eqs. (3.27)–(3.29), which gives a leading order contribution proportional to $1/E_{ji}$. In other words, this is again a fully retarded case for which the static polarizability (3.8) is only atomic property that the

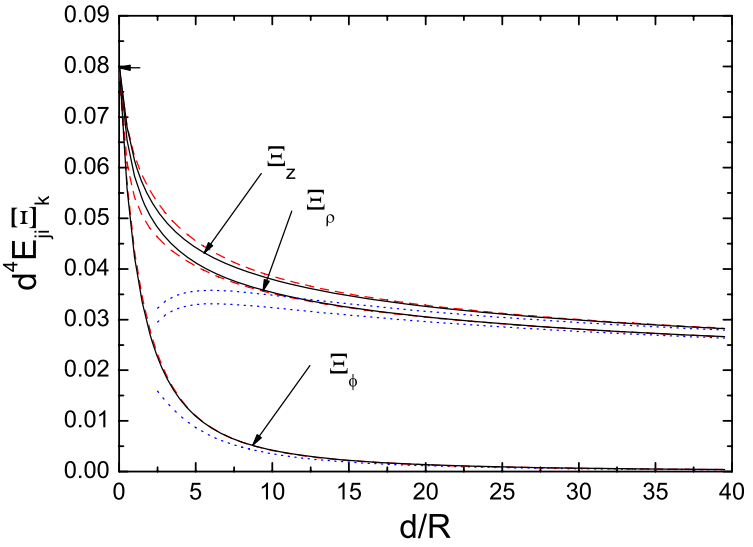

FIGURE 3.2: The contributions to the energy shift in the retarded limit due to the three components of the atomic dipole, multiplied by $E_{ji}d^4$. Solid lines represent the results of exact numerical integration of Eqs. (3.27)–(3.29) in the limit $E_{ji} \to \infty$, whereas the dashed (red) lines represent the approximations (3.33)–(3.35). For large d the asymptotic behaviour is dominated by the lowest m terms in the sums, given by (3.38)–(3.40) and shown as dotted (blue) lines. The arrow on the vertical axis indicates the exact value in the limit $d \to 0$, Eq. (3.37).

energy shift depends on. For distances d much larger than the wire radius R the dominant contribution to the sum then comes from the summands with the lowest m, so that we need consider only those,

$$\Xi_\rho \approx \frac{1}{2\pi E_{ji}} \left\{ \int_0^\infty \mathrm{d}k\, k^3 \frac{I_0(kR)}{K_0(kR)} [K_1(k\rho)]^2 - 2 \int_0^\infty \mathrm{d}k\, \frac{k}{\rho^2} \frac{I_1'(kR)}{K_1'(kR)} [K_1(k\rho)]^2 \right\}, \tag{3.38}$$

$$\Xi_\phi \approx \frac{1}{2\pi E_{ji}} \left\{ \int_0^\infty \mathrm{d}k\, k \left(k^2 + \frac{2}{\rho^2} \right) \frac{I_1(kR)}{K_1(kR)} [K_1(k\rho)]^2 - 2 \int_0^\infty \mathrm{d}k\, k^3 \frac{I_1'(kR)}{K_1'(kR)} [K_1'(k\rho)]^2 \right\}, \tag{3.39}$$

$$\Xi_z \approx \frac{1}{\pi E_{ji}} \int_0^\infty \mathrm{d}k\, k^3 \frac{I_0(kR)}{K_0(kR)} [K_0(k\rho)]^2 \,. \tag{3.40}$$

The dotted lines in Fig. 3.2 show that these are indeed good approximations for large d/R. Their leading-order behaviour is

$$\Xi_\rho \propto \frac{1}{E_{ji}} \frac{1}{d^4 \ln d}, \quad \Xi_\phi \propto \frac{1}{E_{ji}} \frac{R^2}{d^6}, \quad \Xi_z \propto \frac{1}{E_{ji}} \frac{1}{d^4 \ln d} \,,$$

which is in full agreement with the asymptotic results by [34], even though those are for a metallic wire characterized by a plasma frequency. This is because in the retarded limit the interaction between the atom and the surface depends, to leading order, only on the static polarizability.

As in the electrostatic case, the contributions due to the ρ and z components of the atomic dipole fall off less rapidly than the ϕ contribution. We also note that, just as in the non-retarded case, the series in powers of $1/\ln d$ converge too slowly to be of any practical use, so that estimates must be made with Eqs. (3.38)–(3.40).

3.3.1.6 $R \ll \lambda_{ji} \ll d$

As in the non-retarded cases, the limit of vanishing radius ($R \to 0$) and the retarded limit ($E_{ji} \to \infty$) commute, and we recover the results of the previous section, Eqs. (3.38)–(3.40). This is another manifestation of the fact that the criterion of whether the interaction is retarded depends solely on the distance d between an atom and the surface of the wire, and that the relative size of geometrical features and the wavelength λ_{ji} is irrelevant. This means in particular that there are no resonance effects for λ_{ji} coïnciding with the wire radius R.

3.3.2 Numerical results

For intermediate parameter ranges one has to evaluate Eqs. (3.27)–(3.29) numerically. This is straightforward, and one can employ standard software packages like Mathematica or Maple. The numerical convergence of Eqs. (3.27)–(3.29) is very good, although more terms are needed for small distances d than for large distances. Figs. 3.3–3.5 show the contributions by the ρ, ϕ, and z components of the atomic dipole to the energy shift (3.17) for various values of the typical transition frequency E_{ji} in the atom. We give the distance d and the transition wavelength $1/E_{ji}$ in units of the wire radius R. For plotting we have factored out of $\Xi_{\rho,\phi,z}$ the asymptotic functional dependence of the shift in front of a plane mirror, Eq. (3.37). In Fig. 3.6 we show how these contributions look when we choose the wavelengths $1/E_{ji}$ of a typical internal transition as a lengthscale and plot the

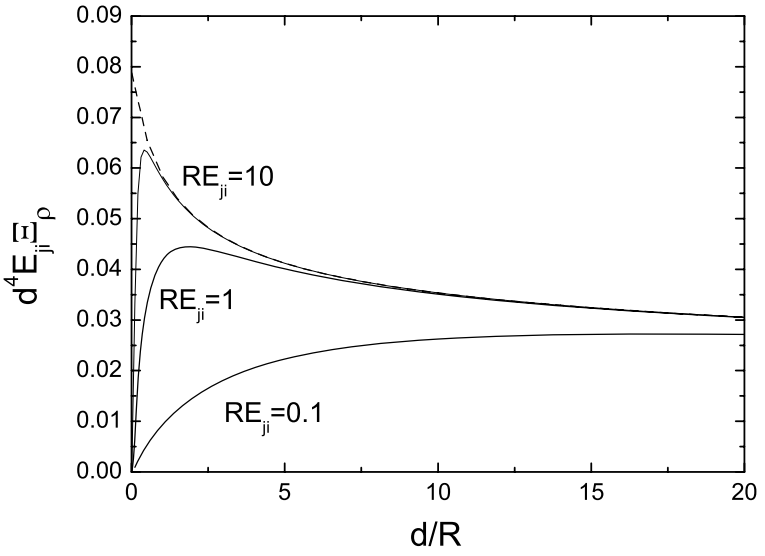

FIGURE 3.3: The contribution (3.27) to the energy shift (3.17) due to the ρ component of the dipole for various typical transition frequencies E_{ji}. The dashed line is this contribution in the retarded limit $E_{ji} \to \infty$.

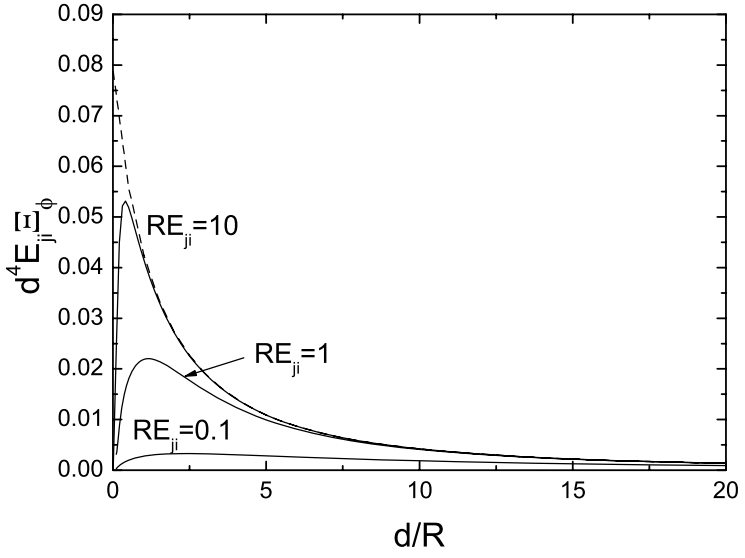

FIGURE 3.4: The contribution (3.28) to the energy shift (3.17) due to the ϕ component of the dipole for various typical transition frequencies E_{ji}. The dashed line is this contribution in the retarded limit $E_{ji} \to \infty$.

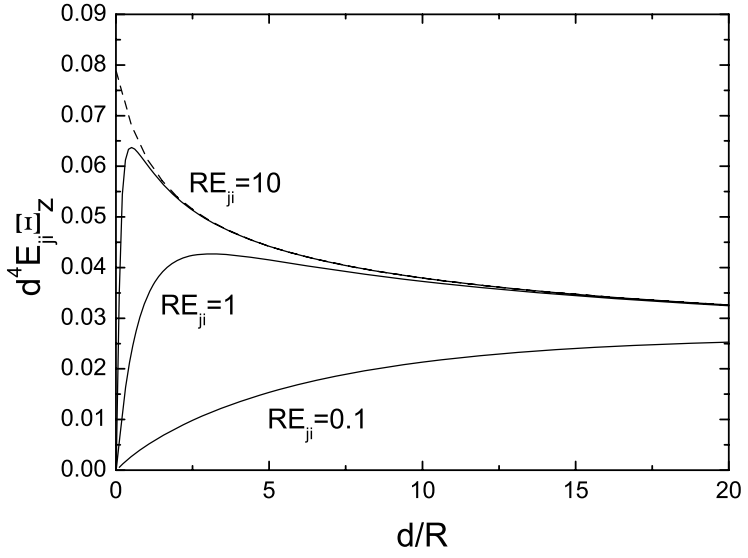

FIGURE 3.5: The contribution (3.29) to the energy shift (3.17) due to the z component of the dipole for various typical transition frequencies E_{ji}. The dashed line is this contribution in the retarded limit $E_{ji} \to \infty$.

contributions to the energy shift for various wire radii R. The larger the value of R the more terms are required in the numerical series.

3.4 Energy shift near a perfectly reflecting semi-infinite half-plane

Next we wish to calculate the energy shift of an atom in the vicinity of a perfectly reflecting half-plane, as illustrated by Fig. 3.7.

The procedure of obtaining the normal modes of the vector potential is analogous to that described in Section 3.3. The scalar solution of the Helmholtz equation (3.4) in the cylindrical coordinates that is best suited to applying boundary conditions on the surface of the half-plane is given by

$$\Phi(\mathbf{x}) = \left[\frac{\alpha}{\sqrt{\pi}}\sin\left(\frac{m}{2}\phi\right) + \frac{\beta}{\sqrt{\pi}}\cos\left(\frac{m}{2}\phi\right)\right] J_{m/2}(k\rho)\,\frac{e^{\mathrm{i}\kappa z}}{\sqrt{2\pi}}\,,$$

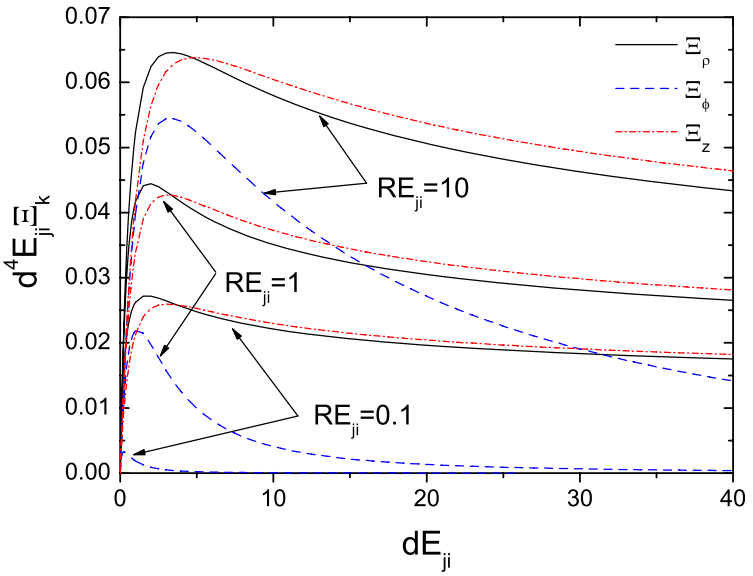

FIGURE 3.6: The contributions (3.27)–(3.29) to the energy shift (3.17) due to the ρ, ϕ, and z components of the dipole for various radii R of the wire.

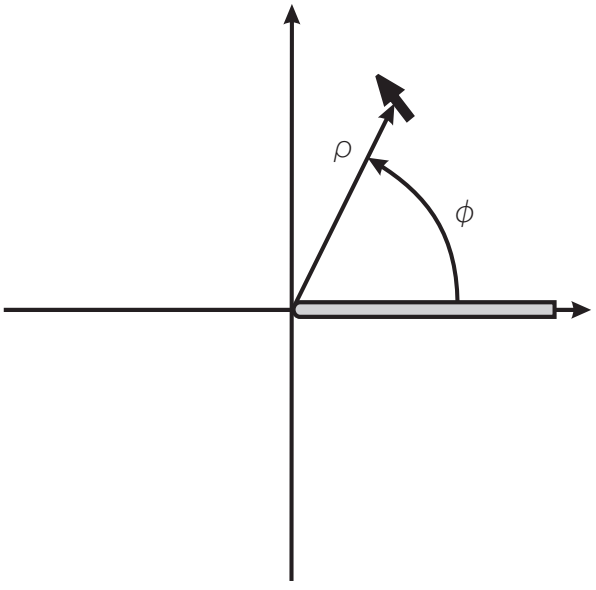

FIGURE 3.7: An atomic dipole in the vicinity of a perfectly reflecting semi-infinite half-plane. The normal modes $\mathbf{F}_\lambda^{(\sigma)}(\mathbf{x})$ in this geometry are given by Eqs. (3.41) and (3.42).

where $J_{m/2}(k\rho)$, with $m = 0, 1, 2, \ldots$, are the regular solutions of Bessel's equation, and the separation constants satisfy $\omega^2 = k^2 + \kappa^2$. We must have $m \geq 0$, as otherwise the solutions are not linearly independent. Note that half-integer indices arise because the angle ϕ is restricted to the interval $[0, 2\pi]$, so that the usual argument of single-valuedness of $e^{im\phi}$ cannot be evoked.

In order to obtain two linearly independent vector solutions we again apply Eqs. (3.10) and (3.11), and impose the boundary conditions for a perfectly reflecting half-plane, $E_\rho = 0 = E_z$ and $B_\phi = 0$ for $\phi = 0$ and $\phi = 2\pi$. In this way we find for the mode functions

$$\mathbf{F}^{(1)}_\lambda(\mathbf{r}) = -\frac{1}{\sqrt{2}\pi}\left[\frac{m}{2k\rho}\sin\left(\frac{m}{2}\phi\right) J_{m/2}(k\rho)\,\hat{\mathbf{e}}_\rho + \cos\left(\frac{m}{2}\phi\right) J'_{m/2}(k\rho)\,\hat{\mathbf{e}}_\phi\right] e^{i\kappa z}, \tag{3.41}$$

$$\begin{aligned}\mathbf{F}^{(2)}_\lambda(\mathbf{r}) = \frac{1}{\sqrt{2}\pi}\Bigg[&\frac{i\kappa}{\omega}\sin\left(\frac{m}{2}\phi\right) J'_{m/2}(k\rho)\,\hat{\mathbf{e}}_\rho + \frac{i\kappa m}{2k\rho\omega}\cos\left(\frac{m}{2}\phi\right) J_{m/2}(k\rho)\,\hat{\mathbf{e}}_\phi \\ &+ \frac{k}{\omega}\sin\left(\frac{m}{2}\phi\right) J_{m/2}(k\rho)\,\hat{\mathbf{e}}_z\Bigg] e^{i\kappa z},\end{aligned} \tag{3.42}$$

where the composite index stands for $\lambda = \{k, m, \kappa\}$. For $m > 0$ these mode functions satisfy the normalization condition (3.13), but the first polarization has an additional mode with $m = 0$ for which Eq. (3.41) must be multiplied by an additional factor $1/\sqrt{2}$ for it to be normalized correctly according to (3.13),

$$\mathbf{F}^{(1)}_{m=0}(\mathbf{r}) = -\frac{1}{2\pi} J'_0(k\rho)\,\hat{\mathbf{e}}_\phi\, e^{i\kappa z}\,. \tag{3.43}$$

Substituting the mode functions (3.41)-(3.43) into Eq. (3.6) and renormalizing the energy shift by subtracting the free-space contribution in the same way as this was done in

Eqs. (3.18)-(3.20), we obtain an energy shift of the form (3.17) with

$$\Xi_\rho = \frac{2}{\pi}\int_0^\infty \mathrm{d}k\, k \int_0^\infty \mathrm{d}\kappa\, \frac{\omega}{E_{ji}+\omega}\left\{\left(\frac{\kappa}{\omega}\right)^2 {\sum_{m=0}^{\infty}}' \left[\sin^2\left(\frac{m}{2}\phi\right) J'^2_{m/2}(k\rho) - J'^2_m(k\rho)\right]\right.$$
$$\left. + \left(\frac{1}{k\rho}\right)^2 \sum_{m=1}^{\infty}\left[\left(\frac{m}{2}\right)^2 \sin^2\left(\frac{m}{2}\phi\right) J^2_{m/2}(k\rho) - m^2 J^2_m(k\rho)\right]\right\}, \tag{3.44}$$

$$\Xi_\phi = \frac{2}{\pi}\int_0^\infty \mathrm{d}k\, k \int_0^\infty \mathrm{d}\kappa\, \frac{\omega}{E_{ji}+\omega}\left\{{\sum_{m=0}^{\infty}}' \left[\cos^2\left(\frac{m}{2}\phi\right) J'^2_{m/2}(k\rho) - J'^2_m(k\rho)\right]\right.$$
$$\left. + \left(\frac{\kappa}{k\rho\omega}\right)^2 \sum_{m=1}^{\infty}\left[\left(\frac{m}{2}\right)^2 \cos^2\left(\frac{m}{2}\phi\right) J^2_{m/2}(k\rho) - m^2 J^2_m(k\rho)\right]\right\}, \tag{3.45}$$

$$\Xi_z = \frac{2}{\pi}\int_0^\infty \mathrm{d}k\, k \int_0^\infty \mathrm{d}\kappa\, \frac{\omega}{E_{ji}+\omega}\left\{\left(\frac{k}{\omega}\right)^2 {\sum_{m=0}^{\infty}}' \left[\sin^2\left(\frac{m}{2}\phi\right) J^2_{m/2}(k\rho) - J^2_m(k\rho)\right]\right\}, \tag{3.46}$$

where the primes on the sums indicate that the $m = 0$ terms are weighted by an additional factor of $1/2$. In order to simplify these expressions, the sums over the Bessel functions need to be evaluated. Recently, similar summations have been carried out [47, 50], but the results obtained do not include our particular case of sums involving Bessel functions of the half-integer order.

We proceed along the following lines. First, we split each sum into two, one over Bessel functions of integer orders, and the other over half-integer orders. For the first we can apply the standard summation formula [21, 9.1.79]

$${\sum_{m=0}^{\infty}}' \cos 2m\phi\, J^2_m(z) = \frac{1}{2} J_0(2z\sin\phi)\,, \tag{3.47}$$

and we choose to represent the right-hand side in terms of an integral [21, 9.1.24]

$$\frac{1}{2} J_0(2z\sin\phi) = \frac{1}{\pi}\int_1^\infty \mathrm{d}t\, \frac{\sin(2zt\sin\phi)}{\sqrt{t^2-1}}\,. \tag{3.48}$$

For the half-integer sum we use a summation formula of [51, 5.7.17.(11.)], which in our case gives

$$\sum_{m=0}^{\infty} \cos(2m+1)\phi\, J^2_{m+\frac{1}{2}}(z) = \frac{1}{\pi}\int_1^{1/\sin\phi} \mathrm{d}t\, \frac{\sin(2zt\sin\phi)}{\sqrt{t^2-1}}\,. \tag{3.49}$$

We note that, if we use the integral representation (3.48), the sums over integer and over

half-integer Bessel functions are very similar; the only difference is the upper limit of the t integral in (3.48) and (3.49). As these t integrals and their derivatives will arise repeatedly, we define the following auxiliary functions:

$$F(z,\phi) \equiv \int_1^{1/\sin\phi} \mathrm{d}t \, \frac{\sin(2zt\sin\phi)}{\sqrt{t^2-1}} \,, \tag{3.50}$$

$$G(z,\phi) \equiv \int_1^{\infty} \mathrm{d}t \, \frac{\sin(2zt\sin\phi)}{\sqrt{t^2-1}} \,. \tag{3.51}$$

Further we note that the κ integrals in Eqs. (3.44)-(3.46) suffer from the same convergence problems as already discussed in Section 3.3. We avoid these by introducing polar coordinates with $k = \omega\sin\alpha$ and $\kappa = \omega\cos\alpha$. At the same time we parametrize the denominator arising from perturbation theory by

$$\frac{1}{E_{ji}+\omega} = \int_0^{\infty} \mathrm{d}x \; e^{-(E_{ji}+\omega)x} \,, \tag{3.52}$$

with $E_{ji}+\omega = E_{ji}+\sqrt{k^2+\kappa^2} \geq 0$. Then Eqs. (3.44)-(3.46) become

$$\begin{aligned} \Xi_\rho \;=\; & \frac{2}{\pi}\int_0^{\infty}\mathrm{d}x \; e^{-E_{ji}x}\int_0^{\infty}\mathrm{d}\omega \; \omega^3 e^{-\omega x}\int_0^{\pi/2}\mathrm{d}\alpha\sin\alpha \\ & \times\left\{\sigma_1(\omega\rho\sin\alpha)+\sigma_3(\omega\rho\sin\alpha)\cos^2\alpha\right\}, \end{aligned} \tag{3.53}$$

$$\begin{aligned} \Xi_\phi \;=\; & \frac{2}{\pi}\int_0^{\infty}\mathrm{d}x \; e^{-E_{ji}x}\int_0^{\infty}\mathrm{d}\omega \; \omega^3 e^{-\omega x}\int_0^{\pi/2}\mathrm{d}\alpha\sin\alpha \\ & \times\left\{\sigma_2(\omega\rho\sin\alpha)\cos^2\alpha+\sigma_4(\omega\rho\sin\alpha)\right\}, \end{aligned} \tag{3.54}$$

$$\begin{aligned} \Xi_z \;=\; & \frac{2}{\pi}\int_0^{\infty}\mathrm{d}x \; e^{-E_{ji}x}\int_0^{\infty}\mathrm{d}\omega \; \omega^3 e^{-\omega x}\int_0^{\pi/2}\mathrm{d}\alpha\sin\alpha \\ & \times\left\{\sigma_5(\omega\rho\sin\alpha)\sin^2\alpha\right\}. \end{aligned} \tag{3.55}$$

The sums $\sigma_i(z)$ appearing in these expressions can be calculated by using Eqs. (3.47)–(3.51) and standard derivative formulae for Bessel functions [21, 9.1.27]; we obtain in

terms of (3.50) and (3.51):

$$\begin{aligned}
\begin{bmatrix} \sigma_1(z) \\ \sigma_2(z) \end{bmatrix} &= \frac{1}{z^2}\sum_{m=1}^{\infty}\left\{\left(\frac{m}{2}\right)^2\begin{bmatrix} \sin^2(m\phi/2) \\ \cos^2(m\phi/2) \end{bmatrix} J_{m/2}^2(z) - m^2 J_m^2(z)\right\} \qquad (3.56)\\
&= \frac{1}{8\pi z^2}\left[\pm\frac{\partial^2 G(z,\phi)}{\partial\phi^2} + \frac{\partial^2 G(z,\phi)}{\partial\phi^2}\bigg|_{\phi=0} \pm \frac{\partial^2 F(z,\phi)}{\partial\phi^2} - \frac{\partial^2 F(z,\phi)}{\partial\phi^2}\bigg|_{\phi=0}\right],\\
\begin{bmatrix} \sigma_3(z) \\ \sigma_4(z) \end{bmatrix} &= {\sum_{m=0}^{\infty}}'\left\{\begin{bmatrix} \sin^2(m\phi/2) \\ \cos^2(m\phi/2) \end{bmatrix} J_{m/2}'^2(z) - J_m'^2(z)\right\}\\
&= -\begin{bmatrix} \sigma_1(z) \\ \sigma_2(z) \end{bmatrix} + \frac{1}{2\pi}\big[F(z,0) - G(z,0)\big] \mp \frac{\cos 2\phi}{2\pi}\big[F(z,\phi) + G(z,\phi)\big]\\
&\quad + \frac{\cos 2z}{2\pi z}(1 \mp \cos\phi)\,, \qquad (3.57)
\end{aligned}$$

$$\begin{aligned}
\sigma_5(z) &= {\sum_{m=0}^{\infty}}'\left\{\sin^2(m\phi/2)\, J_{m/2}^2(z) - J_m^2(z)\right\}\\
&= \frac{1}{2\pi}\big[F(z,0) - F(z,\phi) - G(z,\phi) - G(z,0)\big]\,. \qquad (3.58)
\end{aligned}$$

We now carry out the various integrations in the following order. First we evaluate the α integrals, which all give Bessel functions J_1 or J_0 [49, 3.715(10),(14)]. Next we carry out the integrations over ω, which involve integrals of the type [49, 6.611(1.)]

$$\int_0^\infty \mathrm{d}z\; e^{-az} J_\nu(bz) = \frac{b^{-\nu}\left(\sqrt{a^2+b^2} - a\right)^\nu}{\sqrt{a^2+b^2}}\,.$$

Finally, we calculate the t integrals that came in through the auxiliary functions F and G, Eqs. (3.50) and (3.51). These are all elementary. At the very end we calculate the ϕ derivatives of Eq. (3.56) and take the limit $\phi \to 0$ in the appropriate terms. The end results then still contain the parameter integral (3.52) over x, which we now scale by substituting $x = 2\rho\eta$. Then the final results read

$$\begin{aligned}
\Xi_\rho &= \frac{1}{16\pi\rho^3}\int_0^\infty \mathrm{d}\eta\; e^{-2\rho E_{ji}\eta}\left\{\frac{3\eta^4+6\eta^2+4}{\eta^4(1+\eta^2)^{3/2}} - \frac{4}{\eta^4}\right.\\
&\quad + \frac{4}{(\eta^2+\sin^2\phi)^3}\left[(2\eta^2+1)\sin^2\phi - \eta^2\right] + \frac{\cos\phi}{(1+\eta^2)^{3/2}(\eta^2+\sin^2\phi)^3}\\
&\quad \times \left.\left[(2+\eta^2)\sin^4\phi + 2\sin^2\phi(3\eta^4+6\eta^2+2) - \eta^2(3\eta^4+6\eta^2+4)\right]\right\}, \qquad (3.59)
\end{aligned}$$

$$\begin{aligned}\Xi_\phi &= \frac{1}{16\pi\rho^3}\int_0^\infty \mathrm{d}\eta\, e^{-2\rho E_{ji}\eta}\left\{\frac{3\eta^6+6\eta^4+10\eta^2+4}{\eta^4(1+\eta^2)^{5/2}}-\frac{4}{\eta^4}\right.\\ &+ \frac{4}{(\eta^2+\sin^2\phi)^3}\left[(1-2\eta^2)\sin^2\phi+\eta^2\right]+\frac{\cos\phi}{(1+\eta^2)^{5/2}(\eta^2+\sin^2\phi)^3}\\ &\times \left[(2-2\eta^2-\eta^4)\sin^4\phi+2\sin^2\phi(2+2\eta^2-6\eta^4-3\eta^6)\right.\\ &\left.\left.+\eta^2(3\eta^6+6\eta^4+10\eta^2+4)\right]\right\}, \qquad (3.60)\end{aligned}$$

$$\begin{aligned}\Xi_z &= \frac{1}{16\pi\rho^3}\int_0^\infty \mathrm{d}\eta\, e^{-2\rho E_{ji}\eta}\left\{\frac{9\eta^4+10\eta^2+4}{\eta^4(1+\eta^2)^{5/2}}-\frac{4}{\eta^4}\right.\\ &+ 4\frac{\sin^2\phi-\eta^2}{(\eta^2+\sin^2\phi)^3}-\frac{\cos\phi}{(1+\eta^2)^{5/2}(\eta^2+\sin^2\phi)^3}\\ &\times \left.\left[(\eta^2-2)\sin^4\phi+2(\eta^4-4\eta^2-2)\sin^2\phi+\eta^2(9\eta^4+10\eta^2+4)\right]\right\}. \qquad (3.61)\end{aligned}$$

Inserted into Eq. (3.17) the Eqs. (3.59)–(3.61) give the final result for the energy shift of an atom near a perfectly reflecting half-plane. Some of the integrations over the auxiliary variable η could in principle be carried out, but those would yield complicated hypergeometric functions. Thus it is preferable to have the result in the form of an integral over elementary functions. It converges quickly and can therefore be very easily evaluated numerically by using standard software packages. In addition, we shall go on to determine asymptotic expressions in the non-retarded and retarded regimes.

3.4.1 Asymptotic regimes

3.4.1.1 Plane-mirror limit

In the limit of the polar angle ϕ being very small, the atom is very close to the half-plane but far away from the edge, so that the energy shift should be the same as for an atom in front of a plane, infinitely extended mirror. The component of the atomic dipole that is normal to the surface should then give the contribution listed in Eq. (3.31) to the shift, and the parallel components should contribute that shown in Eq. (3.32). As the distance d of the atom from the half-plane is $\rho\sin\phi$, we take Eqs. (3.59)–(3.61) and scale $\eta\to\eta\sin\phi$, so as to get an exponential with the same argument as in Eqs. (3.31) and (3.32). If we subsequently take the limit $\phi\to 0$, we recover Eqs. (3.31) and (3.32), as expected. Note, however, that the geometry is different from the cylindrical case: the ϕ component of the atomic dipole is now normal to the surface and its contribution Ξ_ϕ to the energy shift is

given by (3.31), and the ρ and z components are parallel so that Ξ_ρ and Ξ_z are given by (3.32).

3.4.1.2 Non-retarded regime

If $\rho E_{ji} \ll 1$ then the atom is very close to the half-plane, compared to the wavelength of a typical internal transition. This means that the interaction of the atom and the surface is instantaneous, as the atom evolves on a much longer timescale. In this case field quantization is not necessary, and only Coulomb interactions between the atom and the half-plane need to be considered, as was done in Ref. [3], where we derived

$$\begin{aligned}
\Xi_\rho &= \frac{5}{48\pi\rho^3} + \frac{\cos\phi}{16\pi\rho^3\sin^2\phi} + \frac{(\pi-\phi)(1+\sin^2\phi)}{16\pi\rho^3\sin^3\phi} \\
\Xi_\phi &= -\frac{1}{48\pi\rho^3} + \frac{\cos\phi}{8\pi\rho^3\sin^2\phi} + \frac{(\pi-\phi)(1+\cos^2\phi)}{16\pi\rho^3\sin^3\phi} \\
\Xi_z &= \frac{1}{24\pi\rho^3} + \frac{\cos\phi}{16\pi\rho^3\sin^2\phi} + \frac{\pi-\phi}{16\pi\rho^3\sin^3\phi}\,.
\end{aligned}$$

Taking the limit $E_{ji} \to 0$ in Eqs. (3.59)–(3.61) we recover these results, which is an important consistency check on our present calculation.

3.4.1.3 Retarded regime

In the opposite limit of the atom being far away from the half-plane, we need to distinguish whether the atom is located beyond the edge of the half-plane or not. If it is, i.e. for $\pi/2 < \phi < \pi$ the distance of the atom to the half-plane is its distance to the edge, namely ρ, so that the condition for the interaction to be fully retarded is $\rho E_{ji} \gg 1$. If, on the other hand, $0 < \phi < \pi/2$ then the distance to the half-plane is $\rho\sin\phi$, and consequently the criterion for full retardation is $\rho\sin\phi E_{ji} \gg 1$, cf. Fig. 3.7.

Taking the limit $E_{ji} \to \infty$ in the integrals (3.59)-(3.61) is straightforward, since, according to Watson's lemma [22], the integral is then dominated by contributions from the vicinity of $\eta = 0^+$, so that one just needs to factor out the exponential and expand the rest of the integrand in the curly brackets in a Taylor series about this point. The leading terms of these Taylor expansions turn out to be constants with respect to η in each case. Thus in

the retarded limit we obtain

$$\Xi_\rho = \frac{1}{64\pi\rho^4 E_{ji}}\left[3+\frac{1}{\sin^4(\phi/2)}+\frac{2}{\sin^2(\phi/2)}\right] \tag{3.62}$$

$$\Xi_\phi = \frac{1}{64\pi\rho^4 E_{ji}}\left[-3+\frac{1}{\sin^4(\phi/2)}+\frac{2}{\sin^2(\phi/2)}\right] \tag{3.63}$$

$$\Xi_z = \frac{1}{64\pi\rho^4 E_{ji}}\left[3+\frac{1}{\sin^4(\phi/2)}+\frac{2}{\sin^2(\phi/2)}\right], \tag{3.64}$$

which, for the case of isotropic polarizability, is in agreement with the result of Ref. [46]. Here again, the energy shift (3.17) depends only on the static polarizability (3.8) of the atom, as follows from general considerations in the retarded limit [48]. In the light of our comments above, we emphasize again that the results (3.62)–(3.64) are only valid when the distance of the atom from the half-plane exceeds several wavelengths λ_{ji}. This means that for small angles ϕ one needs to revert to the plane-mirror limit discussed in Section 3.4.1.1 above, because in the region $0 < \phi < \pi/2$ Eqs. (3.62)–(3.64) apply only if $\sin\phi \gg \lambda_{ji}/\rho$. However, taking the limit $\rho \to \infty$ together with $\phi \to 0$ while keeping $\rho\sin\phi = d$ fixed is legitimate, and reproduces the well-known Casimir-Polder result [13] for the retarded interaction between an atom and a plane mirror, Eq. (3.37).

Taking the limit $\phi \to \pi$ in Eqs. (3.62)–(3.64) shows that for an atomic dipole that is polarized azimuthally the interaction vanishes when the atom is located exactly above the edge of the half-plane. This conclusion actually holds not just in the retarded regime, but generally for any distance, as Eq. (3.60) also vanishes in the limit $\phi \to \pi$. Purely from symmetry one would expect there to be no azimuthal component to the Casimir-Polder force directly above the edge, but the fact that there is no radially directed force either is surprising. Since we have worked in the cylindrical coordinates, the direction of the unit vectors $\hat{\mathbf{e}}_\rho$ and $\hat{\mathbf{e}}_\phi$ depends on the position coordinates ρ and ϕ. In this context it is curious that, in the retarded limit, all three components of the atomic dipole contribute to the energy shift with exactly the same angular dependence.

3.5 Summary

We have calculated the energy shift in a neutral atom caused by the presence at arbitrary distance of perfectly reflecting microstructures of two different geometries. For an atom at

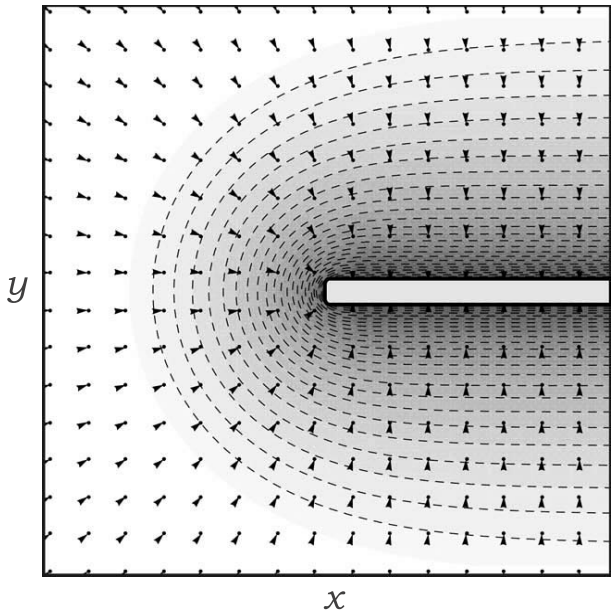

FIGURE 3.8: Direction of the retarded Casimir-Polder force acting on the atom with isotropic polarizability. Note from Eqn. (3.60) that an atom that is polarized azimuthally does not experience any force when it is located exactly above the edge of the half-plane.

a distance $d = \rho - R$ from the perfectly reflecting cylindrical wire of radius R we have found an exact expression for the interaction energy, Eq. (3.17) with Eqs. (3.27)-(3.29). As these integrals and sums are in general quite complicated, we have analysed various important limiting cases. The limit of the distance d being small on the scale of the wavelength λ_{ji} of a typical atomic transition requires only electrostatic forces to be considered, which was done in detail in Ref. [3]. The case of purely retarded interactions, which occur when the distance d is much larger than λ_{ji}, has been analysed in Sections 3.3.1.4–6. For a small wire radius the three contributions to the energy shift are well approximated by Eqs. (3.38)–(3.40), and for a large wire radius by Eqs. (3.33)–(3.35).

In the case of an atom close to a perfectly reflecting half-plane the exact analytic analysis can be pushed a little bit further than in the cylindrical case. We have managed to find an exact formula for the energy shift in terms of a simple, rapidly converging integral over elementary functions, Eqs. (3.59)-(3.61), so that they are very easy to study numerically. Nevertheless, we have also derived asymptotic formulae, which agree with previous calculations.

The totality of our results can be used to reliably estimate the energy shift in an atom

close to a variety of common microstructures that consist of a ledge and possibly an electroplated top layer of higher reflectivity. We have determined the energy shifts for the complete range of distances, which is very important for practical applications as in many modern experiments the distance of the atom is neither much larger nor much smaller than the typical wavelength of an atomic transition, but commensurate.

Chapter 4

On the difference between the standard and generalized Coulomb gauge

4.1 Generalized Coulomb gauge

Although the considerations we report here are quite general we would like to make a point by referring to a specific example. Consider a dielectric half-space occupying the $z < 0$ region of space. The dielectric is a non-dispersive one i.e. it's electromagnetic response is described by a single number, the index of refraction n, that is one and the same for all frequencies. Thus model is described by the dielectric constant

$$\epsilon(z) = 1 + \theta(-z)(n^2 - 1) \tag{4.1}$$

where $\theta(z)$ is a Heaviside the step function. The quantization of the electromagnetic field that coexists with such a dielectric can be achieved by the normal-mode expansion [19].

We start with Maxwell's equations (no sources)

$$\begin{aligned} \boldsymbol{\nabla}\cdot\mathbf{D}(\mathbf{r},t) &= 0, && (4.2)\\ \boldsymbol{\nabla}\cdot\mathbf{B}(\mathbf{r},t) &= 0, && (4.3)\\ \boldsymbol{\nabla}\times\mathbf{E}(\mathbf{r},t)+\frac{\partial}{\partial t}\mathbf{B}(\mathbf{r},t) &= 0, && (4.4)\\ \boldsymbol{\nabla}\times\mathbf{H}(\mathbf{r},t)-\frac{\partial}{\partial t}\mathbf{D}(\mathbf{r},t) &= 0. && (4.5) \end{aligned}$$

For non-magnetic material and the non-dispersive dielectric function (4.1) the constitutive relations may be written as

$$\mathbf{B}(\mathbf{r},t)=\mu_0\mathbf{H}(\mathbf{r},t),\quad \mathbf{D}(\mathbf{r},t)=\epsilon_0\epsilon(z)\mathbf{E}(\mathbf{r},t) \tag{4.6}$$

Introducing the electromagnetic potentials in the usual way [10]

$$\mathbf{B}(\mathbf{r},t)=\boldsymbol{\nabla}\times\mathbf{A}(\mathbf{r},t),\quad \mathbf{E}(\mathbf{r},t)=-\frac{\partial}{\partial t}\mathbf{A}(\mathbf{r},t)-\boldsymbol{\nabla}\phi(\mathbf{r},t) \tag{4.7}$$

takes care of (4.3) and (4.4). The remaining two Maxwell equations (4.2) and (4.5) turn into:

$$\begin{aligned} \boldsymbol{\nabla}\cdot[\epsilon(z)\boldsymbol{\nabla}\phi(\mathbf{r},t)]+\frac{\partial}{\partial t}\boldsymbol{\nabla}\cdot[\epsilon(z)\mathbf{A}(\mathbf{r},t)] &= 0, && (4.8)\\ \boldsymbol{\nabla}\times[\boldsymbol{\nabla}\times\mathbf{A}(\mathbf{r},t)]+\frac{\epsilon(z)}{c^2}\frac{\partial^2}{\partial t^2}\mathbf{A}(\mathbf{r},t)+\frac{\epsilon(z)}{c^2}\frac{\partial}{\partial t}\boldsymbol{\nabla}\phi(\mathbf{r},t) &= 0. && (4.9) \end{aligned}$$

The solution of these coupled differential equations can be very much simplified by a suitable choice of the gauge for the electromagnetic potentials. One usually aims to decouple the two equations. The most convenient approach is to work in the so-called generalized Coulomb gauge in which we require that

$$\boldsymbol{\nabla}\cdot[\epsilon(z)\mathbf{A}(\mathbf{r},t)]=\epsilon(z)\boldsymbol{\nabla}\cdot\mathbf{A}(\mathbf{r},t)+(1-n^2)A_z(\mathbf{r},t)\delta(z)=0. \tag{4.10}$$

where Eq. (4.1) has been used. We note that, since $\epsilon(z)$ is not constant but has a finite jump at $z=0$, the generalized Coulomb gauge differs from the standard Coulomb gauge

$$\boldsymbol{\nabla}\cdot\mathbf{A}(\mathbf{r},t)=0 \tag{4.11}$$

only by a surface term, which is proportional to a $\delta(z)$-function. With (4.10) it follows from Eq. (4.8) that in the absence of sources we can set $\phi(\mathbf{r},t)=0$. Thus in generalized Coulomb gauge equation (4.9) reduces to

$$\boldsymbol{\nabla}\times[\boldsymbol{\nabla}\times\mathbf{A}(\mathbf{r},t)]+\frac{\epsilon(z)}{c^2}\frac{\partial^2}{\partial t^2}\mathbf{A}(\mathbf{r},\omega)=0. \tag{4.12}$$

Thus only the vector potential undergoes quantization, which is accomplished by expanding $\mathbf{A}(\mathbf{r},t)$ in a complete set of the mode functions that satisfy

$$\boldsymbol{\nabla}\times[\boldsymbol{\nabla}\times\mathbf{f}_\sigma(\mathbf{r})]-\epsilon(z)\frac{\omega_\sigma^2}{c^2}\mathbf{f}_\sigma(\mathbf{r})=0, \tag{4.13}$$

supplemented by the condition that derives from the gauge we are working in, cf. Eq. (4.10)

$$\boldsymbol{\nabla}\cdot[\epsilon(z)\mathbf{f}_\sigma(\mathbf{r})]=0. \tag{4.14}$$

We have labelled solutions corresponding to the eigenvalue ω_σ by σ. The double-curl operator can be rewritten using (4.14)

$$\boldsymbol{\nabla}\times[\boldsymbol{\nabla}\times\mathbf{f}_\sigma(\mathbf{r})] \;=\; \boldsymbol{\nabla}[\boldsymbol{\nabla}\cdot\mathbf{f}_\sigma(\mathbf{r})]-\nabla^2\mathbf{f}_\sigma(\mathbf{r},\sigma)=-\nabla^2\mathbf{f}_\sigma(\mathbf{r},\sigma), \qquad \text{for } z\neq 0.$$

Thus away from the interface we can work with the Helmholtz equation

$$\nabla^2\mathbf{f}_\sigma(\mathbf{r})+\epsilon(z)\frac{\omega_\sigma^2}{c^2}\mathbf{f}_\sigma(\mathbf{r})=0, \quad z\neq 0, \tag{4.15}$$

which can be solved as usual by considering the two distinct regions of space, $z<0$ and $z>0$, and using Maxwell boundary conditions to match solutions across the interface. Once the mode functions are known, the expansion of the vector potential is written as

$$\mathbf{A}^{\mathrm{gc}}(\mathbf{r},t)=\sum_\sigma\sqrt{\frac{\hbar}{2\epsilon_0\omega_\sigma}}\left[a_\sigma\mathbf{f}_\sigma(\mathbf{r})e^{-i\omega_\sigma t}+\mathrm{C.C.}\right], \tag{4.16}$$

where the superscript reminds us that the expansion is written down in the generalized Coulomb gauge, Eq. (4.10). The quantization is accomplished by the promotion of the expansion coefficients a_σ to operators that satisfy the bosonic commutation rule

$$[\hat{a}_\sigma,\hat{a}^\dagger_{\sigma'}]=\delta_{\sigma,\sigma'}. \tag{4.17}$$

In the present geometry, described by the dielectric function (4.1), the outlined procedure yields the well-known Carnigila-Mandel modes for the vector field operator which naturally splits into two parts describing left-incident and right-incident photons, respectively [52]:

$$\hat{\mathbf{A}}^{\mathrm{gc}}(\mathbf{r},t)=\sum_{\lambda}\int \mathrm{d}^2\mathbf{k}_{\parallel}\left\{\left[\int_0^{\infty}\mathrm{d}k_{zd}\sqrt{\frac{\hbar}{2\epsilon_0\omega_{\mathbf{k}\lambda}}}\,\hat{a}^L_{\mathbf{k}\lambda}(t)\mathbf{f}^L_{\mathbf{k}\lambda}(\mathbf{r})\right]\right.$$
$$\left.+\left[\int_0^{\infty}\mathrm{d}k_{z}\sqrt{\frac{\hbar}{2\epsilon_0\omega_{\mathbf{k}\lambda}}}\,\hat{a}^R_{\mathbf{k}\lambda}(t)\mathbf{f}^R_{\mathbf{k}\lambda}(\mathbf{r})\right]\right\}+\mathrm{H.C.} \tag{4.18}$$

Here λ labels the polarization of the photons $\lambda=\{\mathrm{TE},\mathrm{TM}\}$ and a harmonic time-dependence of the annihilation operator is implicitly assumed i.e. $a_{\mathbf{k}\lambda}(t)=a_{\mathbf{k}\lambda}(0)e^{-i\omega_{\mathbf{k}\lambda}t}$. The mode functions entering the expansion are given by

$$\mathbf{f}^L_{\mathbf{k}\lambda}(\mathbf{r})=\frac{\hat{\mathbf{e}}_{\lambda}(\boldsymbol{\nabla})}{(2\pi)^{3/2}n}\left\{\theta(-z)\left[e^{i\mathbf{k}^+_d\cdot\mathbf{r}}+R^L_{\lambda}e^{i\mathbf{k}^-_d\cdot\mathbf{r}}\right]+\theta(z)\left[T^L_{\lambda}e^{i\mathbf{k}^+\cdot\mathbf{r}}\right]\right\} \tag{4.19}$$

$$\mathbf{f}^R_{\mathbf{k}\lambda}(\mathbf{r})=\frac{\hat{\mathbf{e}}_{\lambda}(\boldsymbol{\nabla})}{(2\pi)^{3/2}}\left\{\theta(z)\left[e^{i\mathbf{k}^-\cdot\mathbf{r}}+R^R_{\lambda}e^{i\mathbf{k}^+\cdot\mathbf{r}}\right]+\theta(-z)\left[T^R_{\lambda}e^{i\mathbf{k}^+_d\cdot\mathbf{r}}\right]\right\} \tag{4.20}$$

where $\mathbf{k}$ and $\mathbf{k}_d$ are the wavevectors in the vacuum and dielectric, respectively

$$\mathbf{k}^{\pm}=(\mathbf{k}_{\parallel},\pm k_z),\quad \mathbf{k}^{\pm}_d=(\mathbf{k}_{\parallel},\pm k_{zd}). \tag{4.21}$$

Their z-components are related to each other via $k_{zd}=\sqrt{n^2k_z^2+(n^2-1)\mathbf{k}_{\parallel}^2}$. The sign of the square root is chosen in such a way that on the real axis we have $\mathrm{sgn}(k_z)=\mathrm{sgn}(k_{zd})$. This ensures that the for a single mode of the electromagnetic field that consists of the incident, reflected and transmitted wave the direction of propagation is consistent. In equations (4.19) and (4.20) a shorthand notation has been introduced to represent the unit polarization vectors $\hat{\mathbf{e}}_{\lambda}$. We defined them as

$$\hat{\mathbf{e}}_{\mathrm{TE}}(\boldsymbol{\nabla}) = \left(-\nabla_{\parallel}^2\right)^{-1/2}(-i\nabla_y,i\nabla_x,0)\,, \tag{4.22}$$

$$\hat{\mathbf{e}}_{\mathrm{TM}}(\boldsymbol{\nabla}) = \left(\nabla_{\parallel}^2\nabla^2\right)^{-1/2}\left(-\nabla_x\nabla_z,-\nabla_y\nabla_z,\nabla_{\parallel}^2\right), \tag{4.23}$$

where it is understood that the derivatives are replaced by the corresponding components of the wave-vector that is present in the relevant exponential e.g. for the right-incident incoming wave $e^{i\mathbf{k}^-\cdot\mathbf{r}}$ we replace ∇_z by $-ik_z$. We note in particular that the polarization vectors do not act on the step functions. This is a convenient notation as the polarization

vectors point in different directions for incident, reflected and transmitted waves, respectively. However, one needs to be careful when carrying out explicit calculations with the mode functions (4.19)-(4.20) and remember that the operator $\hat{\mathbf{e}}_\lambda(\boldsymbol{\nabla})$ is merely a shorthand notation. The Fresnel coefficients are given by

$$\begin{aligned} R^R_{\mathrm{TE}} &= \frac{k_z - k_{zd}}{k_z + k_{zd}}, \quad R^R_{\mathrm{TM}} = \frac{n^2 k_z - k_{zd}}{n^2 k_z + k_{zd}}, \quad R^L_\lambda = -R^R_\lambda, \\ T^R_{\mathrm{TE}} &= \frac{2k_z}{k_z + k_{zd}}, \quad T^R_{\mathrm{TM}} = \frac{2nk_z}{n^2 k_z + k_{zd}}, \quad T^L_\lambda = \frac{k_{zd}}{k_z} T^R_\lambda. \end{aligned} \tag{4.24}$$

The mode functions (4.19)-(4.20) are well-known to satisfy the completeness relation which can be written in the form [19]

$$\sum_\lambda \int \mathrm{d}^2\mathbf{k}_\parallel \left[\int_0^\infty \mathrm{d}k_z \; f^R_{\mathbf{k}\lambda,i}(\mathbf{r}) f^{*R}_{\mathbf{k}\lambda,j}(\mathbf{r}') + \int_0^\infty \mathrm{d}k_{zd} \; f^L_{\mathbf{k}\lambda,i}(\mathbf{r}) f^{*L}_{\mathbf{k}\lambda,j}(\mathbf{r}') \right] = \delta^\epsilon_{ij}(\mathbf{r}, \mathbf{r}') \tag{4.25}$$

where for definiteness throughout the chapter we choose $\mathbf{r}'$ to refer to the outside of dielectric i.e. $z' > 0$. The proof of the relation

$$\begin{aligned} \nabla^2 \sum_\lambda \int \mathrm{d}^2\mathbf{k}_\parallel \left[\int_0^\infty \mathrm{d}k_z \; f^R_{\mathbf{k}\lambda,i}(\mathbf{r}) f^{*R}_{\mathbf{k}\lambda,j}(\mathbf{r}') + \int_0^\infty \mathrm{d}k_{zd} \; f^L_{\mathbf{k}\lambda,i}(\mathbf{r}) f^{*L}_{\mathbf{k}\lambda,j}(\mathbf{r}') \right] \\ = \left(\nabla_i \nabla_j - \delta_{ij} \nabla^2 \right) \delta^{(3)}(\mathbf{r} - \mathbf{r}') \end{aligned} \tag{4.26}$$

has been presented in [53]. Equation (4.26) is of course obtained by acting with the Laplace operator ∇^2 on (4.25). However, at this point it is still not obvious that

$$\nabla^2 \delta^\epsilon_{ij}(\mathbf{r}, \mathbf{r}') = \left(\nabla_i \nabla_j - \delta_{ij} \nabla^2 \right) \delta^{(3)}(\mathbf{r} - \mathbf{r}'). \tag{4.27}$$

The object $\delta^\epsilon_{ij}(\mathbf{r}, \mathbf{r}')$ represents the unit kernel in the subspace of the mode functions that satisfy the generalized Coulomb gauge i.e. if $\mathbf{f}_{\mathbf{k}\lambda}(\mathbf{r})$ satisfies Eq. (4.14) then

$$\int \mathrm{d}^3\mathbf{r}' \delta^\epsilon_{ij}(\mathbf{r}, \mathbf{r}') \mathbf{f}^j_{\mathbf{k}\lambda}(\mathbf{r}') = \mathbf{f}^i_{\mathbf{k}\lambda}(\mathbf{r}). \tag{4.28}$$

We point out that even though the generalized Coulomb gauge differs from the standard Coulomb gauge only by a surface term, cf. Eq. (4.10), the corresponding unit kernels in the position representation differ in the whole of space because of their non-local character,

i.e. even though

$$\boldsymbol{\nabla}\cdot\mathbf{f}_{\mathbf{k}\lambda}(\mathbf{r}) = \boldsymbol{\nabla}\cdot\left[\epsilon(z)\mathbf{f}_{\mathbf{k}\lambda}(\mathbf{r})\right], \text{ for } z\neq 0, \tag{4.29}$$

we have

$$\delta^{\perp}_{ij}(\mathbf{r}-\mathbf{r}') \neq \delta^{\epsilon}_{ij}(\mathbf{r},\mathbf{r}'), \quad \text{for all } z, z'. \tag{4.30}$$

Here, $\delta^{\perp}_{ij}(\mathbf{r}-\mathbf{r}')$ is the usual transverse δ-function

$$\delta^{\perp}_{ij}(\mathbf{r}-\mathbf{r}') = \frac{1}{(2\pi)^3}\int \mathrm{d}^3\mathbf{k}\left(\delta_{ij}-\frac{k_i k_j}{\mathbf{k}^2}\right)e^{i\mathbf{k}\cdot(\mathbf{r}-\mathbf{r}')}, \tag{4.31}$$

i.e. the unit kernel in the subspace of mode functions that satisfy $\boldsymbol{\nabla}\cdot\mathbf{f}_{\mathbf{k}\lambda}(\mathbf{r})=0$. Note in particular that $\delta^{\epsilon}_{ij}(\mathbf{r},\mathbf{r}')$ is not translation-invariant.

It is possible to calculate the $\mathbf{r}$-representation of $\delta^{\epsilon}_{ij}(\mathbf{r},\mathbf{r}')$ by directly evaluating the integrals in (4.25). Before we do so, let us rewrite the transverse delta function (4.31) as

$$\delta^{\perp}_{ij}(\mathbf{r}-\mathbf{r}') = \delta_{ij}\delta^{(3)}(\mathbf{r}-\mathbf{r}') - \nabla_i\nabla'_j G^0(\mathbf{r}-\mathbf{r}'), \tag{4.32}$$

where we have introduced the Green's function of the Poisson equation

$$G^0(\mathbf{r}-\mathbf{r}') = \frac{1}{4\pi}\frac{1}{|\mathbf{r}-\mathbf{r}'|} \tag{4.33}$$

with the free-space boundary conditions. Let us now turn to the explicit evaluation of the LHS of Eq. (4.25). First we deal with the case $z<0$ and $z'>0$ for which we provide a detailed calculation. Plugging the mode functions (4.19)-(4.20) into (4.25) and multiplying out we obtain

$$\begin{aligned}\delta^{\epsilon}_{ij}(\mathbf{r},\mathbf{r}') &= \frac{1}{(2\pi)^3}\sum_{\lambda}\int \mathrm{d}^2\mathbf{k}_{\parallel}e^{i\mathbf{k}_{\parallel}\cdot(\mathbf{r}_{\parallel}-\mathbf{r}'_{\parallel})}\\ &\times\left\{\int_0^{\infty}\frac{\mathrm{d}k_{zd}}{n^2}\left[T^{L*}_{\lambda}\,\hat{e}^{i}_{\lambda}(\mathbf{k}^{+}_{d})\hat{e}^{*j}_{\lambda}(\mathbf{k}^{+})e^{ik_{zd}z-ik^{*}_{z}z'}+R^{L}_{\lambda}T^{L*}_{\lambda}\,\hat{e}^{i}_{\lambda}(\mathbf{k}^{-}_{d})\hat{e}^{*j}_{\lambda}(\mathbf{k}^{+})e^{-ik_{zd}z-ik^{*}_{z}z'}\right]\right.\\ &\left.\int_0^{\infty}\mathrm{d}k_z\left[T^{R}_{\lambda}\,\hat{e}^{i}_{\lambda}(\mathbf{k}^{-}_{d})\hat{e}^{*j}_{\lambda}(\mathbf{k}^{-})e^{-ik_{zd}z+ik_{z}z'}+R^{R}_{\lambda}T^{R}_{\lambda}\,\hat{e}^{i}_{\lambda}(\mathbf{k}^{-}_{d})\hat{e}^{*j}_{\lambda}(\mathbf{k}^{+})e^{-ik_{zd}z-ik_{z}z'}\right]\right\}.\end{aligned} \tag{4.34}$$

where $\hat{e}^i_\lambda(\mathbf{k}^\pm) \equiv \hat{e}^i_\lambda(\boldsymbol{\nabla})e^{i\mathbf{k}^\pm\cdot\mathbf{r}}$. First we focus attention on the k_z and k_{zd} integrals. We convert the k_{zd} integral using the relation $k_{zd} = \sqrt{n^2k_z^2 + (n^2-1)\mathbf{k}_\parallel^2}$

$$\int_0^\infty \mathrm{d}k_{zd} = n^2\int_{i\Gamma}^0 \mathrm{d}k_z \frac{k_z}{k_{zd}} + n^2\int_0^\infty \mathrm{d}k_z \frac{k_z}{k_{zd}}, \tag{4.35}$$

where $\Gamma = |\mathbf{k}_\parallel|(n^2-1)^{1/2}/n$. After the change of variables the result consists of the integral along the real-positive axis (travelling modes) and the integral along the imaginary axis on the interval $k_z \in [\Gamma, 0]$ (evanescent modes)

$$\begin{aligned}
\delta^\epsilon_{ij}(\mathbf{r},\mathbf{r}') &= \frac{1}{(2\pi)^3}\sum_\lambda \int \mathrm{d}^2\mathbf{k}_\parallel e^{i\mathbf{k}_\parallel\cdot(\mathbf{r}_\parallel-\mathbf{r}'_\parallel)} \\
\times\Bigg\{&\int_{i\Gamma}^{0^+}\mathrm{d}k_z\left[\frac{k_z}{k_{zd}}T^{L*}_\lambda\,\hat{e}^i_\lambda(\mathbf{k}^+_d)\hat{e}^j_\lambda(\mathbf{k}^-)e^{ik_{zd}z+ik_zz'} + T^{L*}_\lambda R^L_\lambda\,\hat{e}^i_\lambda(\mathbf{k}^-_d)\hat{e}^j_\lambda(\mathbf{k}^-)e^{-ik_{zd}z+ik_zz'}\right] \\
&+\int_0^\infty \mathrm{d}k_z\left[\frac{k_z}{k_{zd}}T^L_\lambda\,\hat{e}^i_\lambda(\mathbf{k}^+_d)\hat{e}^j_\lambda(\mathbf{k}^+)e^{ik_{zd}z-ik_zz'} + T^R_\lambda\,\hat{e}^i_\lambda(\mathbf{k}^-_d)\hat{e}^j_\lambda(\mathbf{k}^-)e^{-ik_{zd}z+ik_zz'}\right. \\
&\left.+\frac{k_z}{k_{zd}}T^L_\lambda R^L_\lambda\,\hat{e}^i_\lambda(\mathbf{k}^-_d)\hat{e}^j_\lambda(\mathbf{k}^+)e^{-ik_{zd}z-ik_zz'} + R^R_\lambda T^R_\lambda\,\hat{e}^i_\lambda(\mathbf{k}^-_d)\hat{e}^j_\lambda(\mathbf{k}^+)e^{-ik_{zd}z-ik_zz'}\right]\Bigg\},
\end{aligned} \tag{4.36}$$

where the integral on the interval $k_z \in [i\Gamma, 0^+]$ runs on the RHS of the branch cut due to k_{zd} that runs from $k_z = -i\Gamma$ to $k_z = i\Gamma$. The last two terms of (4.36) cancel out by virtue of the relations (4.24) whereas the second-last line can be combined to a single integral running along the interval $k_z \in (-\infty, 0^-] \cap [0^+, \infty)$

$$\begin{aligned}
\delta^\epsilon_{ij}(\mathbf{r},\mathbf{r}') = \frac{1}{(2\pi)^3}\sum_\lambda \int \mathrm{d}^2\mathbf{k}_\parallel e^{i\mathbf{k}_\parallel\cdot(\mathbf{r}_\parallel-\mathbf{r}'_\parallel)}\Bigg\{&\int_{-\infty}^{\infty}\mathrm{d}k_z\left[T^R_\lambda\,\hat{e}^i_\lambda(\mathbf{k}^-_d)\hat{e}^j_\lambda(\mathbf{k}^-)e^{-ik_{zd}z+ik_zz'}\right] \\
+\int_{i\Gamma}^{0^+}\mathrm{d}k_z&\left[\frac{k_z}{k_{zd}}T^{L*}_\lambda\,\hat{e}^i_\lambda(\mathbf{k}^+_d)\hat{e}^j_\lambda(\mathbf{k}^-)e^{ik_{zd}z+ik_zz'} + T^{L*}_\lambda R^L_\lambda\,\hat{e}^i_\lambda(\mathbf{k}^-_d)\hat{e}^j_\lambda(\mathbf{k}^-)e^{-ik_{zd}z+ik_zz'}\right]\Bigg\}.
\end{aligned} \tag{4.37}$$

To proceed any further close inspection of (4.37) is necessary. To illustrate the argument we focus on the TM contributions to the integral. The TE contributions are treated in an exactly analogous way. We start by noting that

$$T^{L*}_{\mathrm{TM}} = \frac{2nk_z}{k_{zd}-n^2k_z}, \qquad \frac{k_z}{k_{zd}}T^{L*}_{\mathrm{TM}}R^L_{\mathrm{TM}} = \frac{2nk_z}{k_{zd}+n^2k_z}, \tag{4.38}$$

where we have used the fact that for purely imaginary k_z we have $k_z^* = -k_z$. Thus, the k_z-integral in the last line of (4.44) can be written as

$$\int_{i\Gamma}^{0^+} \mathrm{d}k_z \left(\frac{2nk_z}{k_{zd} + n^2 k_z}\right) \hat{e}^i_{\mathrm{TM}}(\mathbf{k}_d^-)\hat{e}^j_{\mathrm{TM}}(\mathbf{k}^-)e^{-ik_{zd}z + ik_z z'} + \int_{i\Gamma}^{0^+} \mathrm{d}k_z \left(\frac{2nk_z}{k_{zd} - n^2 k_z}\right) \hat{e}^i_{\mathrm{TM}}(\mathbf{k}_d^+)\hat{e}^j_{\mathrm{TM}}(\mathbf{k}^-)e^{+ik_{zd}z + ik_z z'}. \tag{4.39}$$

We now observe that the second integral differs from the first integral only by the sign of k_{zd}. This allows us to combine the two integrals utilizing the branch-cut due to k_{zd}. We have

$$\begin{aligned}\int_{i\Gamma}^{0^+} \mathrm{d}k_z \left(\frac{2nk_z}{k_{zd} + n^2 k_z}\right) \hat{e}^i_{\mathrm{TM}}(\mathbf{k}_d^-)\hat{e}^j_{\mathrm{TM}}(\mathbf{k}^-)e^{-ik_{zd}z + ik_z z'} \\ + \int_{i\Gamma}^{0^-} \mathrm{d}k_z \left(\frac{2nk_z}{-k_{zd} - n^2 k_z}\right) \hat{e}^i_{\mathrm{TM}}(\mathbf{k}_d^-)\hat{e}^j_{\mathrm{TM}}(\mathbf{k}^-)e^{-ik_{zd}z + ik_z z'} \\ = \int_{\mathcal{C}} \mathrm{d}k_z T^R_{\mathrm{TM}} \hat{e}^i_{\mathrm{TM}}(\mathbf{k}_d^-)\hat{e}^j_{\mathrm{TM}}(\mathbf{k}^-)e^{-ik_{zd}z + ik_z z'}\end{aligned} \tag{4.40}$$

where the contour $\mathcal{C}$ is illustrated in Fig. 4.1. Thus the completeness relation (4.37) may

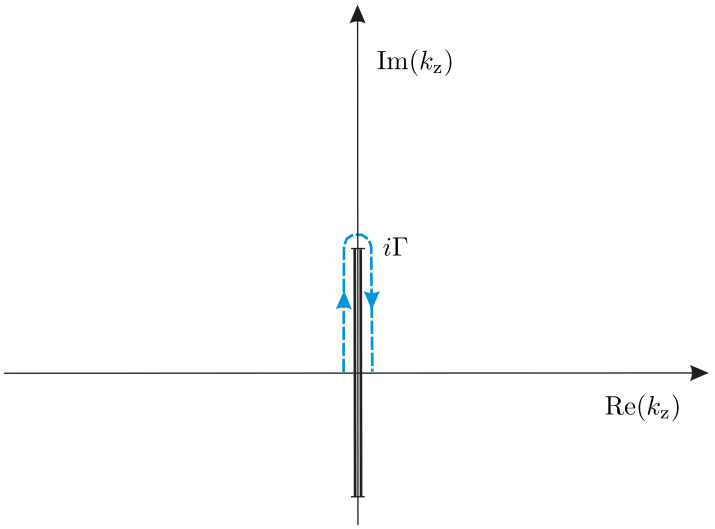

FIGURE 4.1: The dashed line represents the contour $\mathcal{C}$ used to evaluate the k_z-integral in equation (4.40).

be written compactly as

$$\delta^{\epsilon}_{ij}(\mathbf{r},\mathbf{r}') = \frac{1}{(2\pi)^3}\sum_{\lambda}\int \mathrm{d}^2\mathbf{k}_{\parallel} e^{i\mathbf{k}_{\parallel}\cdot(\mathbf{r}_{\parallel}-\mathbf{r}'_{\parallel})}\int_{\gamma}\mathrm{d}k_z T^R_{\lambda}\,\hat{e}^i_{\lambda}(\mathbf{k}^-_d)\hat{e}^j_{\lambda}(\mathbf{k}^-)e^{-ik_{zd}z+ik_z z'} \tag{4.41}$$

where the contour γ runs along the negative real axis from $k_z = -\infty$ to $k_z = 0^-$, then around the branch-cut along the contour $\mathcal{C}$ depicted in Fig. 4.1 and then from $k_z = 0^+$ to $k_z = \infty$. The k_z-integral may now be evaluated with the help of the residue theorem. We note that for $z < 0,\ z' > 0$ the integrand in (4.41) vanishes exponentially in the upper k_z-plane so we might close the contour there. To do so we need to determine the position of the integrand's poles, if any. The Fresnel's coefficients for the half-space geometry are analytic for $\mathrm{Im}(k_z) > 0$ thus it remains to look at the polarization vectors defined in equations (4.22)-(4.23). For the TE mode we immediately note that $\hat{\mathbf{e}}_{\mathrm{TE}}$ are independent of k_z. Thus the transverse electric modes do not contribute to the integral (4.41). For the TM mode, each polarization vector contributes a factor of $1/|\mathbf{k}|$ where $|\mathbf{k}| = \sqrt{k_z^2 + \mathbf{k}_{\parallel}^2}$. Thus for a TM mode the integrand has a simple pole in the upper half-plane at $k_z = i|\mathbf{k}_{\parallel}|$. With this it is a simple matter to show that

$$\delta^{\epsilon}_{ij}(\mathbf{r},\mathbf{r}') = -\nabla_i\nabla'_j G^T(\mathbf{r}-\mathbf{r}'), \qquad z < 0,\ z' > 0 \tag{4.42}$$

where

$$G^T(\mathbf{r}-\mathbf{r}') = \frac{1}{4\pi n^2}\frac{2n^2}{n^2+1}\frac{1}{|\mathbf{r}-\mathbf{r}'|} \tag{4.43}$$

is the transmitted part of the electrostatic Green's function in the half-space geometry, see e.g. [10].

The evaluate (4.25) for the case $z > 0,\ z' > 0$ we again plug the relevant the mode functions (4.19)-(4.20) and after utilizing some straightforward properties of the Fresnel

reflection coefficients we arrive at

$$\begin{aligned}\delta^{\epsilon}_{ij}(\mathbf{r},\mathbf{r}') = \frac{1}{(2\pi)^3}\sum_{\lambda}\int \mathrm{d}^2\mathbf{k}_{\parallel} e^{i\mathbf{k}_{\parallel}\cdot(\mathbf{r}_{\parallel}-\mathbf{r}'_{\parallel})} \\ \times\Bigg\{\int_{-\infty}^{\infty}\mathrm{d}k_z \hat{e}^i_{\lambda}(\mathbf{k}^+)\hat{e}^j_{\lambda}(\mathbf{k}^+)e^{ik_z(z-z')} \\ + \int_{-\infty}^{\infty}\mathrm{d}k_z R^R_{\lambda}\hat{e}^i_{\lambda}(\mathbf{k}^+)\hat{e}^j_{\lambda}(\mathbf{k}^-)e^{ik_z(z+z')} \\ + \int_{i\Gamma}^{0}\mathrm{d}k_z \frac{k_z}{k_{zd}}\left|T^L_{\lambda}\right|^2 \hat{e}^i_{\lambda}(\mathbf{k}^-)\hat{e}^j_{\lambda}(\mathbf{k}^-)e^{ik_z(z+z')}\Bigg\}\end{aligned} \tag{4.44}$$

with $\Gamma = |\mathbf{k}_{\parallel}|(n^2-1)^{1/2}/n$ and $\hat{e}^i_{\lambda}(\mathbf{k}^{\pm}) \equiv \hat{e}^i_{\lambda}(\boldsymbol{\nabla})e^{i\mathbf{k}^{\pm}\cdot\mathbf{r}}$. Now we note that, because of the well-known completeness properties of the polarization vectors, the first term of (4.44) yields the transverse δ-function, Eq. (4.31). The remaining two terms are combined into a single contour integral utilizing the branch cut due to $k_{zd} = \sqrt{n^2k_z^2 + (n^2-1)\mathbf{k}_{\parallel}^2}$. This is done exactly in the same manner as in [53] or [54]. Thus the result reads

$$\delta^{\epsilon}_{ij}(\mathbf{r},\mathbf{r}') = \delta^{\perp}_{ij}(\mathbf{r}-\mathbf{r}') + \frac{1}{(2\pi)^3}\sum_{\lambda}\int \mathrm{d}^2\mathbf{k}_{\parallel} e^{i\mathbf{k}_{\parallel}\cdot(\mathbf{r}_{\parallel}-\mathbf{r}'_{\parallel})}\int_{\gamma}\mathrm{d}k_z R^R_{\lambda}\hat{e}^i_{\lambda}(\mathbf{k}^+)\hat{e}^j_{\lambda}(\mathbf{k}^-)e^{ik_z(z+z')} \tag{4.45}$$

where the contour γ runs along the negative real axis from $k_z = -\infty$ to $k_z = 0^-$, then around the branch cut along the contour $\mathcal{C}$ depicted in Fig. 4.1 and then from $k_z = 0^+$ to $k_z = \infty$. Since the reflection coefficient R^R_{λ} has no poles in the upper k_z-plane we can close the contour there. Then, for the TE mode the integral vanishes because the polarization vectors do not depend on k_z. For the TM mode however, the polarization vectors contribute a pole at $k_z = i|\mathbf{k}_{\parallel}|$. The integral is easily evaluated using the residue theorem and leads to the final result written explicitly as

$$\delta^{\epsilon}_{ij}(\mathbf{r},\mathbf{r}') = \delta_{ij}\delta^{(3)}(\mathbf{r}-\mathbf{r}') - \nabla_i\nabla'_j\left[G^0(\mathbf{r}-\mathbf{r}') + G^R(\mathbf{r},\mathbf{r}')\right] \qquad z,z' > 0 \tag{4.46}$$

with $G^{\mathrm{R}}(\mathbf{r},\mathbf{r}')$ being the reflected part of the electrostatic Green's function in the half-space geometry

$$G^R(\mathbf{r},\mathbf{r}') = -\frac{1}{4\pi}\frac{n^2-1}{n^2+1}\frac{1}{|\mathbf{r}-\bar{\mathbf{r}}'|} \tag{4.47}$$

where $\bar{\mathbf{r}}' = (x', y', -z')$.

The results (4.42) and (4.46) may be compactly written as

$$\delta^{\epsilon}_{ij}(\mathbf{r},\mathbf{r}') = \delta_{ij}\delta^{(3)}(\mathbf{r}-\mathbf{r}') - \nabla_i\nabla'_j G(\mathbf{r},\mathbf{r}'), \qquad z' > 0 \tag{4.48}$$

where

$$G(\mathbf{r},\mathbf{r}') = \frac{1}{4\pi n^2}\frac{2n^2}{n^2+1}\frac{1}{|\mathbf{r}-\mathbf{r}'|}\theta(-z) + \left(\frac{1}{4\pi}\frac{1}{|\mathbf{r}-\mathbf{r}'|} - \frac{1}{4\pi}\frac{n^2-1}{n^2+1}\frac{1}{|\mathbf{r}-\bar{\mathbf{r}}'|}\right)\theta(z) \tag{4.49}$$

is the Green's function of the Poisson equation for the case of a source being outside the dielectric occupying $z < 0$ region of space. We see that the end result has formally the same form as (4.32) only that the free-space Green's function of the Poisson equation is replaced by the Green's function in the presence of a dielectric half-space of refractive index n. The result (4.48) may be formally written as

$$\delta^{\epsilon}_{ij}(\mathbf{r},\mathbf{r}') = \left(\delta_{ij} + \nabla_i\nabla'_j\nabla^{-2}\right)\delta^{(3)}(\mathbf{r}-\mathbf{r}') \tag{4.50}$$

provided an appropriate meaning is attached to the integral operator ∇^{-2}. We would like to remark that it is in this sense the completeness relation proved in [55] holds. There of course, the Green's function is that in the slab geometry, see appendix of [56]. Equation (4.50) is to be compared with (4.27). Note in particular, that the derivative ∇'_j which acts on $\mathbf{r}'$ can not be shifted to act on $\mathbf{r}$ because of the reflection term in (4.49). This is possible only after one acts with Laplace operator on (4.50). Then, replacing ∇'_j with $-\nabla_j$ we recover the result (4.27) derived in [53].

Once the completeness relation of the mode functions has been explicitly calculated it is a simple matter to evaluate the equal-time field commutator. Using Eq. (4.16) we have

$$\left[A^{\mathrm{gc}}_i(\mathbf{r}), \epsilon_0 E_j(\mathbf{r}')\right] = -i\hbar\delta^{\epsilon}_{ij}(\mathbf{r},\mathbf{r}') \tag{4.51}$$

so for the case of the electromagnetic field in the presence of a dielectric half-space the commutator between the vector potential and electric field operator reads

$$\left[A^{\mathrm{gc}}_i(\mathbf{r}), \epsilon_0 E_j(\mathbf{r}')\right] = -i\hbar\delta_{ij}\delta^{(3)}(\mathbf{r}-\mathbf{r}') + i\hbar\nabla_i\nabla'_j G(\mathbf{r},\mathbf{r}'). \tag{4.52}$$

where $G(\mathbf{r},\mathbf{r}')$ is given by (4.49) and we remind the reader that we consider the case $z' > 0$

only. We see that, compared to the standard commutation relations of the QED, the commutator in the presence of the dielectric gains an additional term that represents a reflection from the surface. Note that in the limit of perfect reflectivity i.e. $n \to \infty$ we recover the results obtained in [57][20]. We will come back to this fact at the end of the section 4.2.

4.2 Coulomb gauge

The natural question that arises is whether it is possible to quantize the electromagnetic field in the presence of a dielectric half-space but work in standard Coulomb gauge. A direct approach trying to solve the Maxwell equations (4.8)-(4.9) proves inconvenient but one may exploit gauge transformations to work out the field operators in the standard Coulomb gauge from the ones in the generalized Coulomb gauge. A gauge transformation from the generalized Coulomb gauge to the true Coulomb gauge may be written as follows

$$\mathbf{A}^{\mathrm{c}}(\mathbf{r},t) = \mathbf{A}^{\mathrm{gc}}(\mathbf{r},t) - \boldsymbol{\nabla}\chi(\mathbf{r},t), \tag{4.53}$$

$$\phi^{\mathrm{c}}(\mathbf{r},t) = \phi^{\mathrm{gc}}(\mathbf{r},t) + \frac{\partial}{\partial t}\chi(\mathbf{r},t). \tag{4.54}$$

where we set $\phi^{\mathrm{gc}}(\mathbf{r},t) = 0$ in the absence of charges. It is clear that in the Coulomb gauge, even in the absence of charges, the scalar potential does not vanish. In fact, we shall see shortly that it enters the Hamiltonian on equal footing with the vector potential as a second-quantized operator. We note that the LHS of Eq. (4.53) is transverse, and since $\mathbf{A}^{\mathrm{gc}}$ is not, the gradient of the generating function must compensate for it [16]. In other words we have[1]

$$\nabla_i\chi(\mathbf{r},t) = \int \mathrm{d}^3\mathbf{r}'\delta^{\parallel}_{ij}(\mathbf{r}-\mathbf{r}')A^{\mathrm{gc}}_j(\mathbf{r}',t). \tag{4.56}$$

[1]We aim here to make the LHS of equation (4.53) transverse. Setting $\boldsymbol{\nabla}\chi = \mathbf{A}^{gc}_{\parallel}$ does the job but so does

$$\boldsymbol{\nabla}\chi = \mathbf{A}^{gc}_{\parallel} + \mathbf{f} \tag{4.55}$$

where $\mathbf{f}$ is some function with vanishing divergence i.e. $\boldsymbol{\nabla}\cdot\mathbf{f} = 0$. To convince ourselves that $\mathbf{f}$ necessarily vanishes we note that equation (4.55) implies that $\boldsymbol{\nabla}\times\mathbf{f} = 0$. This in turn implies that $\mathbf{f}$ is given as a gradient of some harmonic function Φ i.e. satisfying $\nabla^2\Phi = 0$. Since we expect the fields to vanish at infinity the function Φ is necessarily zero by the maximum principle, see e.g. [58].

The form of the χ can be easily found if we use the position representation of the longitudinal δ-function

$$\nabla_i \chi(\mathbf{r},t) = \frac{1}{4\pi}\int \mathrm{d}^3\mathbf{r}' \left(\nabla_i \nabla'_j \frac{1}{|\mathbf{r}-\mathbf{r}'|}\right) A_j^{\mathrm{gc}}(\mathbf{r}',t) \tag{4.57}$$

where the primed derivative acts only on the Green's function and not on A_j^{gc}. Thus, after integrating by parts, we identify

$$\chi(\mathbf{r},t) = -\frac{1}{4\pi}\int \mathrm{d}^3\mathbf{r}' \frac{1}{|\mathbf{r}-\mathbf{r}'|} \boldsymbol{\nabla}' \cdot \mathbf{A}^{\mathrm{gc}}(\mathbf{r}',t). \tag{4.58}$$

The generating function can be obtained directly evaluating the integrals in (4.58) using the explicit form of the operator (4.18). Alternatively, we take the divergence of equation (4.53) followed by a time derivative and find that the potential in the coulomb gauge ϕ^c satisfies the Poisson equation

$$-\nabla^2 \dot{\chi}(\mathbf{r},t) = \frac{\sigma(\mathbf{r}_\parallel,t)}{\epsilon_0}\delta(z), \tag{4.59}$$

with the surface charge density given by

$$\sigma(\mathbf{r}_\parallel,t) = -2i\int \mathrm{d}^2\mathbf{k}_\parallel |\mathbf{k}_\parallel| \left\{ \left[\int_0^\infty \mathrm{d}k_{zd} \sqrt{\frac{\hbar\epsilon_0}{2\omega_{\mathbf{k}}}}\, \hat{a}^L_{\mathbf{k}\mathrm{TM}}(t) g^L_{\mathbf{k}}(\mathbf{r}_\parallel) - \mathrm{H.C.}\right] + \left[\int_0^\infty \mathrm{d}k_z \sqrt{\frac{\hbar\epsilon_0}{2\omega_{\mathbf{k}}}}\, \hat{a}^R_{\mathbf{k}\mathrm{TM}}(t) g^R_{\mathbf{k}}(\mathbf{r}_\parallel) - \mathrm{H.C.}\right]\right\}. \tag{4.60}$$

We have introduced the mode functions

$$g^R_{\mathbf{k}}(\mathbf{r}_\parallel) = \frac{1}{(2\pi)^{3/2}} \frac{n^2-1}{2n^2} \left(1 + R^R_{\mathrm{TM}}\right) e^{i\mathbf{k}_\parallel \cdot \mathbf{r}_\parallel}, \tag{4.61}$$

$$g^L_{\mathbf{k}}(\mathbf{r}_\parallel) = \frac{1}{(2\pi)^{3/2}} \frac{n^2-1}{2n^2} \frac{T^L_{\mathrm{TM}}}{n} e^{i\mathbf{k}_\parallel \cdot \mathbf{r}_\parallel}, \tag{4.62}$$

where the reflection coefficients are given by equations (4.24). The solution of Eq. (4.59) can be easily found to be given by

$$\dot{\chi}(\mathbf{r},t) = i\int \mathrm{d}^2\mathbf{k}_\parallel e^{-|\mathbf{k}_\parallel||z|} \left\{ \left[\int_0^\infty \mathrm{d}k_{zd} \sqrt{\frac{\hbar}{2\epsilon_0\omega_{\mathbf{k}}}}\, \hat{a}^L_{\mathbf{k}\mathrm{TM}}(t) g^L_{\mathbf{k}}(\mathbf{r}_\parallel) - \mathrm{H.C.}\right] + \left[\int_0^\infty \mathrm{d}k_z \sqrt{\frac{\hbar}{2\epsilon_0\omega_{\mathbf{k}}}}\, \hat{a}^R_{\mathbf{k}\mathrm{TM}}(t) g^R_{\mathbf{k}}(\mathbf{r}_\parallel) - \mathrm{H.C.}\right]\right\}. \tag{4.63}$$

As promised, the potential $\phi^c = \dot{\chi}$ turns out to be a second-quantized operator. It relates the vector potential in standard Coulomb gauge to that in generalized Coulomb gauge via equation (4.53). It only affects photons with the TM polarization and, interestingly, it's symmetric with respect to the interface i.e. $\dot{\chi}(-z) = \dot{\chi(z)}$. According to (4.54) The generating function χ is found by integrating Eq. (4.63) with respect to time.

Let us now come back to the issue of the commutation relations between the field operators. Clearly we expect

$$\left[A_i^{\mathrm{c}}(\mathbf{r}), \epsilon_0 E_j(\mathbf{r}')\right] = -i\hbar\delta_{ij}^{\perp}(\mathbf{r}-\mathbf{r}') = -i\hbar\delta_{ij}\delta^{(3)}(\mathbf{r}-\mathbf{r}') + i\hbar\nabla_i\nabla'_j G^0(\mathbf{r}-\mathbf{r}') \tag{4.64}$$

which is a consequence of the fact that $\boldsymbol{\nabla}\chi$ is given as a longitudinal part of $\mathbf{A}^{gc}$, cf. Eq. (4.56). This can also be confirmed by an explicit calculation using the mode functions (4.61)-(4.62). The commutator splits as follows

$$\left[A_i^{\mathrm{c}}(\mathbf{r}), \epsilon_0 E_j(\mathbf{r}')\right] = \left[A_i^{\mathrm{gc}}(\mathbf{r}) - \nabla_i\chi(\mathbf{r}), \epsilon_0 E_j(\mathbf{r}')\right] = -ih\delta_{ij}^{\epsilon}(\mathbf{r},\mathbf{r}') - \left[\nabla_i\chi(\mathbf{r}), \epsilon_0 E_j(\mathbf{r}')\right] \tag{4.65}$$

where $\delta_{ij}^{\epsilon}(\mathbf{r},\mathbf{r}')$ is given by equation (4.48) and the reader is reminded that we consider the case $z' > 0$ only. Plugging in the mode functions (4.61)-(4.62) into Eq. (4.65) we find, using the same techniques as in the calculation of the completeness relation (4.25), that

$$\left[\nabla_i\chi(\mathbf{r}), \epsilon_0 E_j(\mathbf{r}')\right] = i\hbar\nabla_i\nabla'_j \begin{cases} -\dfrac{n^2-1}{n^2+1}\, G^0(\mathbf{r}-\mathbf{r}') & z<0, z'>0 \\ G^R(\mathbf{r},\mathbf{r}') & z>0, z'>0 \end{cases}, \tag{4.66}$$

where G^0 and G^R are the Green's functions as introduced in equations (4.33) and (4.47). Equation (4.66) when combined with (4.48) and (4.65) confirms the assertion stated by Eq. (4.64).

The commutator between the vector potential and electric field operators is gauge dependent which has been clearly demonstrated by the above considerations. Therefore, the modification of the QED commutation relations is not a physical effect but rather is related to the choice of gauge in which the electromagnetic field is quantized, which is of course in principle only a matter of convenience. We note that the commutation relation between

the physical fields retain the standard form, as they should. Consider the commutator

$$\left[\mathbf{B}(\mathbf{r}), \mathbf{E}(\mathbf{r}')\right] = \boldsymbol{\nabla} \times \left[\mathbf{A}(\mathbf{r}), \mathbf{E}(\mathbf{r}')\right]. \tag{4.67}$$

We see from (4.53) that regardless of the gauge one uses to calculate the RHS of the above relation the end result is the same. The commutators (4.52) and (4.64) differ only by a longitudinal part that is annihilated by the curl operator. Thus, the shape of the cavity has no impact on the fundamental commutation relations of physical fields.

When the cavity walls are modelled as perfectly reflecting mirrors the generalized Coulomb gauge (4.10) is meaningless. Then, a common way to quantize the electromagnetic field is to work with the free-space form of Eq. (4.9) in standard Coulomb gauge (4.11) and demand that the fields are excluded from interior of the perfect reflector i.e. one solves

$$\begin{aligned} \left(\nabla^2 - \frac{\partial^2}{\partial t^2}\right) \mathbf{A}(\mathbf{r}, t) &= 0, \\ \boldsymbol{\nabla} \cdot \mathbf{A}(\mathbf{r}, t) &= 0, \end{aligned} \tag{4.68}$$

together with the condition that the electric field vanishes for $z \leq 0$. This in particular implies that

$$E_x(z = 0^+) = 0, \; E_y(z = 0^+) = 0. \tag{4.69}$$

The relation between the vector potential and the electric field is taken to be

$$\mathbf{E}(\mathbf{r}, t) = -\frac{\partial \mathbf{A}(\mathbf{r}, t)}{\partial t}, \tag{4.70}$$

and for this reason the boundary conditions for the electric field immediately imply the rules for the vector potential. This method of quantization gives the vector field operator which may be obtained by taking the $n \to \infty$ limit of Eq. (4.18). This in turn implies that the commutation relations for the field operators are given by the perfect reflector limit of the commutation rule (4.52) and *NOT* by Eq. (4.64). Explicitly:

$$\left[A_i(\mathbf{r}), \epsilon_0 E_j(\mathbf{r}')\right] = -i\hbar\delta_{ij}\delta^{(3)}(\mathbf{r} - \mathbf{r}') + \frac{i\hbar}{4\pi}\nabla_i\nabla'_j\left(\frac{1}{|\mathbf{r} - \mathbf{r}'|} - \frac{1}{|\mathbf{r} - \bar{\mathbf{r}}'|}\right), \quad z, z' > 0, \tag{4.71}$$

where $\bar{\mathbf{r}} = (x, y, -z)$. At first it seems surprising that in spite of the Coulomb gauge condition imposed on the vector potential the reflected part of the Green's function appears

in the commutator. This can be explained as follows. In the presence of the perfect reflector the fluctuations of the quantized electromagnetic field imply the existence of the fluctuating charge density on the surface of the perfect reflector. The Gauss's law reads

$$\boldsymbol{\nabla}\cdot\mathbf{E}(\mathbf{r},t)=\frac{\sigma(\mathbf{r}_{\parallel},t)}{\epsilon_0}\delta(z), \tag{4.72}$$

where $\sigma(\mathbf{r}_{\parallel})$ is given as a perfect reflector limit of Eq. (4.60). Relation (4.72) is a consequence of the boundary conditions applied to the electric field at $z=0$ (and vice-versa). We observe that equations (4.68), (4.70) and (4.72) can not be simultaneously satisfied on the surface of the perfect reflector. Thus, the gauge condition in (4.68) should rather read

$$\boldsymbol{\nabla}\cdot\mathbf{A}(\mathbf{r},t)=0 \quad \text{for } z\neq 0 \tag{4.73}$$

which is an adaptation of the generalized Coulomb gauge condition (4.10) to the case of the perfect reflector rather than true Coulomb gauge. This is the origin of the reflected Green's function term appearing in the commutator (4.71) as it has also been recently pointed out in [59]. We can now observe that the oversimplified model of the perfectly reflecting cavity walls obscures the fact that the form of the commutation relation is actually determined by the choice of gauge. We would also like to remark that it is claimed in [59] that the commutator between the physical fields (4.67) is affected by the cavity walls if one assumes them to be perfectly reflecting. We have clearly shown that this is an incorrect conclusion.

4.3 Hamiltonians

Quantum electrodynamics in the presence of dielectrics is most conveniently formulated in the generalized Coulomb gauge. The minimal-coupling Hamiltonian of a charged particle that is placed near dielectric half-space and coupled to the quantized electromagnetic field may be written as [17]

$$H^{gc}=\frac{[\mathbf{p}-q\mathbf{A}^{gc}(\mathbf{r}_0)]^2}{2m}+\frac{1}{2}\int \mathrm{d}^3\mathbf{r}\left\{\epsilon_0\epsilon(z)\left[\frac{\partial\mathbf{A}^{gc}(\mathbf{r})}{\partial t}\right]^2+\frac{\mathbf{B}^2(\mathbf{r})}{\mu_0}\right\}$$
$$+\frac{1}{2}\int \mathrm{d}^3\mathbf{r}\epsilon_0\epsilon(z)\boldsymbol{\nabla}\phi^{gc}(\mathbf{r})\cdot\boldsymbol{\nabla}\phi^{gc}(\mathbf{r}), \tag{4.74}$$

where $\mathbf{r}_0$ is the position of the particle. Here it will prove most convenient to write the Hamiltonian H^f of the electromagnetic field in the form

$$H^f = \sum_{\mathbf{k}} \hbar\omega_{\mathbf{k}} \left(a^\dagger_{\mathbf{k}} a_{\mathbf{k}} + \frac{1}{2} \right). \tag{4.75}$$

The integral involving the scalar potential ϕ^{gc} is a c-number and it contains infinite self-energy of the particle Σ as well as the z_0-dependent electrostatic interaction between the dielectric and the charge

$$\frac{1}{2} \int \mathrm{d}^3\mathbf{r} \epsilon_0 \epsilon(z) \boldsymbol{\nabla}\phi^{gc}(\mathbf{r}) \cdot \boldsymbol{\nabla}\phi^{gc}(\mathbf{r}) = \Sigma + V^{es}, \tag{4.76}$$

with

$$V^{es} = -\frac{q^2}{4\pi\epsilon_0} \frac{n^2-1}{n^2+1} \frac{1}{4z_0}. \tag{4.77}$$

Equation (4.77) can be seen as an interaction energy of a static charge with its image in the dielectric, multiplied by a factor of 1/2. Dropping the irrelevant self-energy of the particle Σ the Hamiltonian H^{gc} may be written as

$$H^{gc} = \frac{\left[\mathbf{p} - q\mathbf{A}^{gc}(\mathbf{r}_0)\right]^2}{2m} + H^f + V^{es}. \tag{4.78}$$

Perhaps the most instructive way of obtaining the Hamiltonian in Coulomb gauge H^c is by using the unitary transformation

$$H^c = e^{iS/\hbar} H^{gc} e^{-iS/\hbar} + i\hbar \left(\frac{d}{dt} e^{iS/\hbar} \right) e^{-iS/\hbar}, \tag{4.79}$$

with the operator S is given by

$$S(\mathbf{r}_0, t) = -q\chi(\mathbf{r}_0, t). \tag{4.80}$$

The generating function $\chi(\mathbf{r}, t)$ is given as an integral of (4.63) with respect to time and is evaluated at the position of the particle $\mathbf{r}_0$. In what follows we set operators to be time-independent (Schrödinger picture) so that the term containing the time derivative in (4.79) does not contribute. Then, using the same methods as in the proof of the completeness

relation (4.25), it is not difficult to show that

$$\begin{aligned} e^{iS/\hbar}\left[\mathbf{p}-q\mathbf{A}^{gc}(\mathbf{r}_0)\right]e^{-iS/\hbar} &= \left[\mathbf{p}-q\mathbf{A}^{c}(\mathbf{r}_0)\right], \\ e^{iS/\hbar}H^f e^{-iS/\hbar} &= H^f+\frac{i}{\hbar}\left[S(\mathbf{r}_0),H^f\right]+\frac{1}{2}\left(\frac{i}{\hbar}\right)^2\left[S(\mathbf{r}_0),\left[S(\mathbf{r}_0),H^f\right]\right] \\ &= H^f+q\dot{\chi}(\mathbf{r}_0)-\frac{n^2-1}{2n^2}V^{es}. \end{aligned} \tag{4.81}$$

With this, the Hamiltonian in the Coulomb gauge is written

$$H^c=\frac{\left[\mathbf{p}-q\mathbf{A}^c(\mathbf{r}_0)\right]^2}{2m}+H^f+q\dot{\chi}(\mathbf{r}_0)+\left(\frac{n^2+1}{2n^2}\right)V^{es}. \tag{4.82}$$

We see that compared to the Hamiltonian written out in the generalized Coulomb gauge, Eq. (4.78), some of the electrostatic interaction energy has been redistributed and is now contained in the second-quantized part of the Hamiltonian H^c. We will demonstrate that it is now shared among two terms

$$H^{es}_{int}=q\dot{\chi}(\mathbf{r}_0)+\left(\frac{n^2+1}{2n^2}\right)V^{es}. \tag{4.83}$$

Working with the standard time-independent perturbation theory applied to the interaction term $q\dot{\chi}(\mathbf{r})$ one finds that the first non-vanishing contribution is of the second-order and is given by

$$\begin{aligned} \Delta E^{es} &= \sum_{\mathbf{k},\mathbf{p}_f}\frac{\left|\langle\mathbf{p}_f;1_{\mathbf{k}\mathrm{TM}}|q\dot{\chi}(\mathbf{r}_0)|\mathbf{p};0\rangle\right|^2}{\dfrac{\mathbf{p}^2}{2m}-\left(\dfrac{\mathbf{p}_f^2}{2m}+\omega_{\mathbf{k}}\right)}\approx -q^2\sum_{\mathbf{k}}\frac{\left|\dot{\chi}(\mathbf{r})\right|^2}{\omega_{\mathbf{k}}} \\ &= -\frac{q^2}{2\epsilon_0}\int \mathrm{d}^2\mathbf{k}_\parallel e^{-2|\mathbf{k}_\parallel|z_0}\left[\int_0^\infty \mathrm{d}k_{zd}\frac{\left|g^L_{\mathbf{k}}(\mathbf{r}_\parallel)\right|^2}{\omega^2_{\mathbf{k}}}+\int_0^\infty \mathrm{d}k_z\frac{\left|g^R_{\mathbf{k}}(\mathbf{r}_\parallel)\right|^2}{\omega^2_{\mathbf{k}}}\right], \end{aligned} \tag{4.84}$$

where we have used no-recoil approximation. The mode functions g are given in Eqs. (4.61)-(4.62). The resulting integrals in (4.84) can be calculated analytically and the result is

$$\Delta E^{es}=\left(\frac{n^2-1}{2n^2}\right)V^{es}. \tag{4.85}$$

Thus, the contributions from both terms in equation (4.83) add up to yield the whole of the electrostatic interaction energy

$$\left(\frac{n^2-1}{2n^2}\right) V^{es} + \left(\frac{n^2+1}{2n^2}\right) V^{es} = V^{es}. \tag{4.86}$$

This is of course what one would expect since both formulations of the theory must lead to the same results.

Chapter 5

Interaction of atoms with layered dielectrics

5.1 Introduction

The question of the interaction between a neutral atom and a macroscopic dielectric body, once of purely academic interest, has recently been promoted to a real-life physics problem, thanks to the rapid developments in nanotechnology and experimental techniques. It is no longer the case this interaction, the so-called Casimir-Polder interaction, is a tiny effect that can be ignored in all practical situations. Instead, on the length-scales that nanotechnology nowadays operates in, dispersion forces as they are also called, become significant and may appreciably influence miniaturized physical systems. The ambition of nanotechnology and cold-atom physics to construct a quantum computer faces, among others, the problem of trapping and extremely accurate guiding of single atoms above dielectric substrates, so-called atom chips. To best utilize such technologies the nearby environment of a trapped atom usually comprises of a complicated arrangement of inhomogeneous dielectrics. The question then arises, what are the magnitudes of the Casimir-Polder forces involved and can one possibly engineer the shapes of surrounding bodies to obtain the optimal ones that would minimize the nuisance of the dispersion forces or positively contribute to the trapping or guiding? However, to search for such possibilities one needs to go beyond simple featureless geometries and ground-state atoms as such models lack

flexibility. Perhaps the least sophisticated but still interesting example to study in this context is to consider a neutral atom, possibly excited, above a layered dielectric half-space, cf. Fig. 5.1. If the atom is in its ground state, then the Casimir-Polder force is always attractive. In such case it is desirable to derive simple analytical formulae that would allow to obtain quick estimates of the magnitudes of the forces involved in terms of the optical properties of the layer and the substrate [56]. On the other hand, if the atom is in its excited state, then as it is widely recognised [27], the potential acquires a oscillatory contribution that can result in a repulsive force. Additionally, the presence of the layer creates the possibility of a resonance between the wavelength of the atomic transition and the thickness of the layer, which could lead to an enhancement of the interaction.

There is a variety of theoretical approaches devised to study the Casimir-Polder interaction (for a comprehensive account of the subject see [60]) but perhaps the most successful ones being the linear response theory [48] and phenomenological macroscopic QED [61]. Consider for example methods developed in [27][62]. They use linear response theory [48] and express the field susceptibilities in terms of Fresnel reflection coefficients. This method allows them to express the Casimir-Polder interaction as an integral along the imaginary frequency axis of the product of the atomic and field susceptibilities. In practice the problem is reduced to the calculation of the classical electromagnetic Green tensor expressed in terms of Fresnel coefficients. Such calculations tend to be tedious and often inevitably lead to the use of the numerical methods. However it is generally beneficial to study problems of QED with methods that are physically transparent and do not obscure basic the physics. In the example of the geometry considered in this Chapter the technique of the electromagnetic field quantization based on the normal-mode expansion [52] seems to be best emphasizing the physics of the problem, namely the fact that the system supports two kinds of modes of the electromagnetic field [63]. These comprise of travelling modes with a continuous spectrum and the trapped modes with discrete spectrum i.e. occurring at only certain allowed frequencies. The trapped modes arise because of repeated total internal reflections within the top layer of higher refractive index than the substrate and emerge as evanescent waves outside the wave-guide. This gives a rise to a complicated structure of evanescent modes outside the layered dielectric where evanescent waves with continuous spectrum, also arising in a half-space geometry [52], are superposed with evanescent modes that arise only in the presence of the slab-like waveguide

[56]. In the framework we apply in this work, in the same spirit as [56][64], the use of standard perturbation theory renders all calculations explicit and it is possible from the outset to track down and remove if necessary any ambiguities that tend to remain hidden in more elaborate theories. For example, linear-response theory results in an integral over the Fresnel reflection coefficients but gives no indication of whether the evanescent waves associated with the trapped modes contribute to the Casimir-Polder interaction or not. The question is answered at once if the normal modes approach is used instead, see [63][65]. Also, it has been recently pointed out [56] that elaborate theories may not only obscure the basic physics but can also lead one to draw incorrect conclusions [66].

The purpose of this Chapter is twofold. Firstly, it aims to support current experimental efforts by providing the analytical formulae useful for quick estimates of the dispersion forces acting on an atom placed in the vicinity of the layered dielectric with the emphasis on the corrections caused by the layer as compared to the standard half-space results reported in [64]. It also investigates the resonant interaction between an excited atom and a layer in the search for the possible enhancement or sign reversal of the Casimir-Polder force. Furthermore, it formulates a simple and explicit theory based on the well understood concepts of theoretical physics such as perturbation theory and electromagnetic field quantization based on normal-modes expansion. The theoretical aspect, although serving only as a means to a practical end result, is interesting in its own right. The perturbative approach used in this work leads to the problem of the summation over the modes of the electromagnetic field, which is non-trivial because of the dual character of the modes of the electromagnetic field. The task of adding the discrete and continuous field modes is elegantly accomplished with the use of complex-integral techniques. This allows us to explicitly show that the canonical commutation relations between the field operators are satisfied, which is equivalent to saying that the completeness relation of the normal-modes holds in the geometry considered. Although this is not a surprise because the field modes are solutions of a Hermitian operator's eigenvalue problem, the explicit calculation we carry out provides us with the mathematics necessary to complete a typical perturbative calculation in this geometry. It also allows us to cast the end result in a simple and elegant form that is easy to study analytically in various asymptotic regimes, which was our goal.

This chapter is organised as follows. First we quantize the electromagnetic field in the presence of the layered dielectric, Section 5.2. Then, in Section 5.2.3, we explicitly prove the completeness relation of the electromagnetic field modes. Equipped with the necessary mathematical tools we proceed to calculate the energy shift in Section 5.3 and then study it analytically (Section 5.4) and numerically (Section 5.5).

5.2 Field quantization in the presence of a layered boundary

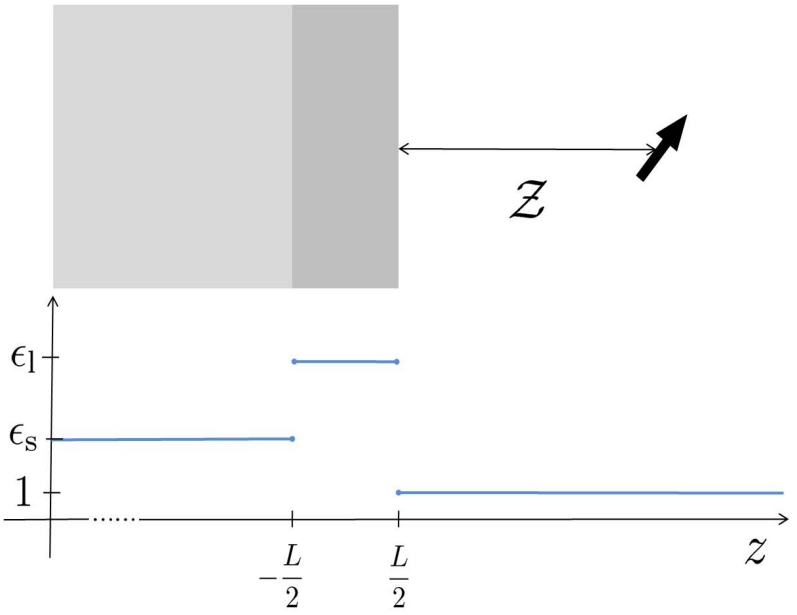

FIGURE 5.1: Atomic dipole moment in the vicinity of the layered dielectric. The dielectric function is a piecewise constant function of the coordinate z.

Our ultimate aim is to work out the energy-level shift in an atom caused by the presence of a layered dielectric. In order to obtain a result that fully takes into account retardation effects, the quantization of the electromagnetic field is necessary. To emphasize the physics of the problem we choose to quantize the electromagnetic field by a normal-mode expansion as described in [19]. The dielectric environment we consider (cf. Fig. 5.1) consists of the substrate, a dielectric half-space occupying the region of space $z < -L/2$ described by a dielectric constant $\epsilon_s = n_s^2$. On top of the substrate we place an additional dielectric layer of thickness L, which has a dielectric constant $\epsilon_1 = n_1^2$. We assume that the dielectric constant of the layer is higher than that of the substrate $\epsilon_1 > \epsilon_s$ in order to account for modes that are trapped inside the layer. Although we work with this assumption the final

result will turn out to be valid even when the reflectivity of the substrate exceeds that of the layer. Throughout the Chapter we shall assume all dielectric constants to be frequency independent so that the optical properties of the system are described solely by a pair of real numbers, $\epsilon_{\rm l}$ and $\epsilon_{\rm s}$.

To solve Maxwell equations for the electromagnetic field operators in the Heisenberg's picture we introduce, in the usual manner [10], the electromagnetic potentials $\mathbf{A}(\mathbf{r},t)$ and $\Phi(\mathbf{r},t)$ and work in the generalized Coulomb gauge

$$\boldsymbol{\nabla}\cdot[\epsilon(\mathbf{r})\mathbf{A}(\mathbf{r})]=0, \tag{5.1}$$

with the dielectric permittivity being a piecewise constant function as plotted in Fig. 5.1. In the absence of free charges one can set $\Phi(\mathbf{r},t)=0$ and work only with the vector potential $\mathbf{A}(\mathbf{r},t)$ which satisfies the wave equation

$$\nabla^2\mathbf{A}(\mathbf{r},t)-\epsilon(z)\frac{\partial^2}{\partial t^2}\mathbf{A}(\mathbf{r},t)=0,\quad |z|\neq L/2. \tag{5.2}$$

Note that right on the interfaces the condition (5.1) is singular due to discontinuities of the dielectric function and equation (5.2) doesn't hold at these points. The normal-modes of the field $\mathbf{f}(\mathbf{r})e^{i\omega t}$ satisfy the Helmholtz equation

$$\nabla^2\mathbf{f}_{\mathbf{k}\lambda}(\mathbf{r})+\epsilon(z)\omega^2\mathbf{f}_{\mathbf{k}\lambda}(\mathbf{r})=0,\quad |z|\neq L/2. \tag{5.3}$$

and we have labelled them by their wave-vector $\mathbf{k}$ and polarization $\lambda=\{\mathrm{TE},\mathrm{TM}\}$. The mode decomposition allows solving the field equation (5.2) in each distinct region of space separately and then stitch up the solutions across the interfaces by demanding that they are consistent with the Maxwell boundary conditions i.e. $\mathbf{E}_{\parallel}$, $D_{\perp}$ and $\mathbf{B}$ are continuous.

The Helmholtz equation (5.3) stems from the Hermitean operator's eigenvalue problem [19]

$$\left[\frac{1}{\sqrt{\epsilon}}\nabla\times\nabla\times\frac{1}{\sqrt{\epsilon}}\right]\sqrt{\epsilon}\mathbf{f}_{\mathbf{k}\lambda}(\mathbf{r})=-\omega^2\sqrt{\epsilon}\mathbf{f}_{\mathbf{k}\lambda}(\mathbf{r}), \tag{5.4}$$

so that we expect the weighted mode functions $\sqrt{\epsilon(\mathbf{r})}\mathbf{f}_{\mathbf{k}\lambda}(\mathbf{r})$ to form a complete set of functions being capable of describing any field configurations. The completeness relation

takes the form

$$\int \mathrm{d}^2\mathbf{k}_\parallel \sum_{k_z} f^i_{\mathbf{k}\lambda}(\mathbf{r})\, f^{*j}_{\mathbf{k}\lambda}(\mathbf{r}') = \delta^\epsilon_{ij}(\mathbf{r},\mathbf{r}'), \quad z, z' > L/2 \tag{5.5}$$

with $\delta^\epsilon_{ij}(\mathbf{r},\mathbf{r}')$ being the unit kernel in the subspace of functions satisfying (5.1), we shall call it the generalized transverse delta-function. From the considerations outlined in the Chapter 4 we expect that it is given by

$$\delta^\epsilon_{ij}(\mathbf{r},\mathbf{r}') = \delta_{ij}\delta^{(3)}(\mathbf{r}-\mathbf{r}') - \nabla_i\nabla'_j\, G(\mathbf{r},\mathbf{r}') \tag{5.6}$$

with the electrostatic Green's function of the Laplace equation given by

$$G(\mathbf{r},\mathbf{r}') = \frac{1}{4\pi}\frac{1}{|\mathbf{r}-\mathbf{r}'|} - \frac{1}{4\pi}\int_0^\infty \mathrm{d}k J_0(k|\mathbf{r}_\parallel - \mathbf{r}'_\parallel|)\frac{\frac{n_1^2-1}{n_1^2+1} - \frac{n_1^2-n_s^2}{n_s^2+n_1^2}e^{-2kL}}{1-\frac{n_1^2-1}{n_1^2+1}\frac{n_1^2-n_s^2}{n_s^2+n_1^2}e^{-2kL}}\, e^{-k(z+z')} \tag{5.7}$$

where we have chosen to confine ourselves to the case $z, z' > L/2$. The J_0 in the above equation is a Bessel function of the first kind [21, 9.1.1] and the outline of the derivation of the Green's function is given in the Appendix D.

The sum over all modes in equation (5.5) is complicated because the spectrum of the field modes has non-trivial structure. It has been shown previously [63][67] that the system supports two kinds of quite distinct types of modes. There are travelling modes going from left to right or in the opposite direction, and there are trapped modes that exist within the dielectric layer, which essentially acts as a wave-guide. The spectrum of the travelling modes is continuous whereas the spectrum of the modes trapped in the dielectric layer is discrete and only some values of the wavevector are allowed, namely those satisfying a certain dispersion relation. This dual character of the spectrum of the field modes is a major obstacle in working out the energy shift but an elegant treatment of the problem has been developed in [55], whose basic idea we follow here.

We choose the normalization convention

$$\int \mathrm{d}^3\mathbf{r}\, \epsilon(z)\mathbf{f}^*_{\mathbf{k}\lambda}(\mathbf{r})\cdot\mathbf{f}_{\mathbf{k}'\lambda'}(\mathbf{r}) = \delta_{\lambda\lambda'} \times \begin{cases} \delta^{(3)}(\mathbf{k}-\mathbf{k}') & \text{travelling modes} \\ \delta^{(2)}(\mathbf{k}_\parallel - \mathbf{k}'_\parallel)\delta_{k_z k'_z} & \text{trapped modes,} \end{cases} . \tag{5.8}$$

Then, the electric field $\mathbf{E}(\mathbf{r}) = -\partial_t \mathbf{A}(\mathbf{r})$ is expanded in terms of the normal modes as

$$\mathbf{E}(\mathbf{r}) = i \sum_{\lambda} \int \mathrm{d}^2\mathbf{k}_{\parallel} \sum_{k_z}^{\mathcal{F}} \sqrt{\frac{\omega_{\mathbf{k}}}{2\epsilon_0}} c_{\mathbf{k}\lambda} \mathbf{f}_{\mathbf{k}\lambda}(\mathbf{r}) e^{-i\omega_{\mathbf{k}} t} + \text{C.C.} \tag{5.9}$$

where C.C. stands for complex conjugate. To promote the classical field (5.9) to an operator, we introduce for each mode photon creation and annihilation operators, $a^{\dagger}_{\mathbf{k}\lambda}$ and $a_{\mathbf{k}\lambda}$, satisfying bosonic commutation relation

$$[a_{\mathbf{k}\lambda}, a^{\dagger}_{\mathbf{k}\lambda'}] = \delta_{\lambda\lambda'} \times \begin{cases} \delta^{(3)}(\mathbf{k} - \mathbf{k}') & \text{travelling photons} \\ \delta^{(2)}(\mathbf{k}_{\parallel} - \mathbf{k}'_{\parallel}) \delta_{k_z k'_z} & \text{trapped photons} \end{cases} . \tag{5.10}$$

These operators replace c-numbers $c_{\mathbf{k}\lambda}$ in the expansion (5.9) which accomplishes the quantization of the electromagnetic field. To be able to write out the field operators explicitly one needs to solve the eigenvalue problem (5.3) and determine the spatial dependence of functions $\mathbf{f}_{\mathbf{k}\lambda}(\mathbf{r})$ so we turn our attention to this now.

5.2.1 Travelling modes

Before the travelling modes are worked out, for further convenience, we introduce Fresnel coefficients for a single interface. Assume that a plane wave is travelling from the medium with refractive index n_{b} to the medium with the refractive index n_{a}, the interface being the $z = 0$ plane. Then, the standard Fresnel reflection and transmission coefficients given by [10]

$$\begin{aligned} r^{\mathrm{ba}}_{\mathrm{TE}} &= \frac{k_{\mathrm{zb}} - k_{\mathrm{za}}}{k_{\mathrm{zb}} + k_{\mathrm{za}}} , \qquad t^{\mathrm{ba}}_{\mathrm{TE}} = \frac{2k_{\mathrm{zb}}}{k_{\mathrm{zb}} + k_{\mathrm{za}}} , \\ r^{\mathrm{ba}}_{\mathrm{TM}} &= \frac{k_{\mathrm{zb}}/n^2_{\mathrm{b}} - k_{\mathrm{za}}/n^2_{\mathrm{a}}}{k_{\mathrm{zb}}/n^2_{\mathrm{b}} + k_{\mathrm{za}}/n^2_{\mathrm{a}}} , \; t^{\mathrm{ba}}_{\mathrm{TM}} = \frac{2k_{\mathrm{zb}}/n_{\mathrm{a}}n_{\mathrm{b}}}{k_{\mathrm{zb}}/n^2_{\mathrm{b}} + k_{\mathrm{za}}/n^2_{\mathrm{a}}} , \end{aligned} \tag{5.11}$$

where k_{zi} are the components of the wavevectors perpendicular to the interface in the medium $\mathrm{i} = \{\mathrm{a}, \mathrm{b}\}$.

The geometry of the problem (cf. Fig. 5.1) naturally divides the space into three distinct regions. Consequently there are three wavevectors to be distinguished. The wavevector in

vacuum ($z > L/2$)

$$\mathbf{k}^{\pm} = (k_{\rm x}, k_{\rm y}, \pm k_{\rm z}) = (\mathbf{k}_{\parallel}, \pm k_{\rm z}), \tag{5.12}$$

the wavevector in the dielectric layer ($|z| < L/2$)

$$\mathbf{k}_{\rm l}^{\pm} = (k_{\rm x}, k_{\rm y}, \pm k_{\rm zl}) = (\mathbf{k}_{\parallel}, \pm k_{\rm zl}), \tag{5.13}$$

and the wavevector in the substrate ($z < -L/2$)

$$\mathbf{k}_{\rm s}^{\pm} = (k_{\rm x}, k_{\rm y}, \pm k_{\rm zs}) = (\mathbf{k}_{\parallel}, \pm k_{\rm zs}). \tag{5.14}$$

The components of the wavevector that are parallel to the surface are the same for all three regions of space. This follows directly from the requirement that the boundary conditions must be satisfied at all points of a given surface i.e. the spatial phase factors $e^{i\mathbf{k}_i\cdot\mathbf{r}}$ must be equal at $z = \pm L/2$ for all $\mathbf{r}_{\parallel}$. The different signs of the z-components of the wavevectors correspond to the waves propagating in different directions. However, the direction of the propagation of a particular mode needs to be consistent in all three layers so we require that on the real axis

$$\mathrm{sign}(\mathrm{k_z}) = \mathrm{sign}(\mathrm{k_{zl}}) = \mathrm{sign}(\mathrm{k_{zs}}). \tag{5.15}$$

Since the frequency ω of a single mode is fixed, the z-components of the wavevectors in the dielectric are related to the vacuum wavevector $k_{\rm z}$ by

$$k_{\rm zl} = \sqrt{(n_{\rm l}^2 - 1)\mathbf{k}_{\parallel}^2 + n_{\rm l}^2 k_{\rm z}^2}\,, \tag{5.16}$$

$$k_{\rm zs} = \sqrt{(n_{\rm s}^2 - 1)\mathbf{k}_{\parallel}^2 + n_{\rm s}^2 k_{\rm z}^2}\,. \tag{5.17}$$

The mode functions $\mathbf{f}_{\mathbf{k}\lambda}(\mathbf{r})$ are transverse everywhere except right on the interfaces $z = \pm L/2$, cf. (5.1). To ensure this transversality, it is convenient to introduce orthonormal polarisation vectors

$$\mathbf{f}_{\mathbf{k}\lambda}(\mathbf{r}) = \hat{\mathbf{e}}_{\lambda}(\mathbf{k}) f_{\mathbf{k}\lambda}(\mathbf{r}) \tag{5.18}$$

defined as

$$\begin{aligned} \hat{\mathbf{e}}_{\rm TE}(\boldsymbol{\nabla}) &= (-\Delta_{\parallel})^{-1/2}\big(-i\nabla_{\rm y}, i\nabla_{\rm x}, 0\big), \\ \hat{\mathbf{e}}_{\rm TM}(\boldsymbol{\nabla}) &= (\Delta_{\parallel}\Delta)^{-1/2}\big(-\nabla_{\rm x}\nabla_{\rm z}, -\nabla_{\rm y}\nabla_{\rm z}, \Delta_{\parallel}\big), \end{aligned} \tag{5.19}$$

with Δ being the Laplace operator expressed in Cartesian coordinates and it is understood that the above operators act on the factors of the type $e^{i\mathbf{k}_{\rm i}^{\pm}\mathbf{r}}$ i.e. $\hat{\mathbf{e}}_\lambda(\mathbf{k}_{\rm i}^{\pm}) \equiv \hat{\mathbf{e}}_\lambda(\nabla)e^{i\mathbf{k}_{\rm i}^{\pm}\mathbf{r}}$. Polarization vectors defined in such a way are normalized to unity provided all three components of the wavevector are real. This statement breaks down in the case of evanescent waves which have wavevectors with pure imaginary components. The spatial dependence of the mode functions is worked out requiring that each mode consists of the incoming, reflected and transmitted parts that are joined together by standard boundary conditions across the interfaces, i.e. $\mathbf{E}_\parallel$, $D_\perp$ and $\mathbf{B}$ are continuous.

With this the travelling modes of the system incident from the left, normalized according to (5.8), are given by

$$\mathbf{f}^L_{\mathbf{k}\lambda}(\mathbf{r}) = \frac{\hat{\mathbf{e}}_\lambda(\nabla)}{(2\pi)^{3/2}n_{\rm s}} \begin{cases} e^{i\mathbf{k}_{\rm s}^{+}\cdot\mathbf{r}} + R^L_\lambda e^{i\mathbf{k}_{\rm s}^{-}\cdot\mathbf{r}} & z < -L/2 \\ I^L_\lambda e^{i\mathbf{k}_{\rm l}^{+}\cdot\mathbf{r}} + J^L_\lambda e^{i\mathbf{k}_{\rm l}^{-}\cdot\mathbf{r}} & |z| < L/2 \\ T^L_\lambda e^{i\mathbf{k}^{+}\cdot\mathbf{r}} & z > L/2 \end{cases}, \tag{5.20}$$

whereas the right-incident modes are given by

$$\mathbf{f}^R_{\mathbf{k}\lambda}(\mathbf{r}) = \frac{\hat{\mathbf{e}}_\lambda(\nabla)}{(2\pi)^{3/2}} \begin{cases} T^R_\lambda e^{i\mathbf{k}_{\rm s}^{-}\cdot\mathbf{r}} & z < -L/2 \\ I^R_\lambda e^{i\mathbf{k}_{\rm l}^{-}\cdot\mathbf{r}} + J^R_\lambda e^{i\mathbf{k}_{\rm l}^{+}\cdot\mathbf{r}} & |z| < L/2 \\ e^{i\mathbf{k}^{-}\cdot\mathbf{r}} + R^R_\lambda e^{i\mathbf{k}^{+}\cdot\mathbf{r}} & z > L/2 \end{cases}. \tag{5.21}$$

For the sake of clarity the reflection and transmission coefficients are listed in full in Appendix C whereas here we only write down the most relevant of them:

$$R^R_\lambda = \frac{r^{\rm vl}_\lambda + r^{\rm ls}_\lambda e^{2ik_{\rm zl}L}}{1 + r^{\rm vl}_\lambda r^{\rm ls}_\lambda e^{2ik_{\rm zl}L}} e^{-ik_{\rm z}L}, \tag{5.22}$$

$$T^L_\lambda = \frac{t^{\rm sl}_\lambda t^{\rm lv}_\lambda e^{(2ik_{\rm zl} - ik_{\rm zs} - ik_{\rm z})L/2}}{1 + r^{\rm sl}_\lambda r^{\rm lv}_\lambda e^{2ik_{\rm zl}L}}. \tag{5.23}$$

5.2.2 Trapped modes

Trapped modes correspond to the repeated total internal reflections within the layer of higher refractive index $n_{\rm l}$. This happens when the angle of incidence of the incoming

wave is sufficiently high and exceeds some critical angle. This critical angle is different for the two opposite waveguide interfaces. First consider the layer-vacuum interface. From equation (5.16) we can obtain the reciprocal relation expressing the k_{z} in terms of the k_{zl}

$$k_{\mathrm{z}} = \frac{1}{n_{\mathrm{l}}}\sqrt{k_{\mathrm{zl}}^2 - (n_{\mathrm{l}}^2 - 1)\mathbf{k}_{\parallel}^2} \tag{5.24}$$

It is seen that whenever $k_{\mathrm{zl}}^2 < (n_{\mathrm{l}}^2 - 1)\mathbf{k}_{\parallel}^2$ the k_{z} becomes pure imaginary

$$k_{\mathrm{z}} = +\frac{i}{n_{\mathrm{l}}}\sqrt{(n_{\mathrm{l}}^2 - 1)\mathbf{k}_{\parallel}^2 - k_{\mathrm{zl}}^2} \tag{5.25}$$

and we have a mode that exhibits evanescent behaviour on the vacuum side. The sign of the square root is chosen so that these modes decay exponentially when moving away from the layer in the positive z-direction. This also ensures that the total internal reflection truly occurs i.e. $|r_{\lambda}^{\mathrm{vl}}|^2 = 1$.

However, since on the other side of the waveguide we have a substrate rather than vacuum not all of the modes internally reflected at the vacuum-layer interface get trapped. From the relation

$$k_{\mathrm{zs}} = \frac{n_{\mathrm{s}}}{n_{\mathrm{l}}}\sqrt{k_{\mathrm{zl}}^2 - \mathbf{k}_{\parallel}^2\left(\frac{n_{\mathrm{l}}^2}{n_{\mathrm{s}}^2} - 1\right)} \tag{5.26}$$

we get the condition of total internal reflection for the substrate-dielectric interface to be $k_{\mathrm{zl}}^2 \leq (n_{\mathrm{l}}^2/n_{\mathrm{s}}^2 - 1)\mathbf{k}_{\parallel}^2$. Therefore, the modes satisfying the condition

$$(n_{\mathrm{l}}^2/n_{\mathrm{s}}^2 - 1)\mathbf{k}_{\parallel}^2 \leq k_{\mathrm{zl}}^2 \leq (n_{\mathrm{l}}^2 - 1)\mathbf{k}_{\parallel}^2 \tag{5.27}$$

are not trapped but appear in vacuum as a continuous spectrum of evanescent waves that are accounted for in the left-incident travelling modes, their quantization was first presented in [52]. The trapped modes occur if

$$0 \leq k_{\mathrm{zl}}^2 \leq (n_{\mathrm{l}}^2/n_{\mathrm{s}}^2 - 1)\mathbf{k}_{\parallel}^2. \tag{5.28}$$

The procedure of obtaining the trapped modes is largely equivalent to that of the travelling modes. They have the form

$$\mathbf{f}^{T}_{\mathbf{k}\lambda}(\mathbf{r}) = N_\lambda \hat{\mathbf{e}}_\lambda(\nabla) \begin{cases} T^{\mathrm{ls}}_\lambda e^{i\mathbf{k}^{-}_{\mathrm{s}}\cdot\mathbf{r}} & z < -L/2 \\ V_\lambda e^{i\mathbf{k}^{-}_{\mathrm{l}}\cdot\mathbf{r}} + e^{i\mathbf{k}^{+}_{\mathrm{l}}\cdot\mathbf{r}} & |z| < L/2 \\ T^{\mathrm{lv}}_\lambda e^{i\mathbf{k}^{+}\cdot\mathbf{r}} & z > L/2 \end{cases} . \tag{5.29}$$

Standard boundary conditions are imposed on both interfaces and from $z = -L/2$ boundary we get

$$\begin{aligned} T^{\mathrm{ls}}_\lambda &= (t^{\mathrm{ls}}_\lambda / r^{\mathrm{ls}}_\lambda) e^{-i(k_{\mathrm{zl}}+k_{\mathrm{zs}})L/2} , \\ V_\lambda &= (1/r^{\mathrm{ls}}_\lambda) e^{-ik_{\mathrm{zl}}L} , \end{aligned} \tag{5.30}$$

whereas from the $z = L/2$ boundary

$$\begin{aligned} T^{\mathrm{lv}}_\lambda &= t^{\mathrm{lv}}_\lambda e^{-i(k_{\mathrm{zl}}-k_{\mathrm{z}})L/2} , \\ V_\lambda &= r^{\mathrm{lv}}_\lambda e^{ik_{\mathrm{zl}}L}. \end{aligned} \tag{5.31}$$

Since both equations, (5.30) and (5.31), need to be simultaneously satisfied we have our dispersion relation

$$1 + r^{\mathrm{vl}}_\lambda r^{\mathrm{ls}}_\lambda e^{2ik_{\mathrm{zl}}L} = 0 \tag{5.32}$$

that determines the allowed values of k_{zl} within the layer. Since we will be dealing with an atom on the vacuum side it will be necessary to express the dispersion relation in terms of k_z rather than k_{zl}. With little effort one can show that the allowed values of the z-component of the evanescent waves' wavevector appearing on the vacuum side are given by numbers q^n_λ:

$$\begin{aligned} q^n_{\mathrm{TE}} &= \{k_{\mathrm{z}} : k_{\mathrm{z}} + ik_{\mathrm{zl}}(k_{\mathrm{z}}) \tan[\phi_{\mathrm{TE}}(k_{\mathrm{z}})] = 0\} , \\ q^n_{\mathrm{TM}} &= \left\{k_{\mathrm{z}} : k_{\mathrm{z}} + ik_{\mathrm{zl}}(k_{\mathrm{z}})/n^2_{\mathrm{l}} \tan[\phi_{\mathrm{TM}}(k_{\mathrm{z}})] = 0\right\} , \end{aligned} \tag{5.33}$$

with

$$\begin{aligned}\phi_{\rm TE}(k_{\rm z}) &= \arg\left[(k_{\rm zl}+k_{\rm zs})e^{-ik_{\rm zl}L}\right],\\ \phi_{\rm TE}(k_{\rm z}) &= \arg\left[(k_{\rm zl}/n_{\rm l}^2+k_{\rm zs}/n_{\rm s}^2)e^{-ik_{\rm zl}L}\right].\end{aligned}$$

The numbers q_λ^n lie on the imaginary $k_{\rm z}$-axis, they satisfy, cf. Eq. (5.25) and (5.28),

$$\left(\frac{1}{n_{\rm l}^2}-1\right)\mathbf{k}_\parallel^2 < (q_\lambda^n)^2 < \left(\frac{1}{n_{\rm s}^2}-1\right)\mathbf{k}_\parallel^2. \tag{5.34}$$

The normalization constant N_λ for trapped modes is easily obtained by the direct evaluation of the integral (5.8). It is given by

$$N_\lambda = \frac{1}{2\pi}\left[2n_{\rm l}^2L + F_\lambda(n_{\rm l},n_{\rm s}) + F_\lambda(n_{\rm l},1)\right]^{-1/2} \tag{5.35}$$

with

$$F_\lambda(n_{\rm l},n_{\rm s}) = \frac{n_{\rm s}^2}{2}|\hat{\mathbf{e}}_\lambda(\mathbf{k}_{\rm s}^-)|^2\frac{|t_\lambda^{\rm ls}|^2}{|k_{\rm zs}|} - \frac{n_{\rm l}}{k_{\rm zl}}{\rm Im}(r_\lambda^{\rm ls})\;\hat{\mathbf{e}}_\lambda^*(\mathbf{k}_{\rm l}^+)\cdot\hat{\mathbf{e}}_\lambda(\mathbf{k}_{\rm l}^-)$$

and the reader is reminded that in (5.35) the z-components of the wavevectors $\mathbf{k}$ and $\mathbf{k}_{\rm s}$ are pure imaginary and because of that the TM polarization vectors $\hat{\mathbf{e}}_{\rm TM}(\mathbf{k}^-)$ and $\hat{\mathbf{e}}_{\rm TM}(\mathbf{k}_{\rm s}^-)$ are no longer normalized to unity.

5.2.3 Field operators and commutation relations. Completeness of the modes.

Now that we have determined the spatial dependence of the mode functions we are in position to write out the vector potential field operator explicitly

$$\begin{aligned}\hat{\mathbf{A}}(\mathbf{r},t) = \Bigg\{ &\int{\rm d}^2\mathbf{k}_\parallel\int_0^\infty{\rm d}k_{\rm z}\frac{1}{\sqrt{2\epsilon_0\omega_{\mathbf{k}}}}\mathbf{f}_{\mathbf{k}\lambda}^R(\mathbf{r})a_{\mathbf{k}\lambda}^R e^{-i\omega_{\mathbf{k}}t}\\ &+\int{\rm d}^2\mathbf{k}_\parallel\int_0^\infty{\rm d}k_{\rm zs}\frac{1}{\sqrt{2\epsilon_0\omega_{\mathbf{k}}}}\mathbf{f}_{\mathbf{k}\lambda}^L(\mathbf{r})a_{\mathbf{k}\lambda}^L e^{-i\omega_{\mathbf{k}}t}\\ &+\int{\rm d}^2\mathbf{k}_\parallel\sum_{k_{\rm zl}}\frac{1}{\sqrt{2\epsilon_0\omega_{\mathbf{k}}}}\mathbf{f}_{\mathbf{k}\lambda}^T(\mathbf{r})a_{\mathbf{k}\lambda}^T e^{-i\omega_{\mathbf{k}}t}\Bigg\} + {\rm H.C.}\end{aligned} \tag{5.36}$$

The sum in the last term runs over the allowed values of the z-component of the layer's wavevector k_{zl} i.e. solutions of the dispersion relation (5.32). For a given type of mode, left-incident, right-incident or trapped, photon creation and annihilation operators appearing in (5.39) satisfy the commutation relations (5.10). Commutators between photon operators corresponding to different types of modes vanish as a consequence of the orthogonality of the field modes (5.8), e.g.

$$\left[a^{L}_{\mathbf{k}\lambda}, \left(a^{R}_{\mathbf{k}'\lambda'}\right)^{\dagger}\right] = 0. \tag{5.37}$$

We would like to explicitly verify the equal-time canonical commutation relation between field operators, say the electric field operator $\hat{\mathbf{E}}(\mathbf{r},t)$ and the vector potential operator $\hat{\mathbf{A}}(\mathbf{r},t)$

$$\left[\hat{A}_i(\mathbf{r},t), \epsilon_0 \hat{E}_j(\mathbf{r}',t)\right] = -i\delta^{\epsilon}_{ij}(\mathbf{r},\mathbf{r}'), \quad z,z' > L/2 \tag{5.38}$$

with $\delta^{\epsilon}_{ij}(\mathbf{r},\mathbf{r}')$ given by Eq. (5.6) and (5.7). To evaluate (5.38) we shall need the electric field operator

$$\begin{aligned}\hat{\mathbf{E}}(\mathbf{r},t) = i\Bigg\{ &\int \mathrm{d}^2\mathbf{k}_{\parallel} \int_0^{\infty} \mathrm{d}k_{\mathrm{z}} \sqrt{\frac{\omega_{\mathbf{k}}}{2\epsilon_0}} \mathbf{f}^{R}_{\mathbf{k}\lambda}(\mathbf{r}) a^{R}_{\mathbf{k}\lambda} e^{-i\omega_{\mathbf{k}}t} \\ &+ \int \mathrm{d}^2\mathbf{k}_{\parallel} \int_0^{\infty} \mathrm{d}k_{\mathrm{zs}} \sqrt{\frac{\omega_{\mathbf{k}}}{2\epsilon_0}} \mathbf{f}^{L}_{\mathbf{k}\lambda}(\mathbf{r}) a^{L}_{\mathbf{k}\lambda} e^{-i\omega_{\mathbf{k}}t} \\ &+ \int \mathrm{d}^2\mathbf{k}_{\parallel} \sum_{k_{\mathrm{zl}}} \sqrt{\frac{\omega_{\mathbf{k}}}{2\epsilon_0}} \mathbf{f}^{T}_{\mathbf{k}\lambda}(\mathbf{r}) a^{T}_{\mathbf{k}\lambda} e^{-i\omega_{\mathbf{k}}t} \Bigg\} + H.C.\end{aligned} \tag{5.39}$$

Plugging in the operators (5.39) and (5.36) into (5.38) and making use of commutation relations (5.10) and (5.37) we are led to result that the LHS of (5.38) is given by

$$\begin{aligned}\mathrm{LHS} = i\mathrm{Re} \sum_{\lambda} \int \mathrm{d}^2\mathbf{k}_{\parallel} \Bigg[&\int_0^{\infty} \mathrm{d}k_{\mathrm{z}}\ f^{R}_{\mathbf{k}\lambda,i}(\mathbf{r}) f^{*R}_{\mathbf{k}\lambda,j}(\mathbf{r}') \\ &+ \int_0^{\infty} \mathrm{d}k_{\mathrm{zs}}\ f^{L}_{\mathbf{k}\lambda,i}(\mathbf{r}) f^{*L}_{\mathbf{k}\lambda,j}(\mathbf{r}') \\ &+ \sum_{k_{\mathrm{zl}}}\ f^{T}_{\mathbf{k}\lambda,i}(\mathbf{r}) f^{*T}_{\mathbf{k}\lambda,j}(\mathbf{r}') \Bigg].\end{aligned} \tag{5.40}$$

The quantity on the right-hand side is the summation over all modes just as prescribed by equation (5.5) and therefore we expect it to be equal to the generalized transverse delta function, Eq. (5.6). This shows that the statement of the completeness of the modes (5.5)

is in fact equivalent to the commutation relation (5.38), as has been noted before in [53].

To prove that the relation

$$\delta^{\epsilon}_{ij}(\mathbf{r},\mathbf{r}') = \sum_{\lambda}\int \mathrm{d}^2\mathbf{k}_{\parallel}\Bigg[\int_0^{\infty}\mathrm{d}k_{\mathrm{z}}\; f^{R}_{\mathbf{k}\lambda,i}(\mathbf{r}) f^{*R}_{\mathbf{k}\lambda,j}(\mathbf{r}') + \int_0^{\infty}\mathrm{d}k_{\mathrm{zs}}\; f^{L}_{\mathbf{k}\lambda,i}(\mathbf{r}) f^{*L}_{\mathbf{k}\lambda,j}(\mathbf{r}') + \sum_{k_{\mathrm{zl}}}\; f^{T}_{\mathbf{k}\lambda,i}(\mathbf{r}) f^{*T}_{\mathbf{k}\lambda,j}(\mathbf{r}')\Bigg] \tag{5.41}$$

holds for $z, z' > L/2$ we need to carry out the sum over all field modes. To get started we carry out a change of variables in (5.41). We convert the k_{zs}-integral and the k_{zl}-sum to run over the values of k_{z}. In the case of the integral it is a simple change of variables according to (5.17)

$$\int_0^{\infty}\mathrm{d}k_{\mathrm{zs}} = n_{\mathrm{s}}^2\int_0^{\infty}\mathrm{d}k_{\mathrm{z}}\frac{k_{\mathrm{z}}}{k_{\mathrm{zs}}} + n_{\mathrm{s}}^2\int_{i\Gamma_{\mathrm{s}}}^{0}\mathrm{d}k_{\mathrm{z}}\frac{k_{\mathrm{z}}}{k_{\mathrm{zs}}} \tag{5.42}$$

with $\Gamma_{\mathrm{s}} = \sqrt{(n_{\mathrm{s}}^2-1)\mathbf{k}_{\parallel}^2}/n_{\mathrm{s}}$. It is seen that the contributions from the left-incident modes split into a travelling part and an evanescent part. The values of k_{z} included in the last integral correspond to the condition stated in equation (5.27). In the case of the sum we change the summation over k_{zl} to run over the values of k_{z} as defined by equation (5.33). Plugging in the mode functions (5.20) and (5.21) into equation (5.41) and utilizing straightforward properties of the reflection and transmission coefficients that hold for real $k_{\mathrm{z}}, k_{\mathrm{zs}}$,

$$R^{*R}_{\lambda}(-k_{\mathrm{z}}) = R^{R}_{\lambda}(k_{\mathrm{z}}), \qquad \frac{k_{\mathrm{z}}}{k_{\mathrm{zs}}}\left|T^{L}_{\lambda}\right|^2 + \left|R^{R}_{\lambda}\right|^2 = 1, \tag{5.43}$$

we can rewrite the completeness relation as

$$\delta^{\epsilon}_{ij}(\mathbf{r},\mathbf{r}') = \delta^{\perp}_{ij}(\mathbf{r}-\mathbf{r}') + \sum_{\lambda}\hat{\mathrm{e}}^{i}_{\lambda}(\nabla)\hat{\mathrm{e}}^{*j}_{\lambda}(\nabla')\int\mathrm{d}^2\mathbf{k}_{\parallel}e^{i\mathbf{k}_{\parallel}(\mathbf{r}_{\parallel}-\mathbf{r}'_{\parallel})}\Bigg\{\sum_{q^n_{\lambda}}|N_{\lambda}|^2\left|T^{\mathrm{lv}}_{\lambda}\right|^2 e^{ik_{\mathrm{z}}(z+z')} + \frac{1}{(2\pi)^3}\int_{i\Gamma_{\mathrm{s}}}^{0}\mathrm{d}k_{\mathrm{z}}\frac{k_{\mathrm{z}}}{k_{\mathrm{zs}}}\left|T^{L}_{\lambda}\right|^2 e^{ik_{\mathrm{z}}(z+z')} + \frac{1}{(2\pi)^3}\int_{-\infty}^{\infty}\mathrm{d}k_{\mathrm{z}}R^{R}_{\lambda}e^{ik_{\mathrm{z}}(z+z')}\Bigg\}. \tag{5.44}$$

The first term in the above equation is the standard transverse delta-function. Therefore, if equation (5.41) is to hold, the term in the curly brackets needs to be proportional to the reflection part of the electrostatic Greens function, cf. Eq. (5.7). Note however that it contains two integrals and a sum and at this stage it is not clear how to proceed with the proof that it is indeed the case. Now it is apparent that the discreteness of the spectrum of the trapped modes is a nuisance that needs to be overcome if one is to complete the

task of summing over the electromagnetic modes successfully. Similar difficulty would appear in any perturbative calculation in this type of geometry, which led Eberlein and Contreras Reyes to address the problem in a considerable detail [55]. We proceed with a completely analogous method to [55] first noting that what we have here can be considered as a superposition of a slab and a half-space geometry, cf. [55] and [53]. One can utilize the branch-cut due to k_{zs} (it runs along the imaginary k_{z} axis between $\pm i\Gamma_{\mathrm{s}}$, cf. Fig. 5.2) to express the integral of $|T_\lambda^L|^2$ in (5.44) as an integral of the reflection coefficient R_λ^R that runs from 0^- along the square root cut up to the branch-point at $+i\Gamma_{\mathrm{s}}$ and then back down to the origin 0^+. Note that the branch-cut due to the k_{zl} is irrelevant because of the symmetry property of the reflection coefficient $R_\lambda^R(-k_{\mathrm{zl}}) = R_\lambda^R(k_{\mathrm{zl}})$. Indeed, the first two integrals in the curly braces in equation (5.44) can be combined together as a single integral in the complex k_{z} plane [53]. This is possible because the relation

$$\frac{k_{\mathrm{z}}}{k_{\mathrm{zs}}}\left|T_\lambda^L\right|^2\Big|_{k_{\mathrm{z}};\, k_{\mathrm{zs}},k_{\mathrm{zl}}>0} = R_\lambda^R\Big|_{k_{\mathrm{z}};\, k_{\mathrm{zs}},k_{\mathrm{zl}}>0} - R_\lambda^R\Big|_{k_{\mathrm{z}};\, k_{\mathrm{zs}},k_{\mathrm{zl}}<0} \tag{5.45}$$

continues to hold for coefficients (5.22) with purely imaginary z-component of the vacuum wavevector k_{z} (cf. [54]). Thus, the contributions from the travelling and evanescent modes can be combined into a one single complex integral along the path γ_{s} depicted in Fig. 5.2 and the term in the curly brackets of equation (5.44) becomes

$$\frac{1}{(2\pi)^3}\int_{\gamma_{\mathrm{s}}} \mathrm{d}k_{\mathrm{z}} R_\lambda^R \hat{e}_\lambda^i(\mathbf{k}^+)\hat{e}_\lambda^j(\mathbf{k}^-)e^{ik_{\mathrm{z}}(z+z')} + \sum_{q_\lambda^n} |N_\lambda|^2 \left|T_\lambda^{\mathrm{lv}}\right|^2 \hat{e}_\lambda^i(\mathbf{k}^+)\hat{e}_\lambda^j(\mathbf{k}^-)e^{ik_{\mathrm{z}}(z+z')}. \tag{5.46}$$

Here we have now included the polarization vectors explicitly in the integrals. This is a crucial step as they alter the analytical structure of the complex k_z-plane. In particular, the TM polarization vector introduces a pole at the points where $k_{\mathrm{z}} = \pm i|\mathbf{k}_{\parallel}|$ due to the factor $1/|\mathbf{k}|^2$ present in the normalization factor. We will see that this is precisely this pole that gives rise to the reflection term present in (5.6).

Recall equation (5.22) which shows that the reflection coefficient contains the phase factor $e^{-ik_{\mathrm{z}}L}$. Since $z + z' - L > 0$ the argument of the exponential in (5.46) is negative in the upper half of the complex k_z plane and we can evaluate the k_{z}-integral in equation (5.46) by closing the contour in the upper half-plane. For this we need to determine the analytical properties of R_λ^R. We note that the denominator of the reflection coefficient (5.22) is

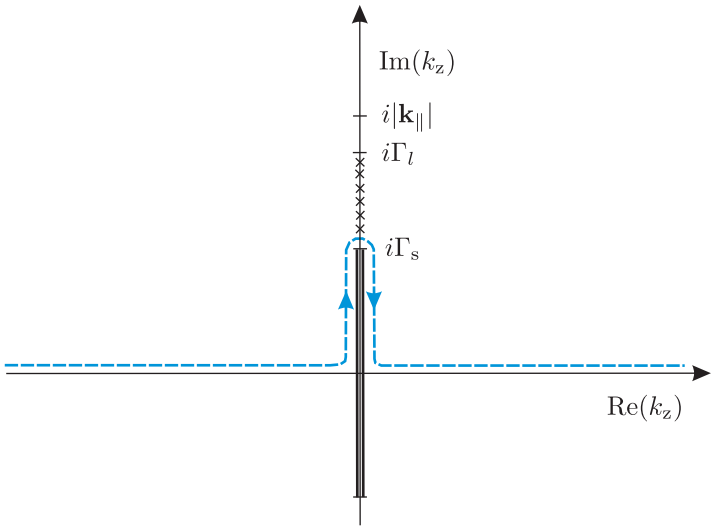

FIGURE 5.2: The dashed line represents the contour γ_s used to evaluate the k_z integral in Eq. (5.46). Here $\Gamma_s = \sqrt{(n_s^2-1)\mathbf{k}_\parallel^2}/n_s$ and $\Gamma_l = \sqrt{(n_l^2-1)\mathbf{k}_\parallel^2}/n_l$. The crosses represent the poles of the reflection coefficient R_λ^R i.e. the solutions to the dispersion relation (5.32).

precisely the dispersion relation (5.32). Rewriting the reflection coefficients in the form

$$R_{\mathrm{TE}}^R = \frac{k_z - k_{zl}\left(\dfrac{1-r_{\mathrm{TE}}^{ls}\exp(2ik_{zl}L)}{1+r_{\mathrm{TE}}^{ls}\exp(2ik_{zl}L)}\right)}{k_z + k_{zl}\left(\dfrac{1-r_{\mathrm{TE}}^{ls}\exp(2ik_{zl}L)}{1+r_{\mathrm{TE}}^{ls}\exp(2ik_{zl}L)}\right)}, \quad R_{\mathrm{TM}}^R = \frac{k_z - \dfrac{k_{zl}}{n_l^2}\left(\dfrac{1-r_{\mathrm{TM}}^{ls}\exp(2ik_{zl}L)}{1+r_{\mathrm{TM}}^{ls}\exp(2ik_{zl}L)}\right)}{k_z + \dfrac{k_{zl}}{n_l^2}\left(\dfrac{1-r_{\mathrm{TM}}^{ls}\exp(2ik_{zl}L)}{1+r_{\mathrm{TM}}^{ls}\exp(2ik_{zl}L)}\right)}$$

allows us to deduce that R_λ^R has a finite number of simple poles on the imaginary axis. When closing the contour we enclose all of them and by Cauchy's theorem the problem is reduced to the evaluation of the residues at these points.

$$\begin{aligned}\sum_\lambda \int_{\gamma_s} \mathrm{d}k_z R_\lambda^R \hat{e}_\lambda^i(\mathbf{k}^+)\hat{e}_\lambda^j(\mathbf{k}^-)e^{ik_z(z+z')} &= 2\pi i \sum_\lambda \sum_{\mathrm{Res}} R_\lambda^R \hat{e}_\lambda^i(\mathbf{k}^+)\hat{e}_\lambda^j(\mathbf{k}^-)e^{ik_z(z+z')} \\ &= 2\pi i \sum_\lambda \sum_{q_\lambda^n} \lim_{k_z\to q_\lambda^n}(k_z - q_\lambda^n)\hat{e}_\lambda^i(\mathbf{k}^+)\hat{e}_\lambda^j(\mathbf{k}^-)\frac{r_\lambda^{vl}+r_\lambda^{ls}e^{2ik_{zl}L}}{1+r_\lambda^{vl}r_\lambda^{ls}e^{2ik_{zl}L}}e^{ik_z(z+z'-L)} \\ &+2\pi i \lim_{k_z\to i|\mathbf{k}_\parallel|}(k_z - i|\mathbf{k}_\parallel|)\hat{e}_{\mathrm{TM}}^i(\mathbf{k}^+)\hat{e}_{\mathrm{TM}}^j(\mathbf{k}^-)\frac{r_\lambda^{vl}+r_\lambda^{ls}e^{2ik_{zl}L}}{1+r_\lambda^{vl}r_\lambda^{ls}e^{2ik_{zl}L}}e^{ik_z(z+z'-L)}\end{aligned}$$

Here, the first term represents the contributions from the poles in the reflection coefficient and corresponds the trapped modes, whereas the second term represents the contributions from the pole that arises due to the TM polarization vector. When carrying out the

calculation explicitly one needs to remember that the two independent variables are k_z and $\mathbf{k}_\parallel$ and that, according to Eq. (5.16) and (5.17), k_zl and k_zs are functions of those. In addition, the denominator of the reflection coefficient is not of the form $f(k_\mathrm{z})(k_\mathrm{z}-q_\lambda^n)$ so that multiplying it with $(k_\mathrm{z}-q_\lambda^n)$ does not remove the singularity, the whole expression is still indeterminate. Therefore, l'Hôpital's rule needs to be used to evaluate the limit. Doing so we find that

$$\begin{aligned}\frac{1}{(2\pi)^3}\int_{\gamma_\mathrm{s}}\mathrm{d}k_\mathrm{z}R_\lambda^R\hat{e}_\lambda^i(\mathbf{k}^+)\hat{e}_\lambda^j(\mathbf{k}^-)e^{ik_\mathrm{z}(z+z')}\\ =-\sum_{q_\lambda^n}|N_\lambda|^2\left|T_\lambda^\mathrm{lv}\right|^2\hat{e}_\lambda^i(\mathbf{k}^+)\hat{e}_\lambda^j(\mathbf{k}^-)e^{ik_\mathrm{z}(z+z')}-\nabla_i\nabla'_jG^R(\mathbf{r},\mathbf{r}')\end{aligned}\tag{5.47}$$

where $G^R(\mathbf{r},\mathbf{r}')$ is the reflected part of the Green's function of the Poisson equation given in Eq. (5.6). We see that the poles of the reflection coefficient R_λ^R yield a term that exactly cancels out the contributions of the trapped modes to the completeness relation (5.44) whereas the pole of the TM polarization vector yields the term proportional to Green's function. Thus, the final result can be written as

$$\begin{aligned}\int\mathrm{d}^2\mathbf{k}_\parallel\sum_{k_z}\!\!\!\!\!\!\int f_{\mathbf{k}\lambda}^i(\mathbf{r})f_{\mathbf{k}\lambda}^{*j}(\mathbf{r}')&=\frac{1}{i}[A_i(\mathbf{r}),-\epsilon_0E_j(\mathbf{r}')]\\ &=\delta_{ij}^\perp(\mathbf{r}-\mathbf{r}')-\nabla_i\nabla'_jG^R(\mathbf{r},\mathbf{r}')\quad z,z'>L/2\end{aligned}$$

which is precisely what we have anticipated on the basis of our discussion in Chapter 4. In the next section we demonstrate how the calculation presented here may be applied to accomplish typical perturbative QED calculation in a layered geometry.

5.3 Energy shift

To work out the energy shift we use standard perturbation theory where the atom is treated by means of the Schrödinger quantum mechanics and only the electromagnetic field is second-quantized. Taking the interaction Hamiltonian to be

$$H_\mathrm{int}=-\boldsymbol{\mu}\cdot\mathbf{E}\tag{5.48}$$

the energy shift of the atomic state i, up to the second-order, is given by

$$\Delta E_i = \langle i;0|H_{\rm int}|i;0\rangle + \sum_{j\neq i}\sum\!\!\!\!\!\!\int_{\mathbf{k},\lambda} \frac{|\langle j;0|H_{\rm int}|i;1_{\mathbf{k}\lambda}\rangle|^2}{E_i-(E_j+\omega_{\mathbf{k}})}.$$

Here, $\boldsymbol{\mu}$ is the atomic electric dipole moment, $|j;n_{\mathbf{k}\lambda}\rangle$ is the state of the system in which the atom is in the state $|j\rangle$ with energy E_j and the photon field contains n photons with momentum $\mathbf{k}$ and polarization λ. Because the electric field operator is linear in the photon creation and annihilation operators the first-order contribution vanishes and the second-order correction is the lowest-order contribution. Since the electric field does not vary appreciably over the size of the atom we use dipole approximation. Then the energy shift can be expressed as

$$\Delta E_i = -\sum_{j\neq i}\sum\!\!\!\!\!\!\int_{\mathbf{k},\lambda} \frac{\omega_{\mathbf{k}}}{2\epsilon_0}\frac{|\langle i|\boldsymbol{\mu}|j\rangle\cdot\mathbf{f}^*_{\mathbf{k}\lambda}(\mathbf{r}_0)|^2}{E_{ji}+\omega_{\mathbf{k}}} \tag{5.49}$$

where we have abbreviated $E_{ji}=E_j-E_i$ and $\mathbf{r}_0=(0,0,z_0)$ is the position of the atom. It is seen that the calculation involves a summation over the modes of the electromagnetic field as carried out in the proof of the completeness relation (5.44). Equation (5.49) can be written out explicitly as

$$\Delta E_i^{\rm tot} = -\frac{1}{2\epsilon_0}\sum_{\lambda}\sum_{j\neq i}|\mu_m|^2\int \mathrm{d}\mathbf{k}_{\parallel}\left(\Delta E^{\rm vac}+\Delta E^{\rm trav}+\Delta E^{\rm evan}+\Delta E^{\rm trap}\right) \tag{5.50}$$

with $|\mu_m|^2\equiv|\langle i|\mu_m|j\rangle|^2$. There are four distinct contributions to the energy shift. $\Delta E^{\rm vac}$ is the position-independent contribution caused by the vacuum fields that corresponds to the Lamb shift in free space

$$\Delta E^{\rm vac} = \frac{1}{(2\pi)^3}\int_{-\infty}^{\infty}\mathrm{d}k_{\rm z}\frac{\omega}{E_{ji}+\omega}\,e_\lambda^m(\mathbf{k}^-)e_\lambda^{m*}(\mathbf{k}^-) \tag{5.51}$$

and the remaining three contributions come from the travelling, evanescent and trapped modes, respectively,

$$\begin{aligned}
\Delta E^{\rm trav} &= \frac{1}{(2\pi)^3}\int_{-\infty}^{\infty}\mathrm{d}k_{\rm z}\frac{\omega}{E_{ji}+\omega}\,R_\lambda^R e_\lambda^m(\mathbf{k}^+)e_\lambda^{m*}(\mathbf{k}^-)e^{2ik_{\rm z}z_0},\\
\Delta E^{\rm evan} &= \frac{1}{(2\pi)^3}\int_{i\Gamma_{\rm s}}^{0}\mathrm{d}k_{\rm z}\frac{\omega}{E_{ji}+\omega}\,\frac{k_{\rm z}}{k_{\rm zs}}|T_\lambda^L|^2 e_\lambda^m(\mathbf{k}^+)e_\lambda^{m*}(\mathbf{k}^+)e^{2ik_{\rm z}z_0},\\
\Delta E^{\rm trap} &= \sum_{q_\lambda^n}\frac{\omega}{E_{ji}+\omega}|N_\lambda|^2|T_\lambda^{\rm lv}|^2 e_\lambda^m(\mathbf{k}^+)e_\lambda^{m*}(\mathbf{k}^+)e^{2ik_{\rm z}z_0},
\end{aligned} \tag{5.52}$$

with z_0 being the position of the atom with respect to the origin. Note that because of the dipole approximation the shorthand notation for polarisation vectors (5.19) can be no longer applied. Normally one is interested in the energy shift caused by the presence of the dielectric boundaries only i.e. the correction to the shift that would appear in the free space. Therefore, we renormalize the energy-level shift (5.50) by subtracting from it it's free space limit i.e.

$$\Delta E_i = \Delta E_i^{\mathrm{tot}} - \lim_{n_\mathrm{l},n_\mathrm{s}\to 1} \Delta E_i^{\mathrm{tot}}. \tag{5.53}$$

The renormalization procedure amounts to the removal of the contributions ΔE^{vac} (5.51) from the energy shift (5.50) and takes care of any infinities that would appear otherwise, provided we treat the remaining parts with care. As noted elsewhere [56], the contributions (5.52) suffer from convergence problems when treated separately. However, appropriate tools to handle the problem have been developed in Sec. 5.2.3. We aim to combine ΔE^{trav}, ΔE^{evan} and ΔE^{trap} into one compact expression easy to handle analytically. We can use the same tricks as in the proof of the completeness relation because the analytical structure of the complex k_z-plane is the same except that the function $\omega = (\mathbf{k}_\parallel^2 + k_\mathrm{z}^2)^{1/2}$ that comes about as the denominator of the perturbation theory introduces additional branch-points at $k_\mathrm{z} = \pm i|\mathbf{k}_\parallel|$ as compared to Fig. 5.2. This poses no difficulties though if one chooses the branch-cuts to lie between $\pm i|\mathbf{k}_\parallel|$ and $\pm i\infty$. Then, the contributions to the energy shift from the travelling modes ΔE^{trav} and the evanescent modes ΔE^{evan} can be combined together into a single complex integral as explained in the steps between Eq. (5.44) and Eq. (5.46). This is possible because for imaginary k_z we have $e_\lambda^{m*}(\mathbf{k}^+) = e_\lambda^m(\mathbf{k}^-)$ whereas for k_z real $e_\lambda^{m*}(\mathbf{k}^-) = e_\lambda^m(\mathbf{k}^-)$ holds. On the other hand, we also know from Eq. (5.47) that the sum in ΔE^{trap} is equal to the integral of the reflection coefficient R_λ^R taken along any clockwise contour enclosing all of it's poles. Choosing this contour to run from $k_\mathrm{z} = 0^- + i\Gamma_\mathrm{s}$ to $k_\mathrm{z} = 0^- + i\Gamma_\mathrm{l}$ and then back down from $k_\mathrm{z} = 0^+ + i\Gamma_\mathrm{l}$ to $k_\mathrm{z} = 0^+ + i\Gamma_\mathrm{s}$, cf. Fig. 5.2, we write down the renormalized energy shift ΔE_i compactly as

$$\Delta E_i = -\frac{1}{2(2\pi)^3\epsilon_0} \sum_{m,\lambda} \sum_{j\neq i} |\mu_m|^2 \int \mathrm{d}\mathbf{k}_\parallel \int_{\gamma_\mathrm{l}} \mathrm{d}k_\mathrm{z}\, \frac{\omega}{E_{ji}+\omega}\, R_\lambda^R e_\lambda^m(\mathbf{k}^+) e_\lambda^m(\mathbf{k}^-) e^{2ik_\mathrm{z}z_0} \tag{5.54}$$

where the contour of integration γ_l is shown in Fig. 5.3. It resembles that of Fig. 5.2 only that now it runs on the imaginary axis up to the point $k_\mathrm{z} = i\Gamma_\mathrm{l}$ enclosing all the poles of the reflection coefficients R_λ^R.

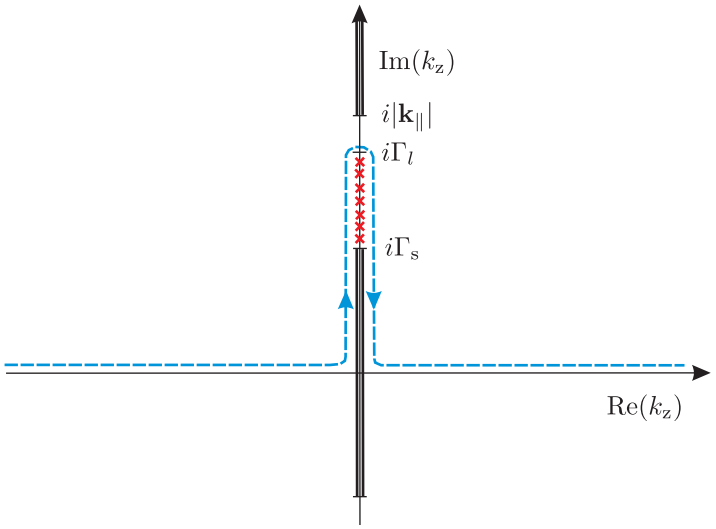

FIGURE 5.3: The dashed line represents the final contour γ_l used to evaluate the energy shift in Eq. (5.54).

The formula (5.54) is equally applicable to the ground-state atoms $|0\rangle$ as it is to the atoms that are in one of the excited states $|i\rangle$ provided we use the contour of integration as given in Fig. 5.3 and interpret the k_z integral as a Cauchy principal-value.

5.3.1 Ground state atoms

In the case of a ground-state atom the energy difference $E_{j0} \equiv E_j - E_0$ is always positive hence the denominator in Eq. (5.54) that originates from second-order perturbation theory, $E_{j0} + \omega$, never vanishes. Then, Eq. (5.54) contains no poles in the upper half of the k_z-plane other than those due to the reflection coefficient R^R_λ. To evaluate the k_z integral we can deform the contour of integration in Eq. (5.54) from that sketched in Fig. 5.3 to the one as shown in Fig. 5.4 which is beneficial from the computational point of view as it simplifies the analysis of Eq. (5.54) considerably. Writing out explicitly the sums over the polarization vectors (5.19) and then expressing the integral in the $\mathbf{k}_\parallel$-plane in polar coordinates, $k_\mathrm{x} = q\cos\phi$, $k_\mathrm{y} = q\sin\phi$, where the angle integral is computable analytically,

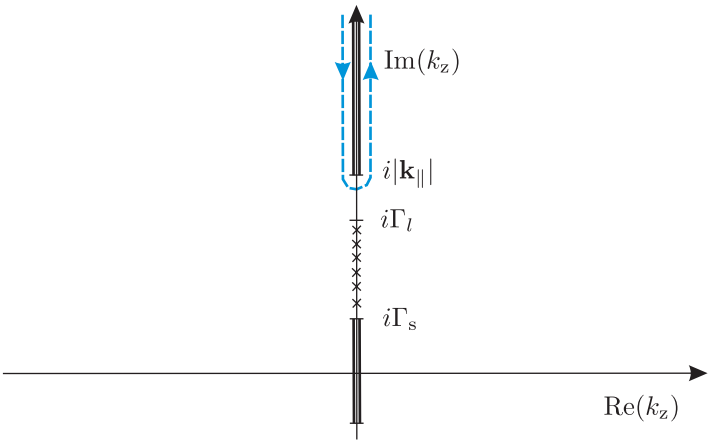

FIGURE 5.4: The final contour $\mathcal{C}$ used to evaluate the energy shift of the ground state atom in Eq. (5.55).

we rewrite the energy shift as

$$\Delta E_0 = \frac{1}{16\pi^2\epsilon_0}\sum_{j\neq 0}\int_0^\infty \mathrm{d}q\, q \int_{\mathcal{C}} \mathrm{d}k_z \frac{\omega}{E_{j0}+\omega} \times \left[|\mu_\parallel|^2\left(\tilde{R}^R_{\mathrm{TE}} - \frac{k_z^2}{\omega^2}\tilde{R}^R_{\mathrm{TM}}\right) + 2|\mu_\perp|^2\frac{q^2}{\omega^2}\tilde{R}^R_{\mathrm{TM}}\right] e^{2ik_z\mathcal{Z}} \tag{5.55}$$

with $\omega(k_z) = \sqrt{q^2+k_z^2}$, $|\mu_\parallel|^2 = |\mu_x|^2 + |\mu_y|^2$ and the contour $\mathcal{C}$ is that in Fig. 5.4 with $|\mathbf{k}_\parallel| = q$. The reflection coefficients $\tilde{R}^R_\lambda$ (of course expressed in terms of new variables) are given by

$$\tilde{R}^R_\lambda = \frac{r^{\mathrm{vl}}_\lambda + r^{\mathrm{ls}}_\lambda e^{2ik_{z\mathrm{l}}L}}{1 + r^{\mathrm{vl}}_\lambda r^{\mathrm{ls}}_\lambda e^{2ik_{z\mathrm{l}}L}}, \tag{5.56}$$

i.e. we have pulled out the phase factor e^{-ik_zL} in order to define $\mathcal{Z} = z_0 - L/2$ as the distance between the atom and the surface, cf. Eq. (5.22).

In order to perform the k_z integration in (5.55) we need to analytically continue the function $\omega = \omega(k_z)$, which is real and positive on the real axis, to the both sides of the branch cut along which the integration is carried out, (cf. Fig. 5.4). Doing so we find that on the LHS of the cut the positive value of the square root needs to be taken, and hence on the RHS of the cut we must take the opposite sign. Therefore we have

$$\int_C \mathrm{d}k_z \frac{\omega}{E_{j0}+\omega} = -\int_{iq}^{i\infty} \mathrm{d}k_z \, \frac{2E_{j0}\omega}{(E_{j0}-\omega)(E_{j0}+\omega)} \, .$$

Now we carry out a sequence of changes of variables. First we express k_z integration in terms of the frequency ω by substitution $\omega = \sqrt{q^2 + k_z^2}$

$$\int_{iq}^{i\infty} \mathrm{d}k_z = \int_0^{i\infty} \mathrm{d}\omega \frac{\omega}{\sqrt{\omega^2 - q^2}}. \tag{5.57}$$

Then, we express the integral to run along the real axis setting $\omega = i\xi$. After this is done, the energy shift of the ground state is expressed as a double integral that covers the first quadrant of the (q, ξ)-plane

$$\Delta E_0 = -\frac{1}{8\pi^2\epsilon_0} \sum_{j\neq i} E_{j0} \int_0^\infty \mathrm{d}q q \int_0^\infty \mathrm{d}\xi \, \frac{e^{-2\sqrt{\xi^2+q^2}\mathcal{Z}}}{\sqrt{\xi^2+q^2}(E_{j0}^2+\xi^2)} \times \left\{ |\mu_\parallel|^2 \left[(\xi^2+q^2)\tilde{R}^R_{\mathrm{TM}} - \xi^2 \tilde{R}^R_{\mathrm{TE}} \right] + 2k^2 \tilde{R}^R_{\mathrm{TM}} |\mu_\perp|^2 \right\}.$$

It seems natural to introduce polar coordinates, $q = \bar{x}\sin\phi, \xi = \bar{x}\cos\phi$. We also choose to scale the radial integration variable $\bar{x} = E_{j0}x$ with $E_{j0} > 0$ and set $y = \cos\phi$. This provides us with the final form of the energy shift that is more suitable for numerical computations and asymptotic analysis

$$\Delta E_0 = \frac{1}{8\pi^2\epsilon_0} \sum_{j\neq i} E_{j0}^3 \int_0^\infty \mathrm{d}x x^3 \int_0^1 \mathrm{d}y \, \frac{e^{-2E_{j0}\mathcal{Z}x}}{1+x^2y^2} \times \left[|\mu_\parallel|^2 \left(y^2 \tilde{R}^R_{\mathrm{TE}} - \tilde{R}^R_{\mathrm{TM}} \right) + 2|\mu_\perp|^2 (y^2-1) \tilde{R}^R_{\mathrm{TM}} \right]. \tag{5.58}$$

The reflection coefficient $\tilde{R}^R_\lambda$ are expressed as in (5.56) but with wavevectors given by

$$k_{z\mathrm{i}} = ixE_{j0}\sqrt{(n_{\mathrm{i}}^2 - 1)y^2 + 1}, \quad n_{\mathrm{i}} = \{1, n_{\mathrm{l}}, n_{\mathrm{s}}\}.$$

Note that even though the wave vector is imaginary, the final result is a real number, as it should, because the Fresnel coefficients contain ratios of wavevectors only.

5.3.2 Excited atoms

As mentioned at the beginning of the previous section the energy level shift of an excited atom is also given by Eq. (5.54). However, one needs to remember that the quantity $E_{ji} \equiv E_j - E_i$ can now become negative for $j < i$ and the denominator originating from

perturbation theory contributes additional poles lying on the path of k_z integration, which is taken as that shown in Fig. 5.3 and is understood as a Cauchy principal-value. The poles are located at $k_z = \pm\sqrt{E_{ji}^2 - \mathbf{k}_\parallel^2}$ and their precise location depends on the value of $|\mathbf{k}_\parallel|$ that is not fixed but varies as we carry out the $\mathbf{k}_\parallel$ integrations in equation (5.54). For $|\mathbf{k}_\parallel| \in [0, |E_{ji}|]$ the poles are located on the real k_z axis but as we increase the value of $|\mathbf{k}_\parallel|$ to exceed $|E_{ji}|$ both poles move onto the positive imaginary axis according to the convention that $\mathrm{Im}(\mathrm{k_z}) > 0$. For $|\mathbf{k}_\parallel|$ belonging to the interval $[|E_{ji}|, n_\mathrm{s}|E_{ji}|]$ the poles are located on the opposite sides of the branch cut due to the k_{zs} and care needs to be taken when evaluating those pole contributions. To evaluate the Cauchy principal-value of the k_z-integral we circumvent the poles and close the contour in the upper half-plane, as was done in the previous section. The contribution from the large semicircle vanishes and equation (5.54) acquires pole contributions that are easily worked out by the residue theorem. The energy shift splits into the a "non-resonant" ground-state-like part ΔE_i and a "resonant" oscillatory part $\Delta E_i^{\mathrm{res}}$ that arises only if the atom is in an excited state. The "non-resonant" part is given by

$$\Delta E_i = \frac{1}{8\pi^2\epsilon_0}\sum_{j\neq i} E_{ji}^3 \int_0^\infty \mathrm{d}x x^3 \int_0^1 \mathrm{d}y\, \frac{e^{-2|E_{ji}|\mathcal{Z}x}}{1+x^2y^2} \times \left[|\mu_\parallel|^2\left(y^2\tilde{R}^R_{\mathrm{TE}} - \tilde{R}^R_{\mathrm{TM}}\right) + 2|\mu_\perp|^2(y^2-1)\tilde{R}^R_{\mathrm{TM}}\right] \tag{5.59}$$

with wavevectors expressed as

$$k_{\mathrm{zi}} = ix|E_{ji}|\sqrt{(n_\mathrm{i}^2-1)y^2+1}, \quad n_\mathrm{i} = \{1, n_\mathrm{l}, n_\mathrm{s}\}, \tag{5.60}$$

whereas the "resonant" part is given by

$$\Delta E_i^{\mathrm{res}} = \mathrm{Re}\frac{i}{8\pi\epsilon_0}\sum_{j<i}|E_{ji}|^3\int_0^\infty \frac{\mathrm{d}k k}{\sqrt{1-k^2}} e^{2i|E_{ji}|\sqrt{1-k^2}\mathcal{Z}} \times \left\{|\mu_\parallel|^2\left[(1-k^2)\tilde{R}^R_{\mathrm{TM}} - \tilde{R}^R_{\mathrm{TE}}\right] - 2|\mu_\perp|^2k^2\tilde{R}^R_{\mathrm{TM}}\right\}, \tag{5.61}$$

with wavevectors expressed as

$$k_{\mathrm{zi}} = |E_{ji}|\sqrt{n_\mathrm{i}^2-k^2}, \quad n_\mathrm{i} = \{1, n_\mathrm{l}, n_\mathrm{s}\}.$$

The reflection coefficients are as usual and are given in (5.56). The integral in (5.61) contains poles because the dispersion relation present in the denominators of the reflection coefficients has now solutions on the real axis when $k \in [n_{\rm s}, n_{\rm l}]$. This signals the contributions from surface excitations (trapped modes). This fact has been discussed in [27] where the interaction of an excited atom with layered dielectric has been studied, although using mainly numerical analysis. Here we will attempt to study the results (5.59) and (5.61) analytically. To do so it will prove beneficial to rewrite equation (5.61) slightly. We change the variables according to $\sqrt{1-k^2} = \eta$ and split the contributions to Eq. (5.61) into two parts. The first one is a contribution from the travelling modes and given by

$$\Delta E_i^{\rm res,trav} = -{\rm Re}\frac{i}{8\pi\epsilon_0}\sum_{j<i}|E_{ji}|^3\int_0^1 {\rm d}\eta e^{2i|E_{ji}|\mathcal{Z}\eta} \times\left\{|\mu_\parallel|^2\left[\tilde{R}^R_{\rm TE}-\eta^2\tilde{R}^R_{\rm TM}\right]+2|\mu_\perp|^2(1-\eta^2)\tilde{R}^R_{\rm TM}\right\} \tag{5.62}$$

where the wavevectors in reflection coefficients are all real and can be expressed as

$$k_{\rm zi} = |E_{ji}|\sqrt{n_{\rm i}^2-1+\eta^2}, \quad n_{\rm i}=\{1,n_{\rm l},n_{\rm s}\}, \tag{5.63}$$

and the second is a contribution from the evanescent modes

$$\Delta E_i^{\rm res,evan} = -{\rm Re}\frac{1}{8\pi\epsilon_0}\sum_{j<i}|E_{ji}|^3\int_0^\infty {\rm d}\eta e^{-2|E_{ji}|\mathcal{Z}\eta} \times\left\{|\mu_\parallel|^2\left[\tilde{R}^R_{\rm TE}+\eta^2\tilde{R}^R_{\rm TM}\right]+2|\mu_\perp|^2(1+\eta^2)\tilde{R}^R_{\rm TM}\right\} \tag{5.64}$$

where the wavevectors in reflection coefficients can be expressed as

$$k_{\rm zi} = |E_{ji}|\sqrt{n_{\rm i}^2-1-\eta^2}, \quad n_{\rm i}=\{1,n_{\rm l},n_{\rm s}\}. \tag{5.65}$$

Finally, it is worth noting that the imaginary part of Eq. (5.61) is actually proportional to the modified decay rates [64]. These have been already studied in [67] so that we focus on energy shifts only. However, the methods of analysis that are reported in the next section allow to write down at once equivalent analytical formulae for the decay rates.

5.4 Asymptotic analysis

The interaction between the atom and the dielectric is electromagnetic in nature and it is mediated by photons. The atomic system in state $|i\rangle$ evolves in time with a characteristic time-scale that is proportional to E_{ji}^{-1}, with E_{ji} being the energy-level spacing between the states $|i\rangle$ and $|j\rangle$ which are connected by the strongest dipole transition. Since it takes a finite time for the photon to make a round trip between an atom and a surface, the atom will have changed by the time the photon comes back. Therefore, the time needed by the photon to reach the surface compared to the typical atomic time-scale is a fundamental quantity that plays decisive role in characterizing the interaction. In natural units, if $2E_{ji}\mathcal{Z} << 1$ we can safely assume that the interaction is instantaneous and we are in the so-called nonretarded or van der Waals regime. If $2E_{ji}\mathcal{Z} >> 1$ the interaction becomes manifestly retarded as the atom will have changed significantly by the time the photon comes back. However, the problem we have considered here provides us with yet another length scale, namely the thickness of the top layer L. We shall now consider the energy shift in various asymptotic regimes.

5.4.1 Ground state atoms. Electrostatic limit, ($2E_{ji}\mathcal{Z} << 1$)

In this limit the interaction is instantaneous (or electrostatic) in nature and the energy shift is obtainable using the Green's function of the classical Laplace equation [3], the derivation is outlined in the Appendix D. It reads

$$\Delta E^{\mathrm{el}} = -\frac{1}{16\pi\epsilon_0}\left(\langle\mu_{\parallel}^2\rangle + 2\langle\mu_{\perp}^2\rangle\right)\int_0^{\infty}\mathrm{d}k k^2 e^{-2k\mathcal{Z}}\left(\frac{\frac{n_{\mathrm{l}}^2-1}{n_{\mathrm{l}}^2+1} - \frac{n_{\mathrm{l}}^2-n_{\mathrm{s}}^2}{n_{\mathrm{s}}^2+n_{\mathrm{l}}^2}e^{-2kL}}{1-\frac{n_{\mathrm{l}}^2-1}{n_{\mathrm{l}}^2+1}\frac{n_{\mathrm{l}}^2-n_{\mathrm{s}}^2}{n_{\mathrm{s}}^2+n_{\mathrm{l}}^2}e^{-2kL}}\right). \tag{5.66}$$

with $\langle\mu_{\parallel}^2\rangle \equiv \langle\mu_x^2\rangle + \langle\mu_y^2\rangle$ and $\langle\mu_{\perp}^2\rangle \equiv \langle\mu_z^2\rangle$.

Now we show that we can also obtain the above result as a limiting case of the results of previous section. Note however that equation (5.58), which has been scaled with E_{ji}, cannot be used to take the electrostatic limit in which we mathematically let $E_{ji} \to 0$. It is best to start from equation (5.54). Equation (5.66) follows immediately if we spot that in the limit $E_{ji} \to 0$ the branch cut due to $\omega = \sqrt{\mathbf{k}_{\parallel}^2 + k_{\mathrm{z}}^2}$ is no longer present and the contour

in Fig. 5.4 collapses to a simple enclosure of the point $k_z = i|\mathbf{k}_\parallel|$. The contributions from the TE mode vanish as the product of the polarization vectors is regular at $k_z = i|\mathbf{k}_\parallel|$ but for the TM mode contributions this point is a simple pole, cf. Eq. (5.19). Therefore we have that

$$\Delta E^{\rm el} = -\frac{1}{(2\pi)^3 2\epsilon_0}\sum_m\sum_{j\neq i}|\mu_m|^2\int {\rm d}\mathbf{k}_\parallel \times 2\pi i \lim_{k_z\to i|\mathbf{k}_\parallel|}(k_z - i|\mathbf{k}_\parallel|)R^R_{\rm TM}e^m_{\rm TM}(\mathbf{k}^+)e^m_{\rm TM}(\mathbf{k}^-)e^{2ik_z z_0}.$$

Taking the limit and expressing the remaining integrals in polar coordinates where the angle integral is elementary yields equation (5.66) with $\langle\mu_m^2\rangle \equiv \sum_{j\neq i}|\langle i|\mu_m|j\rangle|^2 = \langle i|\mu_m^2|i\rangle$. Equation (5.66) can be further analysed depending on the relative values of L and $\mathcal{Z}$.

5.4.1.1 Thin layer ($\mathcal{Z}/L >> 1$)

In this case the distance of the atom from the surface is much greater than the thickness of the layer of refractive index n_1 (but still small enough for the retardation to be neglected). Then, rescaling the integral in equation (5.66) with $k = x/L$ allows us to use the Watson's lemma[1] to derive the following result

$$\Delta E^{\rm el} \approx \Delta E^{\rm el}_{n_{\rm s}} - \frac{1}{64\pi\epsilon_0\mathcal{Z}^3}\left(\langle\mu_\parallel^2\rangle + 2\langle\mu_\perp^2\rangle\right)\left[a_1\frac{L}{\mathcal{Z}} + a_2\frac{L^2}{\mathcal{Z}^2} + O\left(\frac{L^3}{\mathcal{Z}^3}\right)\right], \tag{5.67}$$

with the coefficients a_i given by

$$\begin{aligned} a_1 &= \frac{3}{n_1^2}\frac{n_1^4 - n_{\rm s}^4}{(n_{\rm s}^2+1)^2}, \\ a_2 &= -\frac{6}{n_1^4}\frac{(n_1^4 - n_{\rm s}^4)(n_{\rm s}^2 + n_1^4)}{(n_{\rm s}^2+1)^3}, \end{aligned}$$

where $\Delta E^{\rm el}_{n_{\rm s}}$ is the well-known electrostatic interaction energy between an atom and a dielectric half-space of refractive index $n_{\rm s}$ that can be obtained by the method of images

$$\Delta E^{\rm el}_{n_{\rm s}} = -\frac{1}{64\pi\epsilon_0\mathcal{Z}^3}\frac{n_{\rm s}^2 - 1}{n_{\rm s}^2 + 1}\left(\langle\mu_\parallel^2\rangle + 2\langle\mu_\perp^2\rangle\right). \tag{5.68}$$

[1] The essential idea is to spot that, since the integrand is strongly damped by the exponential, most of the contributions to the integral will come from small values of k. Thus, it is permissible to perform a Taylor expansion of the remaining part of the integrand about $k = 0$. For a more rigorous treatment see [22].

The corrections to this result are represented by the remaining elements of the asymptotic series. Note that if $n_\mathrm{l} > n_\mathrm{s}$ then $a_1 > 0$ and, not surprisingly, the interaction, as compared to a half-space alone, is enhanced by the presence of the thin dielectric layer of higher refractive index n_l.

5.4.1.2 Thick layer ($\mathcal{Z}/L << 1$)

In this case the thickness of the layer is much greater than the distance between the atom and the surface. The top layer now appears from the point of view of the atom almost as a half-space of refractive index n_l only that it is in fact of finite thickness. To analyse the result (5.66) in this limit we cast it in a somewhat different form. Note that, especially when kL is large but not only then,

$$\frac{n_\mathrm{l}^2-1}{n_\mathrm{l}^2+1}\frac{n_\mathrm{l}^2-n_\mathrm{s}^2}{n_\mathrm{s}^2+n_\mathrm{l}^2}e^{-2kL} < 1 \tag{5.69}$$

and the denominator of the integrand in Eq. (5.66) can be written as geometrical series. Since the series is absolutely convergent we can integrate it term by term and obtain the following representation of the electrostatic result

$$\Delta E^\mathrm{el} = \Delta E^\mathrm{el}_{n_\mathrm{l}} + \frac{1}{16\pi\epsilon_0}\left(\langle\mu_\parallel^2\rangle + 2\langle\mu_\perp^2\rangle\right)\frac{n_\mathrm{l}^2}{n_\mathrm{l}^4-1}\sum_{\nu=1}^{\infty}\left(\frac{n_\mathrm{l}^2-1}{n_\mathrm{l}^2+1}\frac{n_\mathrm{l}^2-n_\mathrm{s}^2}{n_\mathrm{s}^2+n_\mathrm{l}^2}\right)^\nu\frac{1}{(\mathcal{Z}+\nu L)^3} \tag{5.70}$$

where $\Delta E^\mathrm{el}_{n_\mathrm{l}}$ is the electrostatic energy shift due to a single half-space of refractive index n_l, i.e. Eq. (5.68) with n_s replaced by n_l. The sum in Eq. (5.70) represents the correction to $\Delta E^\mathrm{el}_{n_\mathrm{l}}$ due to the finite thickness of the layer. For fixed $\mathcal{Z}$ and L it can be easily computed numerically to any desired degree of accuracy. We note however, that to the leading order in $\mathcal{Z}/L$ the interaction is weakened by the same amount independently of the distance of the atom from the surface and therefore is not measurable. The next-to-leading order correction is the first to be distance-dependent and is proportional to $\mathcal{Z}/L^4$, which can be easily seen by expanding the factor in series around $\mathcal{Z}/kL = 0$:

$$\frac{1}{(\mathcal{Z}+kL)^3} \approx \frac{1}{k^3L^3} - \frac{3Z}{k^4L^4} + O\left(\frac{Z^2}{L^5}\right). \tag{5.71}$$

5.4.2 Ground state atoms. Retarded limit, ($2\mathcal{Z}E_{ji} >> 1$)

5.4.2.1 Thin layer ($\mathcal{Z}/L >> 1$)

In this case we study the situation when the top layer is much thinner than the distance between the atom and the surface. To obtain the asymptotic series we use Watson's lemma in much the same way as in the electrostatic case [22]. Series expansion of the integrand in Eq. (5.58) about $x = 0$ decouples the integrals and the resulting integrals can be calculated analytically. Thus, to first approximation, for an atom located sufficiently far from the interface, the impact of the thin dielectric layer on the standard Casimir-Polder interaction can be described by

$$\Delta E^{\mathrm{ret}} = \Delta E^{\mathrm{ret}}_{n_{\mathrm{s}}} - \frac{1}{16\pi^2\epsilon_0\mathcal{Z}^4}\sum_{j\neq i}\left(\frac{a_{\parallel}|\mu_{\parallel}|^2 + 2a_{\perp}|\mu_{\perp}|^2}{E_{ji}}\right)\frac{L}{\mathcal{Z}} + O\left(\frac{L^2}{\mathcal{Z}^2}\right) \tag{5.72}$$

where $\Delta E^{\mathrm{ret}}_{n_{\mathrm{s}}}$ is the retarded limit of energy shift as caused by the single dielectric half-space of refractive index n_{s}, which was calculated in [64]:

$$\Delta E^{\mathrm{ret}}_{n_{\mathrm{s}}} = -\frac{3}{64\pi^2\epsilon_0\mathcal{Z}^4}\sum_{j\neq i}\left(\frac{c_{\parallel}|\mu_{\parallel}|^2 + c_{\perp}|\mu_{\perp}|^2}{E_{ji}}\right), \tag{5.73}$$

with the coefficients c given by

$$c_{\parallel} = -\frac{1}{n_{\mathrm{s}}^2-1}\left(\frac{2}{3}n_{\mathrm{s}}^2 + n_{\mathrm{s}} - \frac{8}{3}\right) + \frac{2n_{\mathrm{s}}^4}{(n_{\mathrm{s}}^2-1)\sqrt{n_{\mathrm{s}}^2+1}}\ln\left(\frac{\sqrt{n_{\mathrm{s}}^2+1}+1}{n_{\mathrm{s}}\left[\sqrt{n_{\mathrm{s}}^2+1}+n_{\mathrm{s}}\right]}\right) + \frac{2n_{\mathrm{s}}^4 - 2n_{\mathrm{s}}^2 - 1}{(n_{\mathrm{s}}^2-1)^{3/2}}\ln\left(\sqrt{n_{\mathrm{s}}^2+1}+n_{\mathrm{s}}\right),$$

$$c_{\perp} = \frac{1}{n_{\mathrm{s}}^2-1}\left(4n_{\mathrm{s}}^4 - 2n_{\mathrm{s}}^3 - \frac{4}{3}n_{\mathrm{s}}^2 + \frac{4}{3}\right) - \frac{4n_{\mathrm{s}}^6}{(n_{\mathrm{s}}^2-1)\sqrt{n_{\mathrm{s}}^2+1}}\ln\left(\frac{\sqrt{n_{\mathrm{s}}^2+1}+1}{n_{\mathrm{s}}\left[\sqrt{n_{\mathrm{s}}^2+1}+n_{\mathrm{s}}\right]}\right) - \frac{2n_{\mathrm{s}}^2(2n_{\mathrm{s}}^4 - 2n_{\mathrm{s}}^2 + 1)}{(n_{\mathrm{s}}^2-1)^{3/2}}\ln\left(\sqrt{n_{\mathrm{s}}^2-1}+n_{\mathrm{s}}\right).$$

The coefficients $a_{\parallel}$ and $a_{\perp}$ in (5.72) are expressed in terms of the elementary functions as follows

$$
\begin{aligned}
a_{\parallel} &= \frac{1}{n_{\rm l}^2}\frac{n_{\rm l}^2-n_{\rm s}^2}{(n_{\rm s}^2-1)^2(n_{\rm s}^2+1)} \\
&\qquad\times\left[n_{\rm s}^5(6n_{\rm s}-3)(n_{\rm l}^2-1)+3n_{\rm s}^2(n_{\rm l}^2+1)-n_{\rm l}^2(2n_{\rm s}^4+3n_{\rm s}^3+3n_{\rm s}-8)\right] \\
&- \frac{n_{\rm l}^2-n_{\rm s}^2}{n_{\rm l}^2(n_{\rm s}^2-1)^{5/2}}\ln\left(\sqrt{n_{\rm s}^2-1}+n_{\rm s}\right)\left[2n_{\rm s}^2n_{\rm l}^2(n_{\rm s}^2-1)^2-2n_{\rm s}^4(n_{\rm s}^2-1)+n_{\rm l}^2\right] \\
&- \frac{n_{\rm s}^4}{2n_{\rm l}^2}\frac{n_{\rm l}^2-n_{\rm s}^2}{(n_{\rm s}^2-1)^2(n_{\rm s}^2+1)^{3/2}}\ln\left(\frac{\sqrt{n_{\rm s}^2+1}+1}{\sqrt{n_{\rm s}^2+1}-1}\frac{\sqrt{n_{\rm s}^2+1}-n_{\rm s}}{\sqrt{n_{\rm s}^2+1}+n_{\rm s}}\right) \\
&\qquad\times\left[2n_{\rm s}^4(n_{\rm l}^2-1)-2n_{\rm s}^2-3n_{\rm l}^2+1\right]
\end{aligned}
$$

$$
\begin{aligned}
a_{\perp} &= \frac{1}{n_{\rm l}^2}\frac{n_{\rm l}^2-n_{\rm s}^2}{(n_{\rm s}^2-1)^2(n_{\rm s}^2+1)} \\
&\times \left[n_{\rm s}^4(4n_{\rm s}^2-3n_{\rm s}-3)-n_{\rm s}^2(12n_{\rm s}^6-6n_{\rm s}^5+2)(n_{\rm l}^2-1)+n_{\rm l}^2(2n_{\rm s}^6+7n_{\rm s}^4-3n_{\rm s}^3+2)\right] \\
&+ \frac{n_{\rm s}^2}{n_{\rm l}^2}\frac{n_{\rm l}^2-n_{\rm s}^2}{(n_{\rm s}^2-1)^{5/2}}\ln\left(\sqrt{n_{\rm s}^2-1}+n_{\rm s}\right)\left[n_{\rm l}^2(4n_{\rm s}^6-6n_{\rm s}^4+3n_{\rm s}^2-1)-n_{\rm s}^2(2n_{\rm s}^2-1)^2\right] \\
&+ \frac{n_{\rm s}^6}{2n_{\rm l}^2}\frac{n_{\rm l}^2-n_{\rm s}^2}{(n_{\rm s}^2-1)^2(n_{\rm s}^2+1)^{3/2}}\ln\left(\frac{\sqrt{n_{\rm s}^2+1}+1}{\sqrt{n_{\rm s}^2+1}-1}\frac{\sqrt{n_{\rm s}^2+1}-n_{\rm s}}{\sqrt{n_{\rm s}^2+1}+n_{\rm s}}\right) \\
&\qquad\times\left[4n_{\rm s}^4(n_{\rm l}^2-1)+2n_{\rm s}^2(n_{\rm l}^2-2)-3n_{\rm l}^2+1\right]
\end{aligned}
$$

Both, $a_{\parallel}$ and $a_{\perp}$, are positive for $n_{\rm l} > n_{\rm s}$ so that, as one would expect, the interaction, as compared to a half-space alone, is enhanced by the thin dielectric layer of the higher refractive index $n_{\rm l}$. The above result simplifies significantly in the case when $n_{\rm s}$ approaches unity i.e. when the situation resembles that of an atom interacting with a dielectric slab of refractive index $n_{\rm l}$. The coefficients $a_{\parallel}$ and $a_{\perp}$ reduce then to those recently calculated in [56] and are given by

$$
\begin{aligned}
a_{\parallel} &= \frac{(n_{\rm l}^2-1)(9n_{\rm l}^2+5)}{10n_{\rm l}^2}\,, \\
a_{\perp} &= \frac{(n_{\rm l}^2-1)(5n_{\rm l}^2+4)}{10n_{\rm l}^2}\,.
\end{aligned}
$$

5.4.2.2 Thick layer ($\mathcal{Z}/L << 1$)

Here we assume that the thickness of the top layer is much greater than the distance between the atom and the surface, but which is still large enough for retardation to occur. Note that the reflection coefficient $\tilde{R}^R_\lambda$ (5.22) can be separated into $L-$dependent and $L-$independent parts in the following manner

$$\tilde{R}^R_\lambda = r^{\rm vl}_\lambda + \frac{[1-(r^{\rm vl}_\lambda)^2] r^{\rm ls}_\lambda e^{2ik_{\rm z l}L}}{1 + r^{\rm vl}_\lambda r^{\rm ls}_\lambda e^{2iLk_{\rm z l}L}}. \tag{5.74}$$

This way of writing the reflection coefficient splits the energy shift (5.58) into a shift due to the single interface of refractive index $n_{\rm l}$ and corrections due to the finite thickness and the underlying material. It can be shown numerically, see Sec. 5.5, that for large values of L the correction term is vanishingly small and can be safely discarded. Brute-force asymptotic analysis allows us to draw similar conclusions as in the electrostatic case, Section 5.4.1.2. To leading order the interaction gets altered by the same amount regardless of the position of the atom with respect to the interface. The next-to-leading-order correction is proportional to $\mathcal{Z}/L^5$.

5.4.3 Excited atoms. Nonretarded limit, ($2\mathcal{Z}|E_{ji}| << 1$)

The energy shift of an excited atom is given by equations (5.59) and (5.61). The "non-resonant" part, i.e. Eq. (5.59) has the same form as the energy shift of the ground state atom and has been analysed in the previous section. Here we focus on the "resonant" part of the interaction that is given by equation (5.61). In order to conveniently obtain the nonretarded limit of (5.61) we will work with its slightly modified form given in equations (5.62) and (5.64).

We start by noting that close to the interface we expect asymptotic series to be in the inverse powers of $\mathcal{Z}$. Equation (5.62), where the η integration runs over $\eta \in [0,1]$, contributes only positive powers of $\mathcal{Z}$. This is most easily seen by expanding the exponential $\exp(2i|E_{ji}|\mathcal{Z}\eta)$ about origin as we may do in the limit $2\mathcal{Z}|E_{ji}| \to 0$. Therefore, to leading-order of the electrostatic limit, only (5.64) contributes. Further we approximate (5.64) by

setting $\eta = k/(|E_{ji}|\mathcal{Z})$. Then, in the limit $|E_{ji}|\mathcal{Z} \to 0$ the wavevectors can be approximated as

$$k_{\rm z} = k_{\rm zl} = k_{\rm zs} = i\frac{k}{|E_{ji}|\mathcal{Z}} \tag{5.75}$$

and the result for the energy shift is seen to reduce to

$$\Delta E^{\rm res,el} = -\frac{1}{8\pi\epsilon_0}\sum_{j<i}\left(|\mu_\parallel|^2 + 2|\mu_\perp|^2\right)\int_0^\infty {\rm d}k k^2 e^{-2k\mathcal{Z}}\frac{\frac{n_{\rm l}^2-1}{n_{\rm l}^2+1} - \frac{n_{\rm l}^2-n_{\rm s}^2}{n_{\rm s}^2+n_{\rm l}^2}e^{-2kL}}{1-\frac{n_{\rm l}^2-1}{n_{\rm l}^2+1}\frac{n_{\rm l}^2-n_{\rm s}^2}{n_{\rm s}^2+n_{\rm l}^2}e^{-2kL}}. \tag{5.76}$$

The final result turns out to have the same dependence on $\mathcal{Z}$ and L as the Coulomb interaction of the ground state atom, cf. Eq. (5.66); therefore we shall not analyse Eq. (5.76) any further. Note however, that the dependence on the atomic states is different in equations (5.66) and (5.76). In the electrostatic limit, *to the order we are considering*, the quantity $\Delta E^{\rm res,el}$ turns out to be real, hence corrections to the decay rates seem to vanish. This conclusion is incorrect for it is known that the change of spontaneous emission in the nonretarded limit is in fact constant for a non-dispersive dielectric half-space [64]. However, any serious analysis of the changes of the decay rates induced by surfaces needs to take into account the absorption of the material, which in the nonretarded limit plays crucial role and can not be neglected. Recall that we have started from Eq. (5.61), that as explained before, contains poles on the real axis signalling the trapped modes. However, the denominator of (5.76) never vanishes which reflects the fact that in the electrostatic limit the trapped modes cease to exist and do not contribute towards the energy shifts, as first mentioned in [27].

5.4.4 Excited atoms. Retarded limit, $(2\mathcal{Z}|E_{ji}| >> 1)$

The leading-order behaviour of equation (5.61) in the retarded limit can be obtained by repeated integration by parts. Unlike in the electrostatic case now both equations, Eq. (5.62) and Eq. (5.64) contribute. We integrate them by parts and note that the non-oscillatory contributions that arise from the boundary terms evaluated at $\eta = 0$ cancel out. It turns out that the leading-order contributions to the energy shift are due to the perpendicular component of the atomic dipole moment. They dominate the retarded interaction energy and behave as $\mathcal{Z}^{-1}$. The contributions due to the component of the atomic

dipole moment that is perpendicular to the surface contribute only terms proportional to $\mathcal{Z}^{-2}$. We find that in the retarded limit the interaction energy up to the leading-order is given by

$$\begin{aligned}\Delta E_i^{\mathrm{res,ret}} = -\frac{1}{8\pi\epsilon_0\mathcal{Z}}\sum_{j<i}|E_{ji}|^2|\mu_{\parallel}|^2\frac{1}{1+2r_{\mathrm{vl}}r_{\mathrm{ls}}\cos(2|Eji|\tau)+r_{\mathrm{vl}}^2r_{\mathrm{ls}}^2}\\ \times\left\{r_{\mathrm{vl}}(1+r_{\mathrm{ls}}^2)\cos(2|E_{ji}|\mathcal{Z})\right.\\ +r_{\mathrm{vl}}^2r_{\mathrm{ls}}\cos[2|E_{ji}|(\mathcal{Z}-\tau)]\\ \left.+r_{\mathrm{ls}}\cos[2|E_{ji}|(\mathcal{Z}+\tau)]\right\},\end{aligned} \tag{5.77}$$

where we have defined the optical thickness of the layer as $\tau = n_{\mathrm{l}}L$ and

$$r_{\mathrm{vl}} = \frac{1-n_{\mathrm{l}}}{1+n_{\mathrm{l}}}, \quad r_{\mathrm{ls}} = \frac{n_{\mathrm{l}}-n_{\mathrm{s}}}{n_{\mathrm{l}}+n_{\mathrm{s}}}. \tag{5.78}$$

The final result agrees with that derived for a half-space in [64] if we take either $L \to 0$ or $n_{\mathrm{l}} \to n_{\mathrm{s}}$, which is a consistency check of our calculation. However, the limit of perfect reflectivity of the top layer does not make sense and one has to start from equation (5.61) and rewrite the reflection coefficient in the form (5.74) in order to study this case. Equation (5.77) is valid only approximately when the distance between the atom and the surface is much greater than the wavelength of the strongest atomic dipole transition. Nevertheless it allows us to draw important conclusion. We note that the interaction is resonant i.e. it is enhanced for certain values of LE_{ji}. The most convenient way to grasp the essence of the resonance effects is to take the slab limit of equation (5.77) i.e. set $n_{\mathrm{s}} = 1$. We have

$$\begin{aligned}\Delta E_i^{\mathrm{res,ret}} = -\frac{1}{8\pi\epsilon_0\mathcal{Z}}\sum_{j<i}|E_{ji}|^2|\mu_{\parallel}|^2\frac{1}{1-2r_{\mathrm{vl}}^2\cos(2|Eji|\tau)+r_{\mathrm{vl}}^4}\\ \times\left\{r_{\mathrm{vl}}(1+r_{\mathrm{vl}}^2)\cos(2|E_{ji}|\mathcal{Z})\right.\\ -r_{\mathrm{vl}}^3\cos[2|E_{ji}|(\mathcal{Z}-\tau)]\\ \left.-r_{\mathrm{vl}}\cos[2|E_{ji}|(\mathcal{Z}+\tau)]\right\}.\end{aligned} \tag{5.79}$$

Then, it is easily seen that whenever $\cos(2|Eji|\tau) = 1$ the interaction vanishes and, conversely, the amplitude of oscillations in equation (5.79) is maximized when $\cos(2|Eji|\tau) = -1$. Therefore we have a condition for resonance in terms of the wavelength of the strongest

atomic dipole transition λ_{ji}

$$\tau = nL = \frac{\lambda_{ji}}{2}\left(k + \frac{1}{2}\right), \quad k = 0, 1, 2 \ldots \tag{5.80}$$

Eq. (5.80) holds for $Z|E_{ji}| >> 1$ but if the value of $Z|E_{ji}|$ approaches unity, the relation looses its validity. The complications arise from the fact that when the atom is close to the surface the evanescent waves come into play whereas the condition (5.80) arises due to the interaction of an atom with travelling modes only. In the nonretarded limit $\mathcal{Z}|E_{ji}| << 1$ the notion of resonance looses its meaning altogether, cf. Eq. (5.76). Exploring the extreme cases in the retarded limit we note that at the anti-resonance i.e. when

$$\tau = \frac{\lambda_{ji}}{2}k, \quad k = 0, 1, 2 \ldots \tag{5.81}$$

equation (5.77) becomes

$$\Delta E_i^{\mathrm{res,ret}} = \frac{1}{8\pi\epsilon_0 \mathcal{Z}} \frac{n_\mathrm{s} - 1}{n_\mathrm{s} + 1} \sum_{j<i} |E_{ji}|^2 |\mu_\parallel|^2 \cos(2|E_{ji}|\mathcal{Z}), \tag{5.82}$$

i.e. the atom does not feel the presence of the layer and the interaction assumes the form of that between an atom and a single half-space of refractive index n_s, cf. [64]. This means that in the retarded regime the interaction between an excited atom and a slab of thickness L vanishes whenever the optical thickness of the slab $\tau = n_\mathrm{l} L$ is equal to a half-integer multiple of the wavelength of the dominant atomic transition λ_{ji}, cf. Fig. 5.11. Conversely, at resonance the shift becomes

$$\Delta E_i^{\mathrm{res,ret}} = \frac{1}{8\pi\epsilon_0 \mathcal{Z}} \frac{n_\mathrm{l}^2 - n_\mathrm{s}}{n_\mathrm{l}^2 + n_\mathrm{s}} \sum_{j<i} |E_{ji}|^2 |\mu_\parallel|^2 \cos(2|E_{ji}|\mathcal{Z}), \tag{5.83}$$

so that the amplitude of oscillations exceeds the amplitude that would have been caused by a single half-space of refractive index n_l. It also reaches the perfect reflector limit $n_\mathrm{l} \to \infty$ more rapidly. Finally, we shall also remark that the meaning of the conditions (5.80) and (5.81) is interchanged if the refractive index of the substrate n_s exceeds that of the layer n_l i.e. when $n_\mathrm{s} > n_\mathrm{l}$.

5.5 Numerical Examples

In this section we present a few numerical results designed to illustrate the influence of the dielectric layer on the usual Casimir-Polder interaction between an atom and a dielectric half-space. In practice, the sum over intermediate states j in Eq. (5.58) and in Eq. (5.61) is restricted to one or a few states to which there are strong dipole transitions. Hence, we assume a two-level system in which E_{ji} is a single number, namely the energy spacing of the levels with the strongest dipole transition. Additionally, we focus just on the contributions to the energy shift due to the component of the atomic dipole that is parallel to the interface of the dielectrics. The contributions due to the perpendicular components of the atomic dipole moment can be easily generated with from Eq. (5.58) using standard computer algebra packages like Mathematica or Maple. We start by simple checks on the asymptotic expansions derived in the previous section.

5.5.1 Ground-state atoms

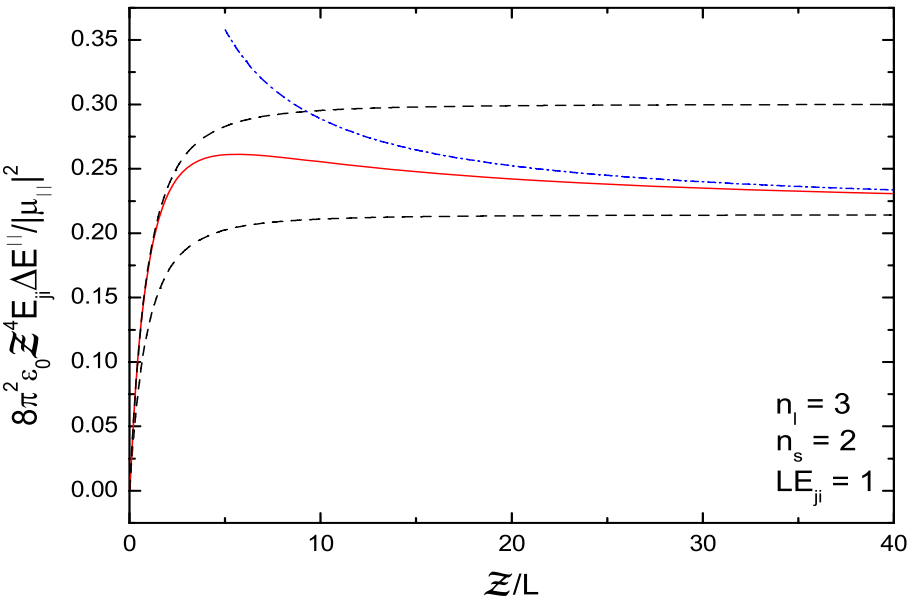

FIGURE 5.5: Plot of the exact energy-level shift contributions $\Delta E^{\parallel}$ (solid), Eq. (5.58), multiplied by $\mathcal{Z}^4$. Dashed lines represent the energy shifts due to the single dielectric half-spaces of refractive indices $n_{\rm l}$ (top) and $n_{\rm s}$ (bottom), whereas the dotted-dashed lines represents the asymptotic approximation (5.72).

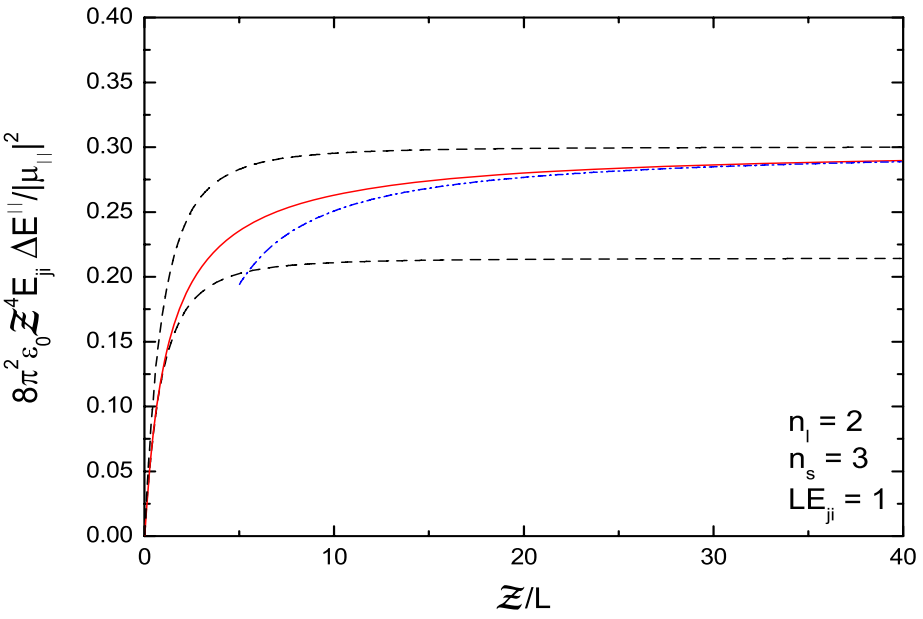

FIGURE 5.6: Plot of the exact energy-level shift $\Delta E^{\parallel}$ (solid), Eq. (5.58), multiplied by $\mathcal{Z}^4$. Dashed lines represent the energy shifts due to the single dielectric half-spaces of refractive indices n_1 (bottom) and n_s (top), whereas the dotted-dashed lines represents the asymptotic approximation (5.72).

We choose to plot the energy level shift ΔE multiplied by $\mathcal{Z}^4$ so that the asymptotic behaviour of it as a function of distance is more apparent, because $\Delta E\mathcal{Z}^4$ for a dielectric half-space approaches constant [64]. Then, one can easily track the variation of the energy shift caused by the top layer as compared to the half-space shifts, Fig. 5.5 and Fig. 5.6. We remark that even though the derivation of the energy shift in this Chapter was based on the assumption $n_1 > n_s$, the result is also valid in the case when the top layer has a smaller reflectivity than the substrate. In such a case the result can be used e.g. to model a thin layer of oxide or any kind of dirt on the substrate which is often present in real cold-atom experiments.

The asymptotic expansion (5.72) works well for large $\mathcal{Z}/L$ and not too high values of the refractive index n_1. This is demonstrated in Fig. 5.7. The increase of the refractive index n_1 has impact on the accuracy of the approximation which is valid provided

$$\mathcal{Z} >> \lambda_{ji} + \tau_1 \tag{5.84}$$

with λ_{ji} being the wavelength of the dominant atomic transition and $\tau_1 = n_1 L$ is the optical thickness of the top layer. In Fig. 5.8 we demonstrate the behaviour of the energy shift

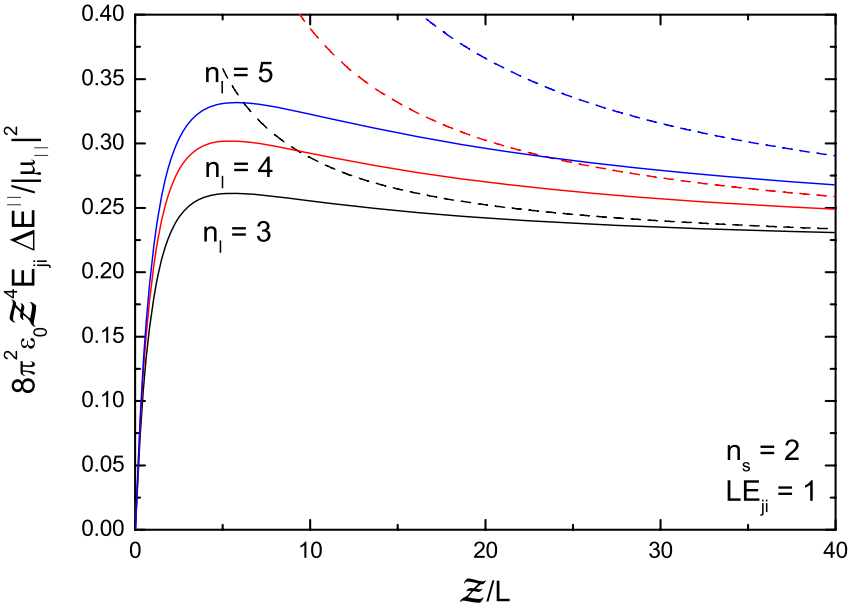

FIGURE 5.7: Plot of the exact energy shift $\Delta E^{\parallel}$, (solid, Eq. (5.58)), multiplied by $\mathcal{Z}^4$ together with the asymptotic approximations (dashed, Eq. (5.72)).

depending on the various values of the parameter E_{ji} measured in units of the layer's thickness. For small E_{ji} we clearly observe linear behaviour that corresponds to the $\mathcal{Z}^{-3}$ dependence of the shift in the electrostatic regime.

We also find it instructive to plot the energy level shift as a function of the thickness of the top layer L for different values of the refractive index n_1 while keeping the distance of the atom from the surface fixed, Fig. 5.9 and Fig. 5.10.

5.5.2 Excited atoms

The energy shift of an excited atom splits into two distinct parts, cf. Eq. (5.59) and Eq. (5.61). The non-oscillatory part displays the same behaviour as the energy shift of the ground-state atoms. We have analysed it numerically in the previous section. Here we will focus on the oscillatory contributions to the level shifts that are given by Eq. (5.61). We choose to plot the dimensionless integrals contained in equations (5.62) and (5.64) as this

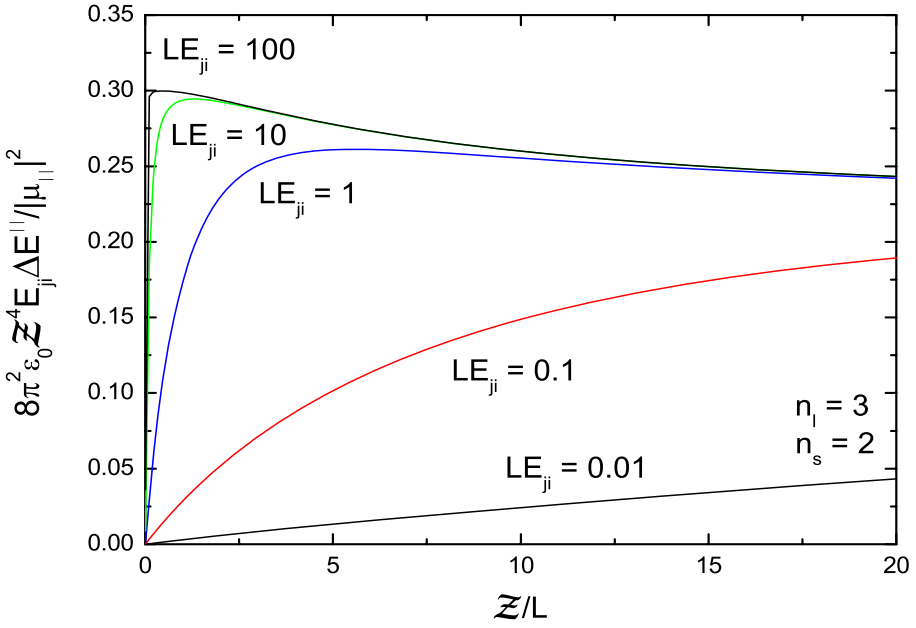

FIGURE 5.8: Plot of the exact energy shift $\Delta E^{\parallel}$ (Eq. (5.58)) multiplied by $\mathcal{Z}^4$ as a function of $\mathcal{Z}/L$ for various values of the retardation parameter $E_{ji}L$.

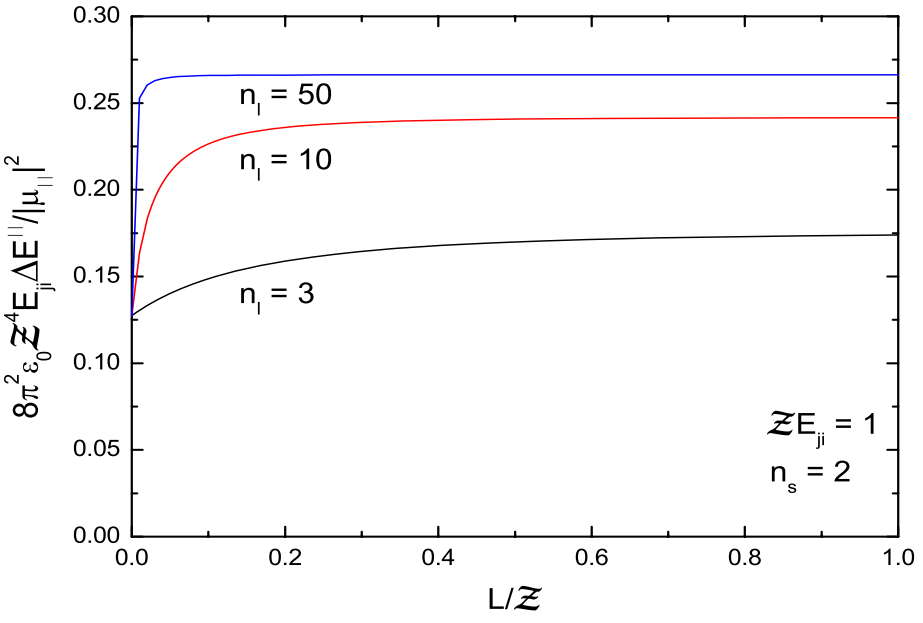

FIGURE 5.9: Plot of the exact energy shift $\Delta E^{\parallel}$ (Eq. (5.58)) multiplied by $\mathcal{Z}^4$ as a function of layer's thickness L measured in units of fixed atom-wall separation $\mathcal{Z}$ for various values of the layer's refractive index $n_l > n_s$.

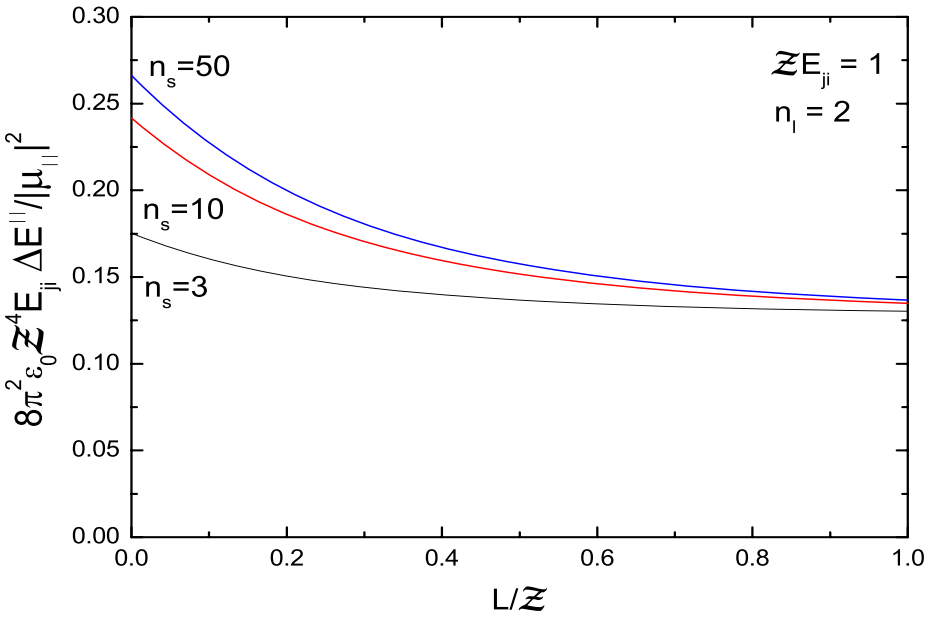

FIGURE 5.10: Plot of the exact energy shift $\Delta E^{\parallel}$ (Eq. (5.58)) multiplied by $\mathcal{Z}^4$ as a function of layer's thickness L measured in units of fixed atom-wall separation $\mathcal{Z}$ for various values of the substrate's refractive index $n_{\rm s} > n_{\rm l}$.

is numerically more efficient than plotting the integral in Eq. (5.61). It should be borne in mind that the reflection coefficients contain the dispersion relation in denominators that now has solutions on the real axis. For the purpose of the present demonstration it is sufficient to simply displace the poles off the real axis by adding small imaginary part to the denominator of the reflection coefficients effectively taking the Cauchy principal-value during numerical integration.

In Fig. 5.11 we demonstrate that indeed, if the anti-resonance condition (5.81) is satisfied, the interaction energy between the excited atom and the slab is strongly suppressed for $\mathcal{Z}E_{ji} >> 1$. In general, for the layered dielectric rather than the slab, the effect of resonance is shown in Fig. 5.12 and Fig. 5.13. Note that the energy level shift in an excited atom due to the layered dielectric can be significantly enhanced. Unlike in the case of the ground state atom where the energy shift caused by the layered structure of refractive indices $n_{\rm l}$ and $n_{\rm s}$ is bounded by the single half-space shifts (compare Fig. 5.5), the excited atom can experience shifts greater than those caused by the unlayered half-space of the refractive index $n = \max(n_{\rm l}, n_{\rm s})$, Fig. 5.12, which is due to resonance effects.

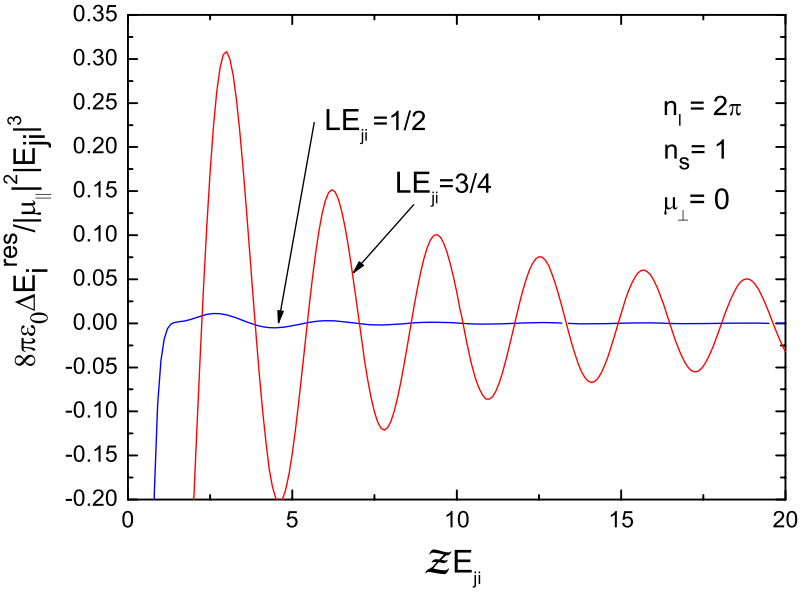

FIGURE 5.11: Plot of the exact energy-level shift (5.61) (resonant part) in an excited atom due to the parallel component of the atomic dipole moment placed in front of a slab of thickness L and refractive index $n_{\rm l} = 2\pi$. The energy spacing of the dominant atomic transition is such that $LE_{ji} = 3/4$ i.e. it satisfies the resonance condition (5.81). As is seen, when $LE_{ji} = 1/2$, the energy shift in the retarded regime is strongly suppressed, cf Eq. (5.77).

Conversely, it is also possible that the interaction with the layer will be unnoticeable if the anti-resonance condition (5.81) is satisfied, Fig. 5.13. Next, in Fig. 5.14, we show that the approximation of Eq. (5.61) derived in (5.77) turns out to be quite accurate and can be safely used to quickly estimate the energy shift in an excited atom caused by the layered dielectric, provided the condition $\mathcal{Z}E_{ji} >> 1$ is satisfied. It is also interesting to plot the resonant part of the energy shift as a function of LE_{ji} while keeping ZE_{ji} fixed. This is done in Fig. 5.15. It is seen that the energy shift indeed experiences the oscillatory resonant behaviour. The subsequent minima and maxima are less and less pronounced as the value of LE_{ji} increases. This is because as we increase LE_{ji} the resonances and anti-resonances move closer and closer together so that their effects cancel out. It is interesting to note that this behaviour could not have been inferred from equation (5.77), which indicates that the approximation (5.77) can be useful only for $LE_{ji} << 1$, which can also be easily verified numerically.

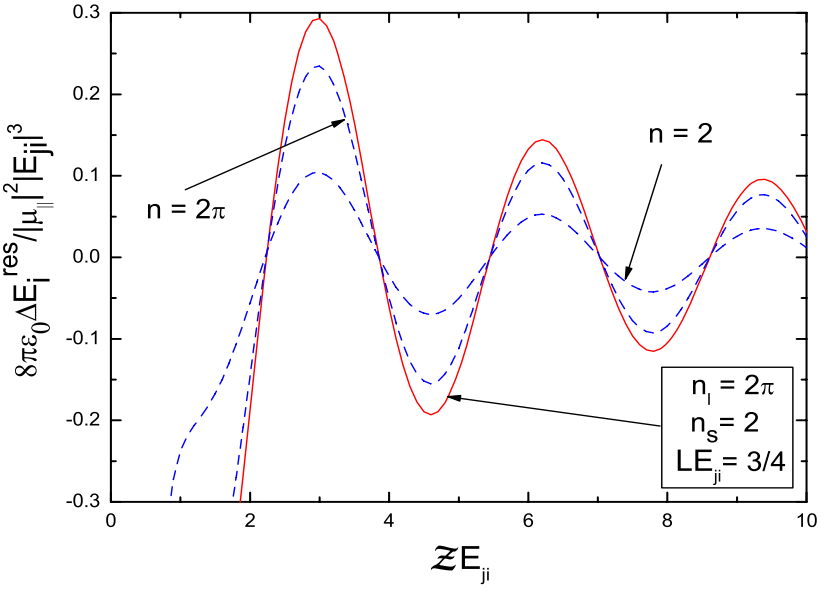

FIGURE 5.12: Plot of the exact energy-level shift (5.61) (resonant part) in an excited atom due to the parallel component of the atomic dipole moment placed in front of the layered dielectric with parameters as shown on the graph (solid). The resonant condition (5.80) is satisfied so that the interaction is enhanced. The amplitude of oscillations exceeds the one that would have been caused by an unlayered half-space of the refractive index $n = 2\pi$, cf. Eq. (5.82). Compare also Fig. 5.5. The dashed lines represent the interaction between an atom and single half-space of refractive index n as indicated.

5.6 Summary

Using perturbation theory we have calculated the energy level shift in a neutral atom placed in front of the layered dielectric half-space, Fig. 5.1. The major difficulty in working out the energy shift is the sum over all modes that appears in this type of calculation, Eq. (5.50), especially when the spectrum of the modes consists of the continuous and discrete parts, Sec. 5.2.1 and 5.2.2. This obstacle can be circumvented by using the complex-variable techniques to express the sum over all modes as a single contour integral in the complex k_z-plane, Eq. (5.54) and Fig. 5.4. Then, the energy shift (5.58) is easily analyzed asymptotically as well as numerically. For a ground-state atom, regardless of whether in retarded or non-retarded regime, we find that the leading-order correction to the interaction of an atom with an unlayered interface is proportional to $L/\mathcal{Z}$. The asymptotic series are given by (5.67) and (5.72) and provide reasonable estimate of the influence

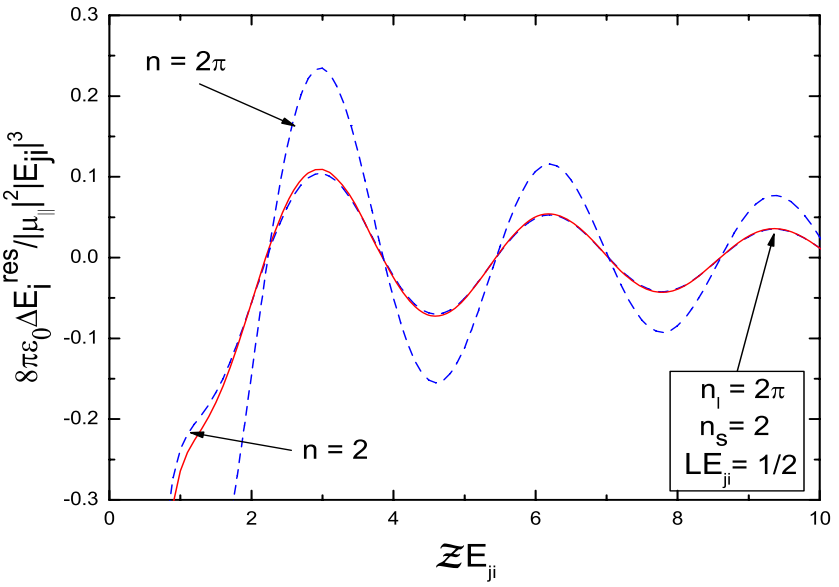

FIGURE 5.13: Plot of the exact energy-level shift (5.61) (resonant part) in an excited atom due to the parallel component of the atomic dipole moment placed in front of the layered dielectric with parameters as shown on the graph (solid). The anti-resonant condition (5.81) is satisfied so that the presence of the layer is almost unnoticeable, cf. Eq. (5.82). The dashed lines represent the interaction between an atom and single half-space of refractive index n as indicated.

of the single dielectric layer on the standard half-space result, Fig. 5.7. In the opposite case of very thick layer i.e. $\mathcal{Z}/L << 1$ we find that the result is well approximated by dielectric half-space [64]. For excited atoms we find that the interaction between an atom and the layered dielectric (5.61) is subject to resonances that occur between the wavelength of the dominant atomic transition λ_{ji} and the thickness of the layer L, Sec. 5.4.4. In particular, the interaction between an atom and the slab can be strongly suppressed in the retarded regime, cf. Fig. 5.11, whenever the optical thickness of the slab τ is equal to the half-integer multiple of the wavelength of the dominant atomic transition λ_{ji}. The existence of resonance effects suggests a physical picture of the excited atom as a radiating dipole. The resonance and anti-resonance correspond to constructive and destructive interference. We have also provided reasonable approximations in the non-retarded (5.76) and retarded (5.77) regimes that can be used to quickly estimate the magnitude of the resonant interaction between an atom and a layered dielectric.

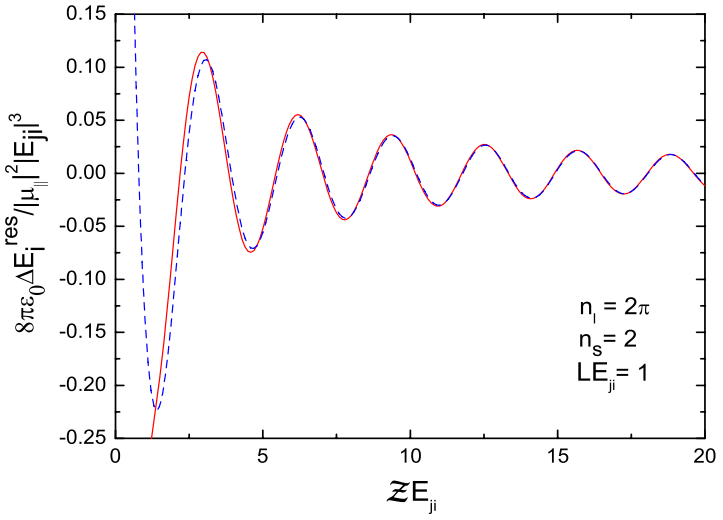

FIGURE 5.14: Plot of the exact energy-level shift (5.61) (resonant part) in an excited atom due to the parallel component of the atomic dipole moment placed in front of the layered dielectric with parameters as shown on the graph (solid). The dashed line represents the approximation in the retarded regime, Eq. (5.77).

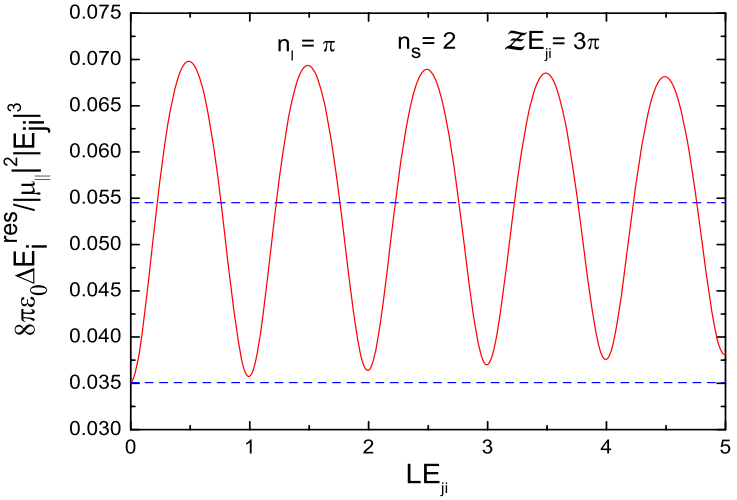

FIGURE 5.15: Plot of the exact energy-level shift (5.61) (resonant part) in an excited atom due to the parallel component of the atomic dipole moment placed in front of the layered dielectric with parameters as shown on the graph (solid). The dashed lines represent energy shifts caused by the single half-spaces of refractive index $n_l = 2\pi$ (top) and $n_s = 2$ (bottom).

Chapter 6

Quantum electrodynamics near a Huttner-Barnett dielectric

6.1 Introduction

The term 'Casimir-Polder shift' refers to the change in the atomic energy-levels induced by a nearby reflecting surface e.g. dielectrics. A similar effect in free-space is the Lamb shift. Crudely speaking, the Casimir-Polder shift can be viewed as a Stark effect where the role of the electric field is played by the non-zero and position-dependent vacuum fluctuations - an unavoidable consequence of the electromagnetic field quantization in the presence of dielectrics [11].

In order to study the Casimir-Polder effect a theory of the quantized electromagnetic field in the presence of boundaries is needed. The methods of field quantization largely depend on how sophisticated the model of material's optical response is. In the simplest case one might assume perfect reflectivity of the surfaces. The quantization of the electromagnetic field can then be achieved by the so-called normal-mode expansion. In this approach the electromagnetic field is expanded in terms of a complete set of solutions of the homogeneous Helmholtz equation. The presence of the boundaries is included by imposing appropriate boundary conditions on the electromagnetic field. Then, to accomplish quantization, the expansion coefficients are promoted to creation and annihilation operators which are required to satisfy bosonic commutation relations. This approach has the advantage of

being simple and therefore workable even for complex geometries [4] but suffers from a lack of physical features e.g. missing evanescent modes [5]. This particular drawback can be removed by considering non-dispersive and non-absorbing dielectrics characterized by a single number - an index of refraction. Then, the goal of field quantization can still be achieved by a similar procedure as for perfect reflectors [19]. However, it is well known that the above-mentioned techniques of the electromagnetic field quantization run into difficulties when one wants to include in the formalism the presence of realistic dielectrics. The response of the material's surface to the electromagnetic radiation in reality depends on the frequency of the impinging radiation. Furthermore, causality requirements demand that any dispersion is always accompanied by absorption. Therefore, in any model of interaction between real dielectrics and the electromagnetic field, the field has to be coupled to a reservoir in order to simulate absorptive degrees of freedom [68][69]. This can be done in a number of ways. One could model the absorptive degrees of freedom by adding to the operator-valued Maxwell equations Langevin-type fluctuating noise-currents that ensure that canonical commutation relations do not decay in time but rather take the expected form [1]. In this approach the field equations are solved using the Green's function of the wave equation and the noise-current operators play a major role in describing the dynamics of the coupled field-dielectric system. A number of papers attempted to provide microscopic justification of such a procedure by deriving the commutative properties of the noise-current operators that otherwise were introduced *ad hoc* [70][71][72].

A more direct approach to the modelling of the interaction between electromagnetic field and an absorptive dielectric is to explicitly include in the Lagrangian (or Hamiltonian) the matter degrees of freedom that are responsible for absorption. The dielectric is then envisaged to consist of a continuum of harmonic oscillators coupled to the reservoir which is just yet another set of harmonic oscillators. This is the so-called quantum model of a classical dielectric introduced by Hopfield [73]. The first Fano-type [74] diagonalization of the resulting Hamiltonian has been achieved for fields in three dimensions in [75] for a bulk dielectric and the general treatment of inhomogeneous dielectrics followed in [71]. The model has also been extended to include spatially dispersive bodies [76] and magnetodielectrics [77]. *Practical applications* of the Huttner-Barnett model, e.g. calculation of spontaneous decay rates [78], work well for bulk dielectrics where simple forms of the relevant operators can be found. However, in a bulk medium the local field corrections

play an important role and need to be included. On the other hand, complications that arise due to inhomogeneities of the dielectric seem to lead to unwieldy and impractical results, see e.g. Appendix in [6].

In this Chapter we aim to demonstrate that starting from the Power-Zienau-Wooley type of Hamiltonian rather than adopting the minimal coupling scheme it is possible to carry out explicit and easy to follow perturbative QED calculations is the presence of inhomogeneous Huttner-Barnett dielectrics. We apply the formalism we develop to the problem of calculating the energy-level shifts and change in spontaneous-decay rates for a neutral atom placed in the vicinity of a dielectric half-space. We successfully rederive the well-known results of phenomenological methods and broaden them by providing the asymptotic expansions that quantify the influence of absorption on the standard Casimir-Polder force calculated in [64]. We use only standard methods of Quantum Field Theory in a similar way as this is done in condensed matter theories. This requires the calculation of quantum propagators, most notably that of the electromagnetic field. This task is non-trivial but manageable. We partially adapt the seemingly overlooked results of [79] and find an exact solution of the Dyson equation satisfied by the photon propagator. In Appendix B we make contact with the phenomenological noise-current approach and calculate the photon propagator using the electromagnetic field operators constructed on the basis of the noise-current operators as developed by the Jena group.

6.2 Hamiltonian of the model and solving strategy

To find the energy-level shifts and change in spontaneous decay rates for an atom placed in the vicinity of an absorptive macroscopic body we adopt essentially the same model as [68]. The dielectric is modelled by a continuum of quantized harmonic oscillators - the polarization field, which is coupled to yet another set of quantized harmonic oscillators - the reservoir, the presence of which leads to a damping in the polarization field so as to allow absorption. Such coupled quantum fields are subsequently allowed to interact with the electromagnetic field via the $\boldsymbol{\mu} \cdot \mathbf{E}$ type of coupling. It turns out that the subsystem consisting of the reservoir, the polarization and the electromagnetic field is exactly soluble (at least for simple geometries of the dielectric); therefore the interaction of the atom with the dielectric can be reduced to the interaction of the atomic electron with the

'dressed' electromagnetic field i.e. the electromagnetic field corrected for the presence of an absorptive body. This approach stems from the theory developed in [80] where the interaction between an atom and a point-like absorptive dielectric (damped harmonic oscillator) was addressed.

Our starting point is the Lagrangian density describing the electromagnetic field and dielectric. It consists of the following parts

$$\mathcal{L}_0 = \mathcal{L}_{\rm EM} + \mathcal{L}_{\rm P} + \mathcal{L}_{\rm R} + \mathcal{L}_{\rm P-EM} \tag{6.1}$$

that are described as follows:

(i). *The Lagrangian density* $\mathcal{L}_{\rm EM}$ *of the free electromagnetic field*:

$$\mathcal{L}_{\rm EM} = \frac{\epsilon_0}{2}\mathbf{E}^2(\mathbf{r}) - \frac{1}{2\mu_0}\mathbf{B}^2(\mathbf{r}), \tag{6.2}$$

where $\mathbf{E}(\mathbf{r})$ is the electric field and $\mathbf{B}(\mathbf{r})$ is the magnetic induction.

(ii). *The Lagrangian density* $\mathcal{L}_{\rm P}$ *of the polarization field*:

$$\mathcal{L}_{\rm P} = \frac{1}{2}\mathcal{M}\dot{\mathbf{X}}(\mathbf{r}) - \frac{1}{2}\mathcal{M}\omega_{\rm T}^2\mathbf{X}^2(\mathbf{r}). \tag{6.3}$$

Here, $\mathbf{X}$ is the dipole moment density of the continuum of harmonic oscillators describing the dielectric. The strength of the restoring force acting on the polarization oscillators is determined by the combination $\mathcal{M}\omega_{\rm T}^2$. Hence, for fixed absorption frequency $\omega_{\rm T}$ of the dielectric, the 'mass' $\mathcal{M}$ is the parameter that determines the susceptibility of the polarization oscillator to an external agent. It has dimensions of (mass) $\times$ (lenght)$^{-1}$ $\times$ (dipole moment density)$^{-2}$ and, in fact, the quantity $(\mathcal{M}\epsilon_0\omega_{\rm T}^2)^{-1}$ will turn out to be the polarizability of the dielectric at zero frequency [73]. The absence of derivatives with respect to $\mathbf{r}$ in equation (6.3) implies that the polarization oscillators at different points in space are mutually independent resulting in a model with no spatial dispersion.

(iii). *The Lagrangian density $\mathcal{L}_{\mathrm{R}}$ of the reservoir*, including its coupling to the polarization field:

$$\mathcal{L}_{\mathrm{R}} = \int_0^\infty \mathrm{d}\nu \left\{ \frac{1}{2}\rho_\nu \dot{\mathbf{Y}}_\nu(\mathbf{r}) - \frac{1}{2}\rho_\nu \nu^2 \left[\mathbf{Y}_\nu(\mathbf{r}) - \mathbf{X}(\mathbf{r})\right]^2 \right\}. \tag{6.4}$$

Here, $\mathbf{Y}$ is the dipole moment density of the bath oscillators and the parameter ρ_ν has dimensions of (mass) $\times$ (lenght)$^{-1}$ $\times$ (dipole moment density)$^{-2}$ per unit frequency. The coupling of the bath to the polarization field leads to the appearance of term proportional to $\dot{\mathbf{X}}(\mathbf{r}, t)$ in the equations of motion for the polarization field, hence it is responsible for damping [81][82]. The 'masses' of the bath oscillators ρ_ν vary continuously with index ν and describe the strength of the coupling between a single polarization oscillator and the continuum of reservoir oscillators for different frequencies ν. The precise profile of ρ_ν is chosen so that the desired absorption spectrum is obtained [83].

(iv). *The Lagrangian density $\mathcal{L}_{\mathrm{P-EM}}$ describing the interaction of the polarization field with the electromagnetic field*:

$$\mathcal{L}_{\mathrm{P-EM}} = g(\mathbf{r})\mathbf{X}(\mathbf{r}) \cdot \mathbf{E}(\mathbf{r}). \tag{6.5}$$

The dimensionless coupling function $g(\mathbf{r})$ specifies where the interaction takes place i.e.

$$g(\mathbf{r}) = \begin{cases} 1 & \text{inside the dielectric} \\ 0 & \text{outside the dielectric} \end{cases}, \tag{6.6}$$

so that $g(\mathbf{r})$ describes the shape of the dielectric body.

It is straightforward to identify the canonical momenta and obtain the corresponding Hamiltonian densities

$$\mathcal{H}_{\rm EM} = \frac{1}{2\epsilon_0}\mathbf{D}^2(\mathbf{r}) + \frac{1}{2\mu_0}\mathbf{B}^2(\mathbf{r}), \tag{6.7}$$

$$\mathcal{H}_{\rm P} = \frac{\mathbf{P}^2(\mathbf{r})}{2\mathcal{M}} + \frac{1}{2}\mathcal{M}\omega_{\rm T}^2\mathbf{X}^2(\mathbf{r}), \tag{6.8}$$

$$\mathcal{H}_{\rm R} = \int_0^\infty {\rm d}\nu \left[\frac{\mathbf{Z}_\nu^2(\mathbf{r})}{2\rho_\nu} + \frac{1}{2}\rho_\nu\nu^2\mathbf{Y}_\nu^2(\mathbf{r})\right], \tag{6.9}$$

$$\mathcal{H}_{\rm P-R} = -\int_0^\infty {\rm d}\nu\rho_\nu\nu^2\mathbf{X}(\mathbf{r})\cdot\mathbf{Y}_\nu(\mathbf{r}), \tag{6.10}$$

$$\mathcal{H}_{\rm P-EM} = -\frac{g(\mathbf{r})}{\epsilon_0}\mathbf{D}(\mathbf{r})\cdot\mathbf{X}(\mathbf{r}), \tag{6.11}$$

where we have separated out the part of the Hamiltonian that represents the frequency shifts

$$\mathcal{H}_{\rm S} = \frac{1}{2}\int_0^\infty {\rm d}\nu\rho_\nu\nu^2\mathbf{X}^2(\mathbf{r}) + \frac{1}{2}\frac{g^2(\mathbf{r})}{\epsilon_0}\mathbf{X}^2(\mathbf{r}). \tag{6.12}$$

The first term of (6.12) arises due the coupling between the polarization field and the reservoir whereas the second term is caused by the coupling between the electromagnetic and the polarization field. Equations (6.7)-(6.12) accompanied by the set of the equal-time commutation relations

$$\left[D_i(\mathbf{r}), B_j(\mathbf{r}')\right] = \frac{\hbar}{(2\pi)^3}\epsilon^{ijm}\int {\rm d}^3\mathbf{k}k_m e^{i\mathbf{k}\cdot(\mathbf{r}-\mathbf{r}')}, \tag{6.13}$$

$$\left[X_i(\mathbf{r}), P_j(\mathbf{r}')\right] = i\hbar\delta_{ij}\delta^{(3)}(\mathbf{r}-\mathbf{r}'), \tag{6.14}$$

$$\left[Y_{i,\nu}(\mathbf{r}), Z_{j,\nu'}(\mathbf{r}')\right] = i\hbar\delta_{ij}\delta^{(3)}(\mathbf{r}-\mathbf{r}')\delta(\nu-\nu'), \tag{6.15}$$

allow one to derive the expected equations of motion for the damped-polariton model, cf. [70]. Here, $\mathbf{D}(\mathbf{r}) \equiv \epsilon_0\mathbf{E}(\mathbf{r}) + g(\mathbf{r})\mathbf{X}(\mathbf{r})$ is the displacement field which is in fact the negative of the momentum conjugate to $\mathbf{A}(\mathbf{r})$, with $\mathbf{A}(\mathbf{r})$ being the vector potential. The fact that it is the displacement field that plays the role of the electromagnetic conjugate momentum is a result of the $\boldsymbol{\mu}\cdot\mathbf{E}$ type of coupling chosen in (6.5). The terms of the Hamiltonian density (6.12) shift the eigenfrequency of the polarization field $\omega_{\rm T}$, i.e.

$$\omega_{\rm T}^2 \to \tilde{\omega}_{\rm T}^2 = \omega_{\rm T}^2 + \frac{1}{\mathcal{M}}\int_0^\infty {\rm d}\nu\rho_\nu\nu^2 + \frac{g^2(\mathbf{r})}{\epsilon_0\mathcal{M}}. \tag{6.16}$$

The second term contains the parameter ρ_ν that pertains to the shape of the absorption

spectrum. For our choice of ν-dependence, see Appendix E, it turns out to be infinite. However, this is not problematic as the observable quantities, most notably the dielectric function, stay physically meaningful. Additionally, the last term in (6.16) in principle introduces position dependence of the frequency $\tilde{\omega}_{\mathrm{T}}$ through the coupling function $g(\mathbf{r})$. At this stage it is not yet apparent but this position dependence will happen to be irrelevant. Hence, we now set $g(\mathbf{r}) = 1$ but promise, when the time comes, to point out why we are allowed to do so. Then, we can incorporate equation (6.12) in the Hamiltonian density of the polarization field writing

$$\mathcal{H}_{\mathrm{P}} = \frac{\mathbf{P}^2(\mathbf{r})}{2\mathcal{M}} + \frac{1}{2}\mathcal{M}\tilde{\omega}_{\mathrm{T}}^2\mathbf{X}^2(\mathbf{r}), \tag{6.17}$$

with

$$\tilde{\omega}_{\mathrm{T}}^2 = \omega_{\mathrm{T}}^2 + \omega_{\mathrm{P}}^2 + \frac{1}{\mathcal{M}}\int_0^\infty \mathrm{d}\nu\rho_\nu\nu^2. \tag{6.18}$$

Although our model does not allow for free electrons, by hindsight, we have introduced notation $\omega_{\mathrm{P}}^2 = (\epsilon_0\mathcal{M})^{-1}$ in analogy to plasma frequency.[1]

Our aim is to investigate the influence of an absorbing dielectric on the properties of an atom such as the energy-level shift and spontaneous decay rates. Therefore, for our Hamiltonian to be complete we have to supplement it by the atomic part. The full Hamiltonian reads

$$H = \int \mathrm{d}^3\mathbf{r}\left(\mathcal{H}_{\mathrm{EM}} + \mathcal{H}_{\mathrm{P}} + \mathcal{H}_{\mathrm{R}} + \mathcal{H}_{\mathrm{P-R}} + \mathcal{H}_{\mathrm{P-EM}} + \mathcal{H}_{\mathrm{A}} + \mathcal{H}_{\mathrm{A-EM}}\right), \tag{6.19}$$

where $\mathcal{H}_A$ is the Hamiltonian density of the non-interacting atom and $\mathcal{H}_{A-EM}$ describes its coupling to the electromagnetic field. We consider a one-electron atom and treat the atomic electron non-relativistically by representing it as a quantum of the Schrödinger field satisfying the fermionic anticommutation relations. Thus, the Hamiltonian density $\mathcal{H}_A$ of the non-interacting[2] atomic electron can be written as

$$\mathcal{H}_A = \Psi^\dagger(\mathbf{r})\left[-\frac{\hbar^2}{2m}\nabla^2 + V(|\mathbf{r}-\mathbf{R}|)\right]\Psi(\mathbf{r}), \tag{6.20}$$

[1] At this stage the analogy between the quantity $(\epsilon_0\mathcal{M})^{-1}$ and the plasma frequency, as commonly introduced in the free-electron model of plasma, is not yet apparent. This choice of notation will justify itself once the precise form of ρ_ν in Eqs. (6.17)-(6.18) is chosen so that the dielectric function of the model is specified, for details see Appendix E.

[2] Here, by non-interacting we mean the absence of interactions with the quantized part of the electromagnetic field.

where $\Psi(\mathbf{r})$ is the Schrödinger field operator satisfying the anticommutator relation

$$\left\{\Psi(\mathbf{r}), \Psi^\dagger(\mathbf{r})\right\} = \delta^{(3)}(\mathbf{r}-\mathbf{r}'), \tag{6.21}$$

and $V(|\mathbf{r}-\mathbf{R}|)$ is the potential due to the immobile nucleus which we choose to be always located well outside the dielectric at a position $\mathbf{R}$ so that there is no wave-function overlap between the atom and the solid. The atom is coupled to the electric field via its electric dipole moment. The Hamiltonian density describing this coupling in the dipole approximation may be written as

$$\mathcal{H}_{A-EM} = -\boldsymbol{\mu}\cdot\mathbf{E}(\mathbf{r})\ \delta^{(3)}(\mathbf{r}-\mathbf{R}), \tag{6.22}$$

with delta function ensuring that we evaluate the electric field at the position of the nucleus. Here, $\boldsymbol{\mu}$ is the electric-dipole moment operator which may be written as

$$\boldsymbol{\mu} = -e\int \mathrm{d}^3\mathbf{r}'\Psi^\dagger(\mathbf{r}')\ \boldsymbol{\rho}\ \Psi(\mathbf{r}'), \tag{6.23}$$

with $-e$ being the charge of the electron and $\tilde{\boldsymbol{\rho}}$ is the negative[3] of its position with respect to the nucleus i.e. $\tilde{\boldsymbol{\rho}} = \mathbf{r}' - \mathbf{R}$. It is convenient to expand the field operator $\Psi(\mathbf{r})$ in terms of the complete set of atomic wave-functions satisfying

$$\left[-\frac{\hbar^2}{2m}\nabla^2 + V(|\mathbf{r}-\mathbf{R}|)\right]\phi_n(\mathbf{r}) = E_n\phi_n(\mathbf{r}). \tag{6.24}$$

We have

$$\Psi(\mathbf{r}) = \sum_m c_m\phi_m(\mathbf{r}), \quad \Psi^\dagger(\mathbf{r}) = \sum_m c_m^\dagger\phi_m^*(\mathbf{r}) \tag{6.25}$$

where the operators c_m and $c_n^\dagger$ can be shown to satisfy the anticommutation relation

$$\left\{c_n, c_m^\dagger\right\} = \delta_{mn}. \tag{6.26}$$

This property follows directly from (6.21) and the fact that the eigenfunctions $\phi_n(\mathbf{r})$ are orthonormal. We use equations (6.25) and (6.26) to rewrite Hamiltonians H_A and H_{EM}

[3]The minus sign ensures the consistency with the conventional definition of the electric dipole moment $\boldsymbol{\mu} = -e\boldsymbol{\rho}$ where $\boldsymbol{\rho}$ points from the position of the negative charge to that of the positive one.

in a more useful form

$$H_A = \int \mathrm{d}^3\mathbf{r}\, \mathcal{H}_A = \sum_n E_n c_n^\dagger c_n, \tag{6.27}$$

$$H_{A-EM} = \int \mathrm{d}^3\mathbf{r}\, \mathcal{H}_{A-EM} = -e \sum_{ij} c_i^\dagger c_j \langle i|\boldsymbol{\rho}|j\rangle \cdot \mathbf{E}(\mathbf{R}), \tag{6.28}$$

where $\langle i|\boldsymbol{\rho}|j\rangle$ are the dipole matrix elements i.e. the expectation value of the electron's position operator $\boldsymbol{\rho}$

$$\langle i|\boldsymbol{\rho}|j\rangle = \int \mathrm{d}^3\boldsymbol{\rho}\, \phi_i^*(\boldsymbol{\rho})\, \boldsymbol{\rho}\, \phi_j(\boldsymbol{\rho}). \tag{6.29}$$

We calculate the energy-level shifts and spontaneous decay rates using Green's function approach in the same manner as in [80]. In this approach the energy shifts and decay rates of the atom are given as poles of the atomic propagator which in our case is accessible only perturbatively. To perform the perturbative calculations we work in the interaction picture where the general expression for the perturbative expansion of a Green's function of the field Ψ under the influence of the interaction H_I is [84]

$$\mathcal{G}(\mathbf{r},\mathbf{r}',t,t') = \sum_{n=0}^{\infty} \left(-\frac{i}{\hbar}\right)^{n+1} \int \mathrm{d}t_1 \ldots \int \mathrm{d}t_n \times \left\langle \Omega|\mathrm{T}\left[\Psi(\mathbf{r},t)\Psi^\dagger(\mathbf{r}',t') H_\mathrm{I}(t_1)\ldots H_\mathrm{I}(t_n)\right]|\Omega\right\rangle_{\mathrm{conn}}. \tag{6.30}$$

Wick's theorem states that the terms appearing in the expansion (6.30), when written out explicitly for a specific interaction Hamiltonian, turn out to be given entirely in terms of the propagators of the non-interacting fields

$$\mathcal{G}^{(0)}(\mathbf{r},\mathbf{r}',t,t') = -\frac{i}{\hbar}\langle\Omega|T\left[\Psi(\mathbf{r},t)\Psi^\dagger(\mathbf{r}',t')\right]|\Omega\rangle, \tag{6.31}$$

where now Ψ is the field operator in the Heisenberg picture and $|\Omega\rangle$ is the exact ground state of the non-interacting system. The subscript 'conn' in equation (6.30) indicates that only connected diagrams contribute, as disconnected diagrams drop out in the normalization of $|\Omega\rangle$.

First we determine the non-interacting propagators of the atom, the polarization field, the bath and the electromagnetic field. Then, the interaction of the polarization field with the reservoir is treated exactly. Once this is accomplished the correction to the

electromagnetic-field propagator caused by the presence of the absorptive dielectric can be calculated. This is the dressed photon propagator enters the final perturbative expansion of the atomic propagator whose poles contain the information about energy-level shifts and changes in transition rates.

6.3 Unperturbed Feynman propagators

6.3.1 Atomic-electron propagator

The unperturbed atomic-electron propagator corresponding to the Hamiltonian (6.20) or equivalently (6.27) is defined by

$$G^{(0)}(\mathbf{r},\mathbf{r}',t,t') = -\frac{i}{\hbar}\langle\Omega|T\left[\Psi(\mathbf{r},t)\Psi^{\dagger}(\mathbf{r}',t')\right]|\Omega\rangle, \tag{6.32}$$

where Ψ is the Schrödinger field operator in the Heisenberg picture and $|\Omega\rangle$ is the exact ground state of the non-interacting system. We plug the field operators written out in terms of the atomic eigenfunctions, Eq. (6.25), and remember that we work in the Heisenberg picture so that the operators c_l and $c_m^{\dagger}$ are now time-dependent:

$$G^{(0)}(\mathbf{r},\mathbf{r}',t,t') = \sum_{l,m}\phi_l(\mathbf{r})\phi_m^*(\mathbf{r}')G_{lm}^{(0)}(t,t') \tag{6.33}$$

with

$$G_{lm}^{(0)}(t,t') = -\frac{i}{\hbar}\langle\Omega|T\left[c_l(t)c_m^{\dagger}(t')\right]|\Omega\rangle. \tag{6.34}$$

The time-dependence of the fermionic annihilation and creation operators is determined using the Heisenberg equations of motion, anticommutation relation (6.26) and the Hamiltonian (6.27):

$$i\hbar\dot{c}_n = [c_n,H] = \sum_m E_m[c_n,c_m^{\dagger}c_m] = \sum_m E_m\left(\{c_n,c_m^{\dagger}\}c_m - c_m^{\dagger}\{c_n,c_m\}\right) = \sum_m E_m\delta_{nm}c_m,$$

so that we have

$$c_m(t) = c_m(0)e^{-iE_mt/\hbar}, \qquad c_m^{\dagger}(t) = c_m^{\dagger}(0)e^{iE_mt/\hbar}. \tag{6.35}$$

With equation (6.35) we determine $G^{(0)}_{lm}(t,t')$ to be

$$G^{(0)}_{lm}(t-t') = -\frac{i}{\hbar}\theta(t-t')e^{-iE_l(t-t')/\hbar}\delta_{lm}. \tag{6.36}$$

where we have used the definition of the time ordering operator and the fact that the vacuum state $|\Omega\rangle$ is annihilated by $c_m(0)$. We shall work with the Fourier transform of $G^{(0)}_{lm}(t,t')$ with respect to the time difference $t-t' \equiv \tau$

$$G^{(0)}_{lm}(E) = \int_{-\infty}^{\infty} \mathrm{d}\tau e^{iE\tau/\hbar} G^{(0)}_{lm}(\tau) = \frac{1}{E - E_l + i\eta}\delta_{lm}. \tag{6.37}$$

With this convention of Fourier transform the η-prescription ensures the correct causal behaviour of the propagator and guarantees the convergence of the integrals.

6.3.2 Photon propagator

To calculate the zeroth-order propagator of the displacement field $\mathbf{D}(\mathbf{r},t)$ whose dynamics is governed by the Hamiltonian (6.7) *not including* the coupling term (6.11), we note that the Heisenberg equations of motion imply

$$\frac{\partial D_i(\mathbf{r},t)}{\partial t} = \frac{1}{\mu_0}\epsilon^{ijk}\,\nabla_j B_k(\mathbf{r},t), \tag{6.38}$$

$$\frac{\partial B_i(\mathbf{r},t)}{\partial t} = -\frac{1}{\epsilon_0}\epsilon^{ijk}\,\nabla_j D_k(\mathbf{r},t), \tag{6.39}$$

where ϵ^{ijk} is the Levi-Civita symbol and the sum over doubly occurring Cartesian indices is implied. Thus the displacement field $\mathbf{D}(\mathbf{r},t)$ satisfies the homogeneous wave equation

$$(\nabla_i\nabla_j - \delta_{ij}\nabla^2)D_j(\mathbf{r},t) + \frac{\partial^2}{\partial t^2}D_i(\mathbf{r},t) = 0. \tag{6.40}$$

Formal definition of the photon propagator reads:

$$D_{ij}(\mathbf{r},\mathbf{r}',t,t') = -\frac{i}{\hbar}\langle 0|T\left[D_i(\mathbf{r},t)D_j(\mathbf{r}',t')\right]|0\rangle, \tag{6.41}$$

where $D_i(\mathbf{r},t)$ is the displacement field operator in the Heisenberg picture and $|0\rangle$ is the exact ground state of the non-interacting electromagnetic field. We apply the differential wave-operator that appears in (6.40) to the definition of the propagator. One needs to be

careful when evaluating time derivatives which do interact with the time-ordering operator, namely

$$\begin{aligned}\frac{\partial}{\partial t}\mathrm{T}[A(t)B(t')] &= \frac{\partial}{\partial t}\left[\theta(t-t')A(t)B(t')+\theta(t'-t)B(t')A(t)\right]\\ &= \delta(t-t')[A(t),B(t)]+\mathrm{T}\left[\frac{\partial A(t)}{\partial t}B(t')\right]. \end{aligned} \tag{6.42}$$

Applying this formula to calculate time derivatives we find that

$$\begin{aligned}&\left(\nabla_i\nabla_j-\delta_{ij}\nabla^2\right)D^{(0)}_{jk}(\mathbf{r},\mathbf{r}',t,t')+\frac{\partial^2}{\partial t^2}D^{(0)}_{ik}(\mathbf{r},\mathbf{r}',t,t')\\ =\;&\frac{i}{\hbar}\left\langle 0\left|\mathrm{T}\left[\left(\nabla_i\nabla_j-\delta_{ij}\nabla^2\right)D_j(\mathbf{r},t)D_k(\mathbf{r}',t')+\frac{\partial^2}{\partial t^2}D_i(\mathbf{r},t)D_k(\mathbf{r}',t')\right]\right|0\right\rangle\\ +\;&\frac{i}{\hbar}\left[\frac{\partial D_i(\mathbf{r},t)}{\partial t},D_k(\mathbf{r}',t)\right]\delta(t-t')\end{aligned} \tag{6.43}$$

where we have used the fact that spatial derivatives commute with time-ordering operator. By virtue of Eq. (6.40) the second line of (6.43) vanishes and it remains to evaluate the commutator $\left[\dot{D}_i(\mathbf{r},t),D_k(\mathbf{r}',t)\right]$. To do so we use Maxwell's equation (6.38) and the commutator (6.13)

$$\left[\frac{\partial D_i(\mathbf{r},t)}{\partial t},D_k(\mathbf{r}',t)\right]=\frac{i\hbar}{\mu_0}\left(\nabla_i\nabla_k-\delta_{ik}\nabla^2\right)\delta^{(3)}(\mathbf{r}-\mathbf{r}'). \tag{6.44}$$

Thus the displacement field propagator $D^{(0)}_{ij}(\mathbf{r},\mathbf{r}',t,t')$ satisfies the following differential equation

$$\begin{aligned}(\nabla_i\nabla_j-\delta_{ij}\nabla^2)D^{(0)}_{jk}(\mathbf{r}-\mathbf{r}',t-t')+\mu_0\epsilon_0\frac{\partial^2}{\partial t^2}D^{(0)}_{ik}(\mathbf{r}-\mathbf{r}',t-t')&\\ =\frac{\epsilon_0}{(2\pi)^3}\delta(t-t')\int\mathrm{d}^3\mathbf{q}(q_iq_k-\delta_{ik}\mathbf{q}^2)e^{i\mathbf{q}\cdot(\mathbf{r}-\mathbf{r}')}.&\end{aligned} \tag{6.45}$$

We note that the free-space photon propagator depends only on the differences $\mathbf{r}-\mathbf{r}'$ and $t-t'$. This property allows us to find the solution of (6.45) using Fourier transform. As a first step we note that Maxwell's equation (6.38) implies that the displacement field is transverse and so is its propagator

$$\nabla_iD^{(0)}_{jk}(\mathbf{r}-\mathbf{r}',t-t')=0. \tag{6.46}$$

Therefore, Eq. (6.45) simplifies to

$$\nabla^2 D^{(0)}_{jk}(\mathbf{r}-\mathbf{r}',t-t') - \mu_0\epsilon_0 \frac{\partial^2}{\partial t^2} D^{(0)}_{ik}(\mathbf{r}-\mathbf{r}',t-t') \\ = -\frac{\epsilon_0}{(2\pi)^3}\delta(t-t')\int \mathrm{d}^3\mathbf{q}(q_i q_k - \delta_{ik}\mathbf{q}^2)e^{i\mathbf{q}\cdot(\mathbf{r}-\mathbf{r}')}. \tag{6.47}$$

Introducing Fourier transformed propagator

$$D^{(0)}_{ik}(\mathbf{q},\omega) = \int \mathrm{d}^3(\mathbf{r}-\mathbf{r}')e^{-i\mathbf{q}\cdot(\mathbf{r}-\mathbf{r}')}\int_{-\infty}^{\infty}\mathrm{d}(t-t')e^{i\omega(t-t')}D^{(0)}_{ik}(\mathbf{r}-\mathbf{r}',t-t') \tag{6.48}$$

we readily obtain the spectral representation of the propagator

$$D^{(0)}_{ik}(\mathbf{q},\omega) = \epsilon_0 \frac{\delta_{ik}\mathbf{q}^2 - q_i q_k}{\omega^2 - \mathbf{q}^2 + i\eta}, \tag{6.49}$$

where the poles in the denominator have been misplaced so that the result displays causality appropriate for the Feynman propagator. In Appendix A we show that this choice of the η-prescription indeed guarantees the correct behaviour of the propagator when transformed back to the time variable.

6.3.3 Polarization field propagator

The Hamiltonian density (6.17) describes a collection of mutually independent harmonic oscillators i.e. the harmonic oscillator at $\mathbf{r}$ is unaffected by the oscillator at $\mathbf{r}+d\mathbf{r}$. This allows us to introduce, for each harmonic oscillator, creation and annihilation operators, $\mathbf{b}^\dagger(\mathbf{r})$ and $\mathbf{b}(\mathbf{r})$, in a completely the same way as this is done in the well-known algebraical approach to a simple harmonic oscillator in non-relativistic quantum mechanics, see e.g. Chapter 2 of this thesis,

$$\mathbf{X}(\mathbf{r}) = \sqrt{\frac{\hbar}{2\mathcal{M}\tilde{\omega}_\mathrm{T}}}\left[\mathbf{b}^\dagger(\mathbf{r}) + \mathbf{b}(\mathbf{r})\right], \quad \mathbf{P}(\mathbf{r}) = i\sqrt{\frac{\hbar\mathcal{M}\tilde{\omega}_\mathrm{T}}{2}}\left[\mathbf{b}^\dagger(\mathbf{r}) - \mathbf{b}(\mathbf{r})\right]. \tag{6.50}$$

The operators $\mathbf{b}^\dagger(\mathbf{r})$ and $\mathbf{b}(\mathbf{r})$ satisfy equal-time commutation relation

$$\left[b_i(\mathbf{r}), b^\dagger_j(\mathbf{r})\right] = \delta_{ij}\delta^{(3)}(\mathbf{r}-\mathbf{r}') \tag{6.51}$$

which follows directly from their definition and the relation (6.14). The operator $b_i(\mathbf{r})$ has the property that it annihilates the ground state of the oscillator at $\mathbf{r}$ oscillating in the i-th direction. We will use this property, together with the commutation relation (6.51), to directly evaluate the polarization field propagator defined as

$$K_{ij}^{(0)}(\mathbf{r},\mathbf{r}',t,t') = -\frac{i}{\hbar}\langle\Omega|T\left[X_i(\mathbf{r},t)X_j(\mathbf{r}',t')\right]|\Omega\rangle. \tag{6.52}$$

Here $X_i(\mathbf{r},t)$ is the polarization field operator in the Heisenberg picture and $|\Omega\rangle$ is the exact ground state of the non-interacting polarization field. When written out in terms of the creation and annihilation operators the Hamiltonian density (6.17) takes on the diagonal form

$$\mathcal{H}_P = \frac{1}{2}\hbar\tilde{\omega}_{\mathrm{T}}\left[\mathbf{b}^\dagger(\mathbf{r})\cdot\mathbf{b}(\mathbf{r}) + \mathbf{b}(\mathbf{r})\cdot\mathbf{b}^\dagger(\mathbf{r})\right], \tag{6.53}$$

so that the time dependence of the creation and annihilation operators is harmonic

$$\mathbf{b}(\mathbf{r},t) = \mathbf{b}(\mathbf{r},0)e^{-i\tilde{\omega}_{\mathrm{T}}t}, \qquad \mathbf{b}^\dagger(\mathbf{r},t) = \mathbf{b}^\dagger(\mathbf{r},0)e^{i\tilde{\omega}_{\mathrm{T}}t}, \tag{6.54}$$

which follows from the Heisenberg's equations of motion. We plug the polarization field operators expressed in terms of the ladder operators into Eq. (6.52). Due to orthogonality of states only terms proportional to $\mathbf{b}\cdot\mathbf{b}^\dagger$ contribute. Taking care of the appropriate time ordering of operators and using the commutator (6.51) to move the annihilation operators to the right of creation operators, so that they act on the vacuum state $|\Omega\rangle$, we readily obtain

$$K_{ij}^{(0)}(\mathbf{r}-\mathbf{r}',t-t') = -\frac{i}{2\mathcal{M}\tilde{\omega}_{\mathrm{T}}}\delta_{ij}\delta^{(3)}(\mathbf{r}-\mathbf{r}')\left[\theta(t-t')e^{-i\tilde{\omega}_{\mathrm{T}}(t-t')} + \theta(t'-t)e^{+i\tilde{\omega}_{\mathrm{T}}(t-t')}\right], \tag{6.55}$$

where the frequency $\tilde{\omega}_{\mathrm{T}}$ has been defined in Eq. (6.18). We shall need Fourier transform of the polarization propagator with respect to the time difference $t-t'$

$$K_{ij}^{(0)}(\mathbf{r}-\mathbf{r}';\omega) = \int_{-\infty}^{\infty}\mathrm{d}(t-t')e^{i\omega(t-t')}K_{ij}^{(0)}(\mathbf{r}-\mathbf{r}',t-t'), \tag{6.56}$$

which is given by

$$K_{ij}^{(0)}(\mathbf{r}-\mathbf{r}';\omega) = \frac{1}{\mathcal{M}}\frac{1}{\omega^2-\tilde{\omega}_{\mathrm{T}}^2+i\eta}\delta_{ij}\delta^{(3)}(\mathbf{r}-\mathbf{r}'). \tag{6.57}$$

6.3.4 Reservoir propagator

The dynamics of the non-interacting reservoir field is described by the Hamiltonian (6.9) which describes a set of independent harmonic oscillators. The propagator for the free reservoir field can be obtained by repeating the steps needed to derive the propagator for the free polarization field, see Section 6.3.3. Therefore, we don't give detailed derivation but simply copy the structure of results (6.55) and (6.57). In the time domain the reservoir propagator reads

$$H_{ij}^{(0)}(\mathbf{r}-\mathbf{r}',t-t',\nu,\nu') = -\frac{i}{2\rho_\nu\nu}\delta_{ij}\delta^{(3)}(\mathbf{r}-\mathbf{r}')\delta(\nu-\nu') \times\left[\theta(t-t')e^{-i\nu(t-t')}+\theta(t'-t)e^{+i\nu(t-t')}\right]. \tag{6.58}$$

It's Fourier transformation with respect to $t-t'$ is given by

$$H_{ij}^{(0)}(\mathbf{r}-\mathbf{r}',\nu,\nu';\omega) = \int_{-\infty}^{\infty}\mathrm{d}(t-t')e^{i\omega(t-t')}H_{ij}^{(0)}(\mathbf{r}-\mathbf{r}',t-t',\nu,\nu'), \tag{6.59}$$

with

$$H_{ij}^{(0)}(\mathbf{r},\mathbf{r}',\nu,\nu';\omega) = \frac{1}{\rho_\nu}\frac{\delta_{ij}}{\omega^2-\nu^2+i\eta}\delta^{(3)}(\mathbf{r}-\mathbf{r}')\delta(\nu-\nu'). \tag{6.60}$$

6.4 Dressed propagators

Having collected all unperturbed propagators we can proceed to work out the propagators for the coupled fields. We are going to use perturbation theory in its diagrammatic formulation i.e. representing each term of the perturbative expansion (6.30) by an appropriate Feynman diagram [84]. In order to proceed, one needs to establish the correspondence between elements of Feynman diagrams and analytical expressions, the so-called Feynman rules. We have four different free propagators and accordingly we associate with them four distinct lines:

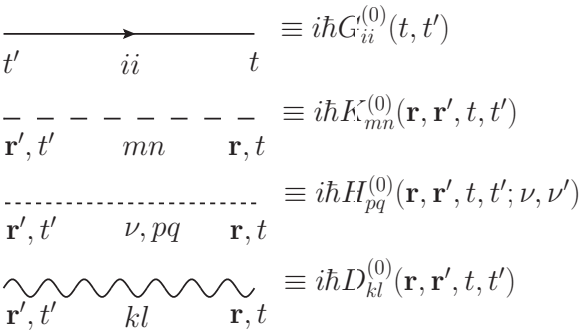

We shall need to consider three interaction Hamiltonians sequentially, $H_{\mathrm{P-R}}$, $H_{\mathrm{P-EM}}$ and $H_{\mathrm{A-EM}}$:

$$H_{\mathrm{P-R}} = -\int \mathrm{d}^3\mathbf{r} \int_0^\infty \mathrm{d}\nu \rho_\nu \nu^2 \mathbf{X}(\mathbf{r}) \cdot \mathbf{Y}_\nu(\mathbf{r}), \tag{6.61}$$

$$H_{\mathrm{P-EM}} = -\frac{1}{\epsilon_0} \int \mathrm{d}^3\mathbf{r} g(\mathbf{r}) \mathbf{D}(\mathbf{r}) \cdot \mathbf{X}(\mathbf{r}), \tag{6.62}$$

$$H_{A-EM} = -\frac{1}{\epsilon_0} \sum_{ij} c_i^\dagger c_j \, \boldsymbol{\mu}_{ij} \cdot \int \mathrm{d}^3\mathbf{r} \, \mathbf{D}(\mathbf{r}) \delta^{(3)}(\mathbf{r} - \mathbf{R}), \tag{6.63}$$

where we have introduced shorthand notation $\boldsymbol{\mu}_{ij} = \langle i|\boldsymbol{\mu}|j\rangle$ for the matrix elements of the atomic electric dipole moment operator $\boldsymbol{\mu}$. These interaction Hamiltonians yield the following rules for the vertices between the lines defined above:

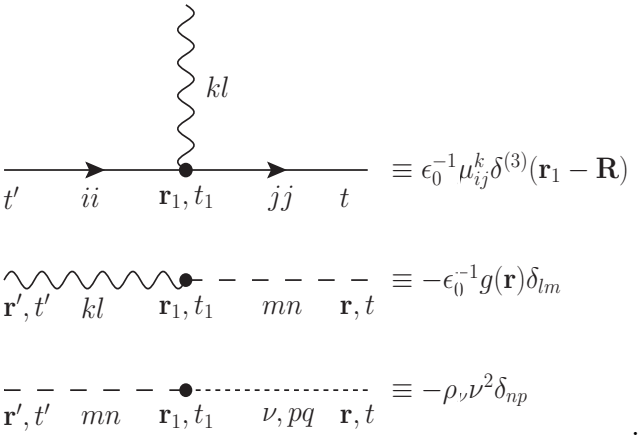

To compute a diagram one has to sum over all internal indices and integrate over internal times, internal coordinates and reservoir oscillator frequencies ν and ν'. We remind the reader that the subscript 'conn' in equation (6.30) means that the summation runs only

over the terms that correspond to the connected Feynman diagrams. Topologically equivalent diagrams i.e. those that can be obtained by permuting the factors $H_{\rm I}(t_i)$ in (6.30) are counted only once therefore we have omitted the usual factor of $1/n!$ that would have otherwise arisen in a straightforward expansion of the time-ordered exponential.

6.4.1 Dressing the polarization line

We chose to represent the dressed polarization propagator with a bold dashed line:

$$\equiv i\hbar K_{mn}(\mathbf{r},\mathbf{r}',t,t')$$

From the Feynman rules for the interaction Hamiltonian (6.61) one can see that the polarization line can only ever join one reservoir line, hence the following sequence of Feynman diagrams corresponding to the expansion (6.30) can be drawn:

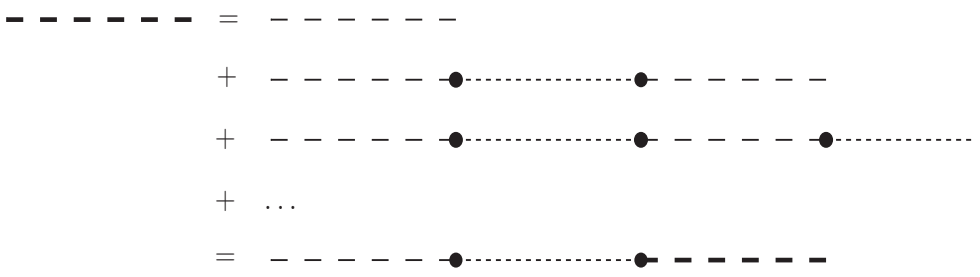

The equivalent analytical expression, which is the integral Dyson equation satisfied by the dressed polarization propagator, then reads

$$\begin{aligned} K_{mn}(\mathbf{r},\mathbf{r}',t,t') &= K^{(0)}_{mn}(\mathbf{r},\mathbf{r}',t,t') \\ &+ \int_{-\infty}^{\infty}\mathrm{d}t_1\int_{-\infty}^{\infty}\mathrm{d}t_2\int\mathrm{d}^3\mathbf{r}_1\int\mathrm{d}^3\mathbf{r}_2\int_0^{\infty}\mathrm{d}\nu\int_0^{\infty}\mathrm{d}\nu'\; K^{(0)}_{ml}(\mathbf{r},\mathbf{r}_1,t,t_1) \\ &\times H^{(0)}_{lp}(\mathbf{r}_1,\mathbf{r}_2,t_1,t_2,\nu,\nu')K_{pn}(\mathbf{r}_2,\mathbf{r}',t_2,t') \end{aligned} \tag{6.64}$$

The above equation is easily solved exactly. Both spatial integrations are trivially calculated, cf. Eqs. (6.57) and (6.60). Then, we Fourier transform with respect to $t-t'$

$$K_{mn}(\mathbf{r},\mathbf{r}';\omega) = \int_{-\infty}^{\infty}\mathrm{d}(t-t')e^{i\omega(t-t')}K_{mn}(\mathbf{r},\mathbf{r}',t-t') \tag{6.65}$$

and find the following expression for the dressed polarization field propagator in the frequency domain

$$K_{mn}(\mathbf{r}-\mathbf{r}';\omega) = K_{mn}(\mathbf{r}-\mathbf{r}';\omega) = K(\omega)\delta^{(3)}(\mathbf{r}-\mathbf{r}')\delta_{mn} \tag{6.66}$$

with

$$K(\omega) = \frac{1}{\mathcal{M}}\left[\omega^2 - \omega_{\mathrm{T}}^2 - \omega_{\mathrm{P}}^2 - \frac{\omega^2}{\mathcal{M}}\int_0^\infty \mathrm{d}\nu \frac{\rho_\nu \nu^2}{\omega^2 - \nu^2 + i\eta}\right]^{-1}. \tag{6.67}$$

Note that $K(\omega)$ is an even function of ω.

6.4.2 Dressing the photon line

The coupling between the (dressed) polarization field and the electromagnetic field (6.62) has formally the same form as the coupling between the polarization field and the bath (6.61). Therefore, by analogy with the previous section, we write down the graphical equation for the dressed photon propagator:

where the bold dashed line denotes the dressed photon propagator i.e.

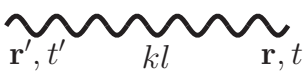

$$\equiv i\hbar D_{kl}(\mathbf{r}, \mathbf{r}', t, t')$$

The corresponding analytical expression is given by

$$\begin{aligned} D_{ik}(\mathbf{r}, \mathbf{r}', t, t') = {} & D_{ik}^{(0)}(\mathbf{r}-\mathbf{r}', t-t') \\ & + \frac{1}{\epsilon_0^2}\int_{-\infty}^{\infty}\mathrm{d}t_1 \int_{-\infty}^{\infty}\mathrm{d}t_2 \int \mathrm{d}^3\mathbf{r}_1 \int \mathrm{d}^3\mathbf{r}_2\, g(\mathbf{r}_1) g(\mathbf{r}_2) D_{ij}^{(0)}(\mathbf{r}-\mathbf{r}_1, t-t_1) \\ & \times K_{jl}(\mathbf{r}_1-\mathbf{r}_2, t_1, t_2) D_{lk}(\mathbf{r}_2, \mathbf{r}', t_2, t'). \end{aligned} \tag{6.68}$$

Now recall the remark made after Eq. (6.16) where we have discussed the shifted eigenfrequency $\tilde{\omega}_{\mathrm{T}}$ of the polarization field. It enters the Dyson equation (6.68) through the dressed polarization field propagator $K_{jl}(\mathbf{r}_1-\mathbf{r}_2, t_1, t_2)$. We noted there, that according to Eq. (6.16), it suffers a jump in the region where the polarization field is coupled to the

electromagnetic field i.e. in the region where the coupling function $g(\mathbf{r}) = 1$. It is now apparent that this discontinuity of the frequency $\tilde{\omega}_{\mathrm{T}}$ is not problematic because all spatial integrations in (6.68) are limited to the region of space where $g(\mathbf{r}) = 1$.

To simplify (6.68) we note that one of the spatial integrations is trivial due to the δ-function, cf. Eq. (6.66), and after we carry out the Fourier transformation with respect to time difference $t - t'$

$$D_{ik}(\mathbf{r}, \mathbf{r}'; \omega) = \int_{-\infty}^{\infty} \mathrm{d}(t - t') e^{i\omega(t-t')} D_{ik}(\mathbf{r}, \mathbf{r}', t, t') \tag{6.69}$$

we find the Dyson equation for the dressed photon propagator in the frequency domain

$$D_{ik}(\mathbf{r}, \mathbf{r}'; \omega) = D^{(0)}_{ik}(\mathbf{r} - \mathbf{r}'; \omega) + \frac{K(\omega)}{\epsilon_0^2} \int \mathrm{d}^3\mathbf{r}_1 g(\mathbf{r}_1) D^{(0)}_{ij}(\mathbf{r} - \mathbf{r}_1; \omega) D_{jk}(\mathbf{r}_1, \mathbf{r}'; \omega). \tag{6.70}$$

The dimensionless coupling function $g(\mathbf{r})$ is as defined in equation (6.6), $D^{(0)}_{ik}(\mathbf{r} - \mathbf{r}', \omega)$ is the real-space photon propagator in an unbounded vacuum i.e. the inverse Fourier transform of (6.49)

$$D^{(0)}_{ik}(\mathbf{r} - \mathbf{r}', \omega) = \frac{\epsilon_0}{(2\pi)^3} \int \mathrm{d}^3\mathbf{q}\, e^{i\mathbf{q}(\mathbf{r}-\mathbf{r}')} \frac{\delta_{ik}\mathbf{q}^2 - q_i q_k}{\omega^2 - \mathbf{q}^2 + i\eta}. \tag{6.71}$$

Function $K(\omega)$ is the frequency-dependent complex function that arose from the dressed polarization field propagator and is given in (6.67); it will be shown to be related to the dielectric permittivity. Interestingly, the geometry of the dielectric enters the calculations only through $g(\mathbf{r})$, which effectively defines the limits of the integration in equation (6.70).

Solution of the integral equation (6.70) is much less trivial than the case of dressing the polarization line, Section 6.4.1. This is because of the translation invariance has been lost when the inhomogeneous dielectric has been introduced into the system. In the next section we are going to solve the Dyson equation satisfied by the dressed photon propagator for the two geometries - the half-space and the gap. To illustrate the different methods we will first determine the propagator in the half-space geometry somewhat indirectly. We will convert the integral equation to a differential equation and then solve the resulting boundary value problem. Next we will determine the propagator for the gap geometry. In this case we will solve the integral equation directly by iteration. The iteration method applied here largely relies on the developments reported in [79]. We will also illustrate how

the iteration technique works for the half-space geometry and point out a peculiar issue of the convergence of the iterative expansion. In Appendix B, for comparison with other theories, we will also construct a photon propagator using an alternative method based on phenomenological noise-current approach.

6.4.2.1 The half-space

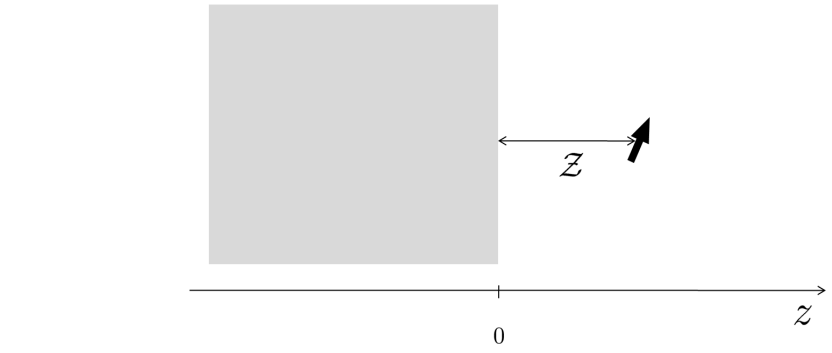

FIGURE 6.1: Atomic dipole moment at a distance $\mathcal{Z}$ away from the dielectric half-space of complex and frequency-dependent permittivity $\epsilon(\omega)$. The transverse propagator of the displacement field $D_{ik}(\mathbf{r}, \mathbf{r}'; \omega)$ in this geometry is given by Eq. (6.108).

The integral equation satisfied by the dressed photon propagator was derived in Section 6.4.2. For convenience we write it down again here:

$$D_{ik}(\mathbf{r}, \mathbf{r}'; \omega) = D^{(0)}_{ik}(\mathbf{r} - \mathbf{r}'; \omega) + \frac{K(\omega)}{\epsilon_0^2} \int \mathrm{d}^3\mathbf{r}_1 g(\mathbf{r}_1) D^{(0)}_{ij}(\mathbf{r} - \mathbf{r}_1; \omega) D_{jk}(\mathbf{r}_1, \mathbf{r}'; \omega). \quad (6.72)$$

To recall, $D^{(0)}_{ik}(\mathbf{r} - \mathbf{r}')$ is the photon propagator in free space, Eq. (6.71), and $g(\mathbf{r})$ is a dimensionless coupling constant that is equal to unity in the region occupied by the dielectric and vanishes otherwise. We now specify the geometry of the problem to describe a dielectric half-space occupying the $z < 0$ region of space, as illustrated in Fig. 6.1. This choice of the dielectric's geometry is realized by taking

$$g(\mathbf{r}_1) = \theta(-z_1) \quad (6.73)$$

where θ is the Heaviside step function. Knowing that the free-space propagator satisfies the differential equation (6.45) we apply the same differential operator to equation (6.72)

and obtain

$$\left(\nabla_i\nabla_j - \delta_{ij}\nabla^2\right) D_{jk}(\mathbf{r},\mathbf{r}';\omega) - \omega^2 D_{ik}(\mathbf{r},\mathbf{r}';\omega) = \frac{\epsilon_0}{(2\pi)^3}\int \mathrm{d}^3\mathbf{q}\left(q_iq_k - \delta_{ik}\mathbf{q}^2\right) e^{i\mathbf{q}\cdot(\mathbf{r}-\mathbf{r}')} + \frac{1}{(2\pi)^3}\frac{K(\omega)}{\epsilon_0}\int \mathrm{d}^3\mathbf{r}_1\theta(-z_1)\int \mathrm{d}^3\mathbf{q}\, e^{i\mathbf{q}\cdot(\mathbf{r}-\mathbf{r}_1)}\left(q_iq_j - \delta_{ij}\mathbf{q}^2\right) D_{jk}(\mathbf{r}_1,\mathbf{r}';\omega). \tag{6.74}$$

Now we write out the factor $\left(q_iq_j - \delta_{ij}\mathbf{q}^2\right)$ in the last term as derivatives acting on exponential and pull it outside the integrals. Then, interchanging the order of $\mathbf{q}$ and $\mathbf{r}_1$ integration we arrive at the differential equation satisfied by the photon propagator in the half-space geometry

$$\left(\nabla_i\nabla_j - \delta_{ij}\nabla^2\right)\left[1 + \theta(-z)\frac{K(\omega)}{\epsilon_0}\right] D_{jk}(\mathbf{r},\mathbf{r}';\omega) - \omega^2 D_{ik}(\mathbf{r},\mathbf{r}';\omega) = \frac{\epsilon_0}{(2\pi)^3}\int \mathrm{d}^3\mathbf{q}\left(q_iq_k - \delta_{ik}\mathbf{q}^2\right) e^{i\mathbf{q}\cdot(\mathbf{r}-\mathbf{r}')}. \tag{6.75}$$

The quantity that appears on the RHS can be written as

$$-\frac{1}{(2\pi)^3}\int \mathrm{d}^3\mathbf{q}\left(\mathbf{q}^2\delta_{ik} - q_iq_k\right) e^{i\mathbf{q}\cdot(\mathbf{r}-\mathbf{r}')} = \nabla^2\delta^{\perp}_{ik}(\mathbf{r}-\mathbf{r}') \tag{6.76}$$

where $\delta^{\perp}_{ik}(\mathbf{r}-\mathbf{r}')$ is the standard transverse delta-function. Now it is more apparent that the RHS of (6.75) contains a distribution and, unlike the transverse delta function, it is a *local* distribution i.e. it is sharply localized around the point $\mathbf{r} = \mathbf{r}'$, the non-local part being removed by the Laplacian through the relation

$$-\nabla^2\left(\frac{1}{4\pi|\mathbf{r}-\mathbf{r}'|}\right) = \delta^{(3)}(\mathbf{r}-\mathbf{r}'). \tag{6.77}$$

The locality of $\nabla^2\delta^{\perp}_{ik}(\mathbf{r}-\mathbf{r}')$ is a very fortunate property of the differential equation (6.75), which is essentially a scattering problem. Its RHS contains distribution which represents a unit source and our task is to work out reflection and transmission at a boundary of the dielectric. Therefore, in order to proceed any further, we need to specify physical situation i.e. decide on which side of the boundary the source is localized. Since our ultimate aim is to work out the energy-shift in an atom located outside the dielectric, we choose to first consider the case $z' > 0$. Then, Eq. (6.75) may be written in a "piecewise" manner i.e.

on the vacuum side we have

$$\left(\nabla_i\nabla_j - \delta_{ij}\nabla^2\right) D_{jk}(\mathbf{r},\mathbf{r}';\omega) - \omega^2 D_{ik}(\mathbf{r},\mathbf{r}';\omega) = \epsilon_0\nabla^2\delta^{\perp}_{ik}(\mathbf{r}-\mathbf{r}'), \quad z>0, \tag{6.78}$$

whereas on the dielectric side we have

$$\left(\nabla_i\nabla_j - \delta_{ij}\nabla^2\right) D_{jk}(\mathbf{r},\mathbf{r}';\omega) - \xi(\omega)\omega^2 D_{ik}(\mathbf{r},\mathbf{r}';\omega) = 0, \quad z<0, \tag{6.79}$$

and the behaviour of the propagator $D_{jk}(\mathbf{r},\mathbf{r}';\omega)$ across the interface $z=0$ is still to be determined. Note how the local character of the RHS of equation (6.75) simplifies the solution of Eqs. (6.78)-(6.79). It is this property that allows us to set the RHS of (6.79) to zero. The function $\xi(\omega)$ that appeared in (6.79) is an even function of ω and, on the positive real axis, it coincides with the dielectric function of the bulk dielectric[4], see Appendix E. It is explicitly written out as

$$\begin{aligned}\xi(\omega) = \frac{1}{1+\dfrac{K(\omega)}{\epsilon_0}} &= 1+\frac{1}{\epsilon_0\mathcal{M}}\left[\omega_{\mathrm{T}}^2-\omega^2-\frac{\omega^2}{\mathcal{M}}\int_0^\infty \mathrm{d}\nu\,\frac{\rho_\nu\nu^2}{\nu^2-\omega^2-i\eta}\right]^{-1}\\ &= 1+\frac{\omega_{\mathrm{P}}^2}{\omega_{\mathrm{T}}^2-\omega^2-2i\gamma\sqrt{\omega^2}}.\end{aligned} \tag{6.82}$$

To solve Eqs. (6.78)-(6.79) we start with the following ansatz

$$D_{ik}(\mathbf{r},\mathbf{r}';\omega) = \theta(-z)D^{(t)}_{ik}(\mathbf{r},\mathbf{r}';\omega) + \theta(z)\left[D^{(0)}_{ik}(\mathbf{r}-\mathbf{r}';\omega) + D^{(r)}_{ik}(\mathbf{r},\mathbf{r}';\omega)\right], \tag{6.83}$$

which we justify as follows. On the vacuum side the solution is written as a sum that consists of the particular solution[5] $D^{(0)}_{ik}(\mathbf{r}-\mathbf{r}';\omega)$ and the solution $D^{(r)}_{ik}(\mathbf{r},\mathbf{r}';\omega)$ of the

[4]Note the difference in the η prescription in equations (E.10) and (6.82). This is because equation (6.82) originates from the Feynman propagator for the polarization field, Eq. (6.57), that is defined as

$$K_{ij}(\mathbf{r},\mathbf{r}',t,t') = -\frac{i}{\hbar}\langle 0|T\left(X_i(\mathbf{r},t)X_j(\mathbf{r}',t')\right)|0\rangle, \tag{6.80}$$

whereas the response function (E.10) is related to the retarded propagator of the polarization field

$$K^{\mathrm{ret}}_{ij}(\mathbf{r},\mathbf{r}',t,t') = -\frac{i}{\hbar}\langle 0|\left[X_i(\mathbf{r},t),X_j(\mathbf{r}',t')\right]|0\rangle, \tag{6.81}$$

for details see [80].

[5]We already know the particular solution of Eq. (6.78) because we have derived it in Section 6.3.2, Eq. (6.45).

homogeneous equation, i.e. Eq. (6.78) with the RHS set to zero, which represents the correction due to reflection at the boundary. The solution on the dielectric side $D_{ik}^{(t)}(\mathbf{r},\mathbf{r}';\omega)$ represents the transmitted part and satisfies the homogeneous equation (6.79). The homogeneous solutions $D_{ik}^{(r)}(\mathbf{r},\mathbf{r}';\omega)$ and $D_{ik}^{(t)}(\mathbf{r},\mathbf{r}';\omega)$ are chosen in such a way that the general solution given in Eq. (6.83) satisfies appropriate boundary conditions across the interface $z=0$. To see what these boundary conditions should be recall the formal definition of the dressed propagator

$$D_{ij}(\mathbf{r},\mathbf{r}';\omega) = -\frac{i}{\hbar}\langle\Omega|T\left[D_i(\mathbf{r},t)D_j(\mathbf{r}',t')\right]|\Omega\rangle. \tag{6.84}$$

The displacement operator $D_i(\mathbf{r},t)$ satisfies Maxwell's equations which follow from Heisenberg's equations of motion, see Appendix E. Therefore, the photon propagator, by virtue of its definition (6.84), when taken as a function of argument $\mathbf{r}$ and index i, is required to satisfy Maxwell's boundary conditions across the interface:

$$\begin{aligned}
&\mathbf{E}_{\|} \quad \text{continuous} \quad \Rightarrow \quad \epsilon^{-1} D_{\|j}\Big|_{z=0^-} = D_{\|j}\Big|_{z=0^+} \\
&D_z \quad \text{continuous} \quad \Rightarrow \quad D_{3j}\Big|_{z=0^-} = D_{3j}\Big|_{z=0^+} \\
&\mathbf{B}_{\|} \quad \text{continuous} \quad \Rightarrow \quad \epsilon^{-1}\nabla_z D_{\|j}\Big|_{z=0^-} = \nabla_z D_{\|j}\Big|_{z=0^+}
\end{aligned} \tag{6.85}$$

with $\|= \{1,2\}$. Another way to see it is to think about the relation

$$D_k(\mathbf{r};\omega) = \int \mathrm{d}^3\mathbf{r}'\; D_{kl}(\mathbf{r},\mathbf{r}';\omega)\; j_l(\mathbf{r}';\omega) \tag{6.86}$$

which expresses the displacement field $\mathbf{D}(\mathbf{r};\omega)$ as a function of some given current $\mathbf{j}(\mathbf{r};\omega)$. If $D_k(\mathbf{r};\omega)$ is to satisfy Maxwell's boundary conditions so is the propagator with respect to variable $\mathbf{r}$ and index k. The apparent complication arising from the appearance of the non-standard distribution in the boundary-value problem (6.75) is an initial illusion. In fact, it is easier to find the solution of (6.75) than it is to solve the standard differential equation satisfied by the Green's function of the wave equation, for example see [85]. Equations (6.78)-(6.79), together with the boundary conditions (6.85), form a boundary-value problem which is equivalent to the integral equation (6.72) with the choice $g(\mathbf{r}_1) = \theta(-z_1)$ (dielectric occupying $z<0$ half-space) and $z'>0$ (source of radiation located in vacuum).

Because of the boundary the problem has lost translational invariance in the z-direction, but not in directions parallel to the surface. In other words, the propagator depends only on the difference $\mathbf{r}_\parallel - \mathbf{r}'_\parallel$ but separately on z and z'. We shall work with quantities Fourier transformed with respect to $\mathbf{r}_\parallel - \mathbf{r}'_\parallel$ i.e.

$$D_{ij}(z, z'; \mathbf{q}_\parallel, \omega) = \int \mathrm{d}^2(\mathbf{r}_\parallel - \mathbf{r}'_\parallel) e^{-i\mathbf{q}_\parallel \cdot (\mathbf{r}_\parallel - \mathbf{r}'_\parallel)} D_{ij}(\mathbf{r}_\parallel - \mathbf{r}_\parallel, z, z'; \omega). \tag{6.87}$$

Our first task is to find representation of the free-space propagator (6.71) as a two-dimensional integral over the momenta parallel to the surface. We write

$$\begin{aligned} D^{(0)}_{ik}(\mathbf{r} - \mathbf{r}', \omega) &= \frac{\epsilon_0}{(2\pi)^3} \int \mathrm{d}^3\mathbf{q} \frac{\delta_{ik}\mathbf{q}^2 - q_i q_k}{\omega^2 - \mathbf{q}^2 + i\eta} \, e^{i\mathbf{q}(\mathbf{r}-\mathbf{r}')} \\ &= -\frac{\epsilon_0}{(2\pi)^3} \left(\nabla_i \nabla_k - \delta_{ik}\nabla^2\right) \int \mathrm{d}^2\mathbf{q}_\parallel e^{i\mathbf{q}_\parallel \cdot (\mathbf{r}_\parallel - \mathbf{r}'_\parallel)} \int_{-\infty}^{\infty} \mathrm{d}q_z \frac{e^{iq_z(z-z')}}{(q_z - k_z)(q_z + k_z)} \end{aligned}$$

and use the residue theorem to evaluate the q_z integral. The result is written in a compact form as

$$D^{(0)}_{ik}(\mathbf{r} - \mathbf{r}', \omega) = -\frac{i\epsilon_0}{2(2\pi)^2} \left(\nabla_i \nabla_k - \delta_{ik}\nabla^2\right) \int \mathrm{d}^2\mathbf{q}_\parallel e^{i\mathbf{q}_\parallel \cdot \left(\mathbf{r}_\parallel - \mathbf{r}'_\parallel\right)} \frac{e^{ik_z|z-z'|}}{k_z} \tag{6.88}$$

where k_z is the z-component of the wavevector in vacuum and is given by $k_z = \sqrt{\omega^2 - \mathbf{q}_\parallel^2 + i\eta}$. The square-root is taken such that the imaginary part of k_z is always positive. Equation (6.88) shows that Fourier transform of the free-space photon propagator with respect $\mathbf{r}_\parallel - \mathbf{r}'_\parallel$ is singular when crossing the $z = z'$ plane. We now note a very useful relation

$$q^2\delta_{ik} - q_i q_k = \omega^2 \left[e_i^{\mathrm{TE}}(\mathbf{q}) e_k^{\mathrm{TE}}(\mathbf{q}) + e_i^{\mathrm{TM}}(\mathbf{q}) e_k^{\mathrm{TM}}(\mathbf{q})\right] \tag{6.89}$$

with $\mathbf{q} = (\mathbf{q}_\parallel, k_z)$ being the vacuum wavevector and we have introduced the unit polarization vectors

$$\mathbf{e}^{\mathrm{TE}}(\mathbf{q}_\parallel) = \frac{1}{|\mathbf{q}_\parallel|}(-q_y, q_x, 0), \quad \mathbf{e}^{\mathrm{TM}}(\mathbf{q}_\parallel, k_z) = \frac{1}{|\mathbf{q}_\parallel|\omega}(q_x k_z, q_y k_z, -\mathbf{q}_\parallel^2). \tag{6.90}$$

This relation follows from the completeness property of the polarization vectors (6.90). We may now write

$$\left(\nabla_i\nabla_k - \delta_{ik}\nabla^2\right) e^{i\mathbf{q}_\parallel\cdot\left(\mathbf{r}_\parallel-\mathbf{r}'_\parallel\right)+ik_z|z-z'|} = \omega^2 \sum_\lambda \begin{cases} e_i^\lambda(\mathbf{q}_\parallel,k_z)e_k^\lambda(\mathbf{q}_\parallel,k_z) & z>z' \\ e_i^\lambda(\mathbf{q}_\parallel,-k_z)e_k^\lambda(\mathbf{q}_\parallel,-k_z) & z<z' \end{cases} \tag{6.91}$$

so that the representation of the free-space propagator (6.88) may be written as

$$D_{ij}^{(0)}(z,z';\mathbf{q}_\parallel,\omega) = -\frac{i\epsilon_0\omega^2}{2k_z}\sum_\lambda \begin{cases} e_i^\lambda(\mathbf{q}_\parallel,k_z)e_k^\lambda(\mathbf{q}_\parallel,k_z)e^{ik_z(z-z')} & z>z' \\ e_i^\lambda(\mathbf{q}_\parallel,-k_z)e_k^\lambda(\mathbf{q}_\parallel,-k_z)e^{-ik_z(z-z')} & z<z' \end{cases}. \tag{6.92}$$

Warning: The above representation of the free-space propagator is valid away from the point $z=z'$. At this point the z-derivatives in (6.88), when acting on $e^{ik_z|z-z'|}$, produce terms proportional to the delta function and its derivative. We will use Eq. (6.92) in the process of matching the boundary conditions. This is safe because then we consider $z=0^\pm$ and the source located at z' is always well away from the boundary.

To proceed further we note that taking the divergence of the integral equation (6.72) and using the fact that $\nabla_i D_{ik}^{(0)}(\mathbf{r}-\mathbf{r}';\omega)=0$ one infers that the dressed photon propagator is transverse everywhere

$$\nabla_i D_{ik}(\mathbf{r},\mathbf{r}';\omega) = 0. \tag{6.93}$$

With this, equations (6.78)-(6.79) simplify further and in the $(\mathbf{q}_\parallel,z)$-space may be written as

$$\begin{aligned} &\left(\nabla_z^2 - \mathbf{q}_\parallel^2 + \omega^2\right) D_{ij}(z,z';\mathbf{q}_\parallel,\omega) = \epsilon_0\left(\mathbf{q}_\parallel^2 - \nabla_z^2\right)\delta_{ij}^\perp(\mathbf{q}_\parallel,z-z'), && z>0 \\ &\left(\nabla_z^2 - \mathbf{q}_\parallel^2 + \xi(\omega)\omega^2\right) D_{ij}(z,z';\mathbf{q}_\parallel,\omega) = 0, && z<0 \end{aligned} \tag{6.94}$$

where $\delta_{ij}^\perp(\mathbf{q}_\parallel,z-z')$ is Fourier transform of $\delta_{ij}^\perp(\mathbf{r}-\mathbf{r}')$ with respect to $\mathbf{r}_\parallel-\mathbf{r}'_\parallel$:

$$\delta_{ij}^\perp(\mathbf{q}_\parallel,z-z') = \int \mathrm{d}^2(\mathbf{r}_\parallel-\mathbf{r}'_\parallel)e^{-i\mathbf{q}_\parallel\cdot(\mathbf{r}_\parallel-\mathbf{r}'_\parallel)}\delta_{ij}^\perp(\mathbf{r}-\mathbf{r}'). \tag{6.95}$$

Equations (6.94) provide us with very important information, namely that the homogeneous solutions $D_{ik}^{(r)}(\mathbf{r},\mathbf{r}';\omega)$ and $D_{ik}^{(t)}(\mathbf{r},\mathbf{r}';\omega)$, as postulated in (6.83), must necessarily

take the form

$$D_{ij}^{(r)}(z,z';\mathbf{q}_\parallel,\omega) = -\frac{i\epsilon_0}{2}\left[R_{ij}(\mathbf{q}_\parallel,z')e^{ik_z z}+S_{ij}(\mathbf{q}_\parallel,z')e^{-ik_z z}\right],\quad z>0, \tag{6.96}$$

$$D_{ij}^{(t)}(z,z';\mathbf{q}_\parallel,\omega) = -\frac{i\epsilon_0}{2}\left[T_{ij}(\mathbf{q}_\parallel,z')e^{-ik_{zd} z}+U_{ij}(\mathbf{q}_\parallel,z')e^{ik_{zd} z}\right],\quad z<0, \tag{6.97}$$

with $k_z = \sqrt{\omega^2-\mathbf{q}_\parallel^2+i\eta}$ and $k_{zd} = \sqrt{\xi(\omega)\omega^2-\mathbf{q}_\parallel^2}$ and we take the square-roots such that k_z and k_{zd} have always positive imaginary part. With this choice of the sign for the square-roots, we observe that terms of the homogeneous solutions (6.96)-(6.97) that contain exponentials $e^{-ik_z z}$ and $e^{ik_{zd}z}$ are unphysical for they represent waves that diverge at infinity. For this reason we may set $S_{ij}=U_{ij}=0$. The remaining two matrices R_{ij} and T_{ij} are chosen so that the general solution (6.83) satisfies the boundary conditions (6.85). To impose the boundary conditions and work out the amplitudes R_{ij} and T_{ij} we observe that the transversality of the dressed propagator (6.93) imposes rather stringent constraints on both of them. For example, the matrix R_{ij} needs to be written in the form

$$R_{ij} = v_i(\mathbf{q}_\parallel)r_j(\mathbf{q}_\parallel,z'), \tag{6.98}$$

where the vector $\mathbf{v}$ is such that

$$\mathbf{q}\cdot\mathbf{v}=0 \quad\Rightarrow\quad \mathbf{v}=\left(v_x,v_y,-\frac{q_x v_y+q_y v_x}{k_z}\right), \tag{6.99}$$

with $\mathbf{q}\equiv(\mathbf{q}_\parallel,k_z)$. By hindsight, we pick $v_x=-q_y$ and $v_y=q_x$ so that

$$\mathbf{v}=(-q_y,q_x,0)\,. \tag{6.100}$$

However, this choice is too restrictive on its own. There is no *a priori* reason for $D_{3j}^{(+)}$ to vanish. Therefore, an additional basis vector is needed in order to span the amplitude R_{ij} in full generality. An obvious and convenient choice is to choose a vector that is orthogonal to both $\mathbf{q}$ and $\mathbf{v}$

$$\mathbf{w}=\mathbf{v}\times\mathbf{q}=(q_x k_z, q_y k_z, -\mathbf{q}_\parallel^2). \tag{6.101}$$

We represent R_{ij} as a linear combination

$$R_{ij} = [\alpha\mathbf{v}+\beta\mathbf{w}]_i\, r_j(\mathbf{q}_\parallel,z') \equiv e_i^{\mathrm{TE}}(\mathbf{q}_\parallel,k_z)r_j^{\mathrm{TE}}(\mathbf{q}_\parallel,z')+e_i^{\mathrm{TM}}(\mathbf{q}_\parallel,k_z)r_j^{\mathrm{TM}}(\mathbf{q}_\parallel,z'), \tag{6.102}$$

where we have recognized in the above argument, apart from normalization factors, the transverse electric and transverse magnetic polarization vectors, cf. Eq. (6.90). Similarly we have

$$T_{ij} = e_i^{\mathrm{TE}}(\mathbf{q}_\parallel, -k_{zd}) t_j^{\mathrm{TE}}(\mathbf{q}_\parallel, z') + e_i^{\mathrm{TM}}(\mathbf{q}_\parallel, -k_{zd}) t_j^{\mathrm{TM}}(\mathbf{q}_\parallel, z'), \tag{6.103}$$

with

$$\mathbf{e}^{\mathrm{TM}}(\mathbf{q}_\parallel, -k_{zd}) = \frac{1}{\sqrt{\xi(\omega)}|\mathbf{q}_\parallel|\omega}(-q_x k_{zd}, -q_y k_{zd}, -\mathbf{q}_\parallel^2). \tag{6.104}$$

We have intentionally written out the k_z-dependence of the polarization vectors even though in reality k_z and k_{zd} are expressible in terms of frequency ω and parallel wave-vector $\mathbf{q}_\parallel$. This is useful as it explicitly indicates the wave-vector to which a given polarization vector is orthogonal to. The decomposition into transverse electric and transverse magnetic components significantly simplifies the matching of boundary conditions. The dressed photon propagator can now be written in the form

$$\begin{aligned} D_{ij}(z, z'; \mathbf{q}_\parallel, \omega) = -\frac{i\epsilon_0}{2} \sum_\lambda \Bigg\{ & \left[e_i^\lambda(\mathbf{q}_\parallel, -k_{zd}) t_j^\lambda e^{-ik_{zd}z} \right] \theta(-z) \\ & + \left[e_i^\lambda(\mathbf{q}_\parallel, k_z) r_j^\lambda e^{ik_z z} + \frac{\omega^2}{k_z} e_i^\lambda(\mathbf{q}_\parallel, -k_z) e_j^\lambda(\mathbf{q}_\parallel, -k_z) e^{-ik_z(z-z')} \right] \theta(z) \Bigg\}. \end{aligned} \tag{6.105}$$

The last term appearing in the above expression is the free-space photon propagator given in Eq. (6.92). We have chosen the solution for which $z - z' < 0$ as is appropriate for the boundary conditions matching at $z = 0^\pm$ in the situation when $z' > 0$. Imposing boundary conditions (6.85) we find that

$$\begin{aligned} r_j^\lambda &= r_R^\lambda \, e_j^\lambda(\mathbf{q}_\parallel, -k_z) \frac{\omega^2}{k_z} e^{ik_z z'}, \\ t_j^\lambda &= t_R^\lambda \, e_j^\lambda(\mathbf{q}_\parallel, -k_z) \frac{\xi(\omega)\omega^2}{k_z} e^{ik_z z'}, \end{aligned} \tag{6.106}$$

with r^λ and t^λ being the standard Fresnel's reflection and transmission coefficients

$$\begin{aligned} r_R^{\mathrm{TE}} &= \frac{k_z - k_{zd}}{k_z + k_{zd}}, \quad r_R^{\mathrm{TM}} = \frac{\xi(\omega)k_z - k_{zd}}{\xi(\omega)k_z + k_{zd}}, \\ t_R^{\mathrm{TE}} &= \frac{2k_z}{k_z + k_{zd}}, \quad t_R^{\mathrm{TM}} = \frac{2\sqrt{\xi(\omega)}k_z}{\xi(\omega)k_z + k_{zd}}. \end{aligned} \tag{6.107}$$

For future reference we write out the propagator in a complete form:

$$D_{ij}(\mathbf{r},\mathbf{r}';\omega) = \theta(z)D_{ij}^{(0)}(\mathbf{r}-\mathbf{r}';\omega) - \frac{i\epsilon_0}{(2\pi)^2}\sum_{\lambda}\int \mathrm{d}^2\mathbf{q}_\parallel \frac{\omega^2}{2k_z} e^{i\mathbf{q}_\parallel\cdot(\mathbf{r}_\parallel-\mathbf{r}'_\parallel)} \times\Big\{\theta(-z)\left[\xi(\omega)e_i^\lambda(\mathbf{q}_\parallel,-k_{zd})e_j^\lambda(\mathbf{q}_\parallel,-k_z)t_R^\lambda\right]e^{-ik_{zd}z+ik_zz'} +\theta(z)\left[e_i^\lambda(\mathbf{q}_\parallel,k_z)e_j^\lambda(\mathbf{q}_\parallel,-k_z)r_R^\lambda e^{ik_z(z+z')}\right]\Big\}. \quad (6.108)$$

and we remind the reader that the expression (6.108) is valid for $z' > 0$. In the calculations of the atomic energy-level shifts we will use the propagator for the case $z, z' > 0$, where it splits into a free-space part $D_{ij}^{(0)}(\mathbf{r}-\mathbf{r}';\omega)$, which is not interesting for us as it corresponds to the position-independent Lamb shift, and the correction due to reflection at the boundary $D_{ij}^{(r)}(\mathbf{r},\mathbf{r}';\omega)$ that gives a rise do the distance-dependent Casimir-Polder shift. We recall that we treat the atom-field interaction in the dipole approximation. This effectively means that we will need the reflected part of the propagator $D_{ij}^{(r)}(\mathbf{r},\mathbf{r}';\omega)$ evaluated at equal arguments $\mathbf{r} = \mathbf{r}'$. In such a case it largely simplifies and can be written in the form

$$\mathbf{D}^{(r)}(\mathcal{Z};\omega) = -\frac{i\epsilon_0}{8\pi}\int_0^\infty \mathrm{d}k\frac{k}{k_z}e^{2ik_z\mathcal{Z}}\begin{pmatrix} \omega^2 r_R^{\mathrm{TE}} - k_z^2 r_R^{\mathrm{TM}} & 0 & 0 \\ 0 & \omega^2 r_R^{\mathrm{TE}} - k_z^2 r_R^{\mathrm{TM}} & 0 \\ 0 & 0 & 2k^2 r_R^{\mathrm{TM}} \end{pmatrix} \quad (6.109)$$

with $k_z = \sqrt{\omega^2 - k^2 + i\eta}$ and we have gone to polar coordinates, $q_x = k\cos\phi$, $q_y = k\sin\phi$, where the angle integration annihilated the off-diagonal elements of equal-argument propagator $D_{ik}^{(r)}(\mathbf{r},\mathbf{r};\omega)$.

We can readily apply the methods developed here to obtain the propagator in the case when the source is placed in the dielectric i.e. $z' < 0$. In this case, the integral equation (6.72) is converted to the Fourier transformed set of differential equations

$$\begin{aligned} &\left(\nabla_z^2 - \mathbf{q}_\parallel^2 + \omega^2\right) D_{ij}(z,z';\mathbf{q}_\parallel,\omega) = 0 && z > 0 \\ &\left(\nabla_z^2 - \mathbf{q}_\parallel^2 + \xi(\omega)\omega^2\right) D_{ij}(z,z';\mathbf{q}_\parallel,\omega) = \epsilon_0\xi(\omega)\left(\mathbf{q}_\parallel^2 - \nabla_z^2\right)\delta_{ij}^\perp(\mathbf{q}_\parallel, z-z') && z < 0 \end{aligned} \quad (6.110)$$

with the boundary conditions given in (6.85). The particular solution of Eq. (6.110) for $z < 0$ is given by the displacement propagator in a bulk dielectric $D_{ik}^{(\epsilon)}(\mathbf{r}-\mathbf{r}';\omega)$ i.e. the solution of (6.70) with $g(\mathbf{r}_1) = 1$. It is fairly straightforward to obtain it using the fact that the bulk propagator depends only on the difference $\mathbf{r}-\mathbf{r}'$. Fourier transformation of

(6.72) with respect to $\mathbf{r}-\mathbf{r}'$ reads

$$D_{ik}^{(\epsilon)}(\mathbf{q},\omega)=\epsilon_0\,\frac{\delta_{ik}\mathbf{q}^2-q_iq_k}{\omega^2-\mathbf{q}^2+i\eta}+\frac{K(\omega)}{\epsilon_0}\frac{\delta_{ij}\mathbf{q}^2-q_iq_j}{\omega^2-\mathbf{q}^2+i\eta}\,D_{jk}^{(\epsilon)}(\mathbf{q},\omega). \tag{6.111}$$

This matrix equation becomes an algebraical one by virtue of the transversality of the propagator, Eq. (6.93). The calculation is straightforward and in the real space we obtain

$$D_{ik}^{(\epsilon)}(\mathbf{r}-\mathbf{r}',\omega)=\frac{\epsilon_0\xi(\omega)}{(2\pi)^3}\int\mathrm{d}^3\mathbf{q}\frac{\delta_{ik}\mathbf{q}^2-q_iq_k}{\xi(\omega)\omega^2-\mathbf{q}^2}\,e^{i\mathbf{q}(\mathbf{r}-\mathbf{r}')} \tag{6.112}$$

with $\xi(\omega)=(1+K(\omega)/\epsilon_0)^{-1}$. In order to solve (6.110) we are going to need Fourier transform of (6.112) with respect to $\mathbf{r}_\parallel-\mathbf{r}'_\parallel$. It can be written in the form

$$D_{ij}^{(\epsilon)}(z,z';\mathbf{q}_\parallel,\omega)=-\frac{i\epsilon_0\xi(\omega)\omega^2}{2k_{zd}}\sum_\lambda\begin{cases}e_i^\lambda(\mathbf{q}_\parallel,k_{zd})e_k^\lambda(\mathbf{q}_\parallel,k_{zd})e^{ik_{zd}(z-z')} & z>z'\\ e_i^\lambda(\mathbf{q}_\parallel,-k_{zd})e_k^\lambda(\mathbf{q}_\parallel,-k_{zd})e^{-ik_{zd}(z-z')} & z<z'\end{cases} \tag{6.113}$$

in a complete analogy with the formula for the free space propagator, Eq. (6.92). Here $k_{zd}=\sqrt{\xi(w)\omega^2-\mathbf{q}_\parallel^2}$ is the z-component of wave-vector in medium with always positive imaginary part. Also, make note of the important remark below Eq. (6.92). The homogeneous solutions of equations (6.110) are written as

$$D_{ij}^{(t)}(z,z';\mathbf{q}_\parallel,\omega) = -\frac{i\epsilon_0}{2}\left[T_{ij}(\mathbf{q}_\parallel,z')e^{ik_zz}+S_{ij}(\mathbf{q}_\parallel,z')e^{-ik_zz}\right],\quad z>0, \tag{6.114}$$

$$D_{ij}^{(r)}(z,z';\mathbf{q}_\parallel,\omega) = -\frac{i\epsilon_0}{2}\left[R_{ij}(\mathbf{q}_\parallel,z')e^{-ik_{zd}z}+U_{ij}(\mathbf{q}_\parallel,z')e^{ik_{zd}z}\right],\quad z<0, \tag{6.115}$$

with $k_z=\sqrt{\omega^2-\mathbf{q}_\parallel^2+i\eta}$ and $k_{zd}=\sqrt{\xi(\omega)\omega^2-\mathbf{q}_\parallel^2}$ and we take the roots such that k_z and k_{zd} have always positive imaginary part. With this choice we observe that terms of the homogeneous solutions (6.114)-(6.115) that contain exponentials e^{-ik_zz} and $e^{ik_{zd}z}$ are unphysical, for they represent waves that diverge at infinity. For this reason we set $S_{ij}=U_{ij}=0$. The remaining two matrices, R_{ij} and T_{ij}, are chosen so that the general solution, i.e. the sum of the particular and homogeneous solution, satisfies boundary conditions (6.85). To simplify matching of the boundary conditions we decompose the propagators into transverse electric and transverse magnetic components in exactly the

same manner as it was done in Eqs. (6.98)-(6.104)

$$\begin{aligned} R_{ij} &= e_i^{\mathrm{TE}}(\mathbf{q}_\parallel, -k_{zd}) r_j^{\mathrm{TE}}(\mathbf{q}_\parallel, z') + e_i^{\mathrm{TM}}(\mathbf{q}_\parallel, -k_{zd}) r_j^{\mathrm{TM}}(\mathbf{q}_\parallel, z'), \\ T_{ij} &= e_i^{\mathrm{TE}}(\mathbf{q}_\parallel, k_z) t_j^{\mathrm{TE}}(\mathbf{q}_\parallel, z') + e_i^{\mathrm{TM}}(\mathbf{q}_\parallel, k_z) t_j^{\mathrm{TM}}(\mathbf{q}_\parallel, z'). \end{aligned}$$

With this, the most general and physically admissible solution of Eqs. (6.110) suitable for boundary-condition matching may be written as

$$\begin{aligned} D_{ij}(z, z'; \mathbf{q}_\parallel, \omega) = -\frac{i\epsilon_0}{2} \sum_\lambda \Big\{ \Big[e_i^\lambda(\mathbf{q}_\parallel, k_z) t_j^\lambda e^{ik_z z} \Big] \theta(z) \\ + \left[e_i^\lambda(\mathbf{q}_\parallel, -k_{zd}) r_j^\lambda e^{-ik_{zd} z} + \frac{\omega^2}{k_z} e_i^\lambda(\mathbf{q}_\parallel, k_{zd}) e_j^\lambda(\mathbf{q}_\parallel, k_{zd}) e^{ik_{zd}(z-z')} \right] \theta(-z) \Big\}. \end{aligned} \tag{6.116}$$

The last term appearing in the above expression is the photon propagator in a bulk dielectric given in Eq. (6.113). We have chosen the solution for which $z - z' > 0$ as is appropriate for the boundary conditions matching at $z = 0^\pm$ in the situation when $z' < 0$. Imposing boundary conditions (6.85) we find that

$$\begin{aligned} r_j^\lambda &= r_L^\lambda \, e_j^\lambda(\mathbf{q}_\parallel, k_{zd}) \frac{\omega^2}{k_{zd}} e^{-ik_{zd} z'}, \\ t_j^\lambda &= t_L^\lambda \, e_j^\lambda(\mathbf{q}_\parallel, k_{zd}) \frac{\xi(\omega)\omega^2}{k_{zd}} e^{-ik_{zd} z'}, \end{aligned}$$

with r^λ and t^λ being the Fresnel's reflection and transmission coefficients

$$\begin{aligned} r_L^{\mathrm{TE}} &= \frac{k_{zd} - k_z}{k_z + k_{zd}}, \quad r_L^{\mathrm{TM}} = \frac{k_{zd} - \xi(\omega) k_z}{\xi(\omega) k_z + k_{zd}}, \\ t_L^{\mathrm{TE}} &= \frac{2k_{zd}}{k_z + k_{zd}}, \quad t_L^{\mathrm{TM}} = \frac{2\sqrt{\xi(\omega)} k_{zd}}{\xi(\omega) k_z + k_{zd}}. \end{aligned} \tag{6.117}$$

For future reference we write out the propagator in a complete form:

$$\begin{aligned} D_{ij}(\mathbf{r}, \mathbf{r}'; \omega) = \theta(-z) D_{ij}^{(\epsilon)}(\mathbf{r} - \mathbf{r}'; \omega) - \frac{i\epsilon_0}{(2\pi)^2} \sum_\lambda \int \mathrm{d}_2 \mathbf{q}_\parallel \frac{\xi(\omega)\omega^2}{2k_{zd}} e^{i\mathbf{q}_\parallel \cdot (\mathbf{r}_\parallel - \mathbf{r}'_\parallel)} \\ \times \Big\{ \theta(-z) \left[\xi(\omega) e_i^\lambda(\mathbf{q}_\parallel, -k_{zd}) e_j^\lambda(\mathbf{q}_\parallel, k_{zd}) r_L^\lambda \right] e^{-ik_{zd}(z+z')} \\ + \theta(z) \left[e_i^\lambda(\mathbf{q}_\parallel, k_z) e_j^\lambda(\mathbf{q}_\parallel, k_{zd}) t_L^\lambda e^{ik_z z - ik_{zd} z'} \right] \Big\}, \end{aligned} \tag{6.118}$$

and we remind the reader that the expression (6.118) is valid for $z' < 0$. It is easily verified that $D_{ij}(\mathbf{r}, \mathbf{r}'; \omega)$ is indeed transverse everywhere.

6.4.2.2 The gap

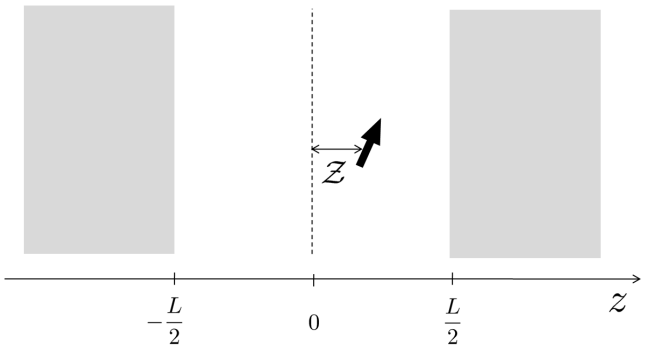

FIGURE 6.2: Atomic dipole moment at a distance $\mathcal{Z}$ away from the middle of the gap formed by parallel dielectric plates of complex and frequency-dependent permittivity $\epsilon(\omega)$. The transverse propagator of the displacement field $D_{ik}(\mathbf{r}, \mathbf{r}'; \omega)$ in this geometry is given by Eq. (6.146).

In the previous section we have calculated the photon propagator in a half-space geometry. This was done by converting the integral equation into the differential equation supported by Maxwell's boundary conditions. In this Section we wish to calculate the photon propagator in a gap geometry, as illustrated in Fig. 6.2, but using a different method. We will solve the integral equation (6.70) directly relying on iteration. We start with the integral equation (6.70) with the coupling function $g(\mathbf{r}_1)$ chosen such that it describes the gap centred at the origin and of width L,

$$D_{ik}(\mathbf{r}, \mathbf{r}'; \omega) = D^{(0)}_{ik}(\mathbf{r} - \mathbf{r}'; \omega) + \frac{K(\omega)}{\epsilon_0^2} \int \mathrm{d}^3\mathbf{r}_1 \left[\theta\left(-\frac{L}{2} - z_1\right) + \theta\left(z_1 - \frac{L}{2}\right)\right] D^{(0)}_{ij}(\mathbf{r} - \mathbf{r}_1; \omega) D_{jk}(\mathbf{r}_1, \mathbf{r}'; \omega), \quad (6.119)$$

where θ is the Heaviside step function. Equation (6.119) defines the problem completely but its not very practical for it does not allow the iterative process. To see what we mean by the iterative process let us write Eq. (6.119) symbolically

$$D = D^0 + K D^0 \otimes D. \quad (6.120)$$

Iterating the above equation leads to the expansion

$$D = D^0 + KD^0 \otimes D^0 + K^2 D^0 \otimes D^0 \otimes D^0 + K^3 D^0 \otimes D^0 \otimes D^0 \otimes D^0 + \ldots \tag{6.121}$$

Such an expansion proves especially useful if the action of the operator $\mathcal{O} = D^0\otimes$ on the free-space propagator D^0 amounts to a simple multiplication i.e.

$$D^0 \otimes D^0 = CD^0, \tag{6.122}$$

where C is some constant. Then, equation (6.121) becomes a geometrical series

$$D = D^0 \left(1 + KC + K^2C^2 + K^3C^3 + \ldots\right) \tag{6.123}$$

which we know how to sum up to all orders. In the language of the integral equation (6.119), the formula (6.122) implies

$$\int \mathrm{d}^3\mathbf{r}_1 \left[\theta\left(-\frac{L}{2} - z_1\right) + \theta\left(z_1 - \frac{L}{2}\right)\right] D^{(0)}_{ij}(\mathbf{r} - \mathbf{r}_1;\omega) D^{(0)}_{jk}(\mathbf{r}_1 - \mathbf{r}';\omega) \stackrel{?}{=} C_{ij} D^{(0)}_{jk}(\mathbf{r} - \mathbf{r}';\omega) \tag{6.124}$$

where C_{ij} is some constant matrix. It so happens that Eq. (6.124) doesn't hold so the iteration of Eq. (6.119) as it stands is not fruitful. However, the situation can be remedied by a clever trick that was developed in [79]. Here we will adapt it to find the solution of (6.119).

We now postulate that if $D^{(-)}_{ik}(\mathbf{r}, \mathbf{r}';\omega)$ denotes the propagator of the displacement field in the geometry where the dielectric occupies the $z < -L/2$ half-space, i.e. the result of the previous Section, cf. Fig. 6.1, translated by $-L/2$, then the solution of the integral equation

$$D_{ik}(\mathbf{r}, \mathbf{r}';\omega) = D^{(-)}_{ik}(\mathbf{r}, \mathbf{r}';\omega) + \frac{K(\omega)}{\epsilon_0^2} \int \mathrm{d}^3\mathbf{r}_1 \theta\left(z_1 - \frac{L}{2}\right) D^{(-)}_{ik}(\mathbf{r}, \mathbf{r}_1;\omega) D_{jk}(\mathbf{r}_1, \mathbf{r}';\omega), \tag{6.125}$$

yields the propagator in the gap geometry as pictured in Fig. 6.2. Similarly, if $D^{(+)}_{ik}(\mathbf{r}, \mathbf{r}';\omega)$ denotes the propagator of the displacement field in the geometry where the dielectric occupies the $z > L/2$ half-space, i.e. the result of the previous Section, cf. Fig. 6.1,

mirror-reflected and translated by $L/2$, then the solution of the integral equation

$$D_{ik}(\mathbf{r},\mathbf{r}';\omega) = D_{ik}^{(+)}(\mathbf{r},\mathbf{r}';\omega) + \frac{K(\omega)}{\epsilon_0^2}\int \mathrm{d}^3\mathbf{r}_1\theta\left(-z_1-\frac{L}{2}\right)D_{ij}^{(+)}(\mathbf{r},\mathbf{r}_1;\omega)D_{jk}(\mathbf{r}_1,\mathbf{r}';\omega) \tag{6.126}$$

also yields the propagator in the gap geometry as pictured in Fig. 6.2. To see that these assertions are correct recall that Hamiltonian density of the electromagnetic field, including its coupling to the polarization field, is given by

$$\mathcal{H} = \mathcal{H}_0 - \frac{g(\mathbf{r})}{\epsilon_0}\mathbf{X}\cdot\mathbf{D} \tag{6.127}$$

where H_0 is Hamiltonian density of the non-interacting electromagnetic field i.e. the electromagnetic field in free-space and $g(\mathbf{r})$ is the coupling function that specifies where the interaction takes place, cf. Eq. (6.7). $\mathbf{X}$ and $\mathbf{D}$ are polarization and displacement field operators, respectively. In the case of the gap geometry the above Hamiltonian can be written as

$$\mathcal{H} = \mathcal{H}_0 - \frac{1}{\epsilon_0}\left[\theta\left(-\frac{L}{2}-z\right)+\theta\left(z-\frac{L}{2}\right)\right]\mathbf{X}\cdot\mathbf{D}. \tag{6.128}$$

The integral equation (6.119) corresponds to the Hamiltonian (6.128) where we take the zeroth-order propagator of the perturbative expansion (6.30) to be the free-space propagator. However, this is by no means necessary. We may just as well rewrite the Hamiltonian (6.128) as

$$\mathcal{H} = \mathcal{H}_0' + \frac{1}{\epsilon_0}\theta\left(z-\frac{L}{2}\right)\mathbf{X}\cdot\mathbf{D} \tag{6.129}$$

with $\mathcal{H}_0' = \mathcal{H}_0 - \theta\left(-L/2-z_1\right)\mathbf{X}\cdot\mathbf{D}/\epsilon_0$ and take the zeroth-order propagator to be the propagator in the presence of the dielectric half-space occupying the $z<-L/2$ region of space. Doing so, the perturbative expansion (6.30) yields the Dyson equation (6.125). We can justify the integral equation (6.126) in a similar way.

From now on we will be working with quantities Fourier transformed with respect to $\mathbf{r}_\parallel - \mathbf{r}_\parallel'$

$$D_{ij}(z,z';\mathbf{q}_\parallel,\omega) = \int \mathrm{d}^2(\mathbf{r}_\parallel-\mathbf{r}_\parallel')e^{-i\mathbf{q}_\parallel\cdot(\mathbf{r}_\parallel-\mathbf{r}_\parallel')}D_{ij}(\mathbf{r}_\parallel-\mathbf{r}_\parallel',z,z';\omega). \tag{6.130}$$

For notational clarity we will suppress the dependence of propagators on frequency ω and parallel wavevector $\mathbf{q}_\parallel$. With this Eqs. (6.125)-(6.126) become

$$D_{ik}(z,z') = D^{(-)}_{ik}(z,z') + \frac{K(\omega)}{\epsilon_0^2}\int_{\frac{L}{2}}^{\infty} \mathrm{d}z_1 D^{(-)}_{ij}(z,z_1)D_{jk}(z_1,z'), \tag{6.131}$$

$$D_{ik}(z,z') = D^{(+)}_{ik}(z,z') + \frac{K(\omega)}{\epsilon_0^2}\int_{-\infty}^{-\frac{L}{2}} \mathrm{d}z_1 D^{(+)}_{ij}(z,z_1)D_{jk}(z_1,z'). \tag{6.132}$$

and we mark this result as a starting point of further analysis.

As promised we will solve the integral equations directly by iteration. To do so we combine equations (6.131) and (6.132) and obtain

$$\begin{aligned} D_{ik}(z,z') = D^{(-)}_{ik}(z,z') &+ \frac{K(\omega)}{\epsilon_0^2}\int_{\frac{L}{2}}^{\infty} \mathrm{d}z_1 D^{(-)}_{ij}(z,z_1)D^{(+)}_{jk}(z_1,z') \\ &+ \frac{K^2(\omega)}{\epsilon_0^4}\int_{\frac{L}{2}}^{\infty}\mathrm{d}z_1\int_{-\infty}^{-\frac{L}{2}} \mathrm{d}z_2 D^{(-)}_{ij}(z,z_1)D^{(+)}_{jl}(z_1,z_2)D_{lk}(z_2,z'). \end{aligned} \tag{6.133}$$

The crucial observation is that, for an appropriate choice of the range of z and z', we can achieve

$$\int_{\frac{L}{2}}^{\infty}\mathrm{d}z_1\int_{-\infty}^{-\frac{L}{2}} \mathrm{d}z_2 D^{(-)}_{ij}(z,z_1)D^{(+)}_{jl}(z_1,z_2)D^{(-)}_{lk}(z_2,z') = C_{ij}D^{(-)}_{jk}(z,z'), \tag{6.134}$$

where C_{ij} is some constant matrix i.e. independent of z and z'. In other words, the double-integral operator in the last line of (6.133), when acting on $D^{(-)}_{jk}$, results in a (matrix) multiplication, that is provided we choose z and z' appropriately. We need to carefully consider all three propagators that enter the double integral. The range of arguments of the middle propagator $D^{(+)}_{jl}(z_1,z_2)$ is fixed by the limits of integration. From Eq. (6.134) we read off

$$z_1 \in \left(\frac{L}{2},\infty\right),\ z_2 \in \left(-\infty,-\frac{L}{2}\right). \tag{6.135}$$

Recall that $D^{(+)}_{jl}(z_1,z_2)$ and $D^{(-)}_{jl}(z_1,z_2)$ denote the propagator of the displacement field in the half-space geometry when the dielectric occupies the $z > L/2$ and $z < -L/2$ region of space, respectively. Thus, the range of arguments (6.135) implies that $D^{(+)}_{jl}(z_1,z_2)$ is given by the transmitted part of the solution (6.108), only that we need to mirror-reflect it and then translate it by $L/2$. This operation is effected by the substitution $(z,z') \to (L/2-z, L/2-z')$ and $e^\lambda_i(\mathbf{q}_\parallel,-k_{zd})e^\lambda_j(\mathbf{q}_\parallel,-k_z) \to e^\lambda_i(\mathbf{q}_\parallel,k_{zd})e^\lambda_j(\mathbf{q}_\parallel,k_z)$. We

write out $D^{(+)}_{jl}(z_1, z_2)$ explicitly

$$\begin{aligned} D^{(+)}_{jl}(z_1, z_2) &= -i\epsilon_0 \frac{\xi(\omega)\omega^2}{2k_z} \sum_\lambda e^\lambda_j(\mathbf{q}_\parallel, k_{zd}) e^\lambda_l(\mathbf{q}_\parallel, k_z) t^\lambda e^{-ik_{zd}(L/2-z_1)+ik_z(L/2-z_2)} \\ &\equiv \sum_\lambda D^{(+)}_{ij}(z_1, z_2)\Big|_\lambda . \end{aligned} \tag{6.136}$$

The choice of the range of arguments z and z' is dictated by the fact that we want (6.134) to hold. We will see shortly that the choice[6]

$$z \in \left(-\infty, -\frac{L}{2}\right), \quad z' \in \left(-\frac{L}{2}, \frac{L}{2}\right). \tag{6.137}$$

does the job. For this choice of z and z', the remaining two propagators on the LHS of (6.134), $D^{(-)}_{ij}(z, z_1)$ and $D^{(-)}_{lk}(z_2, z')$, also consist of a transmitted part of the half-space propagator. They can be obtained by translating the transmitted part of the solution (6.108) by $-L/2$. Explicitly,

$$\begin{aligned} D^{(-)}_{ij}(z, z_1) &= -i\epsilon_0 \frac{\xi(\omega)\omega^2}{2k_z} \sum_\lambda e^\lambda_i(\mathbf{q}_\parallel, -k_{zd}) e^\lambda_j(\mathbf{q}_\parallel, -k_z) t^\lambda e^{-ik_{zd}(z+L/2)+ik_z(z_1+L/2)} \\ &\equiv \sum_\lambda D^{(-)}_{ij}(z, z_1)\Big|_\lambda , \end{aligned} \tag{6.138}$$

and the expression for $D^{(-)}_{lk}(z_2, z')$ is obtained by the replacement $(z, z_1) \to (z_2, z')$. Now we can proceed to show directly that, if the range of z and z' is that given in (6.137), the formula (6.134) is indeed the case. In doing so it is useful to note that the scalar products of polarization vectors with different z-components are diagonal with respect to polarization indices i.e. we have

$$e^\lambda_i(\mathbf{q}_\parallel, q_z) e^\sigma_i(\mathbf{q}_\parallel, p_z) = f^\lambda(q_z, p_z)\delta_{\lambda\sigma}, \tag{6.139}$$

[6]Note however that the propagator which is needed to calculate the atomic energy-level shift is the one where the source of radiation and observation point are located in the vacuum i.e. $z, z' \in (-L/2, L/2)$. First, we find the propagator for the range of arguments (6.137) and once this solution is known the case $z, z' \in (-L/2, L/2)$ can be obtained using the integral equation (6.132).

where the function f is obtained by direct evaluation of the LHS of the above equation. It is always equal to unity for the TE mode and for the TM mode reads

$$f^{\mathrm{TM}}(q_z, p_z) = \frac{q_z p_z + \mathbf{q}_\parallel^2}{\sqrt{\mathbf{q}_\parallel^2 + q_z^2}\sqrt{\mathbf{q}_\parallel^2 + p_z^2}}. \tag{6.140}$$

This is very useful because it shows that the product of propagators can be always split into separate contributions from the transverse electric and transverse magnetic modes i.e. we can always write

$$D_{ij}^{(-)}(z,z_1)D_{jl}^{(+)}(z_1,z_2)D_{lk}^{(-)}(z_2,z') = \sum_\lambda \left. D_{ij}^{(-)}(z,z_1)\right|_\lambda \left. D_{jl}^{(+)}(z_1,z_2)\right|_\lambda \left. D_{lk}^{(-)}(z_2,z')\right|_\lambda .$$

This is true for a product of arbitrary number of half-space propagators. With this in mind we directly evaluate the integral (6.134) and find that

$$\begin{aligned}\int_{\frac{L}{2}}^{\infty} \mathrm{d}z_1 \int_{-\infty}^{-\frac{L}{2}} \mathrm{d}z_2 D_{ij}^{(-)}(z,z_1)D_{jl}^{(+)}(z_1,z_2)D_{lk}^{(-)}(z_2,z') &= \frac{\epsilon_0^4}{K^2(\omega)} \sum_\lambda \left(r^\lambda e^{ik_z L}\right)^2 \\ \times \left(-i\epsilon_0 \frac{\xi(\omega)\omega^2}{2k_z}\right) t^\lambda e_i^\lambda(\mathbf{q}_\parallel, -k_{zd}) e_k^\lambda(\mathbf{q}_\parallel, -k_z) e^{-ik_{zd}(z+L/2)+ik_z(z'+L/2)} & \\ = \frac{\epsilon_0^4}{K^2(\omega)} \sum_\lambda \left(r^\lambda e^{ik_z L}\right)^2 \left. D_{ik}^{(-)}(z,z')\right|_\lambda ,& \end{aligned} \tag{6.141}$$

where we have used the relation between $K(\omega)$ and $\xi(\omega)$, Eq. (6.82). Equation (6.141) tells us two important things: *(i)* the action of the double integral operator appearing in the last line of (6.133) on the propagator $D_{jk}^{(-)}$ amounts to a simple multiplication so that the iteration of the integral equation (6.133) is possible, it results in a geometrical series that can be summed up to all orders; *(ii)* the iteration leads to the two independent series for two polarizations - the transverse electric (TE) and transverse magnetic (TM) modes do not mix up. In order to illustrate iteration more clearly we introduce a shorthand notation

$$\begin{aligned}\int_{-\infty}^{-\frac{L}{2}} \mathrm{d}z_1 D_{ij}^{(..)}(z,z_1)D_{jl}^{(..)}(z_1,z_2) &\equiv \mathbf{D}^{(..)}(z,z_1) \ominus \mathbf{D}^{(..)}(z_1,z'), \\ \int_{\frac{L}{2}}^{\infty} \mathrm{d}z_1 D_{ij}^{(..)}(z,z_1)D_{jl}^{(..)}(z_1,z_2) &\equiv \mathbf{D}^{(..)}(z,z_1) \oplus \mathbf{D}^{(..)}(z_1,z'),\end{aligned}$$

where the symbol $\ominus$ pertains to the integration over the interval $(-\infty, -L/2)$ and similarly

the symbol $\oplus$ pertains to the integration over the interval $(L/2, \infty)$. With this, the integral equation (6.133) is written compactly as

$$\mathbf{D}(z,z') = \mathbf{D}^{(-)}(z,z') + \frac{K(\omega)}{\epsilon_0^2}\mathbf{D}^{(-)}(z,z_1) \oplus \mathbf{D}^{(+)}(z_1,z') + \frac{K^2(\omega)}{\epsilon_0^4}\mathbf{D}^{(-)}(z,z_1) \oplus \mathbf{D}^{(+)}(z_1,z_2) \ominus \mathbf{D}(z_2,z').$$

Likewise, Eq. (6.141) becomes

$$\left[\frac{K(\omega)}{\epsilon_0^2}\right]^2 \mathbf{D}^{(-)}(z,z_1) \oplus \mathbf{D}^{(+)}(z_1,z_2) \ominus \mathbf{D}^{(-)}(z_2,z') = \sum_\lambda \left(r^\lambda e^{ik_z L}\right)^2 \mathbf{D}^{(-)}(z,z')\Big|_\lambda . \quad (6.142)$$

As mentioned before, the iterative process will not mix the transverse electric and transverse magnetic modes, the series will look the same for both polarizations; thus we drop the polarization index for a while. The expansion of the propagator for the case $z < -L/2$ and $|z'| < L/2$ takes the form

$$\begin{aligned}
\mathbf{D}(z,z') &= \mathbf{D}^{(-)}(z,z') \\
&+ \left[\frac{K(\omega)}{\epsilon_0^2}\right] \mathbf{D}^{(-)}(z,z_1) \oplus \mathbf{D}^{(+)}(z_1,z') \\
&+ \left[\frac{K(\omega)}{\epsilon_0^2}\right]^2 \mathbf{D}^{(-)}(z,z_1) \oplus \mathbf{D}^{(+)}(z_1,z_2) \ominus \mathbf{D}^{(-)}(z_2,z') \\
&+ \left[\frac{K(\omega)}{\epsilon_0^2}\right]^3 \mathbf{D}^{(-)}(z,z_1) \oplus \mathbf{D}^{(+)}(z_1,z_2) \ominus \mathbf{D}^{(-)}(z_2,z_3) \oplus \mathbf{D}^{(+)}(z_3,z') \\
&+ \left[\frac{K(\omega)}{\epsilon_0^2}\right]^4 \mathbf{D}^{(-)}(z,z_1) \oplus \mathbf{D}^{(+)}(z_1,z_2) \ominus \mathbf{D}^{(-)}(z_2,z_3) \\
&\qquad \oplus \mathbf{D}^{(+)}(z_3,z_4) \ominus \mathbf{D}^{(-)}(z_4,z') \\
&+ \left[\frac{K(\omega)}{\epsilon_0^2}\right]^5 \mathbf{D}^{(-)}(z,z_1) \oplus \mathbf{D}^{(+)}(z_1,z_2) \ominus \mathbf{D}^{(-)}(z_2,z_3) \\
&\qquad \oplus \mathbf{D}^{(+)}(z_3,z_4) \ominus \mathbf{D}^{(-)}(z_4,z_5) \oplus \mathbf{D}^{(+)}(z_5,z') \\
&\cdots \\
&= \left[\mathbf{D}^{(-)}(z,z') + \frac{K(\omega)}{\epsilon_0^2}\mathbf{D}^{(-)}(z,z_1) \oplus \mathbf{D}^{(+)}(z_1,z')\right] \\
&\qquad \times \left[1 + \left(re^{ik_z L}\right)^2 + \left(re^{ik_z L}\right)^4 + \dots\right] \\
&= \left[\mathbf{D}^{(-)}(z,z') + \frac{K(\omega)}{\epsilon_0^2}\mathbf{D}^{(-)}(z,z_1) \oplus \mathbf{D}^{(+)}(z_1,z')\right] \left(\frac{1}{1-r^2e^{2ik_z L}}\right). \quad (6.143)
\end{aligned}$$

When writing out the second-last line we have used the relation (6.142) whereas the last line follows from the summation of the geometrical series which is possible provided

$$|r_\lambda| < 1. \tag{6.144}$$

This condition will not always be satisfied because we are working with a complex permittivity that, most notably, allows the resonance between the photon's frequency ω and the frequency of the absorption line in the dielectric ω_{T}. In such a resonant situation it is possible for the modulus of the reflection coefficient to exceed unity. A similar situation occurs in electrostatics where, in the case of the non-dispersive media, the famous image factor $(\epsilon - 1)/(\epsilon + 1)$ is bounded by unity but when ϵ becomes complex and frequency-dependent this no longer the case. In fact, one can easily verify that whenever the real part of the dielectric function becomes negative then we can have $|(\epsilon - 1)/(\epsilon + 1)| > 1$. The permittivity that results from our model, see Appendix E, is given by

$$\epsilon(\omega) = 1 + \frac{\omega_{\mathrm{P}}^2}{\omega_{\mathrm{T}}^2 - \omega^2 - 2i\gamma\omega}. \tag{6.145}$$

In the limit when the damping is negligible i.e. $\gamma \to 0$ the real part of $\epsilon(\omega)$ is seen to be negative approximately when $\omega_{\mathrm{T}} < \omega < \sqrt{\omega_{\mathrm{T}}^2 + \omega_{\mathrm{P}}^2}$, a situation which is illustrated in Fig. 6.3. In such case one has to abandon the idea of iteration as the geometric series in (6.143) does not converge. However, we can still obtain the propagator by solving the differential equation derived in the Section 6.4.2.1. This situation is similar to that described in Appendix D of [2].

The last line of Eq. (6.143) gives the photon propagator in the gap geometry for the case $z < -L/2$ and $|z'| < L/2$. This is not quite yet what we need. In order to calculate the energy-level shift and decay rates we will need the propagator for the case when both z and z' lie within the gap between dielectrics i.e. $|z|, |z'| < L/2$. This solution is obtained by plugging the last line of (6.143) into the integral equation (6.132) and evaluating the resulting integrals directly. The calculation is straightforward but somewhat lengthy. After

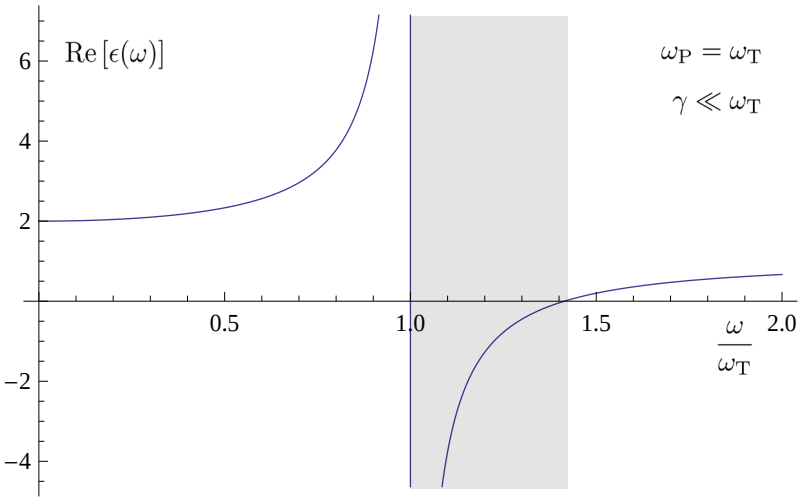

FIGURE 6.3: Plot of the real part of the dielectric function given in Eq. (6.145) as a function of $\omega/\omega_{\rm T}$. The shaded area indicates the range of frequency for which the real part of the dielectric function becomes negative. I this frequency band i.e. when $\omega_{\rm T} < \omega < \sqrt{\omega_{\rm T}^2 + \omega_{\rm P}^2}$ the propagation of photons in the dielectric is not allowed, see also discussion in [86].

some algebra we arrive at expression for the photon propagator needed in our calculations

$$D_{ik}(\mathbf{r},\mathbf{r}';\omega) = D_{ik}^{(0)}(\mathbf{r}-\mathbf{r}';\omega) - \frac{i\epsilon_0}{(2\pi)^2}\sum_{\lambda}\int \mathrm{d}^2\mathbf{q} e^{i\mathbf{q}_\parallel\cdot(\mathbf{r}_\parallel-\mathbf{r}'_\parallel)}\frac{\omega^2}{2k_z}\frac{r^\lambda e^{ik_z L}}{[1-(r^\lambda)^2 e^{2ik_z L}]}$$
$$\times\Big[r^\lambda \hat{e}_i^\lambda(\mathbf{q}_\parallel,k_z)\hat{e}_k^\lambda(\mathbf{q}_\parallel,k_z)e^{ik_z(z-z'+L)} + r^\lambda \hat{e}_i^\lambda(\mathbf{q}_\parallel,-k_z)\hat{e}_k^\lambda(\mathbf{q}_\parallel,-k_z)e^{-ik_z(z-z'-L)}$$
$$+\hat{e}_i^\lambda(\mathbf{q}_\parallel,k_z)\hat{e}_k^\lambda(\mathbf{q}_\parallel,-k_z)e^{ik_z(z+z')} + \hat{e}_i^\lambda(\mathbf{q}_\parallel,-k_z)\hat{e}_k^\lambda(\mathbf{q}_\parallel,k_z)e^{-ik_z(z+z')}\Big]. \tag{6.146}$$

with the Fresnel reflection coefficients given by

$$r^{\rm TE} = \frac{k_z - k_{zd}}{k_z + k_{zd}}, \quad r^{\rm TM} = \frac{\xi(\omega)k_z - k_{zd}}{\xi(\omega)k_z + k_{zd}}. \tag{6.147}$$

The reader is reminded that the formula (6.146) is valid for $|z|, |z'| < L/2$.

In further calculations wee shall need the photon propagator evaluated at equal space arguments $\mathbf{r} = \mathbf{r}'$. In such a case the correction to the free-space propagator due to the gap dielectric splits into the part that depends solely on the width of the cavity L and the part that, in addition, also depends on the position of the within the gap. As we explain later, see Sec. 6.8, we shall be interested in the position-dependent part. In terms of the

distances defined in Fig. 6.2 it is explicitly given by

$$D_{ik}^{(r)}(\mathcal{Z};\omega) = -\frac{i\epsilon_0}{4\pi}\int_0^\infty \mathrm{d}k \frac{k}{k_z}\cos(2k_z\mathcal{Z})e^{ik_zL} \times \begin{pmatrix} \omega^2\mathcal{R}^{\mathrm{TE}} - k_z^2\mathcal{R}^{\mathrm{TM}} & 0 & 0 \\ 0 & \omega^2\mathcal{R}^{\mathrm{TE}} - k_z^2\mathcal{R}^{\mathrm{TM}} & 0 \\ 0 & 0 & 2k^2\mathcal{R}^{\mathrm{TM}} \end{pmatrix} \tag{6.148}$$

where we have abbreviated

$$\mathcal{R}^\lambda = \frac{r^\lambda}{(1-r^\lambda e^{ik_zL})(1+r^\lambda e^{ik_zL})} \tag{6.149}$$

and r^λ are given in (6.147) with $k_z = \sqrt{\omega^2 - k^2 + i\eta}$ having always positive imaginary part. We have exploited polar coordinates, $q_x = k\cos\phi$, $q_y = k\sin\phi$, where the ϕ integration causes the off-diagonal components of the propagator to vanish.

6.4.2.3 The half-space revisited

The methods of the previous section can be readily applied to the geometry in which the dielectric occupies the $z < 0$ half-space thereby providing a verification of the derivation presented in Appendix 6.4.2.1. For the case of a dielectric half-space occupying the $z < 0$ region of space the coupling function becomes $g(\mathbf{r}) = \theta(-z)$, and the integral equation (6.72) becomes

$$D_{ik}(z,z') = D_{ik}^{(0)}(z-z') + \frac{K(\omega)}{\epsilon_0^2}\int_{-\infty}^0 \mathrm{d}z_1 D_{ij}^{(0)}(z-z_1)D_{jk}(z_1,z'), \tag{6.150}$$

where $D_{ik}^{(0)}(z-z')$ is the free-space photon propagator, Eq. (6.88). This integral equation does not lend itself to iteration what can be easily checked by trying. In order to be able to proceed along the same lines as in the case of the gap an auxiliary integral equation that facilitates the iteration process is required. We follow the idea of [79] and note that the following equation will enable the iteration process

$$D_{ik}(z,z') = D_{ik}^{(\epsilon)}(z-z') - \frac{K(\omega)}{\epsilon_0^2}\int_0^\infty \mathrm{d}z_1 D_{ij}^{(\epsilon)}(z-z_1)D_{jk}(z_1,z'), \tag{6.151}$$

where $D^{(\epsilon)}_{ik}(z-z')$ is Fourier transformed propagator in a bulk medium, Eq. (6.113). Equation (6.151) can be justified using the same argument as that spelled out at the beginning of Section 6.4.2.2. Recall that the part of the Hamiltonian density describing the interaction of the photon field with the polarization field has the form

$$\mathcal{H} = \mathcal{H}_0 - \frac{\theta(-z)}{\epsilon_0}\mathbf{X}(\mathbf{r})\cdot\mathbf{D}(\mathbf{r}), \tag{6.152}$$

where $\mathcal{H}_0$ is the Hamiltonian density of the non-interacting electromagnetic field. Using the fact that $\theta(-z)+\theta(z)=1$ the above equation can be written as

$$\mathcal{H} = \mathcal{H}_\epsilon + \frac{\theta(z)}{\epsilon_0}\mathbf{X}(\mathbf{r})\cdot\mathbf{D}(\mathbf{r}), \tag{6.153}$$

where now $\mathcal{H}_\epsilon = \mathcal{H}_0 - \mathbf{X}(\mathbf{r})\cdot\mathbf{D}(\mathbf{r})/\epsilon_0$ corresponds to the Hamiltonian density of the electromagnetic field interacting with an unbounded dielectric. Thus we have a choice, we either correct the free-space propagator for the presence of the dielectric half-space or, equivalently, correct the bulk dielectric propagator for the absence of the dielectric half-space. The second approach yields the integral equation (6.151).

We proceed by plugging equation (6.150) into equation (6.151)

$$\begin{aligned} D_{ik}(z,z') = D^{(\epsilon)}_{ik}(z-z') &- \frac{K(\omega)}{\epsilon_0^2}\int_0^\infty \mathrm{d}z_1 D^{(\epsilon)}_{ij}(z-z_1)D^{(0)}_{jk}(z_1-z') \\ &- \frac{K^2(\omega)}{\epsilon_0^4}\int_0^\infty \mathrm{d}z_1\int_{-\infty}^0 \mathrm{d}z_2 D^{(\epsilon)}_{ij}(z-z_1)D^{(0)}_{jl}(z_1-z_2)D_{lk}(z_2,z') \end{aligned} \tag{6.154}$$

and focus our attention on the solution of the case when $z<0$ and $z'>0$. The solution of the case $z,z'>0$ is then obtained with the use of the integral equation (6.150). The advantage gained by the introduction of equation (6.154) is such that the double-integral operator in the last term, when acting on $D^{(\epsilon)}_{ik}$, results in a simple multiplication i.e.

$$\int_0^\infty \mathrm{d}z_1\int_{-\infty}^0 \mathrm{d}z_2 D^{(\epsilon)}_{ij}(z-z_1)D^{(0)}_{jl}(z_1-z_2)D^{(\epsilon)}_{lk}(z_2-z') = C_{ij}D^{(\epsilon)}_{lk}(z-z'). \tag{6.155}$$

To verify this we first note that the arguments of all three propagators entering Eq. (6.155) have definite sign. Indeed we have

$$z-z_1<0,\quad z_1-z_2>0,\quad z_2-z'<0. \tag{6.156}$$

Therefore, it follows from Eq. (6.92) and (6.113) that the appropriate propagators entering the integral (6.155) are given by

$$\begin{aligned} D_{ij}^{(0)}(z-z') &= -\frac{i\epsilon_0\omega^2}{2k_z}\sum_\lambda e_i^\lambda(\mathbf{q}_\parallel,k_z)e_j^\lambda(\mathbf{q}_\parallel,k_z)e^{ik_z(z-z')} \\ &\equiv \sum_\lambda D_{ij}^{(0)}(z-z')\Big|_\lambda, \qquad (6.157) \\ D_{ij}^{(\epsilon)}(z-z') &= -\frac{i\epsilon_0\xi^2(\omega)\omega^2}{2k_{zd}}\sum_\lambda e_i^\lambda(\mathbf{q}_\parallel,-k_{zd})e_j^\lambda(\mathbf{q}_\parallel,-k_{zd})e^{-ik_{zd}(z-z')} \\ &\equiv \sum_\lambda D_{ij}^{(\epsilon)}(z-z')\Big|_\lambda. \qquad (6.158) \end{aligned}$$

Plugging in the propagators and evaluating the integrals directly we arrive at the result

$$\begin{aligned} \int_0^\infty \mathrm{d}z_1\int_{-\infty}^0 \mathrm{d}z_2 D_{ij}^{(\epsilon)}(z-z_1)D_{jl}^{(0)}(z_1-z_2)D_{lk}^{(\epsilon)}(z_2-z') \\ = \frac{\epsilon_0^4}{K^2(\omega)}\sum_\lambda \frac{r_\lambda^2}{1-r_\lambda^2}D_{lk}^{(\epsilon)}(z-z')\Big|_\lambda, \qquad (6.159) \end{aligned}$$

where we have used the relation between $K(\omega)$ and $\xi(\omega)$, Eq. (6.82), and the fact that the integrals of this type do not mix the TE and TM modes, cf. Eq. (6.139) and the discussion therein. Here r_λ is the half-space Fresnel coefficient, Eq. (6.107). We now introduce a convenient notation in the same spirit as before

$$\begin{aligned} \int_{-\infty}^0 \mathrm{d}z_1 D_{ij}^{(..)}(z,z_1)D_{jk}^{(..)}(z_1,z') \equiv \mathbf{D}^{(..)}(z,z_1)\ominus\mathbf{D}^{(..)}(z_1,z'), \\ \int_0^\infty \mathrm{d}z_1 D_{ij}^{(..)}(z,z_1)D_{jk}^{(..)}(z_1,z') \equiv \mathbf{D}^{(..)}(z,z_1)\oplus\mathbf{D}^{(..)}(z_1,z'). \end{aligned}$$

where the symbol $\ominus$ pertains to the integral along the negative axis and, likewise, $\oplus$ pertains to the integration along the positive axis. With this, Eq. (6.159) becomes

$$\frac{K^2(\omega)}{\epsilon_0^4}\mathbf{D}^{(\epsilon)}(z-z_1)\oplus\mathbf{D}^{(0)}(z_1-z_2)\ominus\mathbf{D}^{(\epsilon)}(z_2-z') = \sum_\lambda \frac{r_\lambda^2}{1-r_\lambda^2}\mathbf{D}^{(\epsilon)}(z-z')\Big|_\lambda. \qquad (6.160)$$

The solution of the integral equation (6.154) can now be obtained by iteration in an exactly analogous way as in the case of the gap. The expansion of the propagator for the case

$z<0$ and $z'>0$ takes the form

$$\begin{aligned}
\mathbf{D}(z,z') &= \mathbf{D}^{(\epsilon)}(z-z') \\
&- \left[\frac{K(\omega)}{\epsilon_0^2}\right] \mathbf{D}^{(\epsilon)}(z-z_1)\oplus\mathbf{D}^{(0)}(z_1-z') \\
&- \left[\frac{K(\omega)}{\epsilon_0^2}\right]^2 \mathbf{D}^{(\epsilon)}(z-z_1)\oplus\mathbf{D}^{(0)}(z_1-z_2)\ominus\mathbf{D}^{(\epsilon)}(z_2-z') \\
&+ \left[\frac{K(\omega)}{\epsilon_0^2}\right]^3 \mathbf{D}^{(\epsilon)}(z-z_1)\oplus\mathbf{D}^{(0)}(z_1-z_2)\ominus\mathbf{D}^{(\epsilon)}(z_2-z_3)\oplus\mathbf{D}^{(0)}(z_3-z') \\
&+ \left[\frac{K(\omega)}{\epsilon_0^2}\right]^4 \mathbf{D}^{(\epsilon)}(z-z_1)\oplus\mathbf{D}^{(0)}(z_1-z_2)\ominus\mathbf{D}^{(\epsilon)}(z_2-z_3) \\
&\qquad \oplus\mathbf{D}^{(0)}(z_3-z_4)\ominus\mathbf{D}^{(\epsilon)}(z_4-z') \\
&- \left[\frac{K(\omega)}{\epsilon_0^2}\right]^5 \mathbf{D}^{(\epsilon)}(z-z_1)\oplus\mathbf{D}^{(0)}(z_1-z_2)\ominus\mathbf{D}^{(\epsilon)}(z_2-z_3) \\
&\qquad \oplus\mathbf{D}^{(0)}(z_3-z_4)\ominus\mathbf{D}^{(\epsilon)}(z_4-z_5)\oplus\mathbf{D}^{(0)}(z_5-z') \\
&\cdots \\
&= \left[\mathbf{D}^{(\epsilon)}(z-z') - \frac{K(\omega)}{\epsilon_0^2}\mathbf{D}^{(\epsilon)}(z-z_1)\oplus\mathbf{D}^{(0)}(z_1-z')\right] \\
&\qquad \times\left[1-\left(\frac{r_\lambda^2}{1-r_\lambda^2}\right)+\left(\frac{r_\lambda^2}{1-r_\lambda^2}\right)^2+\dots\right] \\
&= \left[\mathbf{D}^{(\epsilon)}(z-z') - \frac{K(\omega)}{\epsilon_0^2}\mathbf{D}^{(\epsilon)}(z-z_1)\oplus\mathbf{D}^{(0)}(z_1-z')\right]\left(1-r_\lambda^2\right). \qquad (6.161)
\end{aligned}$$

It now remains to compute the term in square brackets. Here some care needs to be taken. The integral that needs to be evaluated is explicitly written as

$$I_{ik}(z,z') = \frac{K(\omega)}{\epsilon_0^2}\int_0^\infty \mathrm{d}z_1 D_{ij}^{(\epsilon)}(z-z_1)D_{jk}^{(0)}(z_1-z'). \qquad (6.162)$$

Now, the argument of $D^{(\epsilon)}$ is negative definite i.e. $z-z_1<0$ but the sign of z_1-z' can be both positive and negative. In such a case the propagator (6.88) contains components that are discontinuous at $z_1=z$ as well as elements proportional to $\delta(z_1-z)$. To properly take into account all contributions to the integral (6.162) it is convenient to represent the differential operator in (6.88) using the polarization vectors written out symbolically in terms of derivatives, see Eq. (5.19). Using the well-known completeness relation of the

polarization vectors we may write

$$\nabla_i \nabla_k - \delta_{ik}\nabla^2 = -\nabla^2 \sum_\lambda e_i^\lambda(\boldsymbol{\nabla}) e_k^\lambda(\boldsymbol{\nabla}). \tag{6.163}$$

With this, the propagators entering the integral (6.162) are given by

$$D_{ij}^{(0)}(z-z') = -\frac{i\epsilon_0}{2k_z}\left(\mathbf{q}_\parallel^2 - \nabla_{z'}^2\right)\sum_\lambda e_i^\lambda(\mathbf{q}_\parallel, -\nabla_{z'}) e_j^\lambda(\mathbf{q}_\parallel, -\nabla_{z'}) e^{ik_z|z-z'|}, \tag{6.164}$$

$$D_{ij}^{(\epsilon)}(z-z') = -\frac{i\epsilon_0 \xi^2(\omega)\omega^2}{2k_{zd}}\sum_\lambda e_i^\lambda(\mathbf{q}_\parallel, -k_{zd}) e_j^\lambda(\mathbf{q}_\parallel, -k_{zd}) e^{-ik_{zd}(z-z')}. \tag{6.165}$$

Note that we have shifted the z-derivatives to act on z' rather than on z so that they could be pulled outside the integral in (6.162). This is possible thanks to the fact that

$$e_i^\lambda(\mathbf{q}_\parallel, \nabla_z) e^{ik_z|z-z'|} = e_i^\lambda(\mathbf{q}_\parallel, -\nabla_{z'}) e^{ik_z|z-z'|}. \tag{6.166}$$

With this it is not difficult to demonstrate that the integral (6.162) is given by

$$I_{ik}(z,z') = D_{ik}^{(\epsilon)}(z-z') - \frac{i\epsilon_0\xi(\omega)\omega^2}{2k_{zd}}\sum_\lambda \frac{1}{t_R^\lambda} e_i^\lambda(\mathbf{q}_\parallel, -k_{zd}) e_k^\lambda(\mathbf{q}_\parallel, -k_z) e^{-ik_{zd}z + ik_z z'} \tag{6.167}$$

i.e. it contributes a term that exactly cancels out the bulk dielectric propagator in (6.161). The remaining parts combine together to yield the final result

$$D_{ij}(z,z') = -\frac{i\epsilon_0\omega^2}{2k_z}\left[\xi(\omega) e_i^\lambda(\mathbf{q}_\parallel, -k_{zd}) e_j^\lambda(\mathbf{q}_\parallel, -k_z) t_R^\lambda\right] e^{-ik_{zd}z + ik_z z'}. \tag{6.168}$$

This formula is valid for $z<0,\ z'>0$ and agrees with the previous findings, Eq. (6.108), based on the solution of the differential equation. It is a straightforward calculation to plug equation (6.168) into (6.150) and see that the result for the case $z, z' > 0$ also agrees with the result (6.108). As a final remark we would like to comment on the problem of the convergence of the series in (6.161). The expansion will converge provided

$$\left|\frac{r_\lambda^2}{1-r_\lambda^2}\right| < 1. \tag{6.169}$$

At this stage it seems that there is no straightforward physical interpretation of this condition.

6.5 Atomic propagator and electron's self-energy

To perform perturbative expansion of the atomic propagator we start with the formula (6.30) with the field operators Ψ and $\Psi^\dagger$ being replaced by the atomic creation and annihilation operators, c_i and $c_i^\dagger$, respectively

$$G_{ii}(t,t') = \sum_{n=0}^{\infty} \left(-\frac{i}{\hbar}\right)^{n+1} \int \mathrm{d}t_1 \ldots \int \mathrm{d}t_n \times \left\langle \Omega \left| \mathrm{T}\left[c_i(t) c_i^\dagger(t') H_{\mathrm{A-EM}}(t_1) \ldots H_{\mathrm{A-EM}}(t_n)\right] \right| \Omega \right\rangle_{\mathrm{conn}} . \tag{6.170}$$

Using the Wick's theorem to evaluate the ground-state expectation value of the time-ordered product of operators one easily sees that the zeroth-order term is a propagator for non-interacting system. The first-order correction vanishes simply because it is not possible to contract all of the operators.

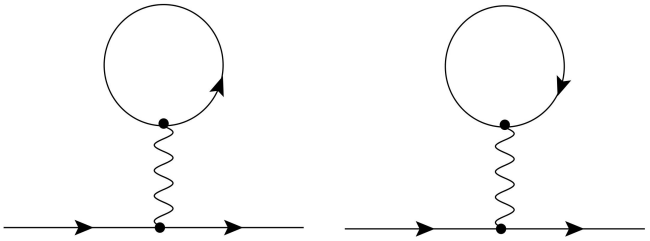

FIGURE 6.4: The figure illustrates two tadpole diagrams that one can draw having at disposal two vertices, three atomic lines and one photon line. The contributions from these diagrams contain equal-time atomic propagators and vanish identically.

The first non-vanishing contributions come from the term of order e^2. Having two vertices at our disposal we see that apart from the irrelevant disconnected diagrams we can draw the so-called 'tadpole' diagram, which is also irrelevant, see Fig. 6.4, and a self-energy diagram that contains the information about the energy-level shifts and decay rates

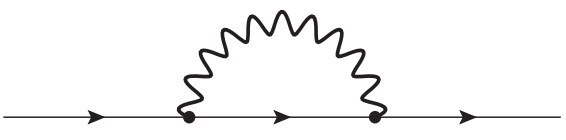

.

In fact, it is more convenient to perform partial summation and consider the following series of diagrams

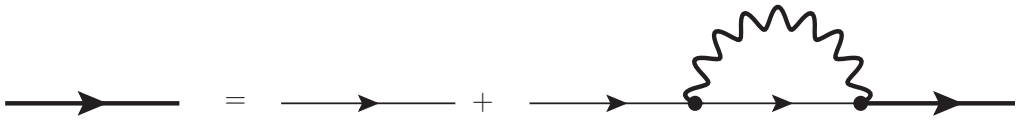

where the thick solid line represents the dressed atomic propagator. The location of poles of such constructed propagator is much more straightforward to work out. The analytical expression corresponding to the above graphical equation is given by

$$G_{ii}(t,t') = G_{ii}^{(0)}(t,t') + \frac{i\hbar}{\epsilon_0^2}\sum_{k,l,m}\mu_{mi}^k\mu_{im}^l\int_{-\infty}^{\infty}\mathrm{d}t_1\int_{-\infty}^{\infty}\mathrm{d}t_2 \times G_{ii}^{(0)}(t,t_1)G_{mm}^{(0)}(t_1,t_2)D_{kl}(\mathbf{R},\mathbf{R},t_1,t_2)G_{ii}(t_2,t'). \tag{6.171}$$

Since we are looking for the poles of the $G_{ii}(\mathcal{E})$ we need to Fourier-transform (6.171) with respect to $t-t'$. One finds using equation (6.37) that the dressed atomic propagator is given by

$$G_{ii}(\mathcal{E}) = \int_{-\infty}^{\infty}\mathrm{d}(t-t')e^{i(t-t')\mathcal{E}/\hbar}G_{ii}(t-t') = \frac{1}{\mathcal{E}-E_i+i\eta-\Sigma_{ii}(\mathcal{E})} \tag{6.172}$$

with the self-energy insertion identified with

$$\Sigma_{ii}(\mathcal{E}) = \frac{i\hbar}{2\pi\epsilon_0^2}\sum_{k,l,m}\mu_{mi}^k\mu_{im}^l\int_{-\infty}^{\infty}\mathrm{d}\omega\,\frac{D_{kl}(\mathbf{R},\mathbf{R};\omega)}{\mathcal{E}-\hbar\omega-E_m+i\eta}. \tag{6.173}$$

The self-energy insertion (6.173) contains the photon propagator which in the case of an atom outside the dielectric splits into two separate parts; *(i)* the free-space part that gives a rise to the position-independent Lamb shift and *(ii)* the reflected part that gives a rise to the distance-to-surface-dependent Casimir-Polder shift. The zeros of the denominator in (6.172) occur at the atomic energy-levels. Thus, we obtain the spectrum writing

$$\mathcal{E}-E_i = \Sigma_{ii}^{(0)}(\mathcal{E}) + \Sigma_{ii}^{(r)}(\mathcal{E}). \tag{6.174}$$

We want to work out changes in the energy-levels already corrected for the coupling between the electron and the free-space electromagnetic fields. Therefore, the renormalized energy-level shift can be written as

$$\Delta\mathcal{E}_i^{\mathrm{ren}} \equiv \mathcal{E}-\bar{E}_i = \Sigma_{ii}^{(r)}(\mathcal{E}), \tag{6.175}$$

where we have absorbed the self-energy associated with the free-space electromagnetic field into $\bar{E}_i$ so that it represents the atomic energy-levels already corrected for the Lamb shift and free-space decay rates.

Equation (6.175) represents the integral equation which served us only as a convenient way to locate the poles of the atomic propagator. Our result is valid only up to the second-order of the perturbation theory and any attempt of finding exact solution of (6.175) is meaningless. At this stage, to obtain the energy shifts, we simply iterate the integral equation once and arrive at

$$\Delta\mathcal{E}_i^{\mathrm{ren}} \approx \Sigma_{ii}^{(r)}(\bar{E}_i) = -\frac{i}{2\pi\epsilon_0^2}\sum_{k,l,m}\mu_{mi}^k\mu_{im}^l\int_{-\infty}^{\infty}\mathrm{d}\omega\,\frac{D_{kl}^{(r)}(\mathbf{R},\mathbf{R};\omega)}{\omega_{mi}+\omega-i\eta} \tag{6.176}$$

where we have abbreviated $\omega_{mi}=\omega_m-\omega_i$. The ω-integral in (6.176) can be restricted to the positive real axis by writing

$$\frac{1}{\omega+\omega_{mi}-i\eta} = \frac{\omega-\omega_{mi}}{\omega^2-(\omega_{mg}-i\eta)^2} \tag{6.177}$$

and noting that $D_{kr}^{(r)}(\mathbf{R},\mathbf{R};\omega)$ is even in ω, see Section 6.4.2 and Appendix E. Note that the term proportional to ω is odd and vanishes when integrated over the real ω axis. The photon propagator is analytic in the first quadrant of the complex ω-plane therefore it is permissible to rotate the contour of ω-integration by $\pi/2$ i.e. $\omega\to i\omega$. However, one must remember that when we consider an excited state i of the atom then $\omega_{mi}<0$ and there will in general be some poles present in the first quadrant of the ω plane due to the denominator in (6.176). We also remind the reader that the Fresnel's reflection coefficients present in the propagator are famous for signalling trapped electromagnetic modes by poles in the complex plane, cf. Sec. (5.2.2). This doesn't concern us when we consider the half-space or gap but requires attention when considering systems capable of wave-guiding. Next we recall that $D_{kr}^{(r)}(\mathbf{R},\mathbf{R};\omega)$ is diagonal, cf. Eqs. (6.109) and (6.148), and write down the final result in the form

$$\Delta\mathcal{E}_i^{\mathrm{ren}} = \Delta\mathcal{E}_i + \Delta\mathcal{E}_i^{\star} \tag{6.178}$$

with $\Delta\mathcal{E}_i$ and $\Delta\mathcal{E}_i^\star$ given by

$$\Delta\mathcal{E}_i = \frac{1}{\pi\epsilon_0^2}\sum_{k,m}|\mu_{im}^k|^2\int_0^\infty \mathrm{d}\omega\,\frac{\omega_{mi}}{\omega^2+\omega_{mi}^2}D_{kk}^{(r)}(\mathbf{R},\mathbf{R};i\omega) \tag{6.179}$$

$$\Delta\mathcal{E}_i^\star = \frac{1}{\epsilon_0^2}\sum_{k,m}|\mu_{im}^k|^2 D_{kk}^{(r)}(\mathbf{R},\mathbf{R};|\omega_{mi}|)\theta(-\omega_{mi}) \tag{6.180}$$

where $|\mu_{mi}^k| \equiv |\langle m|\mu^k|i\rangle|$ are the matrix elements of the k-th component of the electric dipole moment operator. The quantity $\Delta\mathcal{E}_i^\star$ is a contribution to the self-energy that originates from poles of equation (6.176) that come into play if one considers an excited state i for which $\omega_{mi} < 0$. Equations (6.179) and (6.180) have been derived before by different methods e.g. the linear response theory [48][27] or the noise-current approach to phenomenological QED [87]. The shift $\Delta\mathcal{E}_i$ is real because it is evaluated at complex frequencies where the susceptibilities are real. However, $\Delta\mathcal{E}_i^\star$ is complex and contains the decay rates. In fact we have

$$\begin{aligned}\Delta E_i &= \mathrm{Re}\left(\Delta\mathcal{E}_i^{\mathrm{ren}}\right)\\ \hbar\Delta\Gamma_i &= -2\mathrm{Im}\left(\Delta\mathcal{E}_i^\star\right)\end{aligned} \tag{6.181}$$

where ΔE_i are the renormalized energy-level shifts and $\Delta\Gamma_i$ are the changes in decay rates.

6.6 Energy-level shifts near a half-space

6.6.1 Ground state

Substituting the photon propagator (6.109) into equation (6.179) we find that the energy shift of the ground state $|g\rangle$ is given by

$$\begin{aligned}\Delta E_g = -\frac{1}{8\pi^2\epsilon_0}\sum_m\int_0^\infty \mathrm{d}k k\int_0^\infty \mathrm{d}\omega\,\frac{\omega_{mg}}{\omega^2+\omega_{mg}^2}\frac{e^{-2\sqrt{k^2+\omega^2}\mathcal{Z}}}{\sqrt{k^2+\omega^2}}\\ \times\left\{\left[(k^2+\omega^2)\bar{r}^{\mathrm{TM}}-\omega^2\bar{r}^{\mathrm{TE}}\right]|\mu_{mg}^\parallel|^2+2k^2\bar{r}^{\mathrm{TM}}|\mu_{mg}^\perp|^2\right\},\end{aligned} \tag{6.182}$$

where we have abbreviated $|\mu^{\parallel}_{mi}|^2 = |\mu^x_{mi}|^2 + |\mu^y_{mi}|^2$ and $\omega_{mi} \equiv \omega_m - \omega_i$. The reflection coefficients are defined in (6.107) and are expressed in terms of the new variables as

$$\begin{aligned} \bar{r}^{\mathrm{TE}} &= \frac{\sqrt{\omega^2+k^2} - \sqrt{\epsilon(i\omega)\omega^2+k^2}}{\sqrt{\omega^2+k^2} + \sqrt{\epsilon(i\omega)\omega^2+k^2}} \\ \bar{r}^{\mathrm{TM}} &= \frac{\epsilon(i\omega)\sqrt{\omega^2+k^2} - \sqrt{\epsilon(i\omega)\omega^2+k^2}}{\epsilon(i\omega)\sqrt{\omega^2+k^2} + \sqrt{\epsilon(i\omega)\omega^2+k^2}}. \end{aligned} \tag{6.183}$$

Note that we have replaced $\xi(\omega)$ with $\epsilon(\omega)$ in (6.183) compared to (6.107), as for the frequencies considered both functions coincide, see Section 6.4.2 and Appendix E. If we now introduce polar coordinates according to, $\omega = \omega_{mg} xy, k = \omega_{mg} x\sqrt{1-y^2}$ with $y = \cos\phi$, we obtain the perhaps most useful form of the ground-state shift, especially for numerical analysis and the study of retardation,

$$\begin{aligned} \Delta E_g = -\frac{1}{8\pi^2\epsilon_0} \sum_m \int_0^\infty \mathrm{d}x x^3 \int_0^1 \mathrm{d}y \frac{\omega_{mg}^3}{1+x^2y^2} e^{-2\omega_{mg}\mathcal{Z}x} \\ \times \left[\left(\tilde{r}^{\mathrm{TM}} - y^2\tilde{r}^{\mathrm{TE}}\right) |\mu^{\parallel}_{mg}|^2 + 2\left(1-y^2\right)\tilde{r}^{\mathrm{TM}} |\mu^{\perp}_{mg}|^2 \right]. \end{aligned} \tag{6.184}$$

The result (6.184) formally takes the same form as the results obtained in calculations involving non-dispersive dielectrics, see e.g. [64] and Chapter 5, the only difference being the reflection coefficients that now, through the dielectric constant, depend on the product xy of the integration variables which is the photon frequency,

$$\begin{aligned} \tilde{r}^{\mathrm{TE}} &= \frac{1 - \sqrt{y^2[\epsilon(ixy)-1]+1}}{1 + \sqrt{y^2[\epsilon(ixy)-1]+1}}, \\ \tilde{r}^{\mathrm{TM}} &= \frac{\epsilon(ixy) - \sqrt{y^2[\epsilon(ixy)-1]+1}}{\epsilon(ixy) + \sqrt{y^2[\epsilon(ixy)-1]+1}}. \end{aligned} \tag{6.185}$$

Equation (6.184) is suitable for numerical analysis but doesn't give immediate insight into the behaviour of the interaction energy as a function of the distance from the surface. It is therefore instructive to consider some of its limiting cases.

As has been recognized e.g. in [64], the dimensionless parameter that plays a decisive role in the characteristics of the Casimir-Polder interaction is given by the combination $2\omega_{mg}\mathcal{Z}$ which is the ratio of two time-scales: *(i)* the typical time $2\mathcal{Z}/c$ needed by a virtual photon to make a round trip between the atom and the surface, *(ii)* the typical time-scale ω_{mg}^{-1} at which the atomic system evolves. While equation (6.184) includes a sum over atomic states

$|m\rangle$, in reality contributions to the shift will be dominated by the state which is connected to a ground state by the strongest dipole transition. We call the frequency ω_{mg} that pertains to this strongest transition a 'typical transition frequency' and it is this number that enters the retardation criterion parameter. Briefly speaking, if $2\omega_{mg}\mathcal{Z} << 1$ we are in the so-called nonretarded regime when the time needed by the photon to travel between the dielectric and the atom is negligibly small compared to the typical atomic time-scale. Then, the interaction can be safely approximated as instantaneous and our result should reduce to that calculated in the paper by Barton [2], where it is interpreted as the Coulomb interaction of an atom with surface polaritons. In the opposite case, $2\omega_{mg}\mathcal{Z} >> 1$, the interaction becomes retarded, i.e. by the time the photon has completed a round trip the atomic state has significantly changed. In this case, for reasons that become apparent later, the interaction depends only on static polarizabilities i.e. polarizabilities evaluated at zero frequency

$$\begin{aligned} \alpha_{\nu\nu}(\omega=0) &= \sum_j \frac{2\omega_{ji}\,|\langle j|\mu_\nu|i\rangle|^2}{\omega_{ji}^2-\omega^2}\bigg|_{\omega=0} = 2\sum_j \frac{|\langle j|\mu_\nu|i\rangle|^2}{\omega_{ji}}\,, \\ \frac{\epsilon(\omega=0)}{\epsilon_0} &= 1+\frac{\omega_{\mathrm{P}}^2}{\omega_{\mathrm{T}}^2-\omega^2-2i\gamma\omega}\bigg|_{\omega=0} = 1+\frac{\omega_{\mathrm{P}}^2}{\omega_{\mathrm{T}}^2}\,, \end{aligned} \tag{6.186}$$

where $\alpha_{\nu\nu}$ is the polarizability of the atom and ϵ/ϵ_0-1 is the susceptibility of the dielectric, see Appendix E.

6.6.1.1 Nonretarded limit

The form of the energy shift best suited for taking the non-retarded limit is that in equation (6.182). After changing the variables in the ω integration according to $\mathrm{d}\omega = (2\omega_{mg}\mathcal{Z}k)\,\mathrm{d}s$ we let $2\omega_{mg}\mathcal{Z}\to 0$, as we may do because the 'line' $s=\infty$ does not contribute to the integral, and make approximations:

$$\begin{aligned} k^2+\xi^2 &\to k^2\left[1+(2\omega_{mg}\mathcal{Z})^2 s^2\right]\approx k, \\ k^2+\epsilon\xi^2 &\to k^2\left[1+\epsilon(2\omega_{mg}\mathcal{Z})^2 s^2\right]\approx k. \end{aligned}$$

This significantly simplifies equation (6.182). The k-integral becomes elementary and the final result is written as

$$\Delta E_g^{\text{nonret}} \approx -\frac{1}{32\pi^2\epsilon_0\mathcal{Z}^3}\sum_m \int_0^\infty \mathrm{d}\xi\, \frac{\omega_{mg}}{\xi^2+\omega_{mg}^2}\,\frac{\epsilon(i\xi)-1}{\epsilon(i\xi)+1}\left(|\mu_{mg}^{\parallel}|^2+2|\mu_{mg}^{\perp}|^2\right). \tag{6.187}$$

We observe the expected $\mathcal{Z}^{-3}$ behaviour of the energy level shift in the van der Waals regime. The result (6.187), although written in a slightly less explicit form, is in fact equivalent to that derived in [88], their equation (13). It also confirms the results derived on the basis of the phenomenological quantum electrodynamics, see e.g. [87].

6.6.1.2 Retarded limit

To study the influence of retardation on the energy shift it is convenient to start with equation (6.184) where the criterion parameter $2\omega_{mg}\mathcal{Z}$ is present in the exponential factor which in the limit $2\omega_{mg}\mathcal{Z}\to\infty$ strongly damps the integrand. In such a scenario the main contributions to the integral come from the neighbourhood of $x=0^+$ and it is permissible to expand the integrand in Taylor series around this point. A straightforward calculation leads to

$$\Delta E_g^{\text{ret}} \approx -\frac{3}{64\pi^2\epsilon_0}\sum_m\sum_{\sigma=\parallel,\perp}\left(\frac{c_4^\sigma}{\mathcal{Z}^4}-\frac{4\gamma}{\omega_{\mathrm{T}}^2}\frac{c_5^\sigma}{\mathcal{Z}^5}\right)\frac{|\langle g|\mu^\sigma|m\rangle|^2}{\omega_{mg}}, \tag{6.188}$$

where we have neglected terms of order $(\omega_{mg})\mathcal{Z}$ and higher. First we observe, as it was previously recognized [48], that to leading-order only the static polarizability of the atom matters in the retarded limit

$$\alpha_{kk}(0) = 2\sum_m \frac{|\langle m|\mu_k|g\rangle|^2}{\omega_{mg}}. \tag{6.189}$$

The leading-order behaviour of the energy shift displays a $\mathcal{Z}^{-4}$ distance dependence and in fact is just the well-known retarded limit of the energy shift of a ground state atom interacting with a dielectric half-space described by a static refractive index $n^2(0)\equiv n^2 = 1+\omega_{\mathrm{P}}^2/\omega_{\mathrm{T}}^2$. This case has been studied extensively in [64] where the coefficients $c_4^{\parallel,\perp}$ that depend only

on n have been worked out in an analytical form. For completeness we cite them here

$$c_4^{\parallel} = -\frac{1}{n^2-1}\left(\frac{2}{3}n^2+n-\frac{8}{3}\right)+\frac{2n^4}{(n^2-1)\sqrt{n^2+1}}\ln\left(\frac{\sqrt{n^2+1}+1}{n\left[\sqrt{n^2+1}+n\right]}\right) + \frac{2n^4-2n^2-1}{(n^2-1)^{3/2}}\ln\left(\sqrt{n^2+1}+n\right),$$

$$c_4^{\perp} = \frac{1}{n^2-1}\left(4n^4-2n^3-\frac{4}{3}n^2+\frac{4}{3}\right)-\frac{4n^6}{(n^2-1)\sqrt{n^2+1}}\ln\left(\frac{\sqrt{n^2+1}+1}{n\left[\sqrt{n^2+1}+n\right]}\right) - \frac{2n^2(2n^4-2n^2+1)}{(n^2-1)^{3/2}}\ln\left(\sqrt{n^2-1}+n\right).$$

Hence, we conclude that to leading-order, in the retarded limit, absorption makes no difference and only static polarizabilities, of both, the dielectric and the atom, matter. This is because the wavelength of the electromagnetic radiation that matters the most in the atom-wall interaction is of order of the distance between the atom and the dielectric. Hence for an atom in the so-called far-zone only long wavelengths of electromagnetic radiation come to play i.e. low frequencies.

Now we turn our attention to the next term of the asymptotic expansion which is proportional to $\mathcal{Z}^{-5}$. This is the first term that contains information about corrections to the energy shift due to absorption in the retarded regime. The coefficient in front of $\mathcal{Z}^{-5}$ is given by $\gamma/\omega_T^2 c_5^{\sigma}$ where numbers c_5^{σ} depend only on the static refractive index $n=\sqrt{1+\omega_{\mathrm{P}}^2/\omega_{\mathrm{T}}^2}$ and are given by

$$c_5^{\parallel} = \frac{1}{3(n-1)(n+1)^2(n^2+1)}\Big\{6n^6-3n^5-11n^4+4n^3+2n^2-5n+7 - 6n^2\big(n^5+n^4-n^3-n^2-2n-2\big)\ln\left[n\left(\frac{n+1}{n^2+1}\right)\right]\Big\},$$

$$c_5^{\perp} = \frac{4}{3(n-1)(n+1)^2(n^2+1)}\Big\{-6n^8+3n^7+10n^6-5n^5+3n^4-n^3-6n^2+n+1 + 3n^4\big(2n^5+2n^4-n^3-n^2-3n-3\big)\ln\left[n\left(\frac{n+1}{n^2+1}\right)\right]\Big\}. \quad (6.190)$$

We provide plots of these functions in Fig. 6.5 on page 173 from where a quick estimate of the value of the coefficients can be obtained. Since both $c_5^{\parallel}$ and $c_5^{\perp}$ are positive we see that absorption reduces the magnitude of the ground-state energy shift by an amount that is proportional to the damping constant γ, cf. Fig 6.6 on page 174. We also note that the

correction goes with the inverse square of the absorption frequency ω_{T} in the dielectric so that only absorption lines that lie at sufficiently low frequencies make a significant difference. This happens because the main contribution to the shift of the ground state in the retarded limit comes from large wavelengths or equivalently small values of x (which is a scaled frequency). Therefore, the integral is not sensitive to any absorption line peaks which lie at higher frequencies as there the integrand is highly damped anyway, cf. Eq. (6.184).

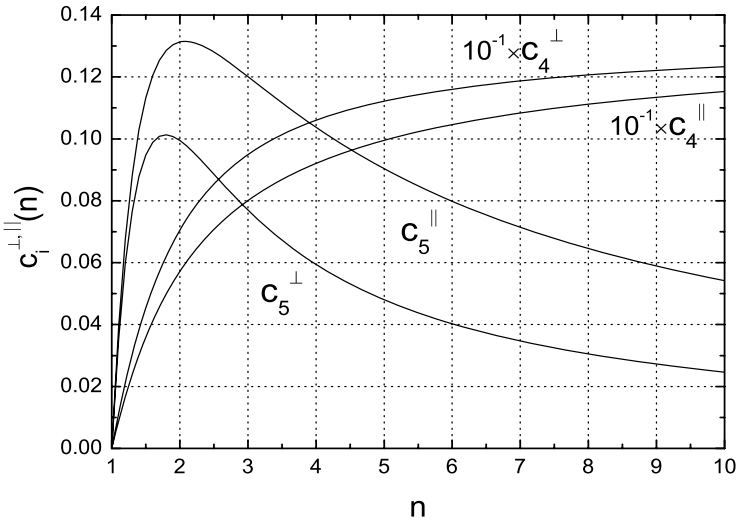

FIGURE 6.5: Plot of the coefficients $c_i^{\sigma}(n)$ that enter equation (6.188) for different values of the static refractive index $n(0)$.

6.6.2 Excited states.

The shift of an excited energy-level gets contributions from both parts of $\Delta\mathcal{E}^{\mathrm{ren}}$, cf. (6.179) and (6.180). The non-residue contributions (6.179) assume exactly the same form as the results of the previous section; therefore we will not analyze them again. Instead we shall have a closer look at equation (6.180).

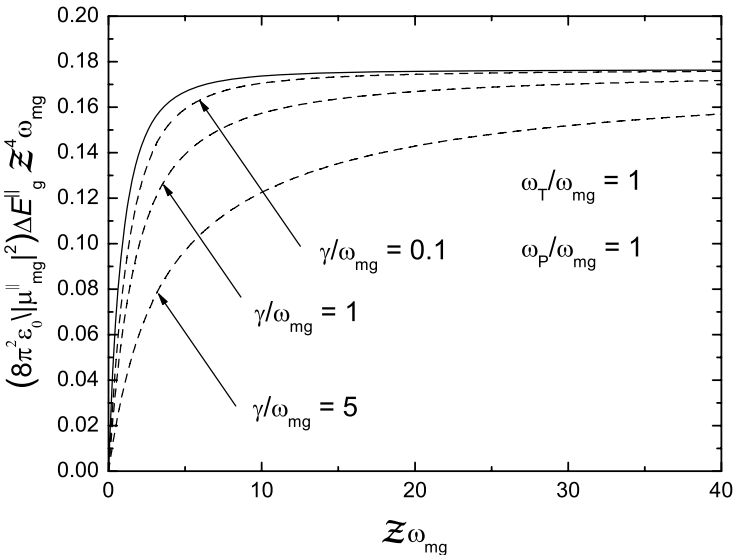

FIGURE 6.6: Plot of the exact ground-state energy shift (contributions due to the perpendicular component of the atomic dipole moment) $\Delta E_g^{\parallel}$, equation (6.182), multiplied by $\mathcal{Z}^4\omega_{mg}$ as a function of $\mathcal{Z}\omega_{mg}$ for various values of the damping parameter γ. Solid line represents the energy shift caused by the non-absorptive and non-dispersive dielectric half-space with static refractive index $n(0)$.

Plugging in the photon propagator (6.109) we find that the energy shift of the excited state $|i\rangle$ is given as a real part of the following expression

$$\Delta\mathcal{E}_i^{\star} = -\frac{i}{8\pi\epsilon_0}\sum_{m<i}\int_0^{\infty}\mathrm{d}k\,\frac{k e^{2i\mathcal{Z}\sqrt{\omega_{mi}^2-k^2}}}{\sqrt{\omega_{mi}^2-k^2+i\eta}} \times\left\{\left[\omega_{mi}^2 r_{mi}^{\mathrm{TE}}-(\omega_{mi}^2-k^2)r_{mi}^{\mathrm{TM}}\right]|\mu_{mi}^{\parallel}|^2+2k^2 r_{mi}^{\mathrm{TM}}|\mu_{mi}^{\perp}|^2\right\}. \tag{6.191}$$

Here, r_{mi}^{λ} are the reflection coefficients of (6.107) evaluated at the atomic transition frequencies $\omega=|\omega_{mi}|$. Also, the restriction of the sum over atomic states to those lying below the state $|i\rangle$ should be noted. To perform the asymptotic analysis of $\Delta\mathcal{E}_i^{\star}$ we change the variable in equation (6.191) to $k_z=\sqrt{\omega_{mi}^2-k^2}/|\omega_{mi}|$ and get

$$\Delta\mathcal{E}_i^{\star} = \frac{i}{8\pi\epsilon_0}\sum_{m<i}|\omega_{mi}|^3\int_1^{i\infty}\mathrm{d}k_z e^{2i|\omega_{mi}|\mathcal{Z}k_z} \times\left\{\left(\bar{r}_{mi}^{\mathrm{TE}}-k_z^2\bar{r}_{mi}^{\mathrm{TM}}\right)|\mu_{mi}^{\parallel}|^2+2\left(1-k_z^2\right)\bar{r}_{mi}^{\mathrm{TM}}|\mu_{mi}^{\perp}|^2\right\}. \tag{6.192}$$

The contour of integration runs from $k_z=1$ along the real axis to $k_z=0$ and then up

along the imaginary axis to $k_z = i\infty$. The reflection coefficients expressed as functions of k_z are

$$\begin{aligned} \bar{r}^{\mathrm{TE}}_{mi}(k_z) &= \frac{k_z - \sqrt{[\epsilon(|\omega_{mi}|) - 1] + k_z^2}}{k_z + \sqrt{[\epsilon(|\omega_{mi}|) - 1] + k_z^2}}, \\ \bar{r}^{\mathrm{TM}}_{mi}(k_z) &= \frac{\epsilon(|\omega_{mi}|)k_z - \sqrt{[\epsilon(|\omega_{mi}|) - 1] + k_z^2}}{\epsilon(|\omega_{mi}|)k_z + \sqrt{[\epsilon(|\omega_{mi}|) - 1] + k_z^2}}. \end{aligned} \tag{6.193}$$

6.6.2.1 Nonretarded limit

First we work out the nonretarded limit of equation (6.192) i.e. we assume $2|\omega_{mg}|\mathcal{Z} << 1$. To do so we split the integration in Eq. (6.192) in a following way

$$\int_1^{i\infty} \mathrm{d}k_z = \int_0^{\infty} \mathrm{d}(ik_z) - \int_0^1 \mathrm{d}k_z \tag{6.194}$$

and note that in the limit $2|\omega_{mi}|\mathcal{Z} \to 0$ the second integral on the RHS contributes to the asymptotic series terms that are proportional to non-negative powers of $\mathcal{Z}$ and therefore can be discarded. The remaining part is given by

$$\begin{aligned} \Delta\mathcal{E}_i^{\star,1} = -\frac{1}{8\pi\epsilon_0} \sum_{m<i} |\omega_{mi}|^3 \int_0^{\infty} \mathrm{d}k_z e^{-2|\omega_{mi}|\mathcal{Z}k_z} \\ \times \left[(\tilde{r}^{\mathrm{TE}}_{mi} + k_z^2 \tilde{r}^{\mathrm{TM}}_{mi}) |\mu^{\parallel}_{mi}|^2 + 2(1 + k_z^2)\tilde{r}^{\mathrm{TM}}_{mi} |\mu^{\perp}_{mi}|^2 \right] \end{aligned} \tag{6.195}$$

where $\tilde{r}^{\lambda}_{im}$ are the reflection coefficients, (6.193), evaluated at imaginary argument $\tilde{r}^{\lambda}_{mi} = \bar{r}^{\lambda}_{mi}(ik_z)$. Scaling the integral again according to $x = 2|\omega_{mi}|\mathcal{Z}\ k_z$ and approximating

$$\sqrt{[\epsilon(|\omega_{mi}|) - 1] - \frac{x^2}{(2|\omega_{mi}|\mathcal{Z})^2}} \approx \frac{ix}{2|\omega_{mi}|\mathcal{Z}} \tag{6.196}$$

we derive that, in the nonretarded limit, equation (6.191) becomes

$$\Delta\mathcal{E}_i^{\star,\mathrm{nonret}} = -\frac{1}{32\pi\epsilon_0\mathcal{Z}^3} \sum_{m<i} \frac{\epsilon(|\omega_{mi}|) - 1}{\epsilon(|\omega_{mi}|) + 1} \left(|\mu^{\parallel}_{mi}|^2 + 2|\mu^{\perp}_{mi}|^2 \right) \tag{6.197}$$

Thus, to leading order the residue contributions to the energy shift of the excited state $|i\rangle$, cf. Eq.(6.180), are given by the real part of the above expression,

$$\Delta E_i^{\star,\mathrm{nonret}} = -\frac{1}{32\pi\epsilon_0\mathcal{Z}^3}\sum_{m<i}\frac{|\epsilon(|\omega_{mi}|)|^2-1}{|\epsilon(\omega_{|mi|})+1|^2}\left(|\mu_{mi}^{\parallel}|^2+2|\mu_{mi}^{\perp}|^2\right). \tag{6.198}$$

We see that in the nonretarded regime the residue contributions behave as $\mathcal{Z}^{-3}$ and therefore are of the same order as the non-residue contributions, cf. Eq. (6.187). The result (6.198) is in fact equivalent to the real part of Eq. (7.10) derived in [2].

6.6.2.2 Retarded limit

Now we turn our attention to the asymptotic behaviour of equation (6.192) in the retarded limit, i.e. when $2|\omega_{mi}|\mathcal{Z} >> 1$. It is again useful to split the integration according to (6.194) only that now both integrals play an important role. The first contribution, the integral along $k_z \in [0, i\infty]$, given in Eq. (6.195), can be tackled by the use of Watson's lemma [22]. Noting that the integrand is strongly damped we separate off the exponential and expand the remaining part into Taylor series about $k_z = 0$. The resulting integrals are elementary and we obtain for the leading term

$$\Delta\mathcal{E}_i^{\star,1,\mathrm{ret}} = \frac{1}{8\pi\epsilon_0}\sum_{m<i}|\omega_{mi}|^3\left\{\frac{|\mu_{mi}^{\parallel}|^2}{2|\omega_{mi}|\mathcal{Z}}+2\left[1-\frac{2i\epsilon(|\omega_{mi}|)}{\sqrt{\epsilon(|\omega_{mi}|)-1}}\frac{1}{2|\omega_{mi}|\mathcal{Z}}\right]\frac{|\mu_{mi}^{\perp}|^2}{2|\omega_{mi}|\mathcal{Z}}\right\}. \tag{6.199}$$

Next we treat the integral on the interval $k_z \in [0, 1]$ which, unlike in the nonretarded case, cannot be discarded. However, its asymptotic expansion in inverse powers of $\mathcal{Z}$ is easily obtained by repeated integration by parts. Interestingly, the asymptotic series contain the non-oscillatory terms that exactly cancel out the contributions given in equation (6.199) and altogether we find that to leading-order

$$\Delta\mathcal{E}_i^{\star,\mathrm{ret}} = \frac{1}{4\pi\epsilon_0}\sum_{m<i}|\omega_{mi}|^3\frac{n(|\omega_{mi}|)-1}{n(|\omega_{mi}|)+1}\,e^{2i|\omega_{mi}|\mathcal{Z}}\left\{\frac{|\mu_{mi}^{\parallel}|^2}{2|\omega_{mi}|\mathcal{Z}}+2i\frac{|\mu_{mi}^{\perp}|^2}{(2|\omega_{mi}|\mathcal{Z})^2}\right\}, \tag{6.200}$$

with $n(|\omega_{mi}|) = \sqrt{\epsilon(|\omega_{mi}|)}$. Thus, it turns out that up to leading-order in $\mathcal{Z}$ only contributions due to the parallel component of the atomic dipole moment are contributing. To see the behaviour of contributions due to the perpendicular component of the atomic dipole moment, one needs to derive the next order of the asymptotic series. We again need

to take the real part of expression (6.200) to get the explicit form of the energy shift

$$\Delta E_i^{\star,\mathrm{ret}} = \frac{1}{4\pi\epsilon_0}\sum_{m<i}\frac{|\omega_{mi}|^3}{|n(\omega_{mi})+1|^2} \times\Bigg\{\Big[(|n(|\omega_{mi}|)|^2-1)\cos(2|\omega_{mi}|\mathcal{Z}) - 2\mathrm{Im}[n(|\omega_{mi}|)]\sin(2|\omega_{mi}|\mathcal{Z})\Big]\frac{|\mu_{mi}^{\parallel}|^2}{2|\omega_{mi}|\mathcal{Z}} -2\Big[(|n(|\omega_{mi}|)|^2-1)\sin(2|\omega_{mi}|\mathcal{Z}) + 2\mathrm{Im}[n(|\omega_{mi}|)]\cos(2|\omega_{mi}|\mathcal{Z})\Big]\frac{|\mu_{mi}^{\perp}|^2}{(2|\omega_{mi}|\mathcal{Z})^2}\Bigg\}. \quad (6.201)$$

We see that in the retarded regime the shift of the excited state consists of two quite differently behaving contributions. The non-residue contributions (6.179) behave as $\mathcal{Z}^{-4}$ (see the analysis of the ground state shift, Section 6.6.1), and the residue contributions (6.201) depend on the distance as $\mathcal{Z}^{-1}$. While it would be tempting to say that equation (6.201) will always dominate, this might however not always be the case as this also depends on the values of the dipole matrix elements which can vary significantly. Additionally, Eq. (6.201) displays oscillatory behaviour and in principle there are sets of parameters for which it vanishes. Finally, we remark that it is easily verified that in the limit of non-absorptive dielectric media our result reduces to that derived in [64].

6.7 Spontaneous decay rates near a half-space

The non-residue contributions to the self-energy (6.179) are real and hence they contribute towards the energy-level shifts only. The decay rates are contained solely in the residue contributions to the self-energy, (6.191), that are complex. In the non-retarded limit they are given by the imaginary part of (6.197)

$$\Delta\Gamma_i^{\mathrm{nonret}} = \frac{1}{8\pi\epsilon_0\mathcal{Z}^3}\sum_{m<i}\frac{\mathrm{Im}[\epsilon(|\omega_{mi}|)]}{|\epsilon(|\omega_{mi}|)+1|^2}\left(|\mu_{mi}^{\parallel}|^2+2|\mu_{mi}^{\perp}|^2\right), \quad (6.202)$$

whereas in the retarded limit by the imaginary part of (6.200):

$$\Delta\Gamma_i^{\mathrm{ret}} = -\frac{1}{2\pi\epsilon_0}\sum_{m<i}\frac{|\omega_{mi}|^3}{|n(\omega_{mi})+1|^2} \times\Bigg\{\Big[(|n(|\omega_{mi}|)|^2-1)\sin(2|\omega_{mi}|\mathcal{Z}) + 2\mathrm{Im}[n(|\omega_{mi}|)]\cos(2|\omega_{mi}|\mathcal{Z})\Big]\frac{|\mu_{mi}^{\parallel}|^2}{2|\omega_{mi}|\mathcal{Z}} +2\Big[(|n(|\omega_{mi}|)|^2-1)\cos(2|\omega_{mi}|\mathcal{Z}) - 2\mathrm{Im}[n(|\omega_{mi}|)]\sin(2|\omega_{mi}|\mathcal{Z})\Big]\frac{|\mu_{mi}^{\perp}|^2}{(2|\omega_{mi}|\mathcal{Z})^2}\Bigg\}. \quad (6.203)$$

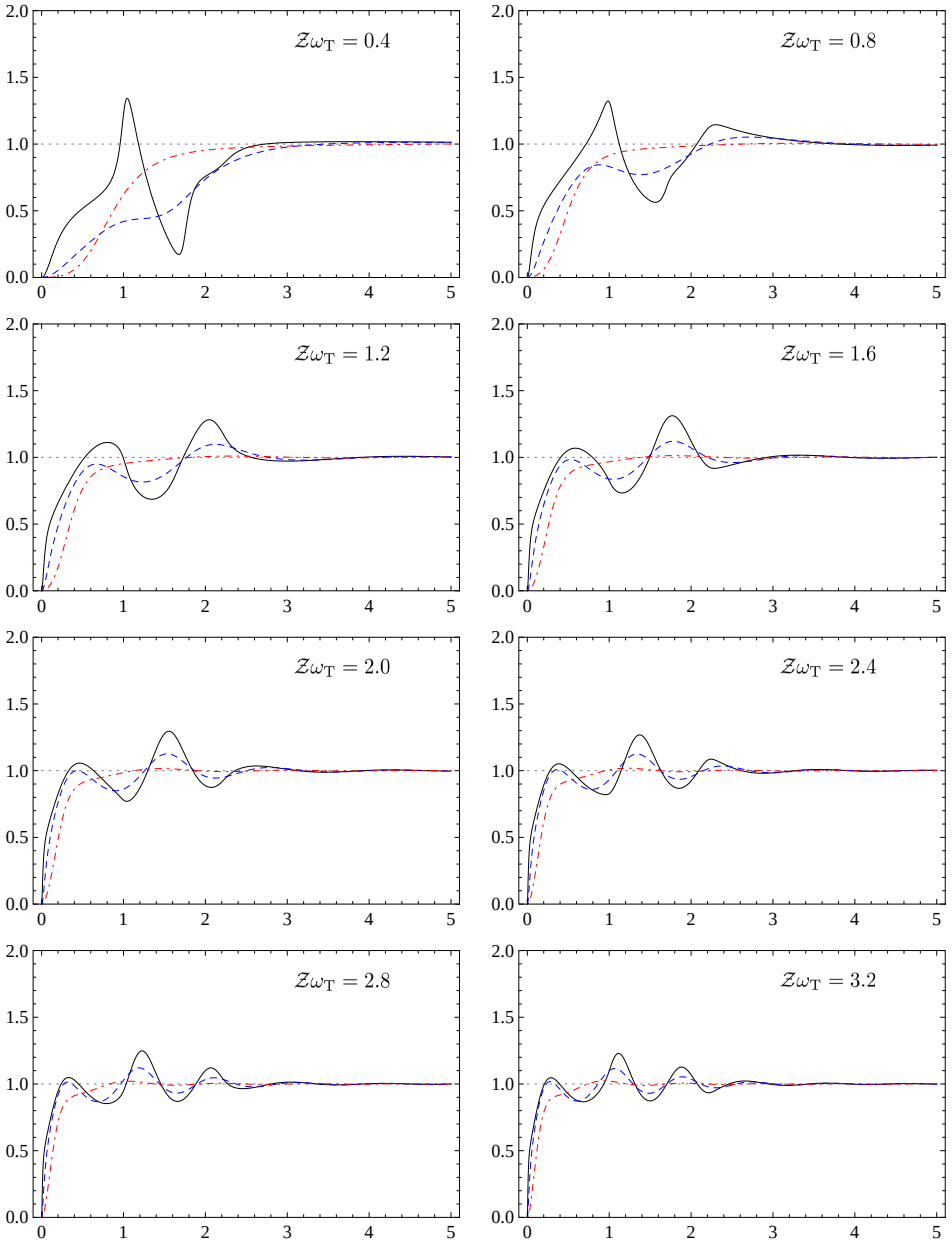

FIGURE 6.7: Normalized lifetime $\tau_{\parallel}$, cf. Eq. (6.204), of the atomic state $|i\rangle$ plotted as a function of $|\omega_{mi}|/\omega_{\mathrm{T}}$ i.e. the frequency of the dipole transition $|i\rangle \to |m\rangle$ measured in units of the transverse resonance frequency of the dielectric ω_{T}. The sequence of graphs corresponds to various distances of the atom from the mirror $\mathcal{Z}\omega_{\mathrm{T}}$, as indicated. The three different line styles (colours) indicate distinct choices of the damping constant in the dielectric γ. We have: $\gamma/\omega_{\mathrm{T}} = 0.05$ (black, solid), $\gamma/\omega_{\mathrm{T}} = 0.5$ (blue, dashed), $\gamma/\omega_{\mathrm{T}} = 5$ (red, dot-dashed). Evidently, for sufficiently high frequencies $|\omega_{mi}|$ the dielectric becomes transparent whereas, if the atom is close to the surface and the absorption is small, the interaction is resonant at $|\omega_{mi}|/\omega_{\mathrm{T}} \approx 1$ i.e. when the frequency of the atomic transition coincides with the absorption line of the dielectric.

The result (6.202) is found to be in an agreement with that derived in [6], their Eq. (128), whereas equation (6.203) reduces to the results given in [64] if we assume $n(\omega)$ to be real and frequency-independent.

As a numerical example we wish to plot the normalized lifetime of the atomic state $|i\rangle$ decaying into some state $|m\rangle$. For simplicity we assume a two-level system and $|\mu_{mi}^{\perp}| = 0$ so that the atom is polarized horizontally with respect to the surface, a situation that is of course artificial. Then, the quantity we plot in Fig. 6.7 is given by

$$\tau_{\parallel}^{-1} = \frac{\Delta\Gamma_i}{\Delta\Gamma_i^0} = -\frac{2\,\mathrm{Im}\,(\Delta\mathcal{E}_i^{\star})}{\hbar\Delta\Gamma_i^0} \tag{6.204}$$

where the quantity $\Delta\mathcal{E}_i^{\star}$ is given by the expression (6.191) and $\Delta\Gamma_i^0$ is the well-known decay rate in free-space

$$\Delta\Gamma_i^0 = \frac{|\omega_{mi}|^3|\mu_{mi}|^2}{3\pi\epsilon_0\hbar}. \tag{6.205}$$

6.8 Energy-level shifts in a gap

In this section we are going to study an atom placed between two identical mirrors distance L apart, as depicted in Fig. 6.2. The scenario of the atom and the gap has been studied previously, see e.g. [89][90]. There, for an atom fixed in the middle of the gap, the dependence of the interaction energy on the width of the cavity has been derived[7]. However, modern cold-atom experiments often deal with atoms trapped in nano-structures. In such experiments it is valuable to know the dependence of the energy shift on the position within the gap, in particular, it would be very useful to work out the shape of the Casimir-Polder potential when the atom's position only slightly varies with respect to the centre of the gap. Therefore, in this Section we will deal with the part of the interaction energy that for a fixed width of the cavity L depends on the position within the gap only.

We have derived the photon propagator in a gap geometry in Section 6.4.2.2, the main result is given in Eq. (6.146). However, since we consider the width of the cavity to be fixed, we discard the part of the propagator which does not depend on the position of the atom. Then, the propagator has formally the same form as in the case of the half-space

[7]The original publication of the results [89] contains some errors in asymptotic analysis, see [90] for corrected formulae.

calculation, cf. Eq. (6.109) and Eq. (6.148). For this reason the calculations of the energy shifts and decay rates for an atom in the gap are largely automatic. The general equations retain the same form as those in the case of a half-space only with different reflection coefficients.

6.8.1 Ground state

To work out the energy shift of a ground state $|g\rangle$ we plug the position-dependent part of the photon propagator (6.148) into equation (6.179). Then, the energy shift can be expressed as

$$\Delta E_g = -\frac{1}{4\pi^2\epsilon_0}\sum_m \int_0^\infty \mathrm{d}k \int_0^\infty \mathrm{d}\xi \frac{\omega_{mg}}{\xi^2+\omega_{mg}^2}\frac{k}{\sqrt{k^2+\xi^2}}\cosh\left(2\sqrt{k^2+\xi^2}\mathcal{Z}\right)e^{-\sqrt{k^2+\xi^2}L} \times\left\{\left[\left(k^2+\xi^2\right)\bar{\mathcal{R}}^{\mathrm{TM}}-\xi^2\bar{\mathcal{R}}^{\mathrm{TE}}\right]|\mu_{mg}^{\parallel}|^2+2k^2\bar{\mathcal{R}}^{\mathrm{TM}}|\mu_{mg}^{\perp}|^2\right\}. \quad (6.206)$$

Here, we have abbreviated

$$\bar{\mathcal{R}}^\lambda = \frac{\bar{r}^\lambda}{\left(1-\bar{r}^\lambda e^{-\sqrt{k^2+\xi^2}L}\right)\left(1+\bar{r}^\lambda e^{-\sqrt{k^2+\xi^2}L}\right)}, \quad (6.207)$$

with $\bar{r}^\lambda$ as given in Eq. (6.183). If we now introduce polar coordinates in (6.206) according to, $\omega=\omega_{mg}xy, k=\omega_{mg}x\sqrt{1-y^2}$ with $y=\cos\phi$, we obtain the perhaps most useful form of the ground-state shift, especially for numerical analysis and the study of retardation,

$$\Delta E_g = -\frac{1}{4\pi^2\epsilon_0}\sum_m \int_0^\infty \mathrm{d}x x^3 \int_0^1 \mathrm{d}y \frac{\omega_{mg}^3}{1+x^2y^2}\cosh(2\omega_{mg}\mathcal{Z}x)e^{-\omega_{mg}Lx} \times\left[\left(\tilde{R}^{\mathrm{TM}}-y^2\tilde{R}^{\mathrm{TE}}\right)|\mu_{mg}^{\parallel}|^2+2\left(1-y^2\right)\tilde{R}^{\mathrm{TM}}|\mu_{mg}^{\perp}|^2\right] \quad (6.208)$$

with $\tilde{\mathcal{R}}^\lambda$ explicitly given as

$$\tilde{\mathcal{R}}^\lambda = \frac{\tilde{r}^\lambda}{\left(1-\tilde{r}^\lambda e^{-\omega_{mg}Lx}\right)\left(1+\tilde{r}^\lambda e^{-\omega_{mg}Lx}\right)}. \quad (6.209)$$

Here, the Fresnel's reflection coefficients $\tilde{r}^\lambda$ are those given in Eq. (6.185).

We consider an atom that is approximately in the middle of the gap so that both interfaces are approximately at the same distance away. In order to define the asymptotic regimes we

use the parameter $2\omega_{mg}(L/2) = \omega_{mg}L$. The interaction is nonretarded when $\omega_{mg}L << 1$ and conversely, the interaction is retarded when $\omega_{mg}L >> 1$. For a physical interpretation of this criterion see the discussion at the end of Section 6.6.1.

6.8.1.1 Nonretarded limit

To take the nonretarded limit we work with equation (6.206). If we follow the steps described in Section 6.6.1.1, where we have dealt with the dielectric half-space, remembering that now $L\omega_{mg}$ plays the role of the decisive parameter, we readily derive

$$\Delta E_g^{\text{nonret}} = -\frac{1}{4\pi^2\epsilon_0 L^3}\sum_m \int_0^\infty \mathrm{d}k k^2 \int_0^\infty \mathrm{d}\xi \frac{\omega_{mg}}{\xi^2+\omega_{mg}^2} \times \cosh\left(2k\frac{\mathcal{Z}}{L}\right)\frac{\chi(i\xi)e^{-k}}{1-\chi^2(i\xi)e^{-2k}}\left[|\mu_{mg}^{\parallel}|^2 + 2|\mu_{mg}^{\perp}|^2\right] \tag{6.210}$$

where $\chi(i\xi)$ is an analogue of the electrostatic image factor defined as

$$\chi(i\xi) = \frac{\epsilon(i\xi)-1}{\epsilon(i\xi)+1}. \tag{6.211}$$

Here $\epsilon(\omega)$ is the dielectric function of the model as described in Appendix E. The k-integral could be in principle carried out but gives a combination of special functions therefore renders the result not very useful. Instead, we work out the corrections due to the small displacement from the middle of the gap i.e. we assume that $\mathcal{Z}/L << 1$ and expand the hyperbolic cosine in Taylor series around the origin

$$\cosh\left(2k\frac{\mathcal{Z}}{L}\right) \approx 1 + 2k^2\frac{\mathcal{Z}^2}{L^2}. \tag{6.212}$$

We discard the second term that does not depend on $\mathcal{Z}$. Then, the k-integral yields the combination of the polylogarithm functions, see e.g. [51], and the result is written as

$$\Delta E_g^{\text{nonret}} = -\frac{6}{\pi^2\epsilon_0 L^3}\frac{\mathcal{Z}^2}{L^2}\sum_m \left(|\mu_{mg}^{\parallel}|^2 + 2|\mu_{mg}^{\perp}|^2\right)\int_0^\infty \mathrm{d}\xi \frac{\omega_{mg}}{\xi^2+\omega_{mg}^2} \times \left\{\mathrm{Li}_5\left[\chi(i\xi)\right] - \mathrm{Li}_5\left[-\chi(i\xi)\right]\right\}. \tag{6.213}$$

The image factor $\chi(i\xi)$, Eq. (6.211), when evaluated at imaginary frequencies, is real and bounded by unity. Then, the polylogarithm functions can be represented as series as [91]

$$\mathrm{Li}_n(z) = \sum_{k=1}^{\infty} \frac{z^k}{k^n} \qquad |z| < 1, \tag{6.214}$$

and their combination appearing in (6.213) becomes

$$\mathrm{Li}_5[\chi(i\xi)] - \mathrm{Li}_5[-\chi(i\xi)] = 2\sum_{k=0}^{\infty} \frac{z^{2k+1}}{(2k+1)^n} = 2\left[\chi(i\xi) + \frac{\chi^2(i\xi)}{243} + \frac{\chi^5(i\xi)}{3125} + \ldots\right]. \tag{6.215}$$

The expansion is seen to converge quite quickly regardless of the value of $\chi(i\xi)$ which in the case of the dielectric function resulting from our model, see Appendix E, is given by

$$\chi(i\xi) = \frac{\omega_{\mathrm{P}}^2}{2\xi(2\gamma+\xi) + \omega_{\mathrm{P}}^2 + 2\omega_{\mathrm{T}}^2}, \tag{6.216}$$

and always satisfies $|\chi(i\xi)| < 1$. Thus, we keep only the leading term of (6.215) and write the final result as

$$\Delta E_g^{\mathrm{nonret}} = -\frac{12}{\pi^2\epsilon_0 L^3}\frac{\mathcal{Z}^2}{L^2}\sum_m \left(|\mu_{mg}^{\parallel}|^2 + 2|\mu_{mg}^{\perp}|^2\right)\int_0^{\infty} \mathrm{d}\xi \frac{\omega_{mg}}{\xi^2+\omega_{mg}^2}\chi(i\xi), \quad \mathcal{Z}/L << 1 \tag{6.217}$$

Thus, for a fixed cavity width L, an atom placed in the middle of the gap experiences an upside-down harmonic potential. In other words, the middle of the gap is an unstable point for a ground-state atom. Therefore, the trap must be able to compensate for the Casimir-Polder potential, otherwise the atom will be adsorbed onto the surface.

6.8.1.2 Retarded limit

Now we turn our attention to the retarded limit of the ground-state energy-level shift in an atom placed roughly in the middle of an absorbing cavity of width L. We shall work with equation (6.208). First we assume $2\mathcal{Z}\omega_{mg}$ to be much smaller than the unity and approximate the hyperbolic cosine by its series expansion, cf. Eq. (6.212). Retaining only

the second term depending on the position within the gap we get

$$\Delta E_g = -\frac{\mathcal{Z}^2}{2\pi^2\epsilon_0}\sum_m \int_0^\infty \mathrm{d}x x^5 \int_0^1 \mathrm{d}y \frac{\omega_{mg}^5}{1+x^2y^2} e^{-\omega_{mg}Lx} \times \left[\left(\tilde{R}^{\mathrm{TM}} - y^2\tilde{R}^{\mathrm{TE}}\right)|\mu_{mg}^{\parallel}|^2 + 2\left(1-y^2\right)\tilde{R}^{\mathrm{TM}}|\mu_{mg}^{\perp}|^2\right]. \quad (6.218)$$

In the limit of $\omega_{mg}L \to \infty$ the x-integration in (6.218) receives contributions only from the neighbourhood of $x = 0^+$, because it is strongly damped the exponential $\exp(-\omega_{mg}Lx)$. The asymptotic behaviour of such type of the integral is usually obtained by the Watson's lemma [22]

$$\int_0^\infty \mathrm{d}x e^{-\alpha x} f(x) \approx \int_0^\infty \mathrm{d}x e^{-\alpha x}[f(0) + xf'(0) + ...], \qquad \alpha \to \infty.$$

However, in case of (6.218), one cannot separate the exponential and approximate the remaining part of the integrand by its Taylor series expansion because the reflection coefficients contain factors $\exp(-\omega_{mg}Lx)$ and each term of the Taylor expansion, after integration with respect to x, would produce terms proportional to L^{-6} which on dimensional grounds is the expected leading-order behaviour. Therefore we have to take into account the contributions from all orders of the expansion. We do this by writing

$$\tilde{\mathcal{R}}^\lambda = \tilde{r}^\lambda \sum_{n=0}^{\infty} (\tilde{r}^\lambda e^{-\omega_{mg}Lx})^{2n}, \quad (6.219)$$

which is possible because $|\tilde{r}^\lambda e^{-\omega_{mg}Lx}| < 1$. Then, equation (6.218) becomes

$$\Delta E_g = -\frac{\mathcal{Z}^2}{2\pi^2\epsilon_0}\sum_{n=0}^{\infty}\sum_m \int_0^\infty \mathrm{d}x x^5 \int_0^1 \mathrm{d}y \frac{\omega_{mg}^5}{1+x^2y^2}\, e^{-(2n+1)\omega_{mg}Lx} \times \left\{\left[\left(\tilde{r}^{\mathrm{TM}}\right)^{2n+1} - y^2\left(\tilde{r}^{\mathrm{TE}}\right)^{2n+1}\right]|\mu_{mg}^{\parallel}|^2 + 2\left(1-y^2\right)\left(\tilde{r}^{\mathrm{TM}}\right)^{2n+1}|\mu_{mg}^{\perp}|^2\right\}. \quad (6.220)$$

Now we are in the position to approximate the damped x integrand by its Taylor series. Doing so and carrying out the straightforward x integrations we arrive at

$$\Delta E_g^{\mathrm{ret}} = -\frac{60}{\pi^2\epsilon_0}\frac{\mathcal{Z}^2}{L^2}\sum_m \sum_{\sigma=\parallel,\perp}\frac{1}{\omega_{mg}}\left(\frac{a_4^\sigma}{L^4} - \frac{12\gamma}{\omega_{\mathrm{T}}^2}\frac{a_5^\sigma}{L^5}\right)|\mu_{mg}^\sigma|^2, \qquad \mathcal{Z}/L << 1,$$

with the coefficients $a^{\sigma}_{4,5}$ given by

$$\begin{aligned}
a_4^{\parallel} &= \sum_{k=0}^{\infty}\int_0^1 \mathrm{d}y\, \left[\frac{(\tilde{r}^{\mathrm{TM}})^{2k+1}}{(2k+1)^6} - y^2\frac{(\tilde{r}^{\mathrm{TE}})^{2k+1}}{(2k+1)^6}\right]_{x=0}, \\
a_5^{\parallel} &= \frac{\beta}{\epsilon_0}\sum_{k=0}^{\infty}\int_0^1 \mathrm{d}y\, y\left[\frac{(\tilde{r}^{\mathrm{TM}})^{2k+1}}{(2k+1)^6}\frac{1}{\tilde{r}^{\mathrm{TM}}}\frac{\partial\tilde{r}^{\mathrm{TM}}}{\partial\epsilon}\right. \\
&\qquad\qquad \left. -y^2\frac{(\tilde{r}^{\mathrm{TE}})^{2k+1}}{(2k+1)^6}\frac{1}{\tilde{r}^{\mathrm{TE}}}\frac{\partial\tilde{r}^{\mathrm{TE}}}{\partial\epsilon}\right]_{x=0}, \\
a_4^{\perp} &= \sum_{k=0}^{\infty}\int_0^1 \mathrm{d}y\, 2(1-y^2)\left[\frac{(\tilde{r}^{\mathrm{TM}})^{2k+1}}{(2k+1)^6}\right]_{x=0}, \\
a_5^{\perp} &= \frac{\beta}{\epsilon_0}\sum_{k=0}^{\infty}\int_0^1 \mathrm{d}y\, 2(1-y^2)y\left[\frac{(\tilde{r}^{\mathrm{TM}})^{2k+1}}{(2k+1)^6}\frac{1}{\tilde{r}^{\mathrm{TM}}}\frac{\partial\tilde{r}^{\mathrm{TM}}}{\partial\epsilon}\right]_{x=0}.
\end{aligned}$$

Setting $x = 0$ in the above equations is related to the fact that in the retarded regime the interaction depends only on static polarizabilities, of both atom and the dielectric. The coefficients listed above are well approximated by the $n = 0$ elements of the sums, cf. eq (6.215). Hence the energy shift reduces to

$$\Delta E_g^{\mathrm{ret}} = -\frac{60}{\pi^2\epsilon_0}\frac{\mathcal{Z}^2}{L^2}\sum_m\sum_{\sigma=\parallel,\perp}\frac{1}{\omega_{mg}}\left(\frac{c_4^{\sigma}}{L^4} - \frac{12\gamma}{\omega_{\mathrm{T}}^2}\frac{c_5^{\sigma}}{L^5}\right)|\mu_{mg}^{\sigma}|^2, \qquad \mathcal{Z}/L << 1, \tag{6.221}$$

with coefficients $c^{\sigma}_{4,5}$ being the same as in the case of the half-space, see Fig. 6.5 on page 173 and the discussion preceding equation (6.190). Since coefficients $c^{\sigma}_{4,5}$ are positive we again observe that the ground-state atom experiences an upside-down harmonic potential. Thus for the ground-state atom, in the limit of retarded interaction, the middle of the gap is an unstable point.

6.8.2 Excited states

The calculation of the energy shift of the excited atomic state i is done along the same lines as in the case of the half-space. The non-residue contributions (6.179) assume the same form as those for the ground state, Eqs. (6.217) and (6.221), calculated in the preceding section. To calculate the residue contributions (6.180) we plug in the propagator (6.148)

and arrive at

$$\Delta\mathcal{E}_i^{\star} = -\frac{i}{4\pi\epsilon_0}\sum_{m<i}\int_0^{\infty}\mathrm{d}k k\frac{\cos\left(2\sqrt{\omega_{mi}^2-k^2}\mathcal{Z}\right)}{\sqrt{\omega_{mi}^2-k^2+i\eta}}\,e^{iL\sqrt{\omega_{mi}^2-k^2}} \times\left\{\left[\omega_{mi}^2\mathcal{R}_{mi}^{\mathrm{TE}}-(\omega_{mi}^2-k^2)\mathcal{R}_{mi}^{\mathrm{TM}}\right]|\mu_{mi}^{\parallel}|^2+2k^2\mathcal{R}_{mi}^{\mathrm{TM}}|\mu_{mi}^{\perp}|^2\right\} \tag{6.222}$$

with $\mathcal{R}_{mi}^{\lambda}$ being the reflection coefficients (6.149) evaluated at the atomic transition frequencies $\omega=|\omega_{mi}|$. We proceed to determine an asymptotic expressions for (6.222) in the case when the atom is placed approximately in the middle of the gap i.e. when $Z/L<<1$ is satisfied. As before, we define the interaction to be nonretarded when $|\omega_{mi}|L<<1$ and retarded when $|\omega_{mi}|L>>1$.

6.8.2.1 Nonretarded limit

To find an approximation of equation (6.222) when the interaction is assumed to be instantaneous we replace the integration variable $k_z=\sqrt{\omega_{mi}^2-k^2}/|\omega_{mi}|$ and rewrite it as

$$\Delta\mathcal{E}_i^{\star} = \frac{i}{4\pi\epsilon_0}\sum_{m<i}|\omega_{mi}|^3\int_1^{i\infty}\mathrm{d}k_z\cos(2k_z|\omega_{mi}|\mathcal{Z})e^{ik_z|\omega_{mi}|L} \times\left\{\left(\bar{\mathcal{R}}_{mi}^{\mathrm{TE}}-k_z^2\bar{\mathcal{R}}_{mi}^{\mathrm{TM}}\right)|\mu_{mi}^{\parallel}|^2+2(1-k_z^2)\bar{\mathcal{R}}_{mi}^{\mathrm{TM}}|\mu_{mi}^{\perp}|^2\right\}. \tag{6.223}$$

The contour of integration runs from 1 to 0 along the real axis and then from 0 to $i\infty$ along the imaginary axis. Note that there is no pole at $k_z=0$. The reflection coefficient $\bar{\mathcal{R}}_{mi}^{\lambda}$ is expressed as follows

$$\bar{\mathcal{R}}_{mi}^{\lambda}=\frac{\bar{r}_{mi}^{\lambda}}{(1-\bar{r}_{mi}^{\lambda}e^{ik_z|\omega_{mi}|L})(1+\bar{r}_{mi}^{\lambda}e^{ik_z|\omega_{mi}|L})} \tag{6.224}$$

with $\bar{r}_{mi}^{\lambda}$ given by (6.193). We note that in equation (6.223) the part of the integration on the interval $k_z\in[0,1]$, in the limit $|\omega_{mi}|L\to 0$, produces an asymptotic series in non-negative powers of L and therefore can be discarded (one anticipates a leading-order

behaviour of L^{-3} in the electrostatic limit). The remaining part can be rewritten as

$$\Delta\mathcal{E}_i^\star = -\frac{1}{4\pi\epsilon_0}\sum_{m<i}|\omega_{mi}|^3\int_0^\infty \mathrm{d}k_z\cosh(2k_z\mathcal{Z})e^{-k_zL} \times\left\{\left(\tilde{\mathcal{R}}_{mi}^{\mathrm{TE}}+k_z^2\tilde{\mathcal{R}}_{mi}^{\mathrm{TM}}\right)|\mu_{mi}^{\parallel}|^2+2(1+k_z^2)\tilde{\mathcal{R}}_{mi}^{\mathrm{TM}}|\mu_{mi}^{\perp}|^2\right\} \tag{6.225}$$

and dealt with using by the methods analogous to those described in Sec. 6.6.2. In (6.225) the reflection coefficients $\tilde{\mathcal{R}}_{mi}^{\lambda}$ are as in (6.224) but evaluated at imaginary k_z i.e. $\tilde{\mathcal{R}}_{mi}^{\lambda}(k_z)=\bar{\mathcal{R}}_{mi}^{\lambda}(ik_z)$. Repeating the steps of equations (6.195)-(6.197), we transform equation (6.225) into

$$\Delta\mathcal{E}_i^{\star,\mathrm{nonret}} = -\frac{1}{4\pi\epsilon_0L^3}\sum_{m<i}\int_0^\infty \mathrm{d}x x^2\cosh\left(2\frac{\mathcal{Z}}{L}x\right) \times\frac{\chi(|\omega_{mi}|)e^{-x}}{1-\chi^2(|\omega_{mi}|)e^{-2x}}\left(|\mu_{mi}^{\parallel}|^2+2|\mu_{mi}^{\perp}|^2\right). \tag{6.226}$$

This is perhaps computationally the most convenient representation of the self-energy in the non-retarded limit. The energy shift $\Delta E_i^{\star,\mathrm{nonret}}$ is given by the real part of the above expression. The x integral can be worked out in the limit $|\mathcal{Z}|/L << 1$ yielding the combination of polylogarithm functions as in Eq. (6.213). However, care needs to be taken because the image factor $\chi(|\omega_{mi}|)$ is now evaluated at real frequency and is complex. Its modulus is not necessarily bound by unity and thus the series representation of the polylogarithm functions (6.214) is no longer convergent so that an approximation similar to that in (6.215) is not always possible. However, whenever[8] we have $\mathrm{Re}[\epsilon(|\omega_{mi}|)]>0$ the image factor will satisfy $|\chi(|\omega_{mi}|)|<1$ and it pays to write the first order position dependent term in the limit $|\mathcal{Z}|/L<<1$ as

$$\Delta\mathcal{E}_i^{\star,\mathrm{nonret}} = -\frac{6}{\pi\epsilon_0L^3}\frac{\mathcal{Z}^2}{L^2}\sum_{m<i}\left(|\mu_{mi}^{\parallel}|^2+2|\mu_{mi}^{\perp}|^2\right)\{\mathrm{Li}_5[\chi(|\omega_{mi}|)]-\mathrm{Li}_5[\chi(-|\omega_{mi}|)]\}. \tag{6.227}$$

[8]The real part of the dielectric constant, as introduced in Appendix E, becomes negative approximately, assuming small damping, in the frequency band between ω_{T} and ω_{L}, see [86]

We can write out the energy shift explicitly by extracting the real part of the above expression. Using the series representation of the Li_5, Eq. (6.214), we obtain

$$\Delta E_i^{\star,\mathrm{nonret}} = -\frac{12}{\pi\epsilon_0 L^3}\frac{\mathcal{Z}^2}{L^2}\sum_{m<i}\sum_{k=0}^{\infty}\left\{\frac{|\chi(|\omega_{mi}|)|^{2k+1}}{(2k+1)^5}\right.$$
$$\left.\times\cos[(2k+1)\phi(|\omega_{mi}|)]\right\}\left(|\mu_{mi}^{\parallel}|^2+2|\mu_{mi}^{\perp}|^2\right), \tag{6.228}$$

with

$$\phi(|\omega_{mi}|)=\mathrm{Arg}\left[\chi(|\omega_{mi}|)\right]=\mathrm{Arg}\left[\frac{\omega_{\mathrm{P}}^2}{2(\omega_{\mathrm{T}}^2-\omega_{mi}^2)+\omega_{\mathrm{P}}^2-4i\gamma|\omega_{mi}|}\right]. \tag{6.229}$$

The series in (6.228) converge rapidly, cf. Eq. (6.215), and can be approximated by taking only the first term into account. Thus we find that the excited state i of an atom placed closely to the middle of the gap experiences the energy shift

$$\Delta E_i^{\star,\mathrm{nonret}} \approx -\frac{12}{\pi\epsilon_0 L^3}\frac{\mathcal{Z}^2}{L^2}\sum_{m<i}\frac{|\epsilon(|\omega_{mi}|)|^2+1}{|\epsilon(|\omega_{mi}|)+1|^2}\left(|\mu_{mi}^{\parallel}|^2+2|\mu_{mi}^{\perp}|^2\right). \tag{6.230}$$

We would like to emphasize that equations (6.228) and (6.230) can be used to estimate the energy shift only when the dielectric function of the material $\epsilon(\omega)$ has a positive real part at the atomic transition frequency. Practically it means that $|\omega_{mi}|$ has to be far away from any resonance absorption lines in the dielectric. In the case of the resonant situation the energy shift is given by the real part of Eq. (6.226).

6.8.2.2 Retarded limit

Recall the methods that have been used to derive the energy shift of an excited state for an atom near a dielectric half-space, Eq. (6.201). One might feel tempted to apply the same procedure to equation (6.222) in order to obtain its behaviour in the retarded limit. This however proves unsuccessful for the following reason. In order to derive Eq. (6.201) we have used repeated integration by parts. This method, when applied to formula (6.222), involves taking derivatives of the coefficient $\bar{\mathcal{R}}_{mi}^{\lambda}$ with respect to the integration variable, say k_z. These coefficients however contain factors $\exp\left(-ik_z|\omega_{mi}|L\right)$, and for that reason, each derivative with respect to k_z produces a term that is proportional to L. Therefore, the repeated integration by parts fails to produce the asymptotic series in inverse powers

of L. Moreover, the difficulty can not be overcome by rewriting $\bar{\mathcal{R}}^{\lambda}_{mi}$ as a geometrical series, as we did in the case of a ground-state atom in the gap, cf. Eq. (6.219), because the modulus of the reflection coefficient $\bar{r}^{\lambda}_{mi}$ may now be greater than one. Therefore, one has to find different way of working out the asymptotic behaviour of the shift when $|\omega_{mi}|L >> 1$. We start from equation (6.223) and note that the integrand is an analytic function in the strip $0 < \mathrm{Im}(k_z) \leq 1$. Hence we deform the contour of integration in Eq. (6.223) to run from 1 to $1 + i\infty$ along the line $\mathrm{Re}(k_z) = 1$ and then from $1 + i\infty$ to $i\infty$. The latter part of the contour can contribute only in the limit $|\omega_{mi}|L \to 0$ and therefore can be discarded. After a simple change of variables $k_z = \kappa_z + 1$ we readily obtain

$$\Delta\mathcal{E}^{\star}_{i} = \frac{i}{4\pi\epsilon_0}\sum_{m<i}|\omega_{mi}|^2\int_0^{i\infty}\mathrm{d}\kappa_z\cos[2(\kappa_z+1)|\omega_{mi}|\mathcal{Z}]e^{i(\kappa_z+1)|\omega_{mi}|L}$$
$$\left\{\left[\bar{\bar{\mathcal{R}}}^{\mathrm{TE}}_{mi} - (1+\kappa_z)^2\bar{\bar{\mathcal{R}}}^{\mathrm{TM}}_{mi}\right]|\mu^{\parallel}_{mi}|^2 + 2\left[1-(1+\kappa_z)^2\right]\bar{\bar{\mathcal{R}}}^{\mathrm{TM}}_{mi}|\mu^{\perp}_{mi}|^2\right\} \tag{6.231}$$

with the reflection coefficients given by

$$\bar{\bar{\mathcal{R}}}^{\lambda}_{mi} = \frac{\bar{\bar{r}}^{\lambda}_{mi}}{\left(1-\bar{\bar{r}}^{\lambda}_{mi}e^{i(\kappa_z+1)|\omega_{mi}|L}\right)\left(1+\bar{\bar{r}}^{\lambda}_{mi}e^{i(\kappa_z+1)|\omega_{mi}|L}\right)}.$$

Here, the doubly barred single-interface Fresnel coefficients have become

$$\bar{\bar{r}}^{\mathrm{TE}}_{mi} = \frac{\kappa_z+1-\sqrt{\epsilon(|\omega_{mi}|)-1+(\kappa_z+1)^2}}{\kappa_z+1+\sqrt{\epsilon(|\omega_{mi}|)-1+(\kappa_z+1)^2}},$$
$$\bar{\bar{r}}^{\mathrm{TM}}_{mi} = \frac{\epsilon(|\omega_{mi}|)(\kappa_z+1)-\sqrt{\epsilon(|\omega_{mi}|)-1+(\kappa_z+1)^2}}{\epsilon(|\omega_{mi}|)(\kappa_z+1)+\sqrt{\epsilon(|\omega_{mi}|)-1+(\kappa_z+1)^2}}.$$

Now we scale the variables according to $\kappa_z = x/|\omega_{mi}|L$ and take the limit $|\omega_{mi}|L \to \infty$. For $x/|\omega_{mi}|L << 1$ the reflection coefficients simplify to

$$\bar{\bar{r}}^{\mathrm{TE}}_{mi} = -\bar{\bar{r}}^{\mathrm{TM}}_{mi} = \frac{1-n(|\omega_{mi}|)}{1+n(|\omega_{mi}|)} \tag{6.232}$$

with $n(|\omega_{mi}|)$ being the complex index of refraction, $n(|\omega_{mi}|) = \sqrt{\epsilon(|\omega_{mi}|)}$. Further short calculation reveals that in the retarded limit $\Delta\mathcal{E}_i^{\text{res}}$ can be expressed as

$$\Delta\mathcal{E}_i^{\star,\text{ret}} = \frac{1}{2\pi\epsilon_0 L}\sum_{m<i}|\omega_{mi}|^2\frac{n(|\omega_{mi}|)-1}{n(|\omega_{mi}|)+1}\cos(2|\omega_{mi}|\mathcal{Z}) \times\int_0^\infty \mathrm{d}x\frac{e^{i|\omega_{mi}|L-x}}{1-\left[\frac{n(|\omega_{mi}|)-1}{n(|\omega_{mi}|)+1}\right]^2 e^{2i|\omega_{mi}|L-2x}}\left(|\mu_{mi}^{\parallel}|^2+\frac{2ix}{|\omega_{mi}|L}|\mu_{mi}^{\perp}|^2\right). \tag{6.233}$$

Note that the dominating contribution comes from the atomic dipole moment that is parallel to the surfaces. It is expressible in terms of elementary functions as

$$\Delta\mathcal{E}_i^{\star,\text{ret}}\Big|_{\parallel} = \frac{1}{2\pi\epsilon_0 L}\sum_{m<i}|\omega_{mi}|^2\cos(2|\omega_{mi}|\mathcal{Z})\tanh^{-1}\left[\frac{n(\omega_{mi})-1}{n(\omega_{mi})+1}e^{i|\omega_{mi}|L}\right]|\mu_{mi}^{\parallel}|^2. \tag{6.234}$$

Equation (6.233) contains both decay rates and energy shifts. To extract the shifts we need take the real part what is most conveniently done by representing the integrand of equation (6.233) as a geometrical series. Doing so we arrive at

$$\Delta E_i^{\star,\text{ret}}\Big|_{\parallel} = \frac{1}{2\pi\epsilon_0 L}\sum_{m<i}|\omega_{mi}|^2|\mu_{mi}^{\parallel}|^2\cos(2|\omega_{mi}|\mathcal{Z}) \times\sum_{q=0}^{\infty}\left|\frac{n(\omega_{mi})-1}{n(\omega_{mi})+1}\right|^{2q+1}\frac{\cos[(2q+1)(\phi_n+|\omega_{mi}|L)]}{2q+1}, \tag{6.235}$$

where

$$\phi_n = \text{Arg}\left[\frac{n(\omega_{mi})-1}{n(\omega_{mi})+1}\right]. \tag{6.236}$$

Written in this form the final result suggests that the energy shift of the excited state $|i\rangle$ displays resonant behaviour i.e. it is enhanced for certain relative values of the atomic transition frequency $|\omega_{mi}|$ with respect to the width of the cavity L, as has also been reported in [92]. The infinite series in equation (6.235) are dominated by its first term so that one can state the approximate condition for resonance to be

$$|\cos(\phi_n+|\omega_{mi}|L)| = 1, \tag{6.237}$$

which in terms of the wavelength of the atomic transition gives

$$\frac{L}{\lambda_{mi}} = \frac{1}{2}\left(k-\frac{\phi_n}{\pi}\right), \quad k = 0,1,2\ldots. \tag{6.238}$$

with ϕ_n given in Eq. (6.236). In the absence of absorption vanishes and the condition states that the resonance occurs whenever the width of the cavity is equal to the half-integer multiply of the wavelength of the atomic transition, as one would expect.

6.9 Spontaneous decay rates in a gap

Spontaneous decay rates in the nonretarded and retarded regime are given by the imaginary part of the expressions (6.226) and (6.233), respectively. There is nothing further gained by writing out the imaginary part of (6.226) explicitly. For practical purposes, the electrostatic result is most conveniently computed using the expression (6.226) and taking the imaginary part after the evaluation of the integral, cf. Eq. (6.181). In the case when the interaction is fully retarded the dominant contributions due to the dipole moment that is parallel to the surface can we written out as

$$\Delta\Gamma_i^{\mathrm{ret}}\big|_{\parallel} = -\frac{1}{\pi\epsilon_0 L}\sum_{m<i}|\omega_{mi}|^2|\mu_{mi}^{\parallel}|^2\cos(2|\omega_{mi}|\mathcal{Z}) \times\sum_{q=0}^{\infty}\left|\frac{n(\omega_{mi})-1}{n(\omega_{mi})+1}\right|^{2q+1}\frac{\sin[(2q+1)(\phi_n+|\omega_{mi}|L)]}{2q+1}, \tag{6.239}$$

with ϕ_n given in Eq. (6.236).

6.10 Summary and conclusions

We have showed that starting from a gauge-independent microscopic model represented by the Hamiltonian (6.19) it is possible to develop a formalism which allows to calculate QED corrections in the presence of absorptive and dispersive boundaries. In order to not presume the equivalence between the Green's function of the wave equation and the quantum photon propagator we have used the diagrammatic technique to integrate out the damped polaritons to give a Dyson equation for the photon propagator. We then solved this integral equation exactly using traceable methods. This allowed us to calculate analytically a one-loop self-energy diagram for an electron bound by a nucleus near a dielectric half-space and hence to determine the energy-level shifts and change in transition rates which are proportional to the real and imaginary part of the electron's self energy, respectively.

TABLE 6.1: Equation numbers of the major results of this Chapter. The half-space.

	$\Delta\Gamma$	ΔE ground state	ΔE excited states
non-retarded regime	Eq. (6.202)	Eq. (6.187)	Eq. (6.198)
retarded regime	Eq. (6.203)	Eq. (6.188)	Eq. (6.201)

TABLE 6.2: Equation numbers of the major results of this chapter. The gap.

	$\Delta\Gamma$	ΔE ground state	ΔE excited states
non-retarded regime	Eq. (6.226)	Eq. (6.217)	Eq. (6.226)
retarded regime	Eq. (6.239)	Eq. (6.221)	Eq. (6.235)

We have investigated the role of the material's absorption in some detail and confirmed the previously known result that absorption has the most profound impact on the atomic system in the non-retarded regime i.e. when the distance between the atom and the mirror is much smaller than the wavelength of the dominant dipole transition. If the distance between the atom and the surface far exceeds the wavelength of the dominant transition, then to leading order dispersion and absorption make no difference. The next-to-leading order corrections are proportional to damping constant of the Lorentz-type dielectric function and it turns out that, in the retarded regime, only the material's absorption lines that lie in the low-frequency region have significant impact on the interaction. This suggests that the interaction of macroscopic bodies and quantum systems for which polarizability peaks at low frequencies, e.g. free electron, might be affected in a more substantial way. We provide complete reference to the major results of this Chapter in Table 6.1 and 6.2.

Appendix A

Free-space photon propagator

The spectral representation of the photon propagator derived in Section 6.3.2 using the differential equation (6.45)

$$D_{ik}^{(0)}(\mathbf{q},\omega) = \epsilon_0 \frac{\delta_{ik}\mathbf{q}^2 - q_i q_k}{\omega^2 - \mathbf{q}^2} \tag{A.1}$$

is meaningless unless we specify how do we circumvent the poles of the denominator. This is because the definition of the photon propagator (6.41) is unique whereas (A.1) is not, and we have to put some additional information in. To see the right way of displacing the poles off the real axis we evaluate the matrix elements in equation (6.41) directly using the normal-mode expansion of the of the electric field operator[1]

$$E_i^{\lambda}(\mathbf{r},t) = \frac{i}{(2\pi)^{3/2}} \sum_{\lambda} \int \mathrm{d}^3\mathbf{q} \sqrt{\frac{\hbar\omega_{\mathbf{q}}}{2\epsilon_0}} \left(a_{\mathbf{q}\lambda} e^{i\omega_{\mathbf{q}}t - i\mathbf{q}\cdot\mathbf{r}} - a_{\mathbf{q}\lambda}^{\dagger} e^{-i\omega_{\mathbf{q}}t + i\mathbf{q}\cdot\mathbf{r}} \right) \hat{e}_i^{\lambda}(\mathbf{q}). \tag{A.2}$$

We plug this operator into the definition (6.41) and bear in mind that when calculating the vacuum expectation value of the product of operators $E_i^{\lambda}(\mathbf{r},t)E_j^{\sigma}(\mathbf{r}',t')$ only the terms proportional to $a_{\mathbf{q}\lambda}a_{\mathbf{p}\sigma}^{\dagger}$ survive. Using the commutation relation $[a_{\mathbf{q}\lambda}, a_{\mathbf{p}\sigma}^{\dagger}] = \delta^{(3)}(\mathbf{q}-\mathbf{p})\delta_{\lambda\sigma}$

[1] Note that for the electromagnetic field not interacting with the polarization field the electric field operator and the displacement field operator coincide up to a factor of ϵ_0.

we find that the propagator is given by

$$D_{ij}^{(0)}(\mathbf{r}-\mathbf{r}',t-t') = -\frac{i\epsilon_0}{2(2\pi)^3}\sum_{\lambda}\int \mathrm{d}^3\mathbf{q} e^{-i\mathbf{q}\cdot(\mathbf{r}-\mathbf{r}')}\omega_{\mathbf{q}}\hat{e}_i^{\lambda}(\mathbf{q})\hat{e}_j^{\lambda}(\mathbf{q}) \times \left[\theta(t-t')e^{-i\omega_{\mathbf{q}}(t-t')} + \theta(t'-t)e^{i\omega_{\mathbf{q}}(t'-t)}\right]. \tag{A.3}$$

where $\omega_{\mathbf{q}} = |\mathbf{q}|$. Using the integral representation of the θ-function

$$\theta(t-t') = \frac{1}{2\pi i}\int_{-\infty}^{\infty}\mathrm{d}x\frac{e^{ix(t-t')}}{x-i\eta}, \quad \eta > 0 \tag{A.4}$$

one can quite simply show that the spectral representation of the photon propagator with the correct prescription to handle the poles is indeed given by

$$D_{ik}^{(0)}(\mathbf{q},\omega) = \epsilon_0\frac{\delta_{ik}\mathbf{q}^2 - q_iq_k}{\omega^2 - \mathbf{q}^2 + i\eta}, \tag{A.5}$$

where we have also used the completeness property of the polarization vectors

$$\sum_{\lambda}\hat{e}_i^{\lambda}(\mathbf{q})\hat{e}_j^{\lambda}(\mathbf{q}) = \delta_{ik} - \frac{q_iq_k}{\mathbf{q}^2}. \tag{A.6}$$

At this point one may wonder why even bother with the derivation of the photon propagator presented in Section 6.3.2. This is done in order to determine the differential equation satisfied by the propagator which proves to be useful in calculations of the dressed photon propagator i.e. the propagator of the electromagnetic field interacting with the polarization field.

Appendix B

Photon propagator using the phenomenological QED

The phenomenological theory of quantum electrodynamics, as developed in [1], gives the electric field operator as

$$E_i(\mathbf{r},t) = -i\mu_0 \int \mathrm{d}^3\mathbf{r}' \int_0^\infty \mathrm{d}\omega e^{-i\omega t} G_{ik}(\mathbf{r},\mathbf{r}';\omega) J_k(\mathbf{r}',\omega) + \mathrm{H.C.} \tag{B.1}$$

where $J_k(\mathbf{r},\omega)$ is the so-called noise current operator satisfying the following commutation relation

$$\left[J_i(\mathbf{r},\omega), J_k^\dagger(\mathbf{r}',\omega')\right] = \frac{\hbar\epsilon_0}{\pi}\epsilon'(\mathbf{r},\omega)\omega^2\delta^{(3)}(\mathbf{r}-\mathbf{r}')\delta(\omega-\omega')\delta_{ik}, \tag{B.2}$$

where $\epsilon'(\mathbf{r},\omega)$ is the imaginary part of the phenomenologically introduced dielectric permittivity. $G_{ik}(\mathbf{r},\mathbf{r}';\omega)$ is the Green's function of the wave equation in the usual mathematical sense i.e. it is a solution of

$$(\nabla_i\nabla_j - \delta_{ij}\nabla^2)G_{jk}(\mathbf{r},\mathbf{r}';\omega) - \epsilon(\mathbf{r},\omega)\omega^2 G_{ik}(\mathbf{r},\mathbf{r}';\omega) = \delta_{ik}\delta^{(3)}(\mathbf{r}-\mathbf{r}'), \tag{B.3}$$

with the requirement that it satisfies the retarded boundary conditions in time. For an overview of the theory and some applications see [93].

We want to calculate the Feynman propagator corresponding to the electric field operator i.e. the quantity

$$D^{\mathrm{E}}_{ij}(\mathbf{r},\mathbf{r}',t,t') = -\frac{i}{\hbar}\langle 0|T\left[E_i(\mathbf{r},t)E_j(\mathbf{r}',t')\right]|0\rangle. \tag{B.4}$$

Plugging into the above definition the operator (B.1) and utilizing the commutation relations (B.2) together with some of the properties of the Green's tensor derived in [93] we arrive at

$$D^{\mathrm{E}}_{ij}(\mathbf{r},\mathbf{r}',t,t') = -\frac{i}{\pi\epsilon_0}\int_0^\infty \mathrm{d}\omega\omega^2\left[\theta(t-t')e^{-i\omega(t-t')} + \theta(t'-t)e^{i\omega(t-t')}\right] G''_{ij}(\mathbf{r},\mathbf{r}';\omega)$$

where $G''_{ij}(\mathbf{r},\mathbf{r}';\omega)$ is the imaginary part of the Green's tensor i.e.

$$G_{ij}(\mathbf{r},\mathbf{r}';\omega) = G'_{ij}(\mathbf{r},\mathbf{r}';\omega) + iG''_{ij}(\mathbf{r},\mathbf{r}';\omega). \tag{B.5}$$

Now we carry out the Fourier transform with respect to $t-t'$ using the distributional identities

$$\int_0^\infty \mathrm{d}\tau e^{\pm i\tau\Omega} = \pi\delta(\Omega) \pm i\frac{\mathcal{P}}{\Omega} \tag{B.6}$$

where $\mathcal{P}$ denotes the Cauchy principal value. We arrive at

$$\begin{aligned} D^{\mathrm{E}}_{ij}(\mathbf{r},\mathbf{r}';\Omega) = \frac{2}{\pi\epsilon_0}\mathcal{P}\int_0^\infty \mathrm{d}\omega\frac{\omega^3}{\Omega^2-\omega^2}G''_{ij}(\mathbf{r},\mathbf{r}';\omega) \\ -\frac{i}{\epsilon_0}\int_0^\infty \mathrm{d}\omega\omega^2\left[\delta(\Omega-\omega)+\delta(\Omega+\omega)\right]G''_{ij}(\mathbf{r},\mathbf{r}';\omega). \end{aligned} \tag{B.7}$$

The Green's tensor satisfies the retarded boundary conditions in time to preserve causality. This means that it is analytical in the upper-half of the complex ω plane. Analycity in the upper-half of the ω-plane implies Kramers-Krönig relations [10], thus the Green's tensor may be said to inherit the properties of the permittivity. In particular, its imaginary part is an odd function of frequency ω whereas its real part is even in ω. Having said that we can deal with the principal-value integral in (B.7). Since $G''_{ij}(\mathbf{r},\mathbf{r}';-\omega) = -G''_{ij}(\mathbf{r},\mathbf{r}';\omega)$ and the remaining part of the integrand is also odd we extend the lower integration limit to start from $-\infty$ and multiply by $1/2$. On the other hand, the real part of the Green's tensor is even in ω so that we can replace

$$G''_{ij}(\mathbf{r},\mathbf{r}',\omega) \to \frac{1}{i}G_{ij}(\mathbf{r},\mathbf{r}',\omega) \tag{B.8}$$

without changing the value of the integral. The first line of equation (B.7) becomes

$$\frac{\mathcal{P}}{i\pi\epsilon_0}\int_{-\infty}^{\infty}\mathrm{d}\omega\frac{\omega^3}{\Omega^2-\omega^2}G_{ij}(\mathbf{r},\mathbf{r}';\omega). \tag{B.9}$$

To work out this integral we consider a new contour of integration γ that runs from $-\infty$ to ∞ circumventing the poles at $\omega=\pm\Omega$ from the above and then closes up in the upper half of the ω-plane along the large semicircle $|\omega|=R$. Because the Green's tensor in analytic in the upper half-plane such calculated integral vanishes and we can express the principal-value integral as

$$\mathcal{P}\int = -\int_{\gamma^-} - \int_{\gamma^+} - \int_{\Gamma} \tag{B.10}$$

where $\gamma^{\pm}$ denotes the clockwise contours that go around the poles at $\omega=\pm\Omega$ respectively and Γ denotes the contribution from the large semicircle taken counter-clockwise. Using the residue theorem we derive that the contribution from $\gamma^{\pm}$ is given by

$$-\frac{1}{\epsilon_0}\Omega^2 G'_{ij}(\mathbf{r},\mathbf{r}';\Omega), \tag{B.11}$$

whereas the large semicircle contributes the delta function

$$-\frac{1}{\epsilon_0}\delta_{ij}\delta^{(3)}(\mathbf{r}-\mathbf{r}'), \tag{B.12}$$

where while calculating it we have used the fact that asymptotically the Green's tensor behaves as [93]

$$\lim_{|\omega|\to\infty}\omega^2 G_{ij}(\mathbf{r},\mathbf{r};\omega) = -\delta_{ij}\delta^{(3)}(\mathbf{r}-\mathbf{r}'). \tag{B.13}$$

The second line of equation (B.7) is on the other hand easily seen to be

$$-\frac{i}{\epsilon_0}\Omega^2 G''_{ij}(\mathbf{r},\mathbf{r}';|\Omega|), \tag{B.14}$$

so the final result relating the photon propagator to the Green's function of the wave equation on the real Ω-axis is written compactly as

$$D^{\mathrm{E}}_{ij}(\mathbf{r},\mathbf{r}';\Omega) = -\frac{\Omega^2}{\epsilon_0}G_{ij}(\mathbf{r},\mathbf{r}';|\Omega|) - \frac{1}{\epsilon_0}\delta_{ij}\delta^{(3)}(\mathbf{r}-\mathbf{r}'). \tag{B.15}$$

A similar formula has been given in [94]. We would like to make connection with the

phenomenological QED by comparing this result with the results of Section 6.4.2. It needs to emphasized that what we have calculated here is the propagator for the electric field **E** whereas in Section 6.4.2 the propagator for the displacement field **D** was obtained. Therefore, the results have a chance to coincide only when $\mathbf{r}, \mathbf{r}'$ are pointing to the outside of the dielectric, so we restrict ourselves to this case. Then, the Green's tensor $G_{ij}(\mathbf{r}, \mathbf{r}'; \omega)$ splits into a free-space part $G_{ij}^{(0)}$ and the correction that describes the reflection of the electromagnetic field from the surface $G_{ij}^{(r)}$ and the result can be rewritten as

$$D_{ij}^{\mathrm{E}}(\mathbf{r}, \mathbf{r}'; \Omega) = -\frac{\Omega^2}{\epsilon_0}\left[G_{ij}^{(0)}(\mathbf{r} - \mathbf{r}'; |\Omega|) + \delta_{ij}\delta^{(3)}(\mathbf{r} - \mathbf{r}')\right] - \frac{\Omega^2}{\epsilon_0} G_{ij}^{(r)}(\mathbf{r}, \mathbf{r}'; |\Omega|). \tag{B.16}$$

It is now clear that the Feynman propagator is an even function of Ω unlike the Green's function of the wave equation that has the same analytical structure as the dielectric function. It is not difficult to verify that for the particular geometry considered in Section 6.4.2.1, the half-space, formula (B.16) indeed holds. The terms in square brackets combine to deliver the *transverse* free-space propagator as given in equation (6.49). The reflected part $G_{ij}^{(r)}(\mathbf{r}, \mathbf{r}'; |\Omega|)$, that can be found for example in [1], satisfies the homogeneous wave equation. Therefore, it is automatically transverse

$$\nabla_i G_{ij}^{(r)}(\mathbf{r} - \mathbf{r}'; \omega) = 0 \tag{B.17}$$

and coincides with the reflected part of the photon propagator $D_{ij}^{\mathrm{E}}(\mathbf{r}, \mathbf{r}'; \omega)$ given in equation (6.108) except for a different behaviour in the ω-plane, which of course arises due to the different boundary conditions in time. $D_{ij}^{\mathrm{E}}(\mathbf{r}, \mathbf{r}'; t - t')$ is a Feynman propagator whereas $G_{ij}(\mathbf{r}, \mathbf{r}', t - t')$ describes the retarded solutions of the wave equation.

Appendix C

Fresnel coefficients for layered dielectric

In this section we list the reflection and transmission coefficients appearing in the normal-modes of the system as discussed in Section 5.2.1. For the left-incident modes we find

$$\begin{aligned} R_\lambda^L &= \frac{r_\lambda^{\mathrm{sl}} + r_\lambda^{\mathrm{lv}} e^{2ik_{\mathrm{zl}}L}}{1 + r_\lambda^{\mathrm{sl}} r_\lambda^{\mathrm{lv}} e^{2ik_{\mathrm{zl}}L}} e^{-ik_{\mathrm{zs}}L} \\ I_\lambda^L &= \frac{t_\lambda^{\mathrm{sl}} e^{i(k_{\mathrm{zl}}-k_{\mathrm{zs}})L/2}}{1 + r_\lambda^{\mathrm{sl}} r_\lambda^{\mathrm{lv}} e^{2ik_{\mathrm{zl}}L}} \\ J_\lambda^L &= \frac{t_\lambda^{\mathrm{sl}} r_\lambda^{\mathrm{lv}} e^{(3ik_{\mathrm{zl}}-ik_{\mathrm{zs}})L/2}}{1 + r_\lambda^{\mathrm{sl}} r_\lambda^{\mathrm{lv}} e^{2ik_{\mathrm{zl}}L}} \\ T_\lambda^L &= \frac{t_\lambda^{\mathrm{sl}} t_\lambda^{\mathrm{lv}} e^{(2ik_{\mathrm{zl}}-ik_{\mathrm{zs}}-ik_{\mathrm{z}})L/2}}{1 + r_\lambda^{\mathrm{sl}} r_\lambda^{\mathrm{lv}} e^{2ik_{\mathrm{zl}}L}}. \end{aligned}$$

and for the right-incident modes we get

$$\begin{aligned} R_\lambda^R &= \frac{r_\lambda^{\mathrm{vl}} + r_\lambda^{\mathrm{ls}} e^{2ik_{\mathrm{zl}}L}}{1 + r_\lambda^{\mathrm{vl}} r_\lambda^{\mathrm{ls}} e^{2ik_{\mathrm{zl}}L}} e^{-ik_{\mathrm{z}}L} \\ I_\lambda^R &= \frac{t_\lambda^{\mathrm{vl}} e^{i(k_{\mathrm{zl}}-k_{\mathrm{z}})L/2}}{1 + r_\lambda^{\mathrm{vl}} r_\lambda^{\mathrm{ls}} e^{2ik_{\mathrm{zl}}L}} \\ J_\lambda^R &= \frac{t_\lambda^{\mathrm{vl}} r_\lambda^{\mathrm{ls}} e^{(3ik_{\mathrm{zl}}-ik_{\mathrm{z}})L/2}}{1 + r_\lambda^{\mathrm{vl}} r_\lambda^{\mathrm{ls}} e^{2ik_{\mathrm{zl}}L}} \\ T_\lambda^R &= \frac{t_\lambda^{\mathrm{vl}} t_\lambda^{\mathrm{ls}} e^{(2ik_{\mathrm{zl}}-ik_{\mathrm{zs}}-ik_{\mathrm{z}})L/2}}{1 + r_\lambda^{\mathrm{vl}} r_\lambda^{\mathrm{ls}} e^{2ik_{\mathrm{zl}}L}}. \end{aligned}$$

The standard Fresnel reflection coefficients r_λ^{ab} are given by (5.11).

Appendix D

Electrostatic calculation of the energy-level shift in a ground-state atom in a layered geometry

To provide an additional check on the consistency of our calculations we would like to derive equation (5.66) by means of ordinary electrostatics. We start from the general formula derived in [3] that expresses the electrostatic interaction energy of a electric dipole in the presence of a dielectric in terms of Green's function of the Laplace equation

$$\Delta E = \frac{1}{2}\sum_i \langle \mu_i^2 \rangle \nabla_i \nabla_i' \, G_R(\mathbf{r},\mathbf{r}')\Big|_{\mathbf{r}=\mathbf{r}_0,\mathbf{r}'=\mathbf{r}_0} . \tag{D.1}$$

Here the sum runs over three components of the dipole moment and the subscript R means that only the homogeneous correction to the free-space Green's function (reflected part) that is caused by the presence of the boundary enters the formula. This ensures that the self-energy of the dipole is omitted and guarantees the convergence of the final result. The harmonic function $G_R(\mathbf{r},\mathbf{r}')$ is a solution of the Laplace equation that vanishes for $|z| \to \infty$. Therefore it can be written in the form:

$$G_R(\mathbf{r},\mathbf{r}') = -\frac{1}{4\pi\epsilon_0}\int_0^\infty \mathrm{d}_2\mathbf{k}_\parallel e^{i\mathbf{k}_\parallel\cdot\mathbf{r}_\parallel} \begin{cases} C_1(\mathbf{k}_\parallel,\mathbf{r}')e^{k_z z} & z < L/2 \\ C_2(\mathbf{k}_\parallel,\mathbf{r}')e^{k_z z} + C_3(\mathbf{k}_\parallel,\mathbf{r}')e^{-k_z z} & |z| < L/2 \\ C_4(\mathbf{k}_\parallel,\mathbf{r}')e^{-k_z z} & z > L/2 \end{cases} , \tag{D.2}$$

with $k_z = \sqrt{k_x^2 + k_y^2}$. The C coefficients are easily worked out by applying the continuity conditions, which result from Maxwell's equations, across the interfaces and one finds that

$$G_R(\mathbf{r}, \mathbf{r}') = -\frac{1}{4\pi\epsilon_0} \int_0^\infty \mathrm{d}k J_0(k\rho) \frac{\dfrac{n_\mathrm{l}^2 - 1}{n_\mathrm{l}^2 + 1} - \dfrac{n_\mathrm{l}^2 - n_\mathrm{s}^2}{n_\mathrm{s}^2 + n_\mathrm{l}^2} e^{-2kL}}{1 - \dfrac{n_\mathrm{l}^2 - 1}{n_\mathrm{l}^2 + 1} \dfrac{n_\mathrm{l}^2 - n_\mathrm{s}^2}{n_\mathrm{s}^2 + n_\mathrm{l}^2} e^{-2kL}} e^{-k(z+z')} \tag{D.3}$$

with $\rho = \sqrt{(x - x')^2 + (y - y')^2}$. Application of the formula (D.1) is straightforward and we easily derive that the electrostatic interaction energy of a dipole in a vicinity of the layered dielectric is indeed equal to (5.66).

Appendix E

Simple model of dielectric constant in the Huttner-Barnett model

To determine the dielectric permittivity of the model we use equations of motion for the fields that follow from the Hamiltonian (6.7)-(6.11) and the commutation relations (6.13)-(6.15). It is not difficult to show that temporally Fourier transformed equations of motion read

$$
\begin{aligned}
(\nabla_i\nabla_j - \delta_{ij}\nabla^2)E_j(\mathbf{r},\omega) - \omega^2 E_i(\mathbf{r},\omega) &= g(\mathbf{r})\omega^2 X_i(\mathbf{r},\omega), && \text{(E.1)}\\
\left(\omega_{\mathrm{T}}^2 - \omega^2 + \frac{1}{\mathcal{M}}\int_0^\infty \mathrm{d}\nu\rho_\nu\nu^2\right) X_i(\mathbf{r},\omega) &= \frac{g(\mathbf{r})}{\mathcal{M}}E_i(\mathbf{r},\omega) + \frac{1}{\mathcal{M}}\int_0^\infty \mathrm{d}\nu\rho_\nu\nu^2 Y_{\nu,i}(\mathbf{r},\omega), && \text{(E.2)}\\
(\nu^2 - \omega^2)Y_{\nu,i}(\mathbf{r},\omega) &= \nu^2 X_i(\mathbf{r},\omega). && \text{(E.3)}
\end{aligned}
$$

The susceptibility is defined as the proportionality constant between polarization $\mathbf{X}(\mathbf{r},\omega)$ and electric field $\mathbf{E}(\mathbf{r},\omega)$. In the isotropic case we have

$$\mathbf{X}(\mathbf{r},\omega) = \epsilon_0\Pi^{\mathrm{ret}}(\mathbf{r},\omega)\mathbf{E}(\mathbf{r},\omega). \tag{E.4}$$

Transforming the above relation back to the time variable gives

$$\mathbf{X}(\mathbf{r},t) = \frac{\epsilon_0}{2\pi}\int_{-\infty}^{\infty}\mathrm{d}w\; e^{-i\omega t}\;\Pi^{\mathrm{ret}}(\mathbf{r},\omega)\mathbf{E}(\mathbf{r},\omega). \tag{E.5}$$

If we now introduce

$$\mathbf{E}(\mathbf{r},\omega) = \int_{-\infty}^{\infty} \mathrm{d}t' e^{i\omega t'} \mathbf{E}(\mathbf{r},t') \tag{E.6}$$

and plug it into Eq. (E.5), then, upon interchanging ω and t' integrations we obtain

$$\mathbf{X}(\mathbf{r},t) = \epsilon_0 \int_{-\infty}^{\infty} \mathrm{d}t' \Pi^{\mathrm{ret}}(\mathbf{r},t-t')\mathbf{E}(\mathbf{r},t'). \tag{E.7}$$

On physical grounds we expect that $\mathbf{X}(\mathbf{r},t)$ doesn't depend on $\mathbf{E}(\mathbf{r},t')$ at the times t' later than t, in other words, the relationship between $\mathbf{X}(\mathbf{r},t)$ and $\mathbf{E}(\mathbf{r},t')$ has to be causal. This requirement forces the response function $\Pi^{\mathrm{ret}}(\mathbf{r},t-t')$ to vanish for times $t-t'<0$

$$\Pi^{\mathrm{ret}}(\mathbf{r},t-t') = \begin{cases} \Pi(\mathbf{r},t-t') & t-t'>0 \\ 0 & t-t'<0 \end{cases}, \tag{E.8}$$

and from the relation

$$\Pi^{\mathrm{ret}}(\mathbf{r},t-t') = \frac{1}{2\pi}\int_{-\infty}^{\infty} \mathrm{d}\omega e^{-i\omega(t-t')}\Pi^{\mathrm{ret}}(\mathbf{r},\omega), \tag{E.9}$$

we can see that it's Fourier transform is analytic in the upper half of the complex ω-plane.

To determine the susceptibility $\Pi^{\mathrm{ret}}(\mathbf{r},\omega)$ which follows from our model one has to find the relation between $\mathbf{X}(\mathbf{r},\omega)$ and $\mathbf{E}(\mathbf{r},\omega)$ that follows from equations of motion (E.1)-(E.3). This is straightforward and yields

$$\Pi^{\mathrm{ret}}(\mathbf{r},\omega) = \frac{g(\mathbf{r})}{\epsilon_0 \mathcal{M}}\left[\omega_{\mathrm{T}}^2 - \omega^2 - \frac{\omega^2}{\mathcal{M}}\int_0^{\infty} \mathrm{d}\nu \frac{\rho_\nu \nu^2}{\nu^2-\omega^2}\right]^{-1}. \tag{E.10}$$

However, in order for the relation (E.10) to be meaningful one has to decide how to deal with the poles present in the ν integral. The freedom of choice is constrained by the retarded nature of $\Pi^{\mathrm{ret}}(\mathbf{r},t-t')$, cf. Eq. (E.8). It is known from the previous work [80, App. 2], that the function ρ_ν in (E.10) must be positive, even and have no poles on the real axis. With these properties in mind it is not difficult to show that an appropriate choice to handle the poles is given by

$$\mathbf{Y}_\nu(\mathbf{r},\omega) = \frac{\nu^2}{\nu^2-\omega^2-i\eta\omega}\mathbf{X}(\mathbf{r},\omega). \tag{E.11}$$

This has been also noted in [71].

The specific form of the dielectric permittivity is determined by the choice of the coupling function ρ_ν that describes the interaction between the reservoir and the dielectric, see [83] for some possible choices. Here we choose the coupling function ρ_ν such as to arrive at the simple single-resonance Lorentz model of the dielectric function. This is guaranteed by choosing

$$\rho_\nu = \frac{4\mathcal{M}\gamma}{\pi\nu^2} \tag{E.12}$$

which gives a frequency-independent coupling between the bath and polarization oscillators, cf eq. (6.10). Carrying out the integration gives

$$\Pi^{\mathrm{ret}}(\mathbf{r},\omega) = g(\mathbf{r})\frac{\omega_{\mathrm{P}}^2}{\omega_{\mathrm{T}}^2 - \omega^2 - 2i\gamma\omega}. \tag{E.13}$$

with $\omega_{\mathrm{P}}^2 = (\epsilon_0\mathcal{M})^{-1}$. From the relation

$$\mathbf{D}(\mathbf{r},\omega) = \epsilon_0\mathbf{E} + g(\mathbf{r})\mathbf{X}(\mathbf{r},\omega) = \epsilon(\mathbf{r},\omega)\mathbf{E}(\mathbf{r},\omega) \tag{E.14}$$

we read off

$$\frac{\epsilon}{\epsilon_0} = 1 + g^2(\mathbf{r})\frac{\omega_{\mathrm{P}}^2}{\omega_{\mathrm{T}}^2 - \omega^2 - 2i\gamma\omega}. \tag{E.15}$$

Bibliography

[1] T. Gruner, D. Welsch, Phys. Rev. A **53**, 1818(1996).

[2] G. Barton, Proc. R. Soc. London, Ser. A **453**, 2461(1997).

[3] C. Eberlein, R. Zietal, Phys. Rev. A **75**, 032516(2007).

[4] C. Eberlein, R. Zietal. Phys. Rev. A **80**, 012504(2009).

[5] C. Eberlein, D. Robaschik. Phys. Rev. Lett **92**, 233602(2004).

[6] M. S. Yeung, T. K. Gustafson, Phys. Rev. A **54**, 5227(1996).

[7] P. A. M. Dirac, Proc. R. Soc. Lond. A, **109**, 642(1925).

[8] J. Mehra, H. Rechenberg, Foundations of Physics, **29**, 91(1999).

[9] W. Heisenberg, Zeit. f. Phys, **34**, 858(1925).

[10] J. D. Jackson, *Classical Electrodynamics*, (Wiley, New York, 1962).

[11] P. Milonni, *The Quantum Vacuum*, (Academic Press, 1994).

[12] P. W. Milonni, Phys. Lett. A **82**, 225(1981).

[13] H. B. G. Casimir, D. Polder, Phys. Rev. **73**, 360(1948).

[14] C. C. Tannoudji, J. Dupont-Roc, G. Grynberg, *Photons & Atoms, Introduction to Quantum Electrodynamics*, Wiley-VCH Verlag (2004).

[15] R. Loudon, The Quantum Theory of Light, Oxford University Press (1995).

[16] M. Babiker, R. Loudon, Proc. R. Soc. Lond A **385**, 439(1983).

[17] B. J. Dalton, E. S. Guerra, P. L. Knight, Phys. Rev A **54**, 2292(1996).

[18] J. J. Sakurai, Modern Quantum Mechanics, Addison-Wesley (1994).

[19] R. Glauber, M. Lewenstein, Phys. Rev. A **43**, 467(1991).

[20] E. A. Power, T. Thirunamachandran, Phys. Rev. A **25**, 2473(1982).

[21] *Handbook of Mathematical Functions*, edited by M. Abramowitz and I. Stegun (US GPO, Washington, DC, 1964).

[22] C. M. Bender, S. A. Orszag, *Advanced Mathematical Methods for Scientists and Engineers*, (Springer Science+Business Media, Inc. 1999).

[23] S. Y. Buhmann, S. Scheel, Acta Physica Slovaca **58**, 675(2008).

[24] C. I. Sukenik, M. G. Boshier, D. Cho, V. Sandoghdar, E. A. Hinds, Phys. Rev. Lett. **70**, 560(1993).

[25] H. B. G. Casimir, Haphazard Reality: Half a Century of Science (New York: Harper and Row) p 247 (1983).

[26] G. Barton, J. Phys. B: Atom. Molec. Phys. , **7**, 2134(1974).

[27] J. M. Wylie, J. E. Sipe, Phys. Rev. A **32**, 2030(1985).

[28] G. S. Agrawal, Phys. Rev. Lett. **73**, 703(1974).

[29] K. H. Drexhage, Sci. Am. , **222**, 108(1970).

[30] V. Sandoghdar, C. I. Sukenik, E. A. Hinds, Phys. Rev. Lett. **68**, 3432(1992).

[31] M. Bordag, G. L. Klimchitskaya, U. Mohideen, V. M. Mostepanenko, *Advanves in the Casimir Effect*, (Oxford University Press, 2008).

[32] A. F. Devonshire, Proc. R. Soc. Lond. A **156**, 37(1936).

[33] H. Bender,Ph. W. Courteile, C. Marzok, C. Zimmermann, S. Slama, Phys. Rev. Lett. **104**, 083201(2010).

[34] Yu. S. Barash, A. A. Kyasov, Sov. Phys. JETP **68**, 1(1989).

[35] Ya. B. Zel'dovich, Zh. Eksp. Theor. Fiz. **5**, 22(1935).

[36] V. M. Nabutovskii, V. R. Belosludov, A. M. Korotkikh, Sov. Phys. JETP **50**, 2 (1979).

[37] A. M. Marvin, F. Toigo, Phys. Rev. A **25**, 782(1982).

[38] M. J. Mehl, W. L. Schaich, Phys. Rev. A **16**, 921(1977).

[39] M. J. Mehl, W. L. Schaich, Phys. Rev. A **21**, 1177(1980).

[40] D. Langbein, *Theory of Van der Waals attraction*,(Springer, Berlin, 1974).

[41] A. M. Marvin, F. Toigo, Phys. Rev. A **25**, 803(1982).

[42] D. P. Fussell, R. C. McPhedran, C. Martijn de Sterke, Phys. Rev. A **71**, 013815(2005).

[43] M. Boustimi, J. Baudon, P. Candori, J. Robert, Phys. Rev. B **65**, 155402(2002).

[44] M. Boustimi, J. Baudon, J. Robert, Phys. Rev. B **67**, 045407(2003).

[45] E. V. Blagov, G. L. Klimchitskaya, V. M. Mostepanenko, Phys. Rev. B **71**, 235401(2005).

[46] I. Brevik, M. Lygren, V. N. Marachewsky Ann. Phys. (NY)**267**, 134(1988).

[47] T. N. C. Mendes, F. S. S. da Rosa, A. Tenorio, C. Farina, J. Phys. A **41**, 164029(2008).

[48] A. D. McLachlan, Proc. R. Soc. London, Series A **271**, 387(1963).

[49] I. S. Gradshteyn, I. M. Ryzhik, *Table of Integrals, Series, and Products*, edited by A. Jeffrey (Academic Press, London, 1994), 5th ed.

[50] F. S. S. da Rosa, T. N. C. Mendes, A. Tenorio, C. Farina, Phys. Rev. A **78**, 012105(2008).

[51] A. P. Prudnikov, Yu. A. Brychkov, O. I. Marichev, *Integrals and Series, Volume 2: Special Functions* (Gordon and Breach, New York, 1992), 3rd printing with corrections.

[52] C. K. Carnigila, L. Mandel, Phys. Rev. D **3**, 280(1971).

[53] I. Bialynicki-Birula, J. B. Brojan, Phys. Rev. D **5** 485(1972).

[54] C. Eberlein, D. Robashik, Phys. Rev. D **73**, 025009(2006).

[55] C. Eberlein, A. Contreras Reyes, Phys. Rev. A **79**, 043834(2009).

[56] C. Eberlein, A. Contreras Reyes, Phys. Rev. A **80**, 032901(2009).

[57] P. W. Milonni, Phys. Rev. A **25**, 1315(1982).

[58] T. W. Gamelin, *Complex Analysis*, (Springer Science 2001).

[59] G. Bimonte, J. Phys. A: Math. Theor. **43**, 155402(2010).

[60] S. Y. Buhmann, D. -G. Welsh, Progress in Quantum Electronics, **31**, 51-130, (2007).

[61] S. Y. Buhmann,L. Knoll, D. -G. Welsh, H. Dung, Phys. Rev. A **70**, 052117(2004).

[62] J. M. Wylie, J. E. Sipe, Phys. Rev. A **30**, 1185(1984).

[63] H. Koshravi, R. Loudon, Proc. R. Soc. London, Series A **433**, 337(1991); *ibid.* **436**, 373, (1992).

[64] S. Wu, C. Eberlein, Proc. R. Soc. London, Series A **455**, 2487(1998).

[65] E. Yablonovitch, T. J. Gmitter, R. Bhat, Phys. Rev. Lett. **61**, 2546(1988).

[66] M. Bordag, Phys. Rev. D **70**, 085010(2004); *ibid.* **76**, 065011(2007).

[67] H. P. Urbach, G. L. J. A. Rikken, Phys. Rev. A **57**, 3913(1998).

[68] B. Huttner, J. J. Baumberg, S. M. Barnett, Europhys. Lett, **16**, 177(1991).

[69] B. Huttner, S. M. Barnett, Europhys. Lett, **18**, 487(1992).

[70] L. G. Suttorp, M. Wubs, Phys. Rev. A **70**, 013816(2004).

[71] L. G. Suttorp, A. J. van Wonderen, Europhys. Lett. **67**, 766(2004).

[72] O. Di Stefano, S. Savasta, R. Girlanda, J. Opt. B: Quantum Semiclass. Opt. **3**, 288(2001).

[73] J. J. Hopfield, Phys. Rev. **112**, 1555(1958).

[74] U . Fano, Phys. Rev. **103**, 1202(1956).

[75] B. Huttner, S. M. Barnett, Phys. Rev. A **46**, 4306(1992).

[76] A. Bechler, J. Phys. A: Math. Gen. **39**, 13553(2006).

[77] F. Kheirandish, M. Soltani, Rev. A **78**, 012102(2008).

[78] S. M. Barnett, B. Huttner, R. Loudon , Phys. Rev. Lett. **68**, 3698(1992).

[79] L. Valeri, G. Scharf, quant-ph/052115v1.

[80] C. Eberlein, M. Janowicz, Phys. Rev. A **67**, 063816(2003).

[81] I. R. Senitzky, Phys. Rev. **119**, 670(1960).

[82] G. W. Ford, J. T. Lewis, R. F. O'Connell, Phys. Rev. A **37**, 4419(1988).

[83] Z. Artyszuk, A. Bechler, Acta. Phys. Pol. A **103**, 263(2003).

[84] A. L. Fetter, J. D. Walecka, *Quantum Theory of Many-Particle Systems* (McGraw-Hill, New York, 1971).

[85] A. A. Maradudin, D. L. Mills, Phys. Rev. A **11**, 1392(1975).

[86] C. Kittel, *Introduction to Solid State Physics*, (John Wiley & Sons, 1975).

[87] S. Y. Buhmann, H. T. Dung, D. Welsh, J. Opt. B: Quantum Semiclass. Opt. **6**, S127(2006).

[88] G. Barton, Comments At. Mol. Phys. **1**, 301(2000).

[89] H. Nha,W. Jhe, Phys. Rev. A **54**, 3505(1996).

[90] H. Nha,W. Jhe, Phys. Rev. A **60**, 1729(1999).

[91] L. Lewin, *Dilogarithms and Associated Functions*, (Macdonald - London, 1958).

[92] S. A. Ellingsen, S. Y. Buhmann, S. Scheel, Phys. Rev. A **80**, 022901(2009).

[93] L. Knöll, S. Scheel, D. Welsh, *Coherence and Statistics of Photons and Atoms*, edited by J. Peřina, (John Wiley & Sons, Inc., 2001)

[94] M. S. Tomas, Z. Lenac, Phys. Rev. A **56**, 4197(1997).